



Songsri, Sineenard (2024) *Synthesis of nonproteinogenic amino acids via reactions of enone and ynone functional groups*. PhD thesis.

<https://theses.gla.ac.uk/84250/>

Copyright and moral rights for this work are retained by the author

A copy can be downloaded for personal non-commercial research or study, without prior permission or charge

This work cannot be reproduced or quoted extensively from without first obtaining permission from the author

The content must not be changed in any way or sold commercially in any format or medium without the formal permission of the author

When referring to this work, full bibliographic details including the author, title, awarding institution and date of the thesis must be given

Enlighten: Theses

<https://theses.gla.ac.uk/>
research-enlighten@glasgow.ac.uk

Synthesis of Nonproteinogenic Amino Acids via Reactions of Enone and Ynone Functional Groups

Sineenard Songsri, MSci

A thesis submitted in part fulfilment of the requirements
of the degree of Doctor of Philosophy



University | School of
of Glasgow | Chemistry

School of Chemistry

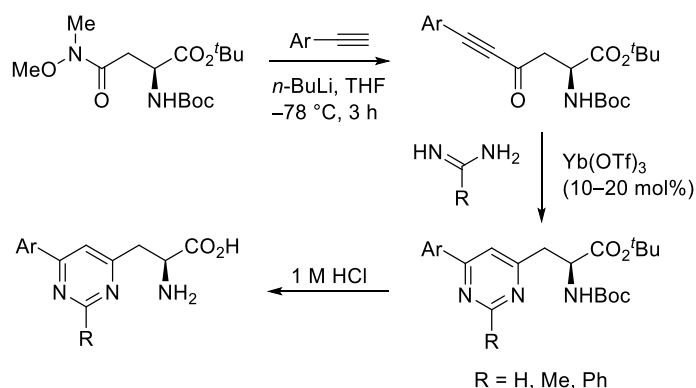
College of Science and Engineering

University of Glasgow

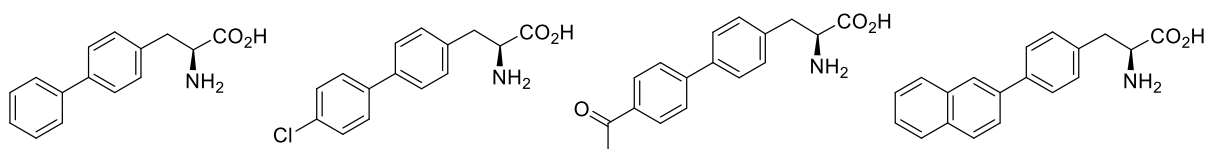
November 2023

Abstract

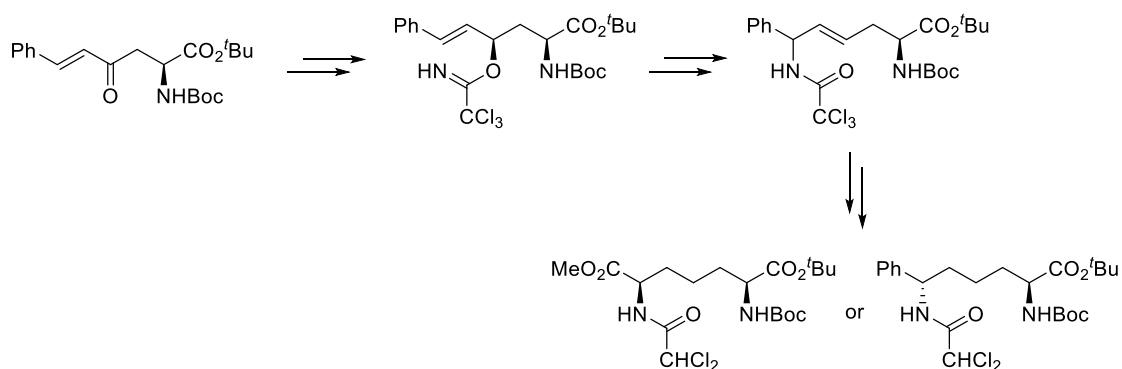
The main aim of this PhD was to develop novel syntheses of functional amino acids using synthetic chemistry involving ynone or enone side-chains. The first project focused on utilising amino acid-derived ynones to synthesise pyrimidine derivatives, that would have application as fluorescence probes for chemical biology. The approach involved starting with readily available chiral pool α -amino acids. These were transformed into Weinreb amide intermediates and subsequent reaction with the anion of an alkyne allowed for the synthesis of the ynone. Lewis acid catalysed heterocyclisation of the ynone with a range of amidines resulted in the efficient synthesis of pyrimidine-derived amino acids. By altering the alkyne side chain, a variety of pyrimidine analogues were prepared. These compounds were readily deprotected in a one-step process under acidic conditions to yield the parent amino acids. Analysis of the photophysical properties of these amino acids showed that electron-deficient pyrimidines with electron-rich or highly conjugated side-chains gave fluorophores with red-shifted emission and the highest quantum yields.



The next project investigated the synthesis of biphenyl amino acids using a short and efficient synthetic route from a readily available tyrosine derivative. The approach involved one-pot nonaflate formation, followed by a Suzuki-Miyaura cross-coupling reaction to create the biphenyl side-chain. Using the nonaflate as an excellent leaving group and the Buchwald XPhos Pd G2 pre-catalyst for the cross-coupling step, rapid access to a variety of biphenyl amino acids was achieved. The optical properties of these amino acids were also investigated and showed the 2-naphthyl derivative as the brightest with a molar attenuation coefficient of $\sim 31,000$ $\text{cm}^{-1} \text{M}^{-1}$ and a quantum yield of 0.18.



The final project describes the development of a new synthetic approach for the preparation of the biologically important *meso*-DAP and L,L-DAP amino acids using enones as key intermediates. An enone intermediate was prepared by the Horner-Wadsworth-Emmons (HWE) reaction of a phosphonate ester-derived amino acid with benzaldehyde. The enone was subjected to a diastereoselective reduction using L-selectride or the (S)-CBS-Me reagent to access either diastereomer. The resulting allylic alcohols were then used to install the amino group via an Overman rearrangement. Hydrogenation, oxidation of the phenyl ring and esterification of the resulting carboxylic acid led to the synthesis of protected DAP amino acids.



2.1.5.2	Fluorescent Properties of the Pyrimidine Derived α -Amino Acids with a C2-Methyl Substituent	58
2.1.5.3	Fluorescent Properties of the Pyrimidine Derived α -Amino Acids with no C2-Substituent	61
2.1.6	Further Analysis of Lead Analogue 122n	66
2.1.7	Conclusions	70
2.1.8	Future Work	70
2.2	Synthesis of Novel Fluorescent Biaryl α-Amino Acids	72
2.2.1	Introduction	72
2.2.2	Project Aims	76
2.2.3	Fluorescent Properties of Biphenyl Amino Acids	79
2.2.4	Conclusions	81
2.2.5	Future Work	81
2.3	New Applications of Enone Derived α-Amino Acids:	
	The Stereoselective Synthesis of Diaminopimelic Acids	83
2.3.1	Introduction	83
2.3.2	Antibiotic Properties of DAP Pathway Inhibitors	85
2.3.2.1	Synthesis of Diaminopimelic Analogues	85
2.3.2.2	Synthesis of Protected DAP Analogues	85
2.3.3	Previous Work in the Sutherland Group	90
2.3.4	Project Aims	94
2.3.5	Synthesis of Diaminopimelic Acid	94
2.3.5.1	Synthesis of Enone-Derived α -Amino Acid 184	94
2.3.5.2	Synthesis of <i>t</i> -Butyl Ester Analogue 186	96
2.3.5.3	Stereoselective Reduction of Enone-Derived α -Amino Acid 196	98
2.3.6	New Approach for the Efficient Synthesis Enone-derived α -Amino Acid 197	98
2.3.6.1	Installation of the Second Amino Group Using an Overman Rearrangement	99
2.3.6.2	Completion of the Synthetic Route to a Protected <i>meso</i> -DAP Analogue	99
2.3.7	Synthesis of Protected L,L-DAP 145	100
2.3.8	Summary	101
2.3.9	Future Work	101

3.0 Experimental	101
3.1 General Experimental	104
3.2 Aryl Substituted Pyrimidine Derived α -Amino Acids Experimental	104
3.3 Biaryl α -Amino Acids Experimental	136
3.4 Enone Derived α -Amino Acids Experimental	144
4.0 References	159

Acknowledgement

I would first like to thank my supervisor, Professor Andrew Sutherland for affording me the opportunity to embark on this PhD journey. Your support and patience have been absolute lifesavers during this academic rollercoaster. Your guidance has been more than just academic—it's been a driving force behind my personal and professional growth. Massive thanks for all the guidance and encouragement, Andy! I would also like to express my gratitude to my second supervisor, Dr Alistair Boyer, for providing invaluable advice on annual report feedback. Thanks to the Royal Thai Government and Maejo Phrae University for funding my research.

I wish to acknowledge the technical staff in the Joseph Black Building, including Karen and Finlay (stores), Andy, Jess, and Gangi (MS), Dave and Alec (NMR), and Stuart and Arlene (IT). Special thanks to Dr William Peveler for his training and allowing me to use the fluorimeter.

My appreciation extends to all members of the Sutherland group, past and present, for making this experience so enjoyable. Martyn, Rebecca, Euan, Holly, Liyao, Rochelle, Amy, Lachlan, Olivia—thank you. I am especially grateful to my friends, Leanne, Joe and Valeria for their unwavering support throughout my PhD journey. You guys are the real MVPs, always having my back. I would like to thank the Hartley group, especially Becca, for your cheerful and positive contributions.

And to my Thai pals, you've been a constant source of strength with your support, delightful Thai meals, and understanding.

Lastly, a huge thank you to my parents, my sisters, Amily, and James for being incredibly supportive throughout my entire university experience. Your unwavering presence, listening ear, and endless encouragement have meant more than words can say. Cheers everyone!

Author's Declaration

I declare that, except where explicit reference is made to the contribution of others, this thesis represents the original work of Sineenard Songsri and has not been submitted for any other degree at the University of Glasgow or any other institution. The research was carried out at the University of Glasgow in the Loudon Laboratory under the supervision of Professor Andrew Sutherland between October 2019 to May 2023. Aspects of the work described herein have been published elsewhere as listed below.

S. Songsri, A. H. Harkiss, and A. Sutherland, Synthesis of Photophysical Properties of Charge-Transfer-Based Pyrimidine-Derived α -Amino Acids, *J. Org. Chem.* **2023** 88 (18), 13214-13224.

Abbreviations

°C	Degrees centigrade
Ac	Acetyl
Ar	Aromatic
Bn	Benzyl
Boc	<i>tert</i> -Butyloxycarbonyl
BODIPY	Boron-dipyrrromethene
br	Broad
Bt	Benzotriazole
Bu	Butyl
BuLi	Butyllithium
Bz	Benzyl
CBS	Corey–Bakshi–Shibata catalyst (a chiral oxazaborolidine)
Cbz	Carboxybenzyl
CDI	<i>N,N'</i> -Carbonyldiimidazole
COD	Cyclooctadiene
COSY	Correlated spectroscopy
d	Doublet
DABCO	1,4-Diazabicyclo[2.2.2]octane
DAP	2,3-Diaminopropanoic acid
dba	Dibenzylideneacetone
DCE	Dichloroethane
DDQ	2,3-Dichloro-5,6-dicyano-1,4-benzoquinone
DEPT	Distortionless enhancement polarisation transfer
DIBAL-H	Diisobutylaluminium hydride
DIEPA	Diisopropylethylamine
DMAP	4-Dimethylaminopyridine
DMF	Dimethylformamide
DMSO	Dimethyl sulfoxide
ee	Enantiomeric excess
EI	Electron impact
ESI	Electrospray ionisation
Et	Ethyl
Fmoc	Fluorenylmethyloxycarbonyl
FRET	Förster resonance energy transfer

g	Grams
GFP	Green fluorescent protein
h	Hour
HBTU	O-(Benzotriazol-1-yl)-N,N,N',N'-tetramethyluronium
HCl	Hydrochloric acid
HRMS	High-resolution mass spectrometry
HSQC	Heteronuclear single quantum correlation spectroscopy
HWE	Horner-Wadsworth-Emmons reaction
Hz	Hertz
ICT	Intramolecular charge transfer
IR	Infrared
ISC	Intersystem crossing
J	NMR spectra coupling constant
<i>m</i> -	<i>Meta</i>
m	Multiplet
M	Molar
m/z	Mass to charge
Me	Methyl
mg	Milligrams
MHz	Megahertz
mL	Millilitres
mM	Millimolar
μM	Micromolar
mmol	Millimole
mol	Mole
MOM	Methoxymethyl
Ms	Mesyl
MW	Microwave
NBS	N-Bromosuccinimide
NHS	N-Hydroxysuccinimide
NIR	Near-infrared
nm	Nanometers
NMM	N-Methyl morpholine
NMP	N-Methyl-2-pyrrolidone
NMR	Nuclear magnetic resonance
NOE	Nuclear Overhauser effect

NOESY	Nuclear Overhauser effect spectroscopy
NPAAs	Non-proteinogenic amino acids
<i>o</i> -	<i>Ortho</i> -
<i>p</i> -	<i>Para</i> -
PBS	Phosphate-buffered saline
PET	Positron emission tomography
Ph	Phenyl
Py	Pyridine
Pr	Propyl
pTyr	Phosphotyrosine
q	Quartet
QY	Quantum yield
R _f	Retention factor
rt	Room temperature
s	Singlet
S ₀	Ground state
S ₁	First excited state
S ₂	Second excited state
S _N Ar	Nucleophilic aromatic substitution
SPPS	Solid phase peptide synthesis
t	Triplet
T ₁	Triplet excited state
TBAF	Tetra- <i>n</i> -butylammonium fluoride
TBDMS	<i>tert</i> -Butyldimethylsilyl
TBS	Tris-buffered saline
TEA	Triethylamine
TFA	Trifluoroacetic acid
THF	Tetrahydrofuran
TLC	Thin layer chromatography
tRNA	Transfer ribonucleic acid
Tr	Trityl
Ts	Tosyl
UV	Ultraviolet
Vis	Visible
XPhos	2-Dicyclohexylphosphino-2',4',6'-triisopropylbiphenyl
Yb(OTf) ₃	Ytterbium(iii) trifluoromethanesulfonate

Δ	Reflux
ϵ	Molar attenuation coefficient
λ_{abs}	Absorbance maximum
λ_{em}	Emission maximum
Φ	Fluorescence quantum yield
μM	Micromolar

1.0 Introduction

1.1 α -Amino Acids

α -Amino acids are defined as organic compounds containing both an amino group (-NH₂) and a carboxylic group (-COOH), which differ in the side chain (R group).¹ They exist as zwitterions and possess amphoteric properties, meaning they can act as an acid and a base (**Figure 1**).² In general terms, α -amino acids serve multiple and diverse roles within the biological realm. They play an important role in a wide range of biochemical systems. These α -amino acids are referred to as coded amino acids or proteinogenic amino acids. The rest of the amino acids are referred to as non-coded amino acids or non-protein amino acids. Although there are hundreds of amino acids in nature, only 20 amino acids act as building blocks for proteins.³



Figure 1: General structure of an α -amino acid.

While twenty amino acids are involved directly in protein structure, a category known as non-proteinogenic amino acids (NPAAs)⁴ do not serve such a role. NPAAs are not inherently encoded within the human genetic code or integrated into polypeptide chains.⁴ However, research has highlighted their significant contribution to various organisms,⁵ including bacteria, fungi, plants, and marine organisms.⁶ These NPAAs serve as fundamental building blocks, participating not only in the constitution of peptides and proteins with versatile functions but also exhibiting diverse roles such as drug compounds **1** and **2** (**Figure 2**),⁷ acting as catalysts **3**,⁸ and enabling biotechnological tools **4** and **5** (**Figure 2**).⁹⁻¹¹

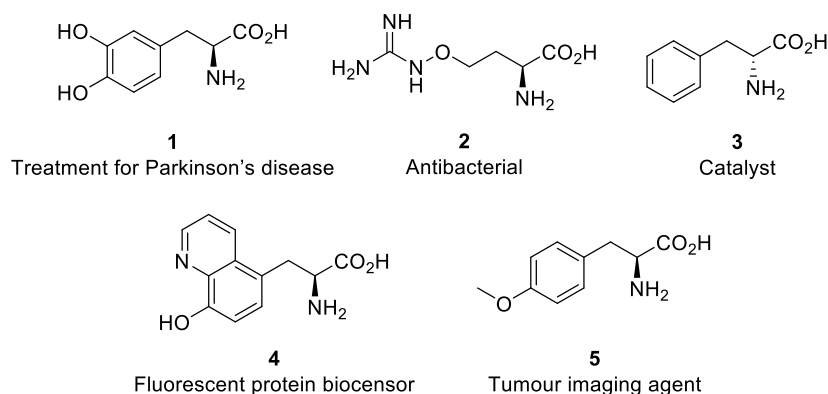


Figure 2: Examples of non-proteinogenic amino acids as drugs, catalysts, and biotechnological tools.⁷⁻¹¹

As chemical biology, biomedical sciences, and life sciences make continual advancements, the utilisation of non-proteinogenic amino acids is progressively expanding. In particular, the measurement of fluorescence spectra, lifetime and polarisation properties are powerful methods for studying biological structure and function. Among the existing techniques for achieving this goal, the incorporation of fluorescent unnatural amino acids is particularly noteworthy. This chapter will primarily concentrate on this approach and explore the recent synthetic methodologies used to create these fluorescent amino acids, considering factors such as structural modifications, spectroscopic properties, and their potential applications.

1.2 Introduction to Fluorescence Spectroscopy

Fluorescence, a type of luminescence, is a process in which a molecule absorbs light energy, becomes electronically excited, and subsequently emits light energy while relaxing to a lower energy state through the emission of a photon without a change in electron spin. These photonic processes involve transitions between electronic and vibrational states of polyatomic fluorescent molecules, also known as fluorophores.

These processes can be represented using a Jabłoński diagram (**Figure 3a**).^{12,13} This partial energy diagram represents the energy of a photoluminescent molecule in its different energy states. The ground and first electronic states are depicted as S_0 , and S_1 , respectively. At each of these electronic energy levels, the fluorophores can exist in a number of vibrational energy levels (denoted by 0, 1, 2, etc.).

The fluorescence phenomenon occurs in three steps: excitation of the fluorophore by the energy absorbed from the incident light (occurring within 10^{-15} s); vibrational relaxation of the fluorophore and emission preparation.¹⁴

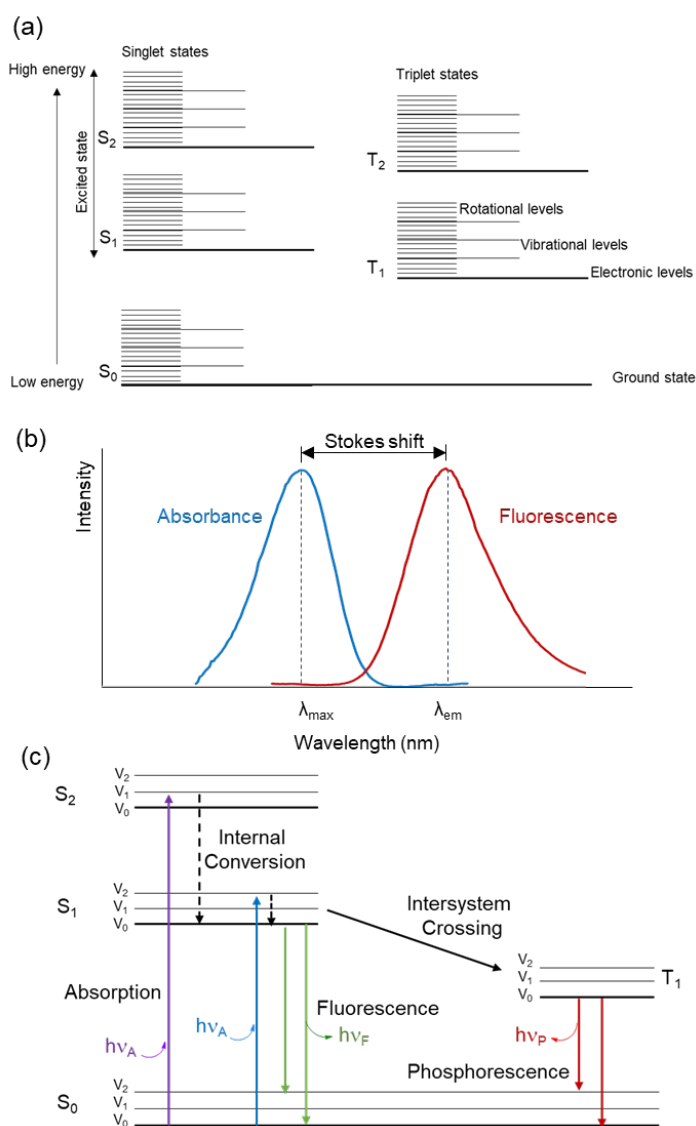


Figure 3: Fluorescence fundamentals, (a) Jablonski diagram displaying the energy states of a molecule,¹³ (b) The absorption and emission spectra of the common fluorophore,¹⁵ (c) various steps in fluorescence excitation and emission and phosphorescence.¹³

Relaxation and Fluorescence

Molecules typically relax to the lowest available vibrational state of the S_1 energy level. This process notably contributes to the Stokes shift, observed, as fluorescence photons are emitted at longer wavelengths than the excitation radiation (**Figure 3b**).¹⁵

In addition, the emission spectrum is typically a mirror image of the absorption spectrum, resulting from the ground to first excited state transition. The change in energy level, following excitation is facilitated by vibrational relaxation. The relaxation of molecules to the lowest available vibrational state of the S_1 energy level occurs by internal conversion and generally occurs in a picosecond or less. This is almost always complete before emission can occur. Several other relaxation pathways that have varying degrees of probability compete with the fluorescence emission process. The excited fluorophore can collide with another molecule to transfer energy in a second type of non-radiative process, for example, quenching or intersystem crossing, which is relatively rare. The latter event describes the relaxation of the molecule from a singlet excited state S_1 to a lower energy, triplet excitation state T_1 through different pathways (**Figure 3c**).¹³

The most favoured transitions will be those where the rotational and vibrational electron density probabilities maximally overlap in both the ground and excited states. However, incident photons of varying wavelengths may have sufficient energy to be absorbed and often produce transitions from other internuclear separation distances and vibrational energy levels.¹² This effect gives rise to an absorption spectrum containing multiple peaks. This happens because of the diverse possibilities for these transitions caused by different photon energies. In most fluorophores, these energy levels are not significantly altered by the different electronic distributions of S_0 and S_1 . In cases where an absorption spectrum of a fluorophore displays distinctive peaks attributed to vibrational energy levels, as observed in anthracene (**Figure 4**),¹⁶ these peaks are the result of transitions from the lowest vibrational level of the S_0 state to higher vibrational levels of the S_1 state. When the fluorophore returns to the S_0 state, it can revert to any of the ground state vibrational levels, which exhibit similar spacing to those in the S_1 state. Interestingly, the emission spectrum also exhibits the same vibrational energy spacing observed in the absorption spectrum. According to the Franck-Condon principle,¹³ all electronic transitions are vertical, implying they occur without any change in the position of the atomic nuclei.

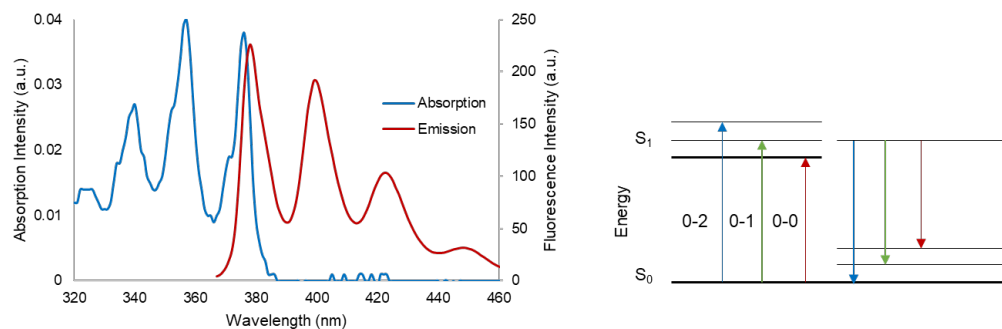


Figure 4: Absorption and emission spectrum of anthracene (5 μM in EtOH). Mirror-image rule and Franck-Condon factors.¹³

In addition to the wavelength at which a fluorophore absorbs and emits light, several parameters are useful to summarise the properties of a fluorophore. These include molar attenuation coefficient, quantum yield and brightness. The molar attenuation coefficient (ϵ) is a measure of how strongly a molecule absorbs light at a given wavelength. The fluorescence quantum yield (ϕ) is a ratio of the number of photons emitted to those absorbed. As such, it is a measure of decay by emission rather than by other non-radiative decay processes, and the closer to unity this value, the brighter a fluorophore is likely to be. Multiplication of the quantum yield and molar attenuation coefficient ($\phi \times \epsilon$) gives the brightness value of the fluorophore.¹⁷

To exhibit fluorescence, a molecule must possess an energy gap between its highest occupied molecular orbital¹⁸ and lowest unoccupied molecular orbital (LUMO), specifically between the energy levels of the relaxed, excited singlet state and the ground state on the potential energy surface.¹³ The critical band gap can be achieved through several common methods, such as incorporating extended π -conjugated systems or combining electron-donating groups with electron-withdrawing groups, often referred to as push-pull or donor-acceptor systems in the literature.¹⁹

1.3 Fluorescence of Organic Compounds

Organic fluorescent compounds typically present aromatic or conjugated double bonds. Organic fluorophores have superior properties over fluorescent proteins, such as a wider spectral range, smaller size, greater photostability, and, in many cases, higher brightness.^{20,21} Small synthetic fluorophores are one of the major classes of fluorophores from the commercially available fluorescent molecules. A key advantage of small-molecule fluorophores is the ability to construct compounds where fluorescence is activated by chemical or biochemical processes.

A wide range of organic molecule-based fluorophores exist and include fluorescein **6**, BODIPY **7**, rhodamine **8**, coumarin **9** and cyanine derivatives **10** (**Figure 5**),²²⁻²⁶ which have been used for the measurement of protein interactions,^{27,28} enzymatic activity,^{29,30} biological imaging,^{31,32} conformation changes,³³ and the ability to observe individual proteins moving in real-time.³⁴

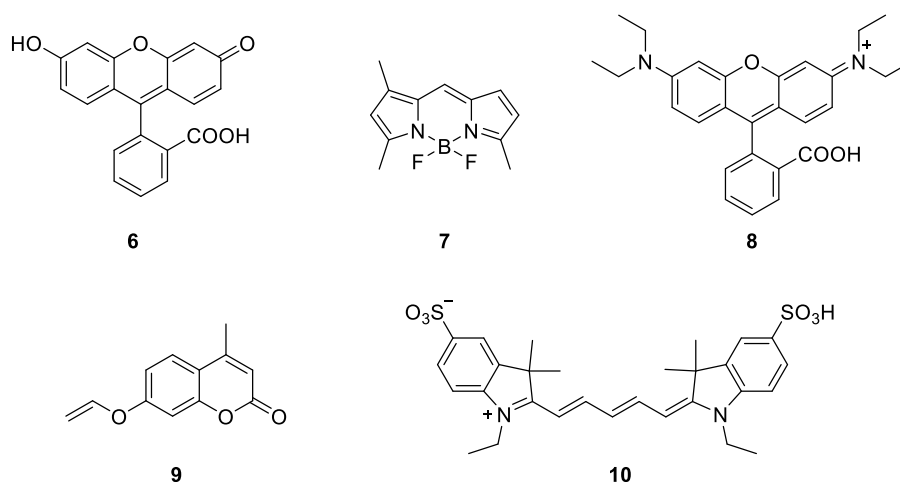
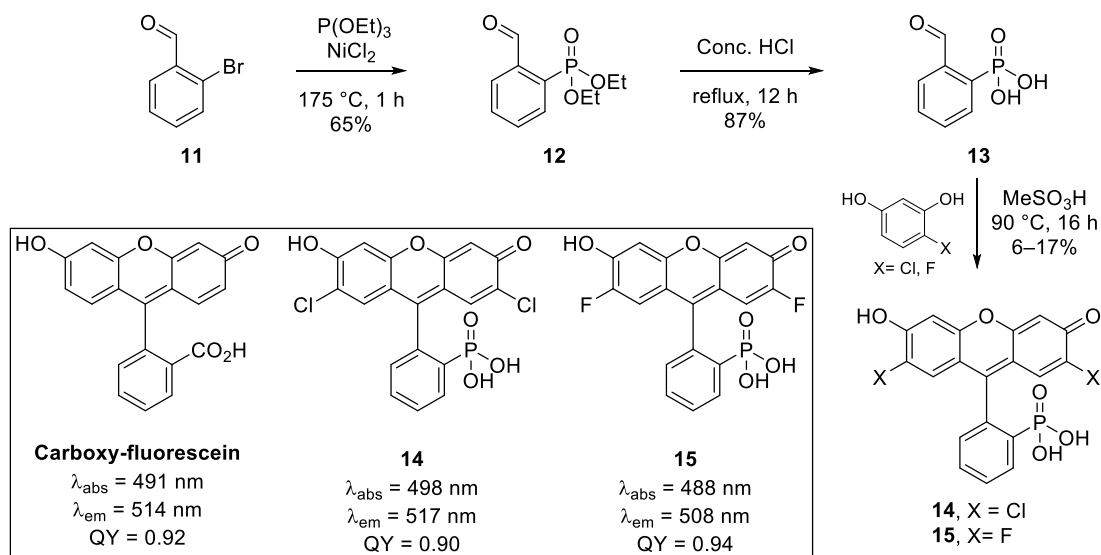


Figure 5: Representative molecules from important fluorophore classes, including fluorescein **6**, BODIPY (BODYPY-FL) **7**, rhodamine (rhodamine B) **8**, coumarin **9** and Cy5-phalloidin **10** cores.

1.3.1 Fluorescein

The well-known xanthene dye fluorescein is particularly prominent among fluorophores due to its remarkable properties, including strong fluorescence, reversible pH sensitivity, and exceptional chemical stability.^{35,36} Fluorescein has served as a starting material to create novel fluorescent probes revealing specific biological activities. In 2021, Miller and co-workers reported a novel class of phosphonic acid-derived fluoresceins (**Scheme 1**).³⁷ The synthetic process involved the preparation of aryl phosphonic ester **12**, which was achieved by the reaction of 2-bromobenzaldehyde **11** and triethyl phosphite with nickel chloride as the catalyst,³² yielding aryl phosphonic ester **12** in 65% yield. Subsequent hydrolysis of **12** under reflux conditions produced compound **13** in 87% yield. Following this, the condensation of **13** with the corresponding resorcinol in neat methanesulfonic acid, yielded dihalogenated phosphonofluoresceins **14** and **15**. However, purifying the crude phosphonofluoresceins proved challenging due to their water-soluble nature, resulting in a lower isolated yield. The optical properties of **14** and **15** are similar to

that of the 3-carboxy derivative. Importantly, 2',7'-dichloro-3-phosphonofluorescein **14** demonstrated enhanced water solubility compared to the 3-carboxy analogue, making it particularly suitable for application in intracellular imaging and membrane potential sensing.



Scheme 1: Synthesis of Phosphonofluoresceins.

1.3.2 BODIPY

BODIPY fluorophores have traditionally found extensive use as fluorescent labels for biomolecules and in cellular imaging.³⁸ These dyes possess several distinctive attributes, including insensitivity of their spectroscopic properties to environmental changes, a small Stokes shift, and an inherent lipophilic nature.³⁹⁻⁴¹ The absorption and fluorescence properties of BODIPYs are profoundly influenced by the electron delocalisation around their core structure and through conjugated substituents.⁴² A simple BODIPY, such as compound **16**, exhibited an absorption maximum at 505 nm, an emission maximum at 511 nm and a high quantum yield of 0.94.⁴³ As expected, by extending the conjugated system through aryl substitution, compound **17** showed absorption and emission at longer wavelengths (λ_{abs} 544 nm and λ_{em} 570 nm).⁴⁴ In addition, by combining the BODIPY motif with other functionalities has provided a broad range of tools available for detecting specific ions, imaging cellular processes, and tracking specific substances within cells (**Figure 6**).^{45,46}

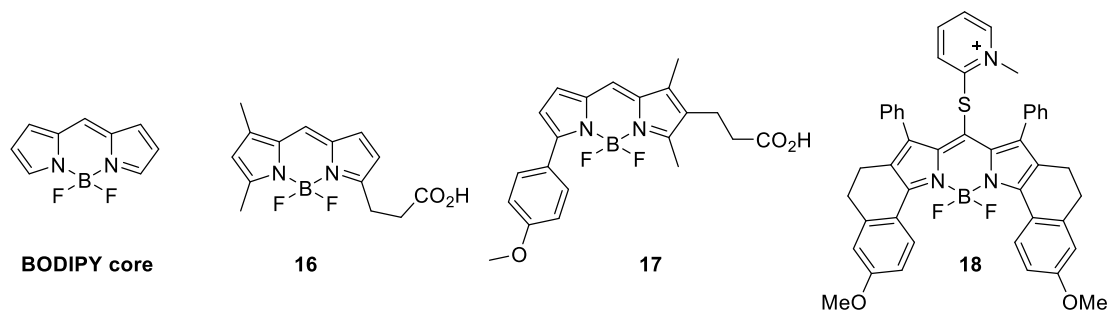
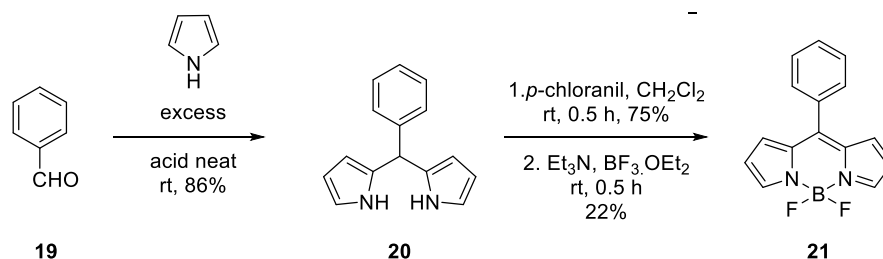


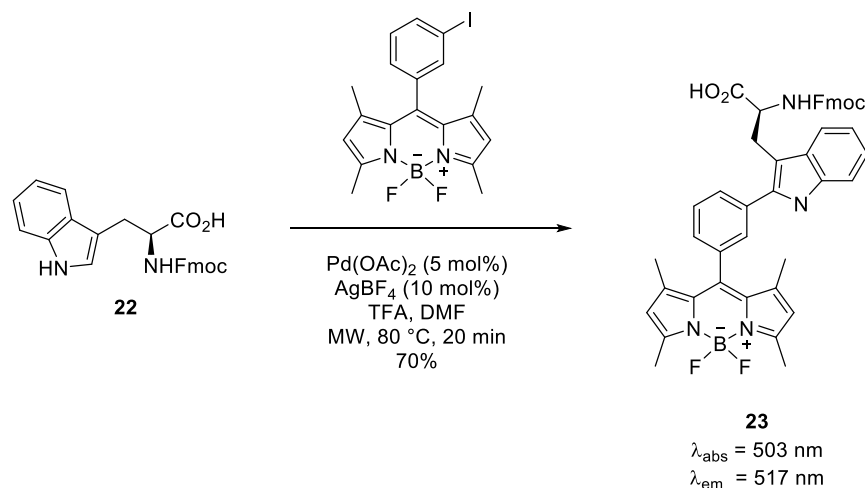
Figure 6: Boron dipyrromethene (BODIPY)-based fluorogenic molecules **16** and **17**, BDP-S-*o*-Pyb **18** (a BODIPY probe to detect cysteine in living cells).⁴⁶

A common approach for the preparation of BODIPY derivatives involves the acid-catalysed condensation of pyrrole with an aromatic aldehyde (**19**), to afford aryldipyrromethanes **20** (Scheme 2).^{38,47} Subsequently, the oxidation of aryldipyrromethanes such as **20** can be conducted with *p*-chloranil to obtain the corresponding dipyrrens in good yields. Subjecting the dipyrren to base and boron trifluoride etherate affords the boron difluoride complex **21**.



Scheme 2: General synthetic route to the BODIPY unit.³⁸

The versatility of BODIPY cores extends to numerous modifications of the *meso*-aryl substituent. Interestingly, these BODIPYs have been incorporated as side chains in amino acids, rendering them highly suitable for imaging various biochemical processes.⁴⁸ For example, a notable application involves the preparation of Trp-BODIPY fluorogenic amino acid for labelling peptides in live cells.⁴⁹ The synthetic method involved the arylation of *m*-iodophenyl-BODIPY at the C2 position of Fmoc-Trp-OH **22** by using Pd-catalysis, leading to the desired Fmoc-Trp(C2-BODIPY)-OH in 70% yield (Scheme 3). Subsequently, the Fmoc-protected compound can be incorporated into peptides for live-cell fluorescence imaging by conventional solid-phase peptide synthesis (SPPS).



Scheme 3: Synthesis of amino acid Fmoc-Trp(C2-BODIPY)-OH (**23**).

1.3.3 Rhodamine

Rhodamine dyes are analogues of fluorescein but with amine substituents. These typically possess high absorption coefficients, high fluorescence quantum yields and photostability.⁵⁰ Other characteristics of this dye class include low pH sensitivity and tuneable spectroscopic properties. The addition of different functionalities at the bottom ring of rhodamines can also be used to modulate fluorescence. The simplest member of the rhodamine family, rhodamine 110 (**24**), shares optical properties similar to fluorescein.⁵¹ More structurally rigid rhodamines, such as the fully alkylated rhodamine derivative rhodamine 101 (**25**), exhibit more substantial spectroscopic shifts with high quantum yield.

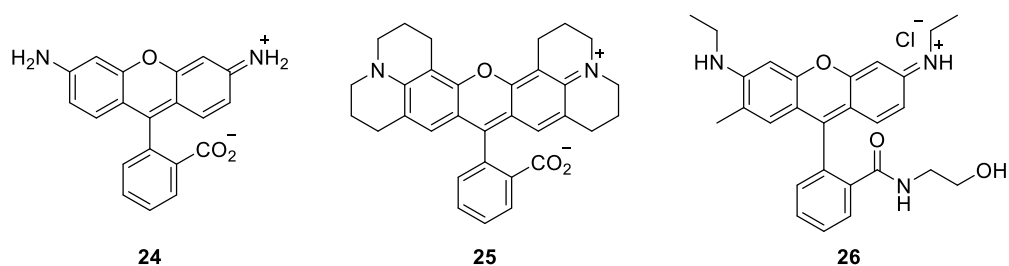
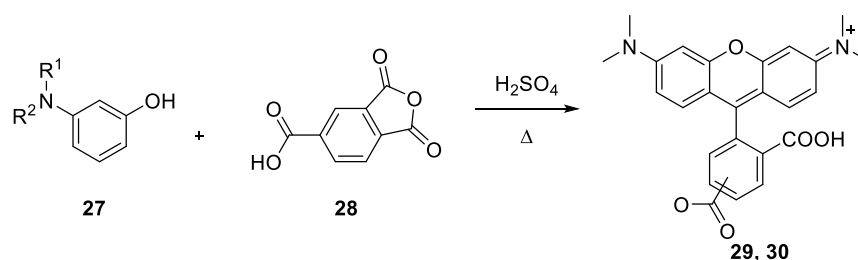


Figure 7: Representative rhodamine derivatives (**24** and **25**) and amide-functionalised pH-sensitive fluorescent probe **26**.^{50,51}

The typical synthesis of the rhodamine core involves condensation of a phthalic anhydride derivative with *N*-alkylated-*m*-aminophenols in the presence of an acid, resulting in the mixture of two isomers, 4'-carboxyrhodamine **29** and 5'-carboxyrhodamine **30** (**Scheme 4**).^{52,53} The separation of the two rhodamine isomers requires complicated purification procedures. Thus, most commercially available rhodamine derivatives are usually sold as a mixture of isomers.

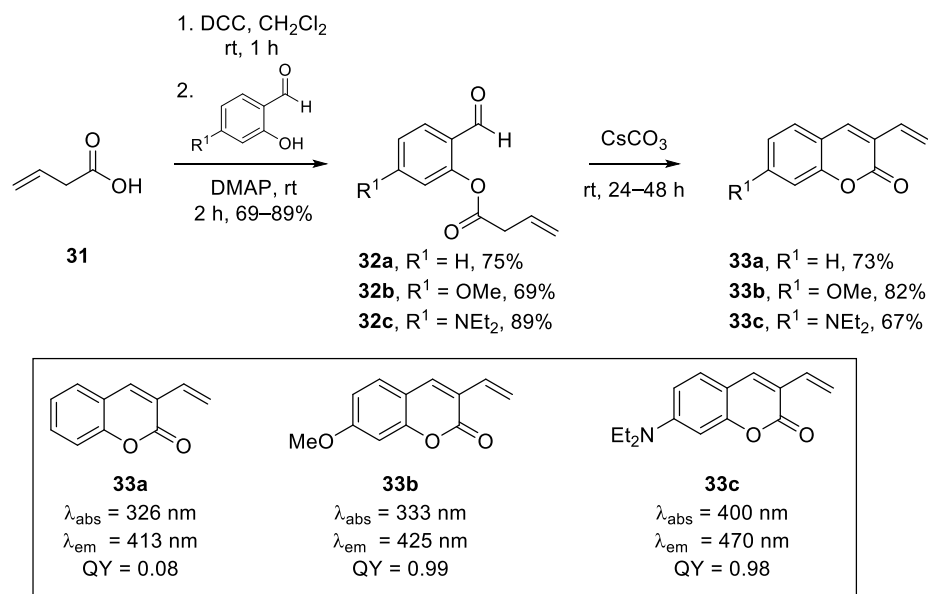


Scheme 4: General synthesis of rhodamine dye (Ceresole-type process).

Rhodamines are known for being pH-insensitive and offer greater photostability compared to fluorescein analogues.⁵⁴ However, their hydrophobic and planar structure can pose challenges. These characteristics often result in low water solubility, non-specific binding of labelled species, and potential fluorescence quenching when used with proteins.

1.3.4 Coumarin

Coumarins constitute a diverse class of compounds that find wide application in natural products, pharmaceutical agents, and fluorophores. While coumarin itself exhibits a low quantum yield, the strategic introduction of appropriate substitutions yields fluorescent derivatives emitting within the blue to green spectroscopic range (400–550 nm).⁵⁵ Branco and co-workers have outlined a general methodology for enhancing the fluorescence properties of coumarin-based fluorophores (**Scheme 5**).⁵⁶ The synthetic approach involves the initial coupling reaction of 3-butenoic acid **31** with salicylaldehydes, forming 2-formylaryl-but-3-enoates **32a–c**. Compounds **32a–c** were then cyclised via an aldol condensation reaction using cesium carbonate, which gave 3-vinylcoumarins **33a–c** in good yields. These derived fluorophores exhibited an absorption above 300 nm and red-shifted emission maxima with fluorescent quantum yields of 0.08, 0.99 and 0.98, respectively. This approach represents a valuable strategy for enhancing the fluorescence properties of coumarin-based compounds, expanding their utility in various applications.



Scheme 5: Synthesis of 3-vinylcoumarins.

1.3.5 Cyanine⁵⁷

Cyanine dyes contain two nitrogen heterocyclic rings connected through a p-conjugated polymethine chain.^{58,59} The absorption and emission characteristics of cyanine dyes are notably influenced by the length of the polymethine bridge with heterocyclic units at the terminal position forcing the formation of a linear shape.⁵⁸ Cyanine dyes are highly valuable as labels for proteins and nucleic acids^{60,61} due to their spectroscopic properties, such as high molar extinction coefficients and good fluorescence quantum yields. Additionally, the spectroscopic position of absorption and emission bands for cyanine dyes, including well-known variants such as Cyanine3 (Cy3) **34**, Cyanine5 (Cy5) **35** and Cyanine5.5 (Cy5.5) **36**, have found application in labelling RNA and DNA for gene expression studies (**Figure 8**).⁶²

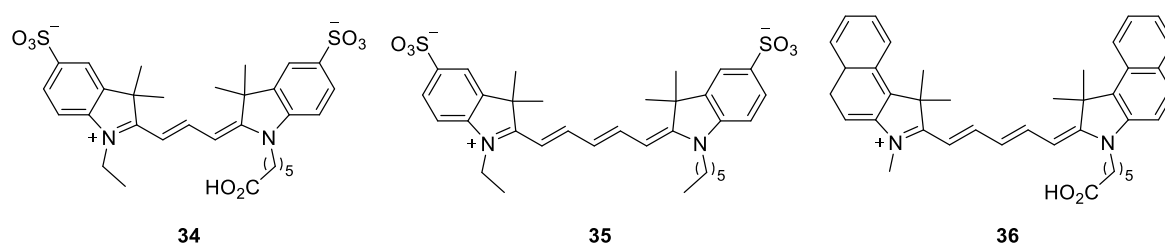
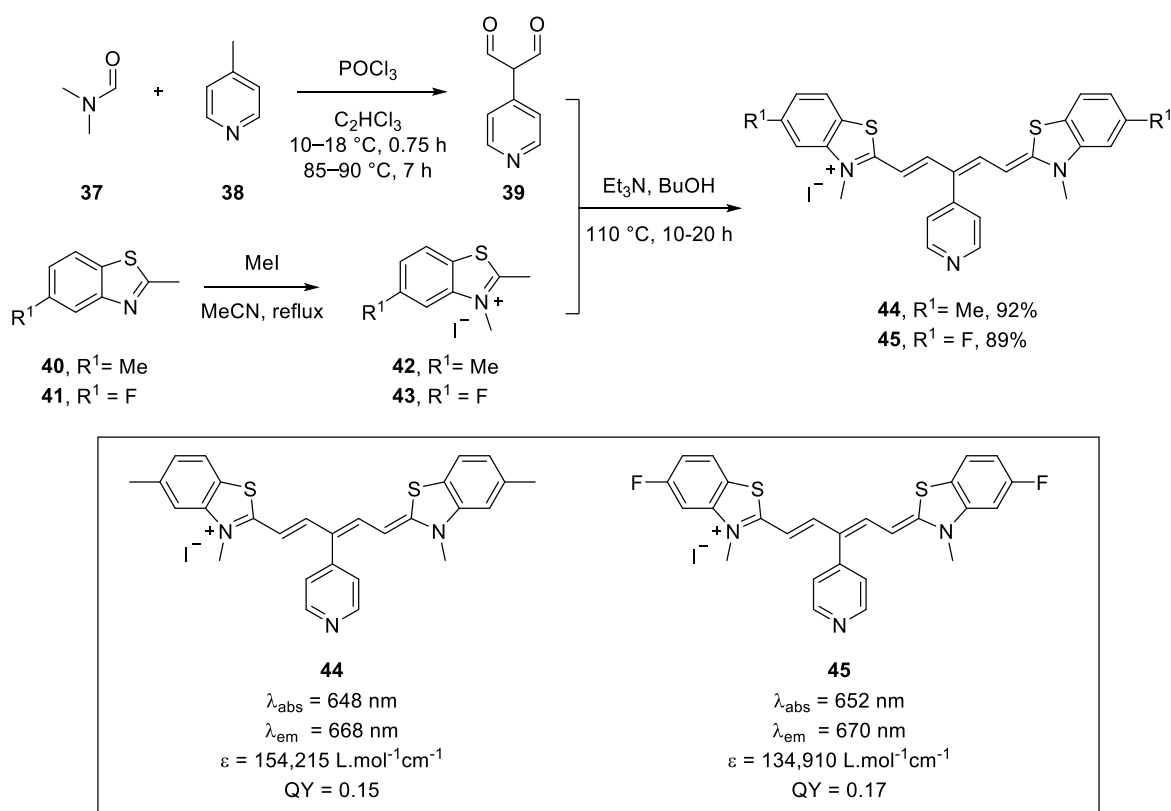


Figure 8: Chemical structures of commonly used cyanine dyes

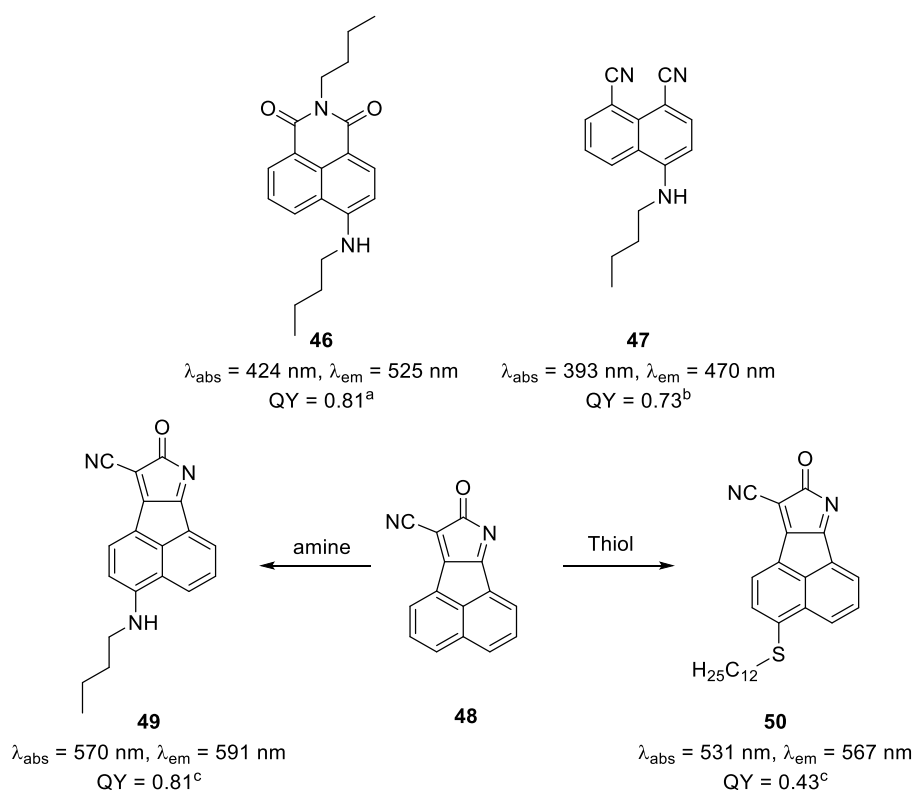
Cyanine dyes are used in diverse applications, including as pH-responsive probes.⁶³ In one instance, benzothiazole-derived pentamethine cyanine dyes were synthesised in three separate steps (**Scheme 6**).⁶⁴ The initial step involved the synthesis of the substituted pentamethine bridge. This was achieved using a Vilsmeier-Haack reaction by treatment of 4-methylpyridine **38** with DMF **37** and phosphorus oxychloride in trichloroethylene, yielding dialdehyde intermediate **39**. The second step was *N*-alkylation of benzothiazoles **40** and **41** using methyl iodide. The final step involved reaction of dialdehyde intermediate **39** with benzothiazolium salts **42** and **43**, forming cyanine dyes **44** and **45**. These dyes feature a pyridine moiety at the *meso*-position of the methine chain and are obtained with a reaction yield of 92 and 89%, respectively.⁶⁴ These types of structures give compounds with red-shifted absorption and emission properties and very large molar attenuation coefficients.



Scheme 6: Synthesis of benzothiazole *meso*-pyridine substituted carbocyanine dyes **44** and **45**.⁶⁴

1.3.6 Other Fluorogenic Scaffolds

Derivatives of polycyclic aromatic compounds represent a widely used subset of fluorescent dyes. Among them, a classic category of synthetic biomolecule labels, utilises the naphthalene-based intramolecular charge transfer (ICT) system. Zhu and co-workers have made significant advances in developing novel ICT fluorophores using a naphthalene-based fluorophore as a starting point.⁶⁵ They replaced the bisimide moiety **46** with stronger electron-withdrawing groups through oxidative S_NArH (nucleophilic substitutions of aromatic hydrogen) reactions of the non-fluorescent precursor **48**. This strategic approach allowed for the direct introduction of various electron-donor moieties at the 4-position, generating strong ICT fluorophores. The two new fluorophores, 4-amino-1,8-dicyanonaphthalene (**47**) and 8-oxo-8*H*-acenaphtho[1,2-*b*]pyrrol-9-carbonitriles (**49** and **50**) have been developed through this convenient procedure (**Scheme 7**).^{66,67} The former emits intense blue light and has been employed in the development of sensors for pH and transition metal ions.⁶⁷ The latter class of fluorophore exhibits tuneable fluorescence properties, offering exciting possibilities for various applications.⁶⁶



Scheme 7: The structures of naphthalene-based push-pull fluorophores (^ain ethanol, ^bin dichloromethane and ^cin chloroform).⁶⁵

Other polycyclic aromatic molecules are also sometimes used to construct useful fluorescent tools. Anthracene has been elaborated to prepare fluorescent sensors incorporating aliphatic or aromatic thiourea moieties (**Figure 9**).^{68,69}

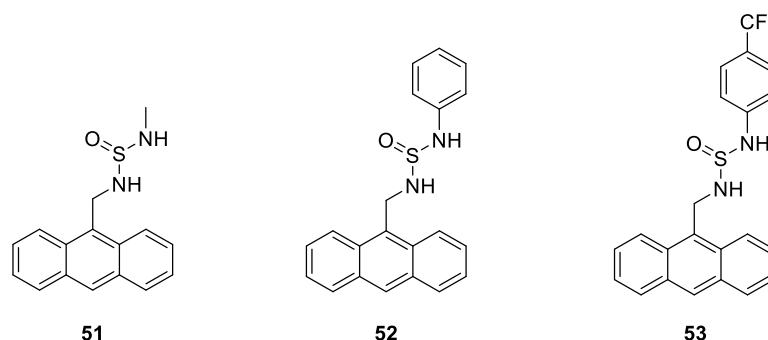


Figure 9: Anthracene PET chemosensors.⁶⁹

Pyrene and their derivatives constitute another intriguing class of fluorophores that exhibit high fluorescence quantum yield, long lifetimes of excited singlet and environment-responsive emission. For example, 8-hydroxypyrene-1,3,6-trisulfonic acid (HPTS) **54a**, a highly water-soluble dye compound, has been used for the measurement of cytoplasmic pH (**Figure 10**).^{70,71}

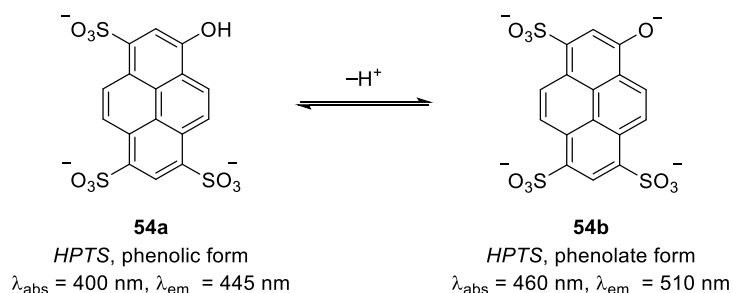


Figure 10: The structures of pyrene-based fluorophores probes.

As a result, most of the fluorophore research has concentrated on a select group of key molecular structures, including BODIPY, coumarin, fluorescein, rhodamine, and cyanine. Nevertheless, numerous current probes face challenges like cell toxicity, limited permeability, low water solubility, and sub-par sensitivity.⁷² Consequently, there is a growing demand for small fluorescent dyes that can be easily prepared and, that have increased brightness, and enhanced photostability, enabling biological insights without relying on genetic engineering.⁷³

1.4 Fluorescent α -Amino Acids

1.4.1 Naturally Occurring Fluorescent Amino Acids⁷⁴

For biological imaging, the available fluorophores include fluorescent proteins, organic fluorescent dyes, fluorescent nano-sensors, quantum dots, fluorescent transition metal complexes and fluorescent amino acids. Among them, fluorescent amino acids are particularly suitable for applications where the fluorophore size needs to be minimised or the chemical structure needs to be similar to the native amino acid it replaces due to concerns of structural or physicochemical changes. Among the 20 genetically encoded amino acids, phenylalanine, tyrosine, and tryptophan are particularly notable due to their aromatic side chains, which confer favourable spectroscopic characteristics.⁷⁵ These amino acids can serve as intrinsic or "built-in" fluorescent probes within proteins and peptides.⁷⁶ When excited by light of specific wavelengths, they undergo π - π^* transitions within their aromatic rings, leading to the emission of fluorescence (**Table 1**).

Table 1: Spectroscopic Properties of Emissive Proteinogenic Amino Acids^{77,78}

Compounds	Lifetime (τ , ns)	Absorptivity (ϵ)	Wavelengths		Quantum yield ⁷⁴ (Φ_F)
			λ_{abs} (nm)	λ_{em} (nm)	
L-Tryptophan (Trp)	3.1	5600	280	348	0.20
L-Tyrosine (Tyr)	3.6	1400	274	310	0.14
L-Phenylalanine (Phe)	6.4	200	257	282	0.01-0.4

Tryptophan is the most fluorescent of the three aromatic amino acids. It contains an indole ring in its side chain, which can absorb ultraviolet light to undergo a π - π^* transition, resulting in strong fluorescence emission upon excitation. Tryptophan serves as a natural fluorescence probe for monitoring protein conformational changes, ligand binding, and protein-protein interactions. The fluorescence spectrum of tryptophan can change due to multiple factors, including electron transfer processes, conformational transitions, conjugation of substituents, substrate binding, or denaturation of the tryptophan residue. These changes are often indicative of alterations in the local environment around the indole group.⁷⁹

Tyrosine contains a phenolic hydroxyl group in its side chain, and its fluorescence properties are related to its phenol chromophore, which has the ability to absorb ultraviolet light and generate a $\pi\text{-}\pi^*$ transition to the excited state.⁸⁰ This hydroxyl group enhances its fluorescence properties compared to phenylalanine. The fluorescence of tyrosine is sensitive to its local environment.⁷⁵ Changes in factors such as polarity and pH can influence its fluorescence properties. Strategically placing tyrosine residues within a biomolecule provides additional information that can monitor changes in the local environment, protein folding, ligand binding, and protein-protein interactions.

Phenylalanine contains a phenyl ring in its side chain. It can exhibit fluorescence, especially in a hydrophobic environment.⁸¹ However, its fluorescence intensity is relatively weak compared to tyrosine and tryptophan. The fluorescence properties of phenylalanine can be influenced by intramolecular charge transfer phenomena. This occurs when the molecule contains groups capable of either donating or accepting electrons, leading to changes in its optical and spectroscopic properties. Despite these attributes, there are a number of issues using naturally occurring proteinogenic α -amino acids from fluorescent imaging of proteins. They can be found at multiple sites and in diverse environments within a protein, making their analysis complex and challenging. To overcome these limitations, substantial research efforts have been directed towards the discovery and development of small, unnatural α -amino acids that can provide enhanced and more versatile fluorescence properties for various applications.⁸²⁻⁸⁴

Designing specialised fluorescent probes with precise excitation and emission wavelengths is often a necessity, particularly when aiming to minimise interference from naturally occurring emissive substances within cells. Ideally, these probes should closely mimic their natural counterparts in terms of size and shape. However, this goal can be challenging to achieve because any modification aimed at changing a molecule's electronic properties, often through the introduction of aromatic residues or extending conjugation, can also impact its steric bulk and, subsequently, its interactions with its surrounding environment. Considering these challenges, there has been a growing interest in the development of small unnatural α -amino acids with distinctive optical characteristics, including environmental sensitivity, responsiveness to metal chelation, and the ability to fine-tune fluorescence emission and lifetime (**Figure 11**).

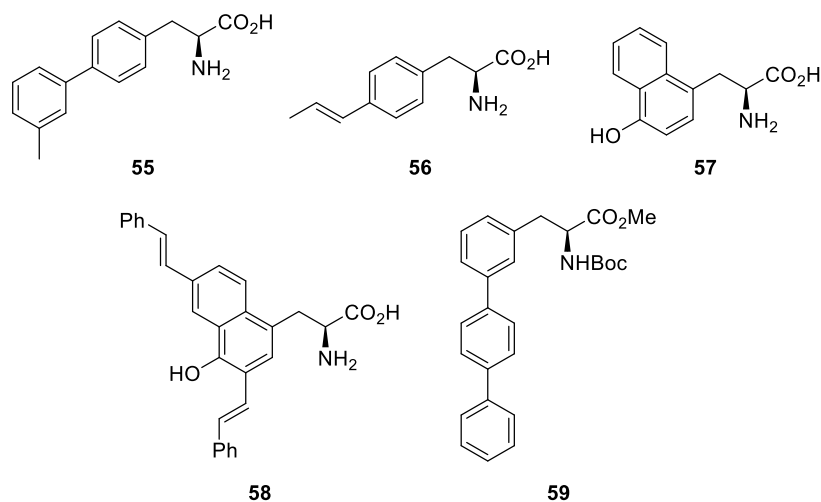
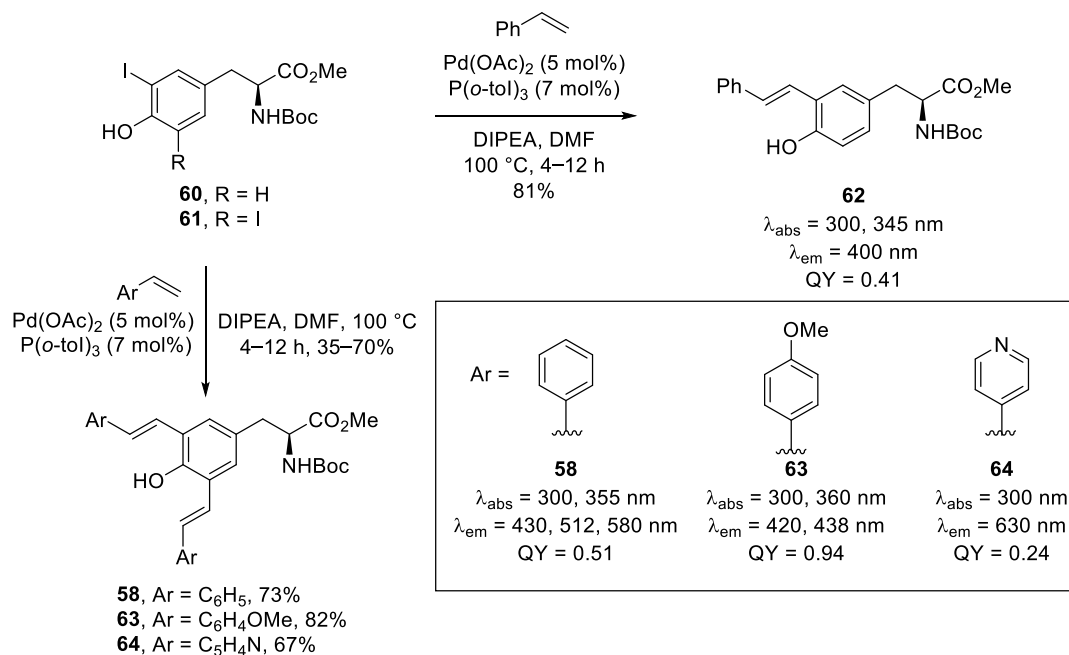


Figure 11: Selected fluorescent unnatural α -amino acids.⁸²⁻⁸⁵

1.4.2 Synthesis of Novel Fluorescent Amino Acids

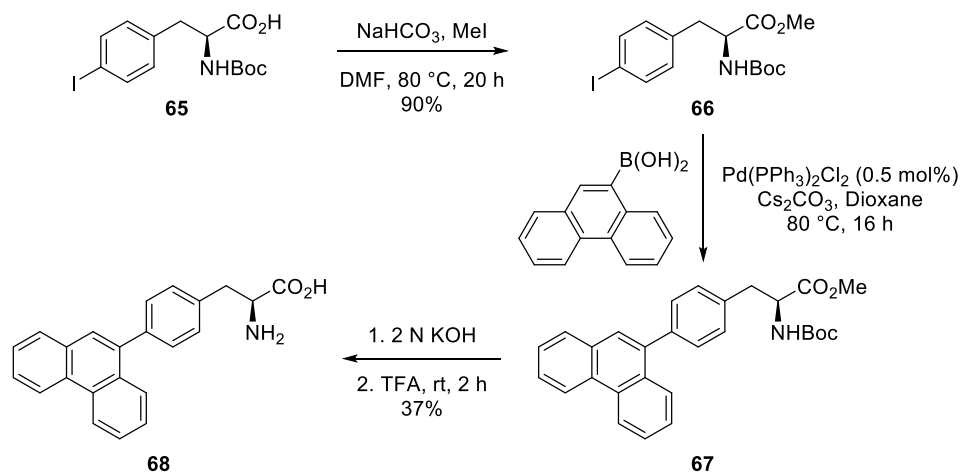
A number of small-molecule fluorescent α -amino acids have been developed through structure modifications aimed at fine-tuning their optical properties. For example, using tyrosine as the core structure, Wang and co-workers investigated improving the optical properties by extending the conjugation (**Scheme 8**).⁸⁵ The *mono*-styryl-L-tyrosine analogue **62** was synthesised using palladium-catalysed Heck coupling reactions. The Boc-protected 3-iodo-L-tyrosine **60** was reacted with styrene in the presence of palladium acetate (5 mol%), allowing incorporation of a *meta*-phenylenevinylene moiety in good yield. In addition, compounds such as the bis-styryl analogues **58**, **63** and **64** were prepared using a method analogous to this approach. A palladium-catalysed double Heck coupling reaction involving α -3,5-diiodo-L-tyrosine derivative with various styrene derivatives gave di-substituted tyrosines with enhanced properties, particularly the *p*-methoxyphenyl analogue **64**, which showed a large Stokes shift and a quantum yield of 0.94.



Scheme 8: Fluorescent unnatural amino acids derived from tyrosine by extending the π -conjugation of the aromatic side chain (properties determined in DMSO).

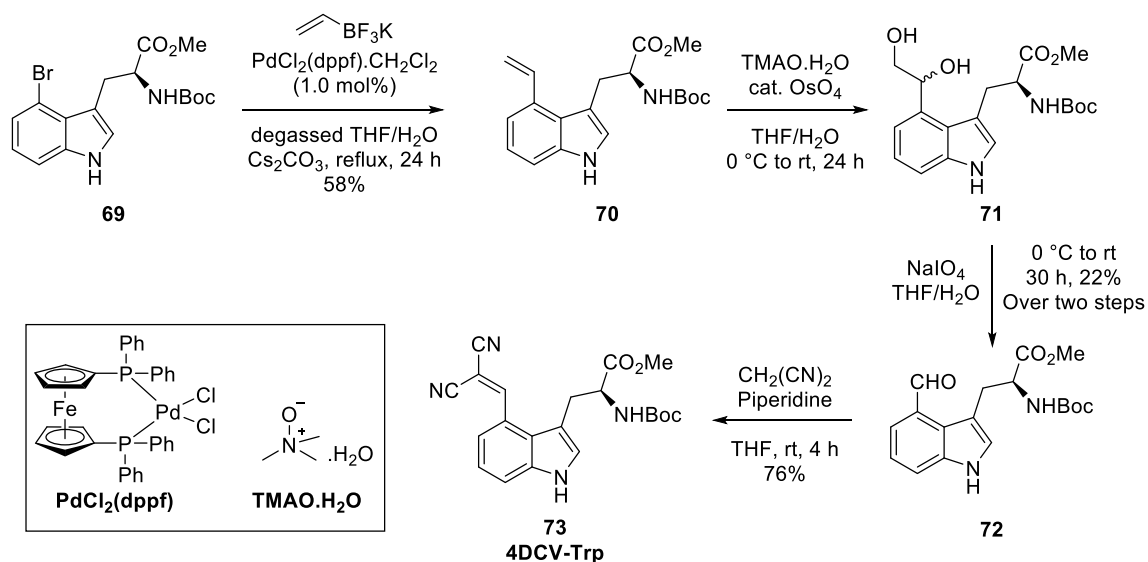
Additionally, incorporation of bis-styryl analogue **63** into a cell-penetrating peptide followed by successful imaging of two different cell lines showed the potential utility of these compounds as intrinsic labels for fluorescent imaging of cells.

A notable study by Gue and coworkers introduced encoded fluorescent α -amino acids that emit greenish-blue light, and have found widespread application in research.⁸⁶ The synthesis of these compounds started with commercially available *N*-(*tert*-butoxycarbonyl)-4-iodo-L-phenylalanine **65**. Following esterification, the key step involved the Suzuki–Miyaura cross-coupling reaction of α -amino acid **66** with polyaromatic boronic acids, which led to the formation *N*-4-(9-phenanthracenyl)-L-phenylalanine methyl ester intermediate **67**.⁸⁷ Removal of methyl and Boc protecting groups under mild conditions gave 4-phenanthracen-9-yl-L-phenylalanine **68**, emitting greenish-blue fluorescence. α -Amino acid **68** exhibited strong fluorescence with an excellent quantum yield of 75% and was used to image live cells at 405 nm.



Scheme 9: Synthesis of α -amino acid **68**.

Using the indole ring of tryptophan as the core motif, Gai and co-workers developed fluorescent amino acids with 4-substituted indoles that emit in the visible region (**Scheme 10**).⁸⁸ The new tryptophan derivatives were synthesised by the introduction of a dicyano-alkene motif to the indole chromophore of tryptophan. This approach was favoured because the electron-withdrawing nitrile group has a charge transfer interaction with the indole chromophore, resulting in a redshift of the spectroscopic properties. Furthermore, the relatively small size of the nitrile group minimally perturbs the protein structure, making it an attractive choice for labelling and studying proteins. 4DCV-Trp **73** was synthesised in four steps from enantioenriched 4-bromotryptophan **69**. Suzuki cross-coupling between **69** and potassium vinyl trifluoroborate (vinylBF₃K) was performed to install the vinyl group, giving intermediate **70** in 58% yield. A modified, two-step Lemieux-Johnson oxidative cleavage of alkene **70** delivered 4-formyltryptophan **72** in low yield (22% over two steps). Lastly, piperidine-catalysed Knoevenagel condensation between aldehyde **72** and malononitrile, CH₂(CN)₂ gave desired 4DCV-Trp **73** in 76% yield.⁸⁸

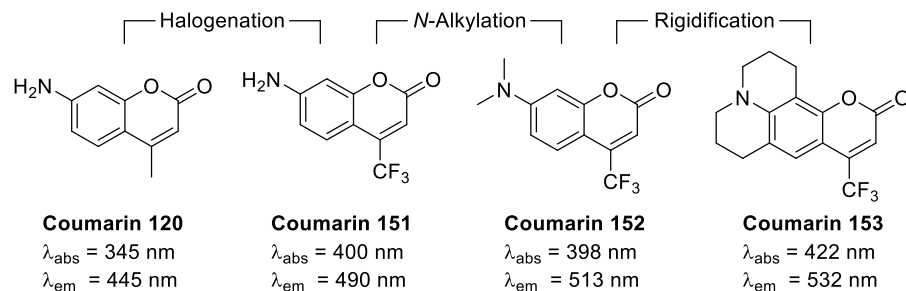


Scheme 10: Synthesis of *N*-Boc-4-DCV-Trp-OMe **73**.

4DCV-Trp is a valuable yellow fluorescence unnatural amino acid widely employed in biological spectroscopy and microscopy. It possesses a maximum absorption wavelength of 430 nm and a Stokes shift of 150 nm in water.⁸⁸ These characteristics make it useful for the design of new fluorescent compounds that can be used for studying biological systems using optical imaging.

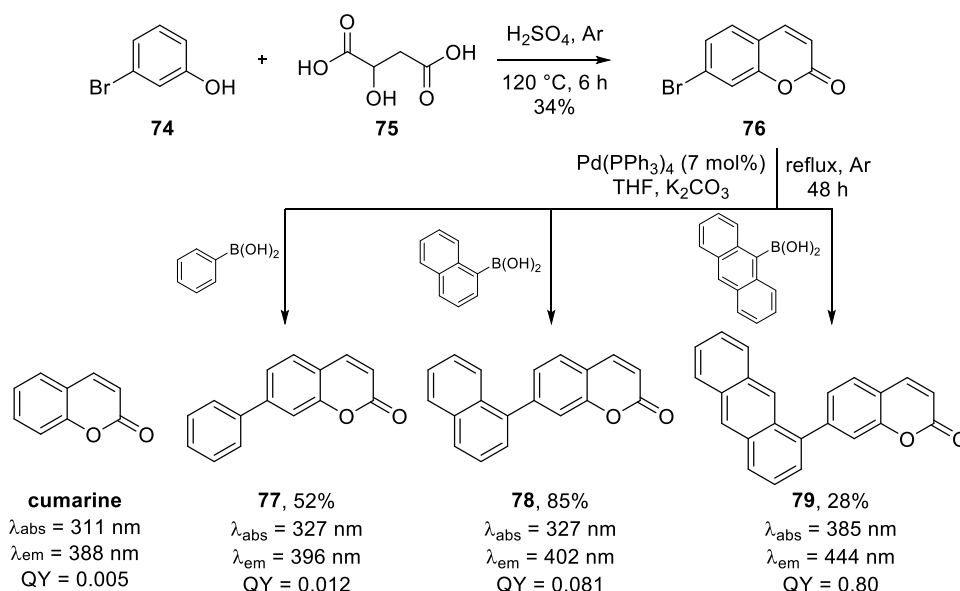
1.4.3 General methods to improve small-molecule fluorophores.

To enhance the photoluminescence properties of fluorophores, several strategies have been explored. Many fluorophores are easily tuneable through functional group transformations, extending conjugation through aryl group additions, or fusing rings together to increase rigidity. This allows for bathochromic shifts to take place with regards to absorption and emission, allowing fluorescence to occur in the green and red areas of the visible spectrum. Structural modifications for many classic fluorophore labels can finely tune and improve fluorescent properties, such as for the coumarin motif. This approach includes the addition of halogen substituents, *N*-alkylation, rigidification, and sulfonation (**Scheme 11**).⁴¹



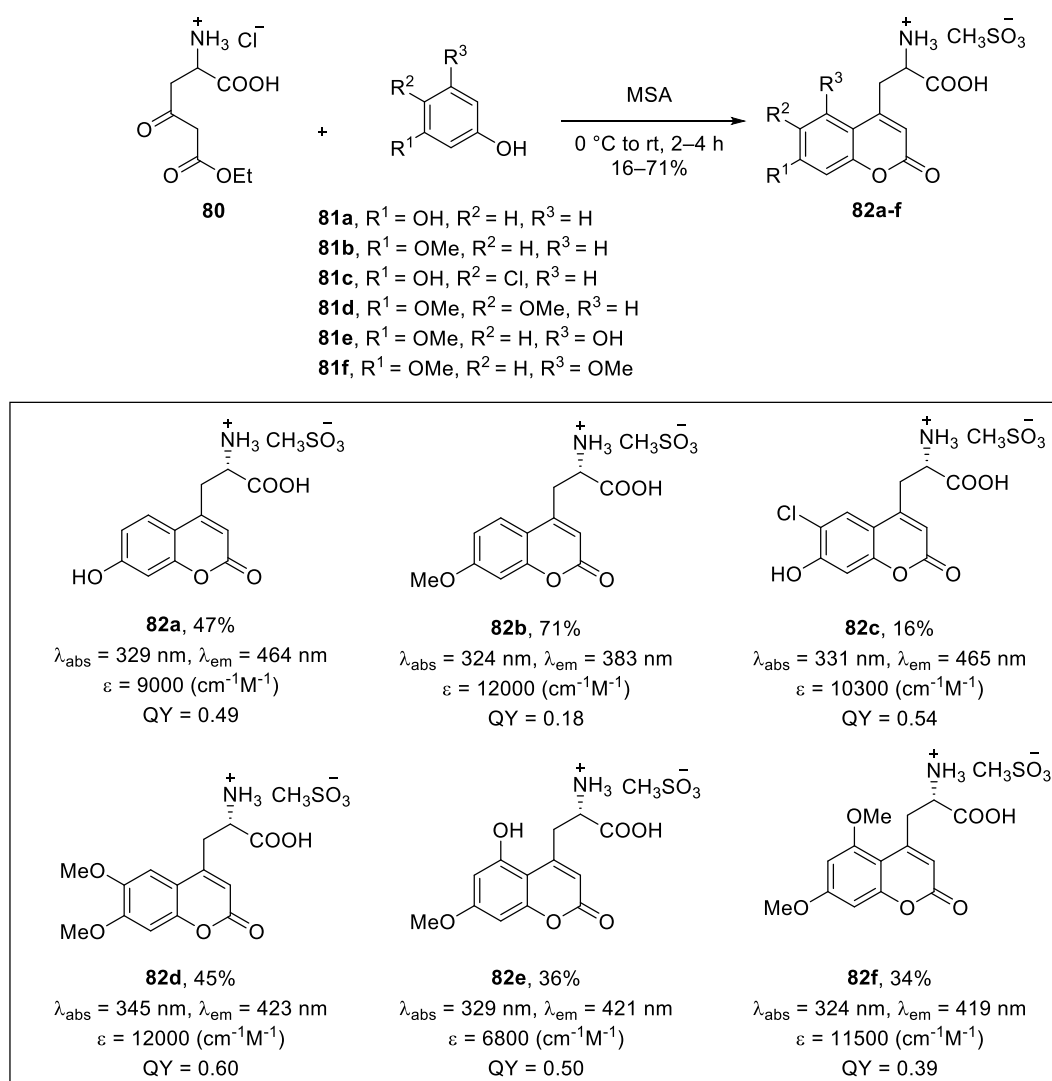
Scheme 11: Structural modifications for the coumarin chromophore.

As well as the modifications described above, simply extending the conjugation of a chromophore, particularly to create a charge transfer system is a useful approach to improve the properties. For example, coumarin analogues with extended conjugation have been prepared by the incorporation of an aryl substituent, such as phenyl, 1-naphthyl, and 9-anthryl moieties (**Scheme 12**).⁸⁹ Aromatic hydrocarbons with extended p-conjugation can donate electrons to the electron-deficient coumarin upon photoexcitation, promoting an intramolecular charge-transfer (ICT) transition. The $n-\pi^*$ transition state was destabilised, and an ICT state was generated, revealing redshifted absorption and emission and improved quantum fluorescence yields compared to the simple bicyclic compounds.



Scheme 12: Syntheses and fluorescence properties of the coumarin compounds (10 μM in cyclohexane).

Incorporation of substituents to the coumarin motif to generate charge transfer chromophores have been utilised for the preparation of fluorescent amino acids. Garbay and colleagues used the von Pechmann reaction, as the key step for the preparation of coumaryl amino acids.⁹⁰ This reaction involved condensation of a phenol with a β -ketoester-derived amino acid, (*S*)- or (*R*)-**80**, under acidic conditions (**Scheme 13**). The use of methanesulfonic acid (MSA) allowed the synthesis of a wide range of structurally diverse coumaryl amino acids **82a–f** with red-shifted absorption and emission properties, strong molar attenuation coefficients and higher quantum yields, relative to proteinogenic amino acids.



Scheme 13: Synthesis of aspartic acid derived coumaryl amino acids **82a–f** (determined in 95% ethanol).

To investigate the potential utility of coumaryl amino acids in biological studies, peptides containing specifically compound **82a** was synthesised by solid-phase

peptide synthesis (SPPS). This was incorporated at the N-terminus of penetratin. After incubation of this peptide in HeLa cells, its internalisation was visualised using confocal microscopy, thus demonstrating the practical use of coumaryl amino acids as intrinsic fluorescent labels in biological research.

As previously mentioned, it is preferable for fluorophores to have red-shifted absorption and emission wavelengths for imaging. An excellent approach to achieve this is through the use of push-pull electronic systems.⁹¹ An example of optical tuning in push-pull molecules is demonstrated by varying the donor groups (D) such as within the 2,2'-bithiophene scaffold **83a–d**, diphenylacetylenes **84a–d** and 2,6-di-*tert*-butylindoanilines **85a–d** (Figure 12 and Table 2).⁹²⁻⁹⁵

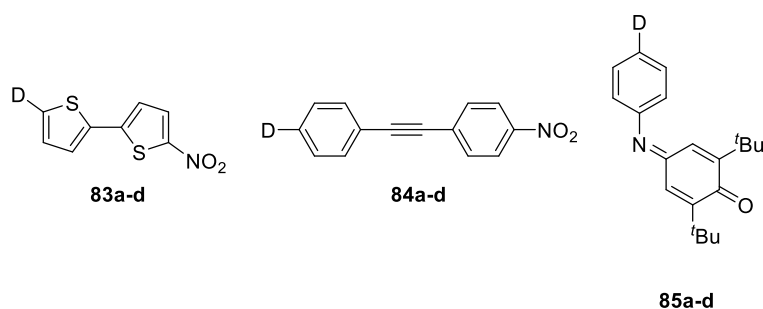


Figure 12: Push-pull 2,2'-bithiophenes **83a–d**, diphenylacetylenes **84a–d** and 2,6-di-*tert*-butylindoanilines **85a–d**.

Table 2: Push–pull molecules **83–85** properties.

Compounds	D	λ_{\max} (nm)
83a	H	375
83b	MeN	408
83c	MeS	391
83d	Me ₂ N	466
84a	MeO	347
84b	MeS	358
84c	H ₂ N	379
84d	MeHN	400
85a	H	428
85b	Br	432
85c	MeS	476
85d	Me ₂ N	558

^a Measured in *n*-hexane, ^b Measured in chloroform.

As can be seen from Table 2, the most red-shifted emission is observed for push-pull systems where the dimethylamino group has been used as the electron-rich component. Based on these results, this approach has been used very effectively for charge-transfer emissive α -amino acids (**Figure 13**). These amino acids all incorporate dimethylamino moieties as the push component, which are conjugated through aromatic systems to the pull component, a ketone or amide group.^{96,97} These α -amino acids, such as aminonaphthyl **87** and aminophthalimides **88** and **89** have been developed as environmentally sensitive probes for various biological processes. Under photoexcitation, charge transfer from the electron donor (D) to the electron acceptor (A) occurs, making them valuable for biological applications.⁹¹

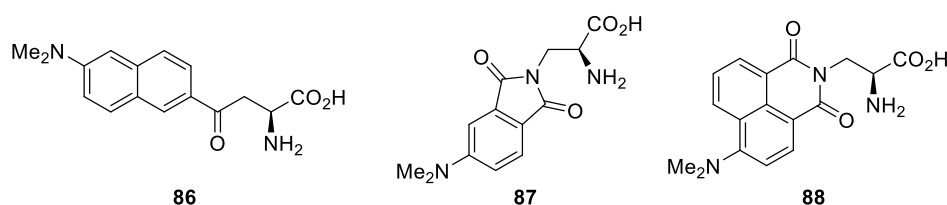
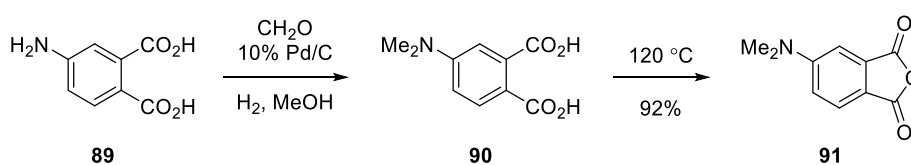


Figure 13: Aminonaphthyl and aminophthalimide-type α -amino acids.

Several syntheses and subsequent biological studies have been conducted with α -amino acids derived from aminophthalimide and aminonaphthyl due to their distinctive functionality. For example, the synthesis of aminophthalimide has been achieved and successfully incorporated into peptides. The key step involved the preparation of the intermediate 4-(*N,N*-dimethylamino)phthalic anhydride **91** (**Scheme 14**).⁹⁸ The synthetic procedure involved the reductive amination of 4-aminophthalic acid **89** with formalin, hydrogen and Pd/C. This gave the desired 4-(*N,N*-dimethylamino)phthalic acid **90**. Subsequently, dehydration of the diacid **90** under reduced pressure afforded the desired anhydride **91** in excellent yield.



Scheme 14: Synthesis of 4-(*N,N*-dimethylamino)phthalic anhydride **91**.⁹⁸

Utilising 4-(dimethylamino)phthalic anhydride **91** as a key intermediate, the synthesis of 4-(dimethylamino)phthalimide **92**, the phthalimide precursor for environment-sensitive fluorophores was achieved (**Figure 14**).^{98,99} 4-(Dimethylamino)phthalimide **93** exhibits convenient excitation and maximum emission wavelengths suitable for biological applications, and is comparable in size to the side-chains of natural amino acids, tyrosine or tryptophan. Consequently, this residue is less disruptive to specific native interactions compared to current environment-sensitive fluorophores. The 4-(dimethylamino)phthalimide fluorophore has been incorporated into amino acids (e.g. **93**), allowing for the monitoring of phosphorylation-dependent peptide binding to proteins and the investigation of protein–protein interactions.

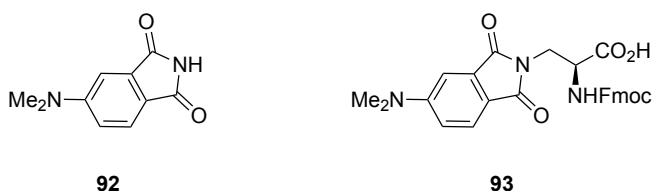
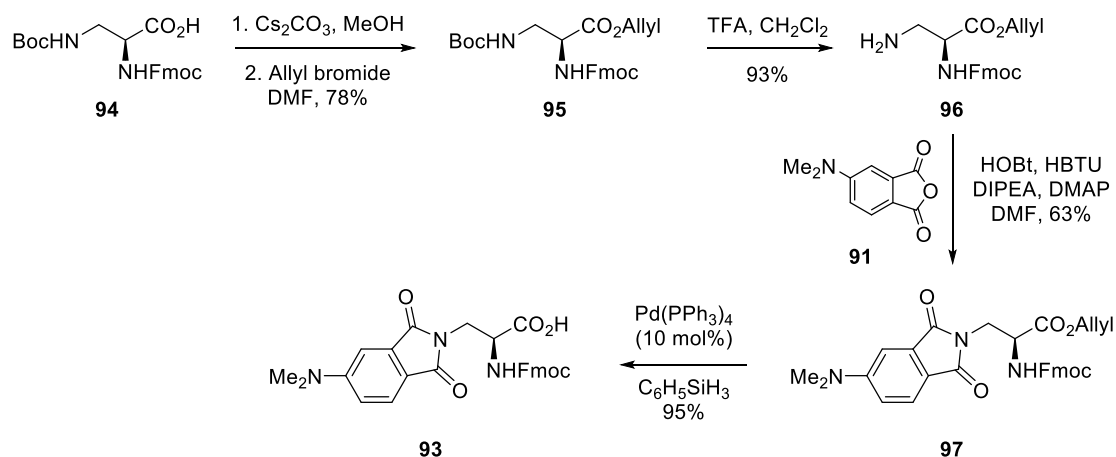


Figure 14: Structures of 4-(dimethylamino)phthalimide **92** and Fmoc-Protected-4-aminophthalimide-derived α -amino acid **93**.

The synthesis of Fmoc-protected-4-aminophthalimide-derived α -amino acid **93** is shown in **Scheme 15**.⁹⁸ Starting with 3-aminoalanine derivative **94**, the carboxylic acid group was protected to yield allyl ester **95**. Upon treatment with TFA and removal of the Boc-group, this produced amine **96**. Amine **96** was then coupled with the intermediate, 4-(*N,N*-dimethylamino)phthalic anhydride **91** using HBTU and HOBT under basic conditions. This gave phthalimide **97** in 63% yield. Subsequent removal of the allyl ester group with Pd(PPh₃)₄ and phenylsilane yielded *N*-Fmoc-4-aminophthalimide-derived α -amino acid **93**. This methodology provides a versatile route for preparing α -amino acids incorporating 4-aminophthalimide, demonstrating potential applications in fluorescence studies.



Scheme 15: Synthesis of 4-dimethylaminophthalimide-derived α -amino acid **93**.⁹⁸

The dimethylaminophthalimide α -amino acid **93**, when incorporated into peptide-based ligands through standard SPPS protocols, proved to be an excellent reporter for binding with 14-3-3 proteins. These proteins play a crucial role in phosphoserine-dependent signalling and are essential for cell signal regulation.⁹⁸ Upon the addition of the protein to a solution of 14-3-3bp-DAPA (**Figure 15**), a significant increase in fluorescence emission intensity is observed. The fluorescence emission intensity at 510 nm becomes six times more intense when the peptide is complexed with 14-3-3 than in the absence of protein. Additionally, the maximum emission intensity undergoes a shift of about 40 nm (from 570 to 531 nm). This shift highlights the high sensitivity of the 4-DMAP side chain to changes in the surrounding environment. It should be noted that this new building block can be incorporated into peptides using Fmoc-based SPPS without requiring any modification of the standard protocols.

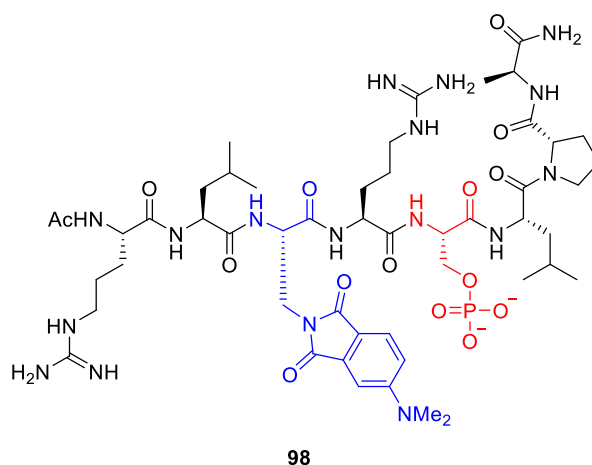
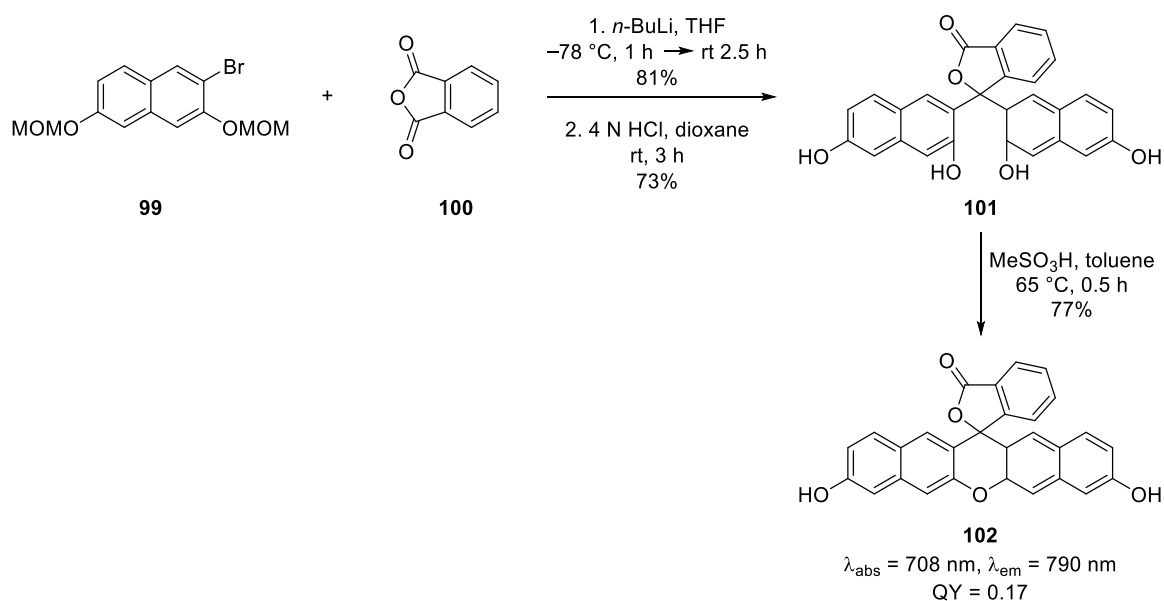


Figure 15: Fluorescently labelled phosphopeptide 14-3-3bp-DAPA **98**.⁹⁸

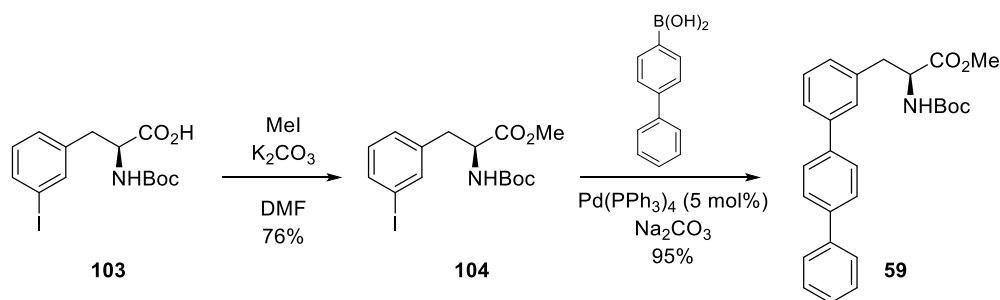
Significantly extending the conjugation of a fluorophore is one method to greatly increase absorption and fluorescence emission maxima. This can be exemplified by tuning the fluorescent properties of fluorescein through structural modifications (**Scheme 15**).¹⁰⁰ The synthetic route to naphthofluorescein involved Friedel–Crafts reactions between arylbenzoic acids and dihydroxynaphthalenes. Initially, the methoxymethyl (MOM)-protected bromonaphthalene **100** was subjected to reaction with *n*-BuLi and phthalic anhydride, resulting in the formation of the phenolic MOM protected compound with an 81% yield. The MOM protecting groups were subsequently removed using 4 N HCl in dioxane, providing compound **101** in a 73% yield. Intramolecular dehydration, carried out under acidic conditions, facilitated the fusion of the benzene rings leading to the formation of naphthofluorescein **102**. This derivative displayed a bathochromic shift with absorption maxima at 708 nm and emission maxima at 790 nm, exhibiting a high absorption coefficient (ϵ) of $5.6 \times 10^4 \text{ M}^{-1} \text{ cm}^{-1}$, and a quantum yield (Φ) of 0.17. Its capacity to emit fluorescent light in the NIR region positions it as a potential NIR fluorescent probe.



Scheme 16: Synthesis of naphthofluorescein **102**¹⁰⁰

This approach of significantly extending conjugation has been used to improve the fluorescent properties of aryl-substituted amino acids. For example, the introduction of a biphenyl unit to *m*-iodophenylalanine derivative **104** via a Suzuki-Miyaura cross-coupling reaction, allowed the highly efficient synthesis of terphenyl amino acid **59** (**Scheme 16**). This gave an amino acid with excellent fluorescent properties and

was used as FRET pair with a coumarin amino acid within a mutase reductase enzyme.¹⁰¹



Scheme 17: Synthesis of fluorescent *para*-terphenyl α -amino acid **59**.¹⁰¹

1.5 Summary

Fluorescent unnatural amino acids are particularly suitable for applications where the fluorophore size needs to be minimised or the chemical structure needs to be similar to the native amino acid it replaces due to structural or physicochemical limitations. Over the years, the synthesis and biological application of fluorescent unnatural α -amino acids have expanded significantly, highlighting their importance in chemical, biological, and medicinal research. These novel fluorophores offer tunable optical properties with absorption and emission peaks in the visible to near-IR regions and high quantum yield values, making them highly desirable. Many of these fluorophores can be easily tuned through Pd functional group modifications, extending conjugation by adding aryl groups, or increasing rigidity by fusing rings. These strategies lead to bathochromic shifts in both absorption and fluorescence. A key synthetic strategy for the preparation of these unnatural amino acids involves starting with readily available chiral pool α -amino acids and then subjecting them to various synthetic transformations to construct novel fluorophores while retaining the α -amino acid throughout the synthesis. Several of these unnatural α -amino acids have been employed as substitutes for tyrosine, phenylalanine and tryptophan, allowing the introduction of a fluorescent tag into peptides and proteins with minimal disruption to their structure and conformation.

1.6 Overall Strategic aim of the PhD project

The overall strategic aim of this PhD was to develop efficient synthetic routes to access functional amino acids using ynone- or enone-derived amino acids. Expanding on prior research conducted within the Sutherland group, which explored the use of amino acids with unsaturated side-chains and their potential applications, this research aimed to advance the understanding and utilisation of these synthetic intermediates for new functional applications. The first aspect of the research aimed to employ amino acid-derived ynones for the synthesis of pyrimidine derivatives, which could serve as fluorescence probes in chemical biology applications. In particular, a strategic aim was to investigate the synthesis of the key pyrimidine ring by cycloaddition of amidines with ynones. A second key aim was to access fluorescent amino acids in relatively few steps. Amino acids with biaryl side-chains were targeted from a readily available tyrosine derivative, using a Suzuki-Miyaura cross-coupling reaction with nonaflates as a coupling partner. The final aim of this PhD was to develop a novel synthetic approach for the synthesis of biologically important *meso*-DAP and L,L-DAP amino acids, utilising enones as key intermediates. The focus of this project was to utilise the enone to install the second amino group via stereoselective reduction, followed by an Overman rearrangement. Through these investigations, the PhD aimed to not only expand synthetic methods for accessing diverse amino acid derivatives but to also explore their applications for various biochemical studies.

2.0 Results and Discussion

2.1 Aryl substituted pyrimidine derived α -amino acids.

2.1.1 Introduction

Unnatural amino acids represent an important class of compound and are valuable tools for studying various areas of research, including biophysics, spectroscopy, bio-orthogonal chemistry, peptide therapeutics, optical probes, protein labelling, mimetics and protein interaction mapping.¹⁰²⁻¹⁰⁵ They have been structurally modified to expand their functionality as they circumvent the limitations of traditional natural amino acids. Unnatural amino acids can be synthesised through chemical modifications of natural amino acids or related compounds. This can involve modifying the side-chain,¹⁰⁶⁻¹⁰⁸ cyclisation,^{109,110} or replacement within the amino acid backbone to introduce new functional groups.¹¹¹

In recent years, there has been increased interest in fluorescent amino acids, including proteinogenic amino acids such as L-phenylalanine, L-tyrosine and L-tryptophan (**Figure 16**).

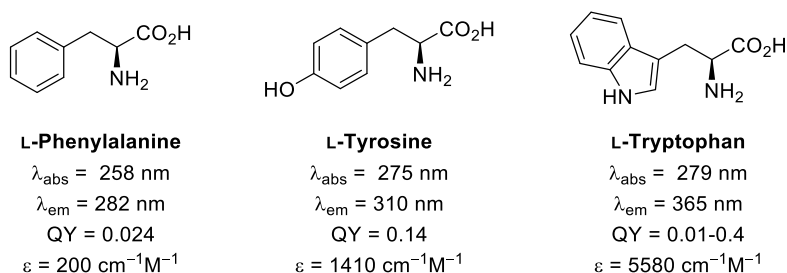


Figure 16: Fluorescent proteinogenic amino acids.

These three amino acids can exhibit fluorescence when incorporated into peptides with aromatic side-chains that can undergo electronic transitions upon excitation with light of specific wavelengths. The intrinsic fluorophores of naturally occurring proteinogenic α -amino acids undergo π - π^* excitation with light of a specific wavelength, resulting in fluorescence emission. While fluorophores derived from natural amino acids serve as useful tools for fluorescence-based assays, they do have certain limitations when applied in biological assays. One major drawback is that their excitation and emission wavelengths may not be optimal for specific applications. Moreover, the fluorescence properties of peptides rely on the presence of these fluorophores to enhance their own fluorescence characteristics, which can pose challenges in terms of compatibility with biological systems.

Due to these limitations, there has been significant interest in discovering fluorescent unnatural α -amino acids that can act as more effective probes for investigating biological systems. Due to their ability to be structurally modified in many ways and their versatile range of functions, the synthesis of modified unnatural α -amino acids, has been developed, including new fluorescent amino acids with side-chain or backbone chromophore systems, which have particular importance as biological probes.

2.1.2 Previous Work in the Sutherland Group.

One of the key objectives of the Sutherland group is the synthesis of unnatural amino acids that are structurally similar to natural amino acids, with enhanced or novel fluorescence properties. For example, benzotriazoles (**105–108**) (**Figure 17**) are similar to L-tryptophan, with an indole-like system in the same position. These compounds not only mimic natural amino acids but also possess an extended conjugated system, thereby enhancing their fluorescence properties.¹¹²⁻¹¹⁴

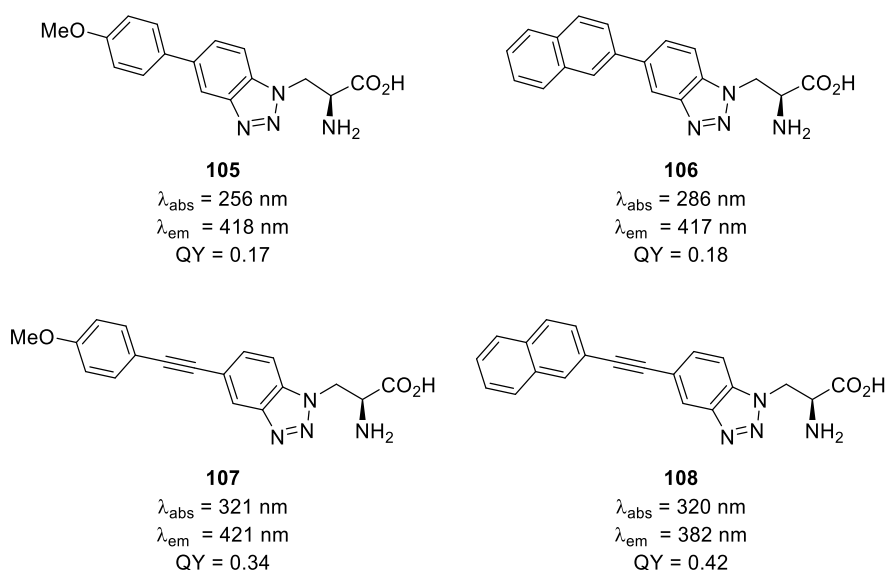
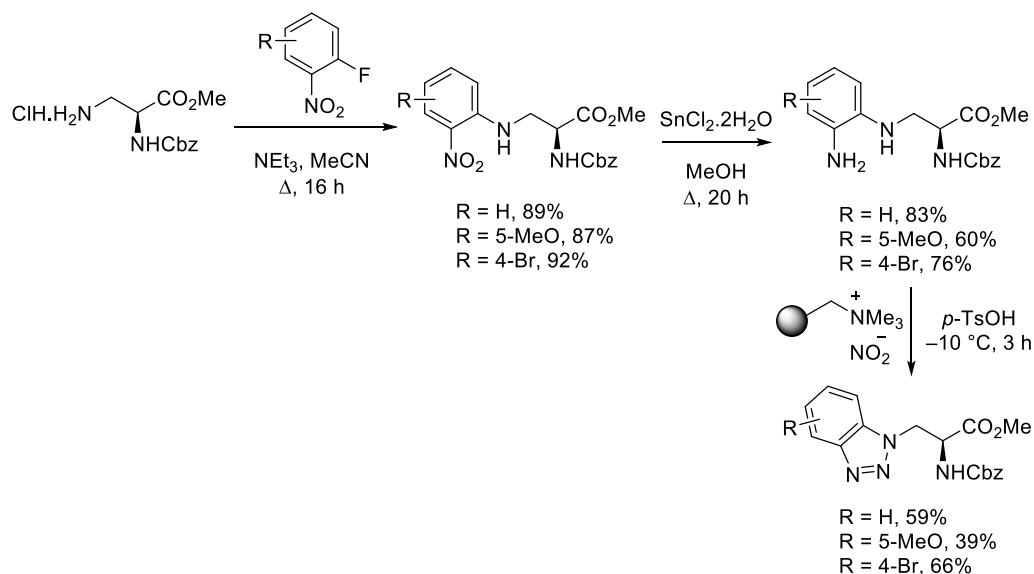


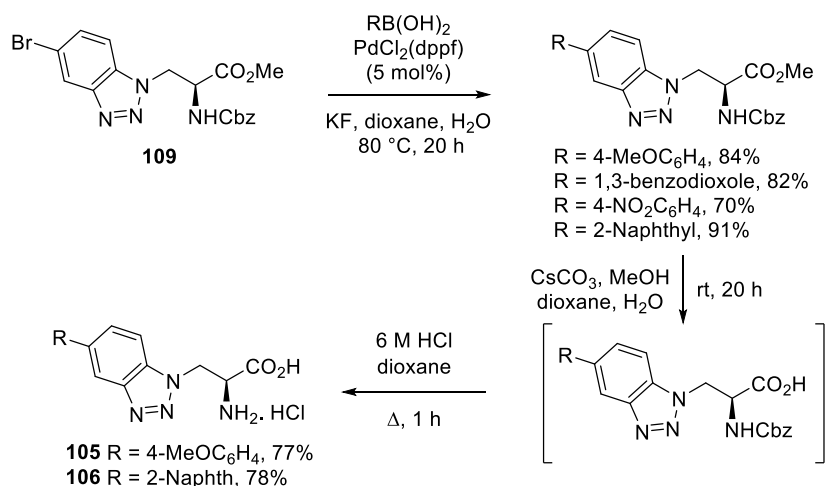
Figure 17: Previously synthesised fluorescent amino acids.

These benzotriazole-derived α -amino acids were easily prepared in relatively few steps using a 3-aminoalanine derivative as the starting material (**Scheme 18**).¹¹³⁻¹¹⁵ Nucleophilic aromatic substitution of the side-chain amino group with a 2-fluoronitrobenzenes was then followed by nitro group reduction. Subsequent one-pot diazotisation and cyclisation allowed access to the benzotriazole moiety.



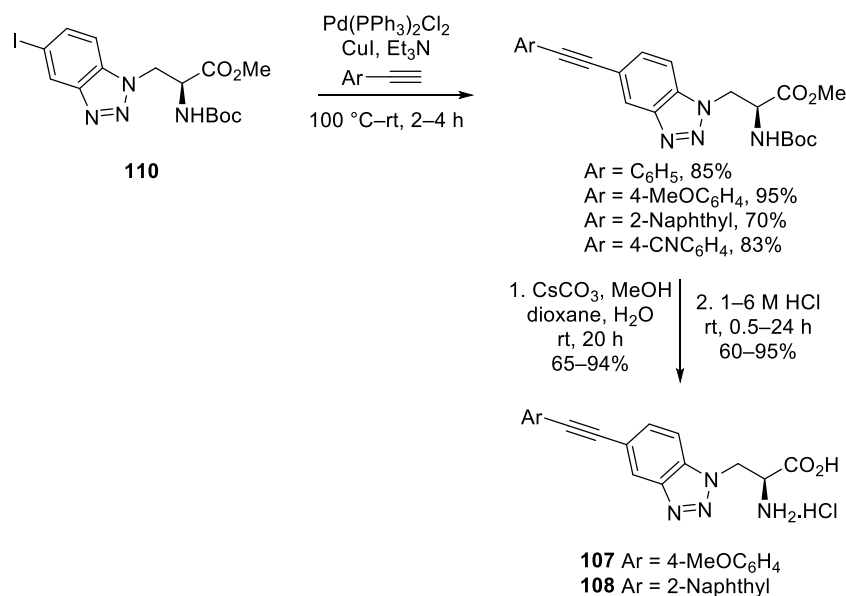
Scheme 18: Synthesis of benzotriazole derived α -amino acids.

As well as benzotriazoles with various substituents, this approach allowed the synthesis of bromide analogue **109**, which was found to be an excellent coupling partner and was utilised for the preparation of a series of benzotriazole-derived α -amino acids with more conjugated side-chains.¹¹⁴ The initial series was prepared via a Suzuki-Miyaura cross-coupling reactions with various aryl boronic acids, resulting in the formation of biaryl products in yields of 60–91% (**Scheme 19**). The electron-rich, *p*-methoxyphenyl substituted benzotriazole **105** showed strong fluorescence with emission maxima in the visible region (418 nm) and was one of the brightest α -amino acid among this series. 2-Naphthyl-substituted benzotriazole **106** also displayed red shifted emission maxima (417 nm) and a good quantum yield (18%).



Scheme 19: Synthesis of 5-aryl benzotriazole-derived α -amino acids.

A challenge that arose from this work was that the absorption bands of these biaryl analogues closely resembled those of natural amino acids such as L-tryptophan and L-tyrosine (250–300 nm). This similarity in absorption spectra can limit the ability to distinguish and selectively study the fluorescence properties of these unnatural amino acids in the presence of natural amino acids in biological systems. To overcome this limitation, other analogues were prepared with extended conjugation that were proposed to absorb at longer wavelengths. By introducing additional conjugation or charge transfer moieties, a molecule's electronic structure can be modified, resulting in a longer wavelength (red shift) that can be tuned to avoid overlap with the absorption of natural amino acid residues. To address the limitation of the biaryl compounds, a novel class of alkynyl benzotriazole-derived amino acids were prepared.¹¹⁵ Following the synthesis of an iodinated benzotriazole moiety in a similar manner as described above, the key step involved a Sonogashira cross-coupling reaction to introduce the extended side-chain (**Scheme 20**).

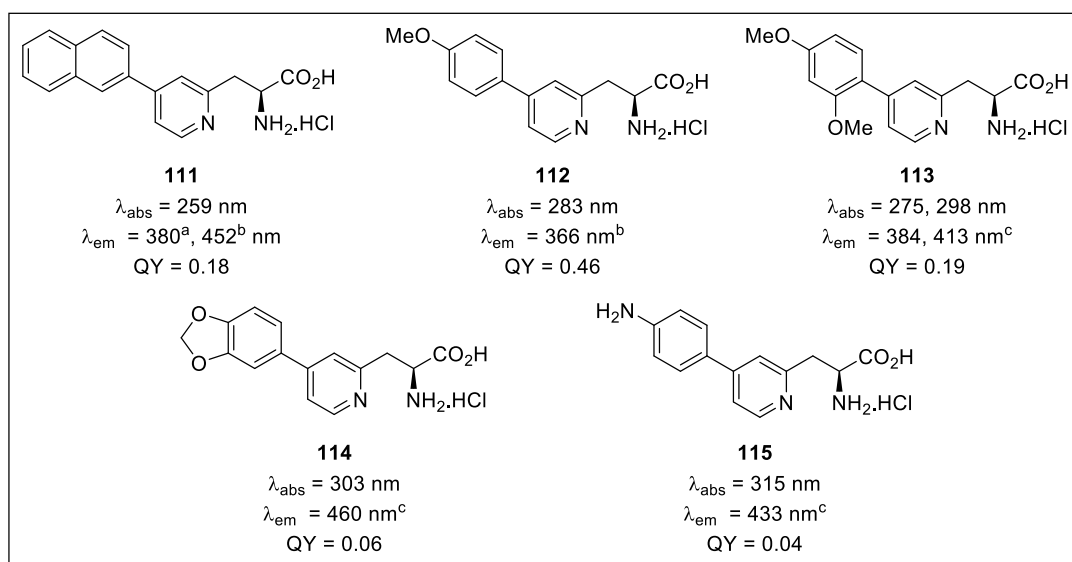
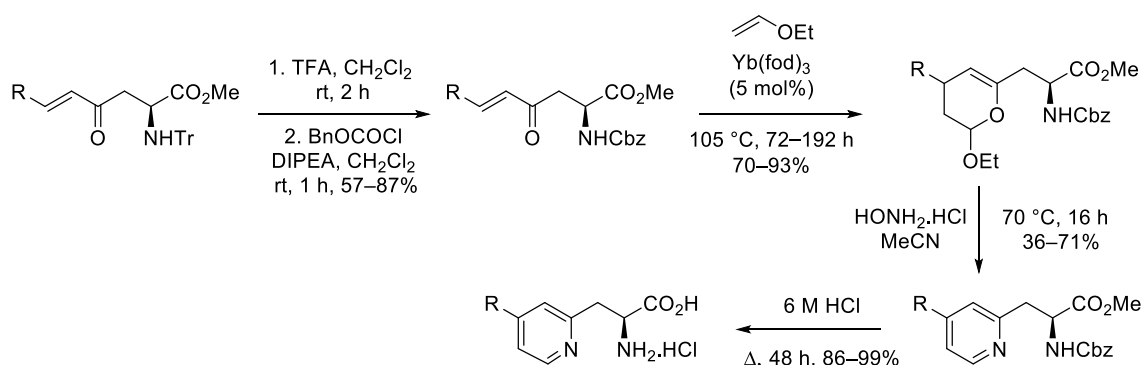


Scheme 20: Synthesis of alkynyl-fused benzotriazole-derived α -amino acids.

Alkynyl analogues *p*-methoxyphenyl **107** and naphthyl-substituted alkynyl-fused benzotriazoles **108** exhibited high quantum yields of 34% and 42%, respectively, and demonstrated strong brightness with red-shifted absorption and emission maxima.¹¹⁵ By extending the conjugated system of the benzotriazole analogues with different electron-rich arenes generated fluorescence amino acids with Mega Stokes shifts that are very different to natural amino acids such as tryptophan.

The development of conjugated fluorescent molecules with a small-sized chromophore has become one of the alternative approaches for developing fluorescent amino acids. Among these efforts, a novel class of β -pyridyl α -amino acids has been specifically investigated to study the influence of charge transfer effects on their fluorescence properties.¹¹³ These amino acids were synthesised by incorporating an electron-rich aryl group that interacts with an electron-withdrawing pyridine moiety, resulting in the formation of a charge transfer chromophore. The design and synthesis of these β -pyridyl α -amino acids aimed to exploit the electronic interactions between the aryl and pyridine groups. The synthesis of the β -pyridyl α -amino acids began with a Horner-Wadsworth-Emmons reaction of various aryl aldehydes and a β -ketophosphonate ester derivative of an amino acid. The resulting enone-derived α -amino acids were subsequently explored as substrates for the following pyridine-forming process, which involved a two-stage sequence of reactions. The first step involved a highly regioselective hetero-Diels Alder reaction of enones with ethyl vinyl ethers in the presence of the Lewis acid, $\text{Yb}(\text{fod})_3$ (5

mol%), which gave the dihydropyran as single regioisomers (**Scheme 21**).¹¹³ This was followed by a modified Knoevenagel-Stobbe reaction of the dihydropyrans with hydroxylamine hydrochloride to give the pyridine ring system in moderate to good yields. The pyridine-derived amino acids were then deprotected in one-step under acidic conditions.



Scheme 21: The synthesis of β -pyridyl- α -amino acids. Measured in MeOH at ^a $0.5 \times 10^{-5} \text{ M}$, ^b $1.0 \times 10^{-7} \text{ M}$ or ^c $1 \times 10^{-5} \text{ M}$.

As expected, pyridines with electron-rich substituents showed strong fluorescence properties with emission maxima from 366 to 460 nm with large Stoke shifts.¹¹³ Interestingly, naphthyl analogue **111** gave a red-shifted emission spectra at 452 nm and a Mega Stoke shift of 193 nm. *para*-Methoxypyridine **112** was of great interest because of its photophysical properties, with a large Stokes shift, the highest brightness ($11,923 \text{ cm}^{-1} \text{ M}^{-1}$) and a very good quantum yield (46%). The *para*-methoxypyridine derived α -amino acid **112** was incorporated into a cell-penetrating

peptide using solid-phase peptide synthesis (SPPS) for the preparation of a biologically relevant hexapeptide.

2.1.3 The synthesis of pyrimidine derived α -amino acids.

Based on the above interesting results of the β -pyridyl- α -amino acids,¹¹³ it was proposed that by changing the pyridine ring to a pyrimidine ring may improve the optical properties further. Using a more π -deficient heterocycle in combination with an electron-rich side chain would increase the charge transfer (push-pull) across the chromophore, resulting in amino acid probes with more red-shifted absorption and emission maxima than the β -pyridyl α -amino acids (**Figure 18**). This approach would provide an opportunity to expand the range of fluorescent amino acid analogues and further explore their applications in various fields.

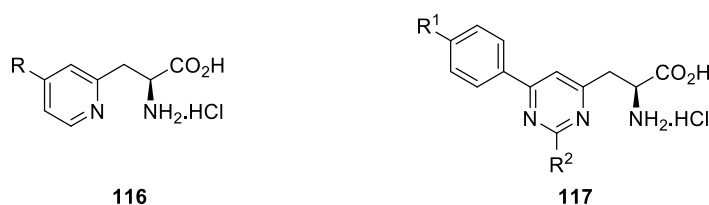
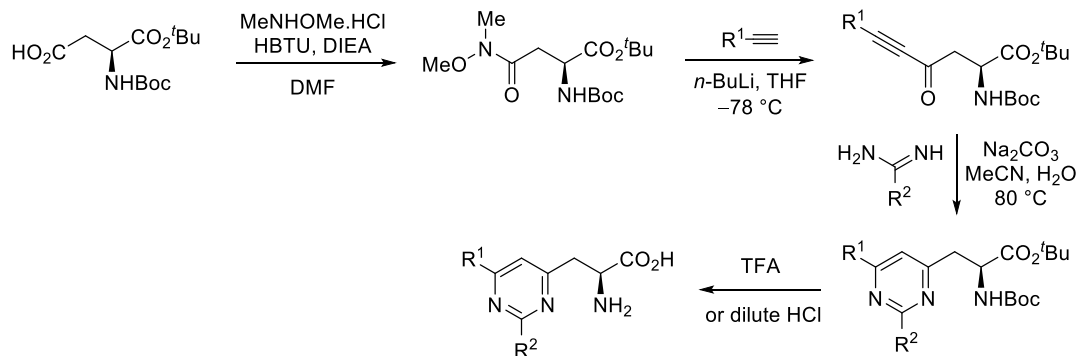


Figure 18: Aryl substituted pyridine **116** and pyrimidine **117** derived α -amino acids.

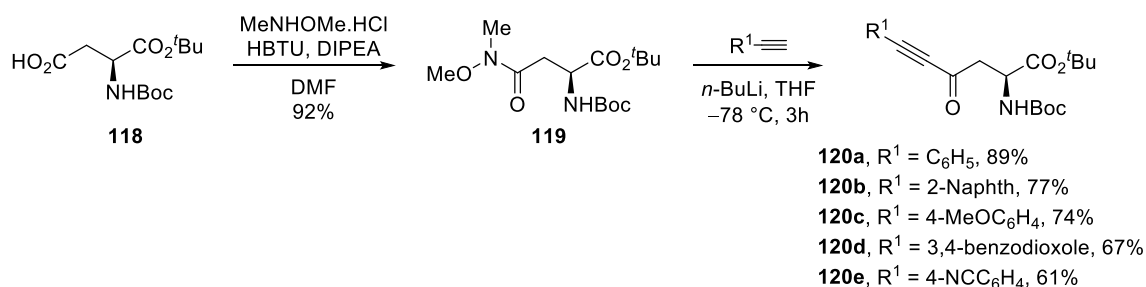
The main aim of this project was to develop an efficient approach for the synthesis of pyrimidine-derived α -amino acids (**Scheme 22**). The first step would involve the preparation of a Weinreb amide that would then be used in a regioselective substitution reaction with lithium salts of alkynes to generate the corresponding ynones. The alkynyl analogues would then be subjected to a cycloaddition reaction with amidines to generate the pyrimidine ring. Removal of both acid-sensitive protecting groups with hydrochloric acid under mild conditions would give the final products. A key aspect of this route is that the pyrimidine rings can be diversified by using different alkynes during the ynone synthesis or by variation of the amidine, leading to a range of products. On synthesis of the final products, the fluorescent properties of these compounds would be investigated.



Scheme 22: Proposed synthesis of pyrimidine derived α -amino acids.

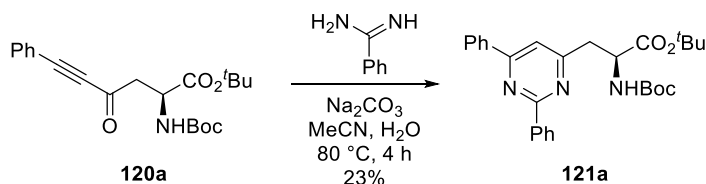
2.1.4 Synthesis of pyrimidine-derived amino acids

In a previous study, Renault and co-workers described an effective method for the preparation of ynones.¹¹⁶ With some changes, this was used for the preparation of ynones **120a–120f** (**Scheme 23**). Initially, commercially available N -Boc L-aspartic acid t -butyl ester **118** was converted to Weinreb amide **119** by reaction with dimethyl hydroxylamine, the coupling reagent, HBTU and using DIPEA as a base. This gave Weinreb amide **119** in 92% yield.¹¹⁶ Reaction of Weinreb amide **119** with the lithium anion of various alkynes, generated by deprotonation with n -butyl lithium, gave ynones **120** in moderate to excellent yields. The majority of alkynes chosen for this study contained either an electron-donating group (e.g. 4-MeOPh) or were highly conjugated (e.g. 2-naphthyl), which would result in a charge transfer chromophore in the final pyrimidine. However, for completeness, two alkynes with electron withdrawing aryl groups (e.g. 4-CNC₆H₄) were also synthesised to examine the effect of this type of side-chain with the pyrimidine.



Scheme 23: Synthesis of ynones **120a–e**.

Using ynone **120a**, with the simplest side-chain (Ph), an initial heterocyclisation reaction with benzamidine was attempted using literature conditions for this type of transformation (**Scheme 24**).¹¹⁷ Using sodium carbonate as a base and a reaction temperature of 80 °C, this gave pyrimidine **121a** in 23% yield after a 4 hour reaction time.



Scheme 24: The synthesis of pyrimidine amino acid **121a**.

While the reaction was successful, an optimisation study was conducted in an attempt to improve the yield (**Table 3**). Initially, the temperature of the reaction was lowered to minimise the decomposition of both starting materials and products. Using THF as the solvent gave an improved yield of 42% (**entry 2**), while the use of acetonitrile gave 39% (**entry 3**). Other based mediated methods reported for the synthesis of pyrimidines from ynones and amidines have also given moderate yields.¹¹⁸ To overcome the moderate yields, other approaches were considered. Previous work by Bagley and co-workers demonstrated the synthesis of pyridines by activation of ynones using Lewis acid ytterbium salts.¹¹⁹ Thus, to improve the yield further, the use of ytterbium triflate as a Lewis acid catalyst was studied.¹¹ Initially, the reaction was investigated at 40 °C, with a slight increase in the amount of benzamidine (**entry 4**). However, this showed slow conversion and therefore, the reaction temperature was increased to 50 °C. This gave **121a** in 69% overall yield, after a reaction time of 48 hours. The structure of pyrimidine **121a** was confirmed by ¹H NMR spectroscopy, which showed the presence of the 5'-H hydrogen atom at the characteristic position of around 7.5 ppm (**Figure 19**). A repeat of this reaction at 50 °C for 48 hours, gave a reproducible yield of 63% for pyrimidine **121a** (**entry 5**).

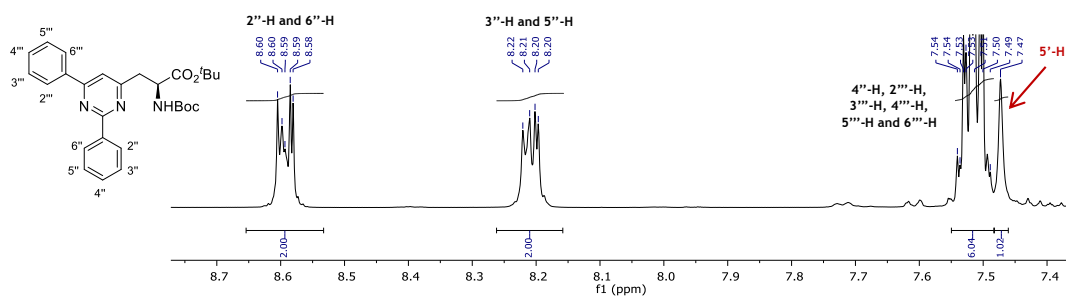
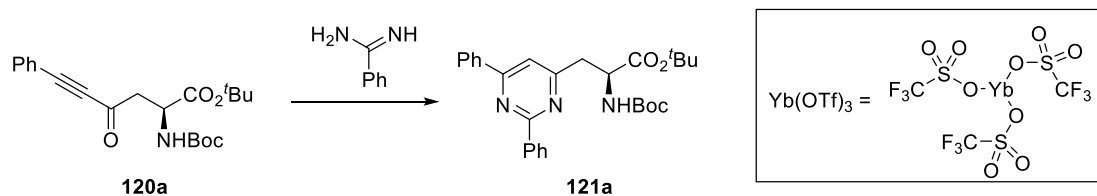


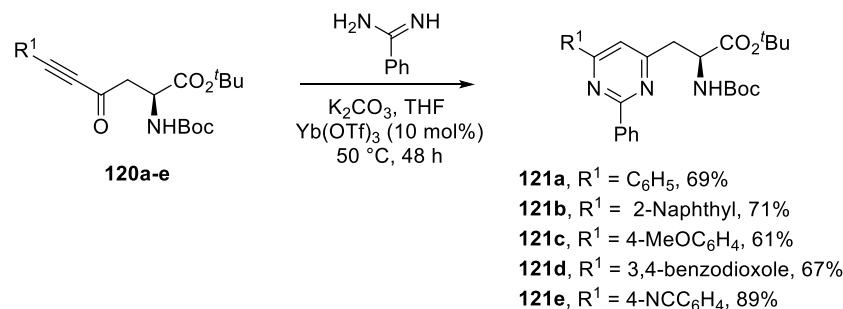
Figure 19: ^1H NMR spectrum of pyrimidine **121a**, measured in CD_3OD (region from 7.4–8.7 ppm).

Table 3: Optimisation of the reaction conditions.



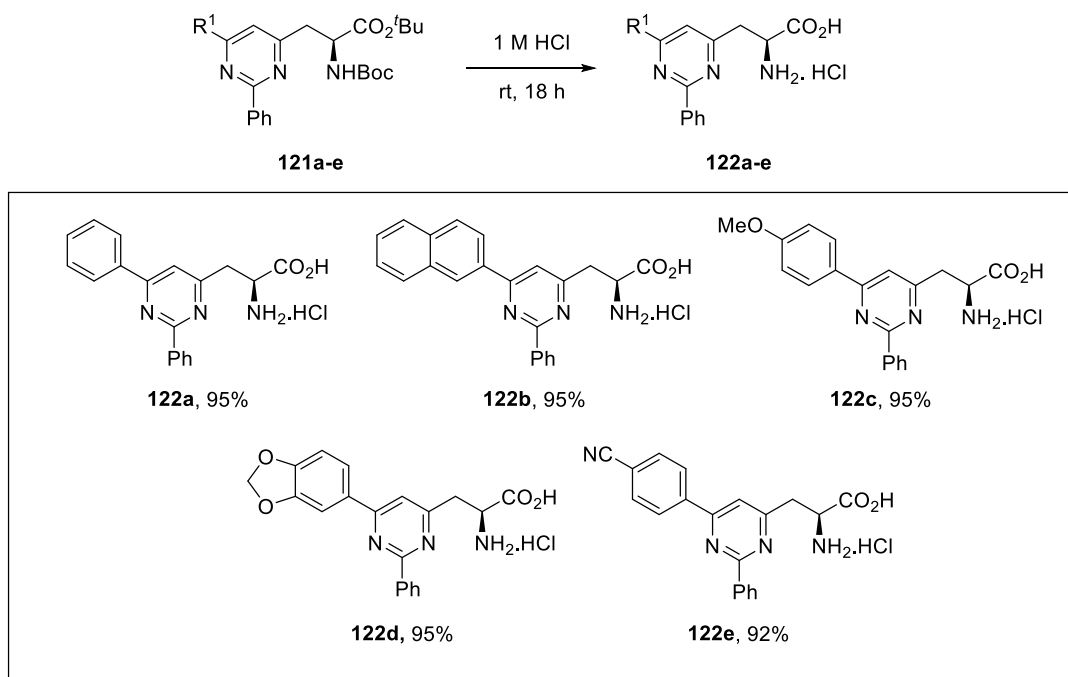
Entry	SM:Amidine (ratio)	Solvent	Yb(OTf) ₃ ¹²⁰ (cat. load)	Temperature (°C)	Time (h)	Yield (%)
1	1:1.2	MeCN	-	80	4	23
2	1:1.2	THF	-	50	24	42
3	1:1.2	MeCN	-	50	24	39
4	1:1.5	THF	10%	40 (24 h) to 50 (24 h)	48	69
5	1:1.5	THF	10%	50	48	63

With the optimised reaction conditions in hand, this method was then used to prepare a series of pyrimidine-derived amino acids (**Scheme 25**). Reaction of ynones **120a–120e** with benzamidine using ytterbium triflate (10 mol%) gave a series of pyrimidine-derived amino acids in 61–89% yields.



Scheme 25: Synthesis of *N*-Boc protected pyrimidines **121a–e**.

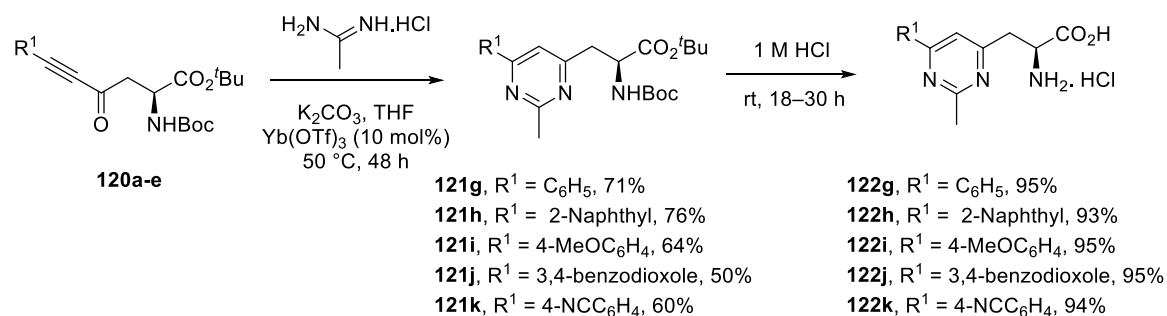
Finally, pyrimidine analogues **121a–121e** were deprotected to the parent amino acid (**Scheme 26**). This was done using 1 M hydrochloric acid, under mild conditions and gave amino acids **122a–122e** in excellent yields.



Scheme 26: Synthesis of pyrimidine-derived α -amino acids **122a–e**.

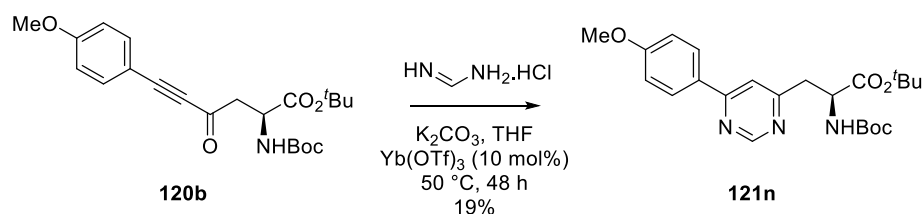
To explore the scope of this methodology and the effect of substituents at the 2-position of the pyrimidine ring, it was proposed to investigate the reaction of ynones with other amidine reagents. Therefore, ynones **120a–e** were also reacted with acetamidine and formamidine. Initially, aryl substituted ynones **120a–e** were subjected to the cyclisation reaction with acetamidine under the standard conditions using THF as the solvent in the presence of ytterbium triflate (10 mol%) and potassium carbonate to neutralise the amidine salt (**Scheme 27**). Using a reaction

temperature of 50 °C and a reaction time of 48 h gave 2-methylpyrimidines **121g–k** in moderate to good yield (50–76%). As for the 2-phenyl analogues, the protecting groups were removed under mild conditions using 1 M HCl at room temperature for 24 hours, which gave the second series of pyrimidine derived α -amino acids **122g–k**.



Scheme 27: Synthesis of pyrimidine-derived α -amino acids **122g–k**.

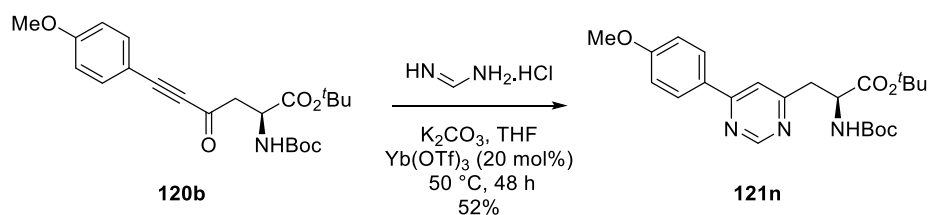
Under the standard Lewis acid-catalysed conditions, the reaction of the ynone-derived amino acids with benzamidine and acetamidine proceeded smoothly, leading to the formation of the corresponding pyrimidine analogues. The yield of the desired compounds was significantly improved using Lewis acid-catalysis, rather than base-mediated conditions. However, attempted heterocyclisation of *p*-methoxyphenyl substituted ynone **120b** with formamidine hydrochloride using the optimised Lewis acid conditions gave a low yield (19%) of the desired product (**Scheme 28**).



Scheme 28: Synthesis of pyrimidine-derived α -amino acids **121n**.

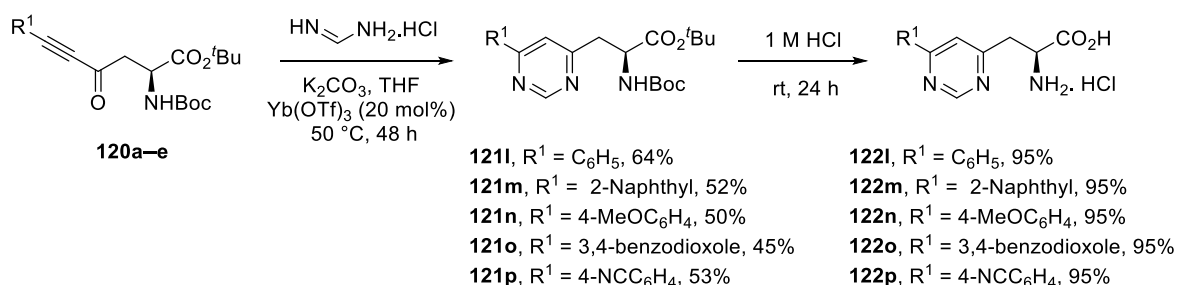
A brief study was conducted to enhance the yield of pyrimidine synthesis using formamidine. It was found that increasing the catalyst loading of the Lewis acid,

ytterbium triflate to 20 mol%, resulted in an improved 50% yield for pyrimidine-derived α -amino acid **120n** (**Scheme 29**).



Scheme 29: Synthesis of pyrimidine-derived α -amino acid **18n** using ytterbium triflate (20 mol%).

Similar results were observed with other yrones, suggesting that increasing the catalyst loading was a viable strategy for enhancing the yield of heterocyclisations using formamidine (**Scheme 30**). Having successfully synthesised a small library of pyrimidine derived α -amino acids from yrones and formamidine, the deprotection process was carried out using 1 M hydrochloric acid under mild conditions. Recrystallisation of the resulting amino acids gave the parent amino acids in excellent yields.



Scheme 30: Synthesis of pyrimidine-derived α -amino acids **121l-p**.

2.1.5 Fluorescent Properties of Pyrimidine Derived α -Amino acids.

The pyrimidine ring is a well-known electron-deficient π -system due to the electronegativity of the two nitrogen atoms. By attaching different substituents to the pyrimidine ring, it is possible to modulate the extent of intramolecular charge transfer across the chromophore.

2.1.5.1 Fluorescent properties of the pyrimidine derived α -amino acids with a C2-phenyl substituent.

The absorption and emission spectra of amino acids **122a–122e** were recorded at 5 mM in methanol (methanol were chosen as solvent due to its ability to dissolve these fluorophores). The photophysical properties of this series showed significant variation based on the C4-pyrimidine substituent. In the case of **122a** with a weakly donating C4-phenyl substituent, the main absorption band was found at 262 nm. As expected, **122** displayed weak fluorescence, with an emission band at 396 nm (**Figure 20**). It was observed that pyrimidine analogues bearing highly conjugated (naphthyl) and electron-donating (4-MeOC₆H₄ and 3,4-benzodioxole) groups exhibited interesting properties. Compounds **122b** (naphthyl), **122c** (4-MeOC₆H₄) and **122d** (3,4-benzodioxole)¹²¹ displayed absorption bands above 300 nm, significantly longer than those observed in naturally occurring amino acids and the previously reported pyridine-derived amino acids.¹¹³ Naphthyl analogue **122b** showed the strongest, red-shifted fluorescence with the main band at 495 nm (**Figure 21**). The methoxy analogue **122c** displayed a red shifted absorption peak at 310 nm and an emission maximum at 386 nm (**Figure 22**). Similarly, the 3,4-benzodioxole **122d** exhibited a comparable absorption band at 305 nm and emission maxima at 405 nm (**Figure 23**). The properties displayed by these three amino acids primarily rely on the intramolecular charge transfer characteristics resulting from the difference in push-pull abilities between the donor and acceptor moieties. Compound **122e**, which contains a C4-electron-withdrawing substituent (4-NCC₆H₄), exhibited spectroscopic characteristics similar to those of compound **122a**, which has a weakly donating substituent. An absorption band was observed at 265 nm and the emission maximum was relatively weak at 499 nm (**Figure 24**). Apart from the weak fluorescence, the other issue with both amino acids is they absorb at similar wavelengths to fluorescent proteinogenic amino acids and therefore could not be used in peptides containing these residues.

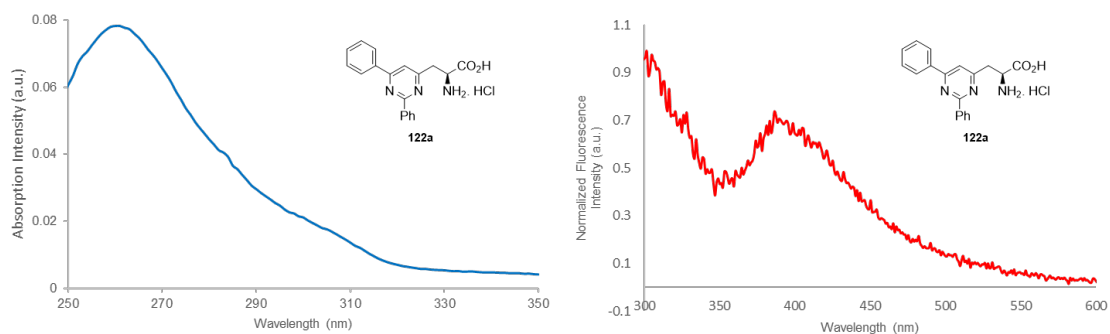


Figure 20: Absorption and emission spectra of **122a** recorded at 5 μM in methanol.

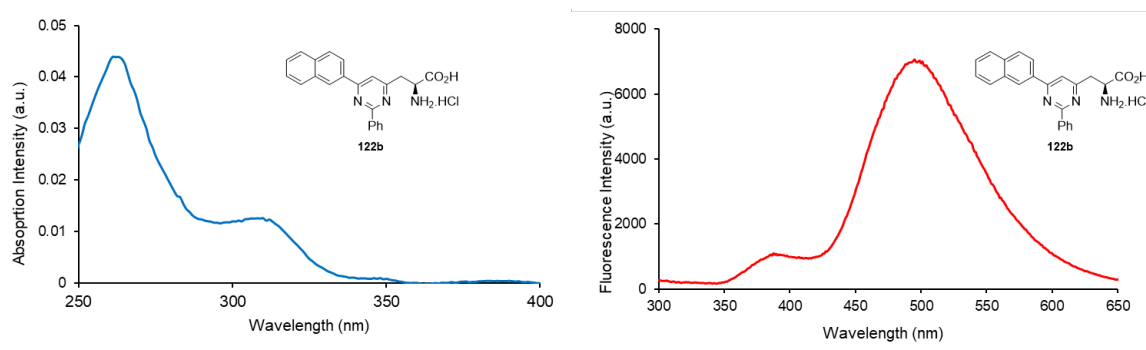


Figure 21: Absorption and emission spectra of **122b** recorded at 5 μM in methanol.

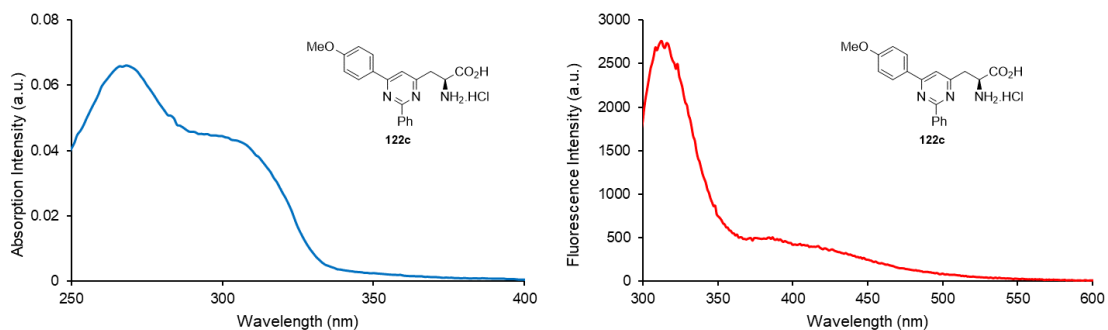


Figure 22: Absorption and emission spectra of **122c** recorded at 5 μM in methanol.

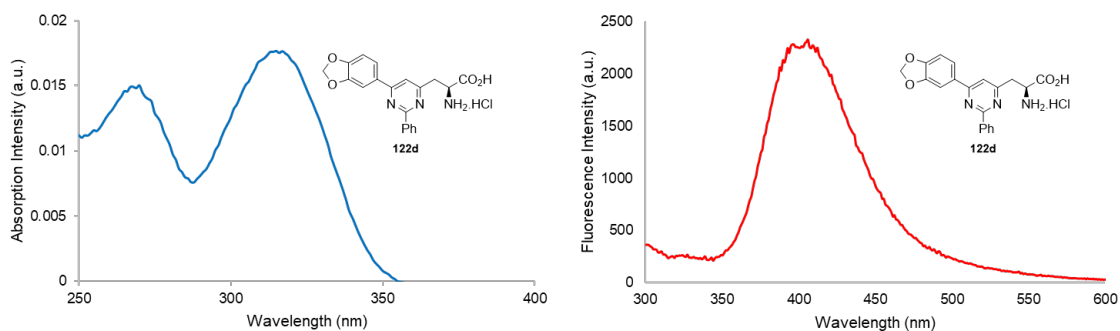


Figure 23: Absorption and emission spectra of **122d** recorded at 5 μM in methanol.

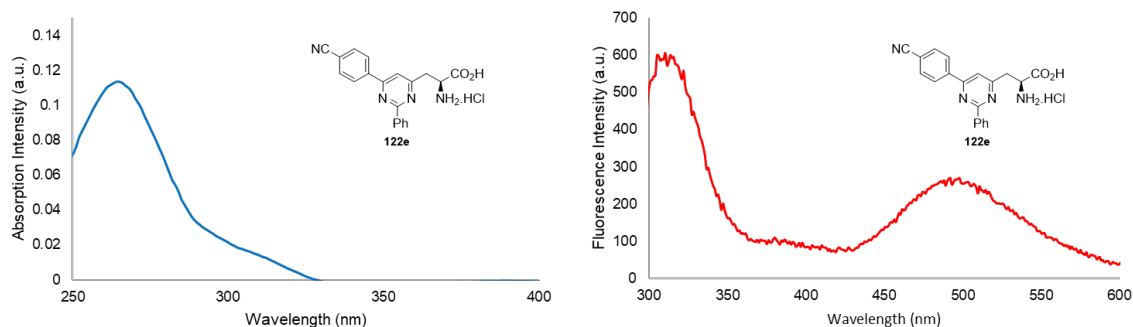
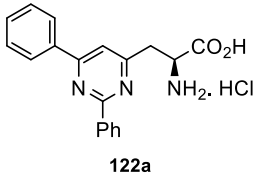
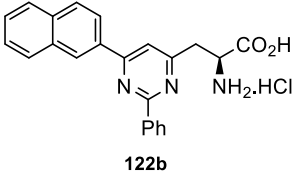
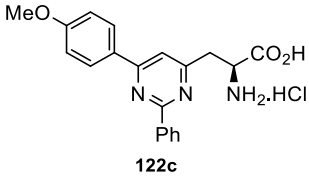
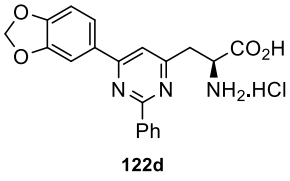
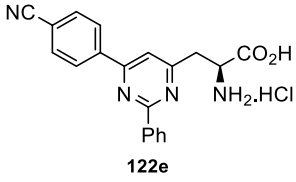


Figure 24: Absorption and emission spectra of **122e** recorded at 5 μ M in methanol.

The complete data for amino acids **122a–122e** is presented in **Table 4**. In addition to the previously discussed absorption and emission data, amino acids, **122a**, **122b** and **122e** were found to possess Mega Stokes shifts (this is where the Stokes shift is >100 nm). Only amino acid **122b** showed a good quantum yield of 12%. All other analogues displayed low quantum yields. This may be due to twisting of the C4-substituent due to the presence of the C2-phenyl group. The C2-phenyl group may induce a distorted conformation, consequently, the emission arises from twisted intramolecular charge transfer excited states, leading to reduced brightness and quantum yield.

Table 4. Photophysical Data of Pyrimidine-Derived α -Amino Acids **122a–e**.

Amino acids	Absorption Maximum (nm)	Emission Maximum (nm)	Stokes Shift (nm)	Molar Extinction Coefficient ($\text{cm}^{-1} \text{M}^{-1}$)	Quantum Yield (Φ_F)	Brightness ($\text{cm}^{-1} \text{M}^{-1}$)
 122a	260	414	154	27,800	0.0017	47
 122b	263, 311	393, 497	130, 186	24,000	0.12	2880
 122c	269, 310	315, 386	46, 76	12,700	0.008	90
 122d	270, 315	335, 405	65, 90	3100	0.015	47
 122e	265, 312	316, 499	51, 187	38,700	0.004	155

2.1.5.2 Fluorescent properties of the pyrimidine derived α -amino acids with a C2-methyl substituent.

Next, the photophysical properties of the second series of amino acids, bearing 2-methylpyrimidines were analysed. The absorption and emission spectra of amino acids **122g–122k** were recorded at 5 mM in methanol. The phenyl derivative **122g** exhibited an absorption peak at 279 nm and a weak emission band at 308 nm (**Figure 25**). The naphthyl analogue **122h** with its highly conjugated side-chain displayed excellent photophysical properties, with a red-shifted absorption maximum at 305 nm and emission maxima at 485 nm (**Figure 26**). The methoxy analogue **122i** showed an absorption band at 299 nm and two emission bands at 314 and 381 nm (**Figure 27**). The dual emission displayed by **122i** may be due to emission from both planar localised emission (LE) and twisted intramolecular charge

transfer (TICT) excited states. The 3,4-benzodioxole analogue **122j** displayed an absorption band at 319 nm and emission maximum at 417 nm (**Figure 28**). Finally, and as expected, the 4-cyanophenyl analogue **122k** exhibited weak fluorescence and low brightness (**Figure 29**).

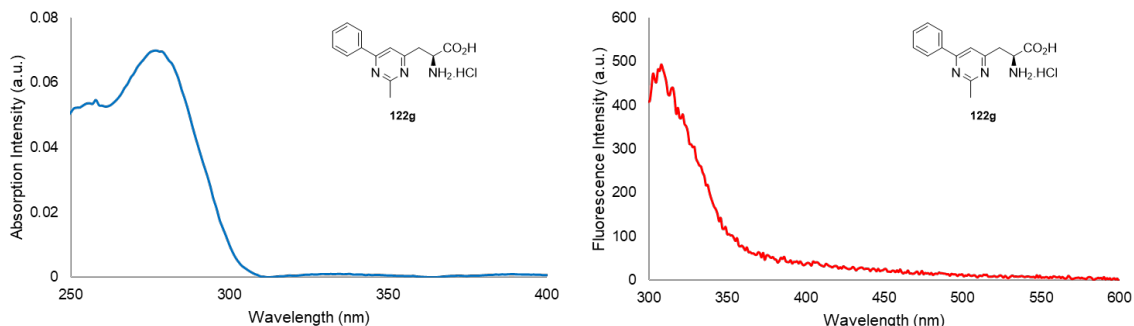


Figure 25: Absorption and emission spectra of **122g** recorded at 5 μM in methanol.

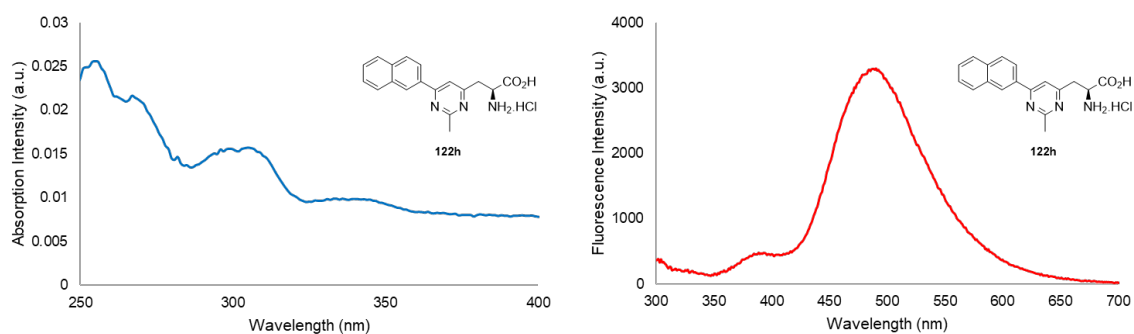


Figure 26: Absorption and emission spectra of **122h** recorded at 5 μM in methanol.

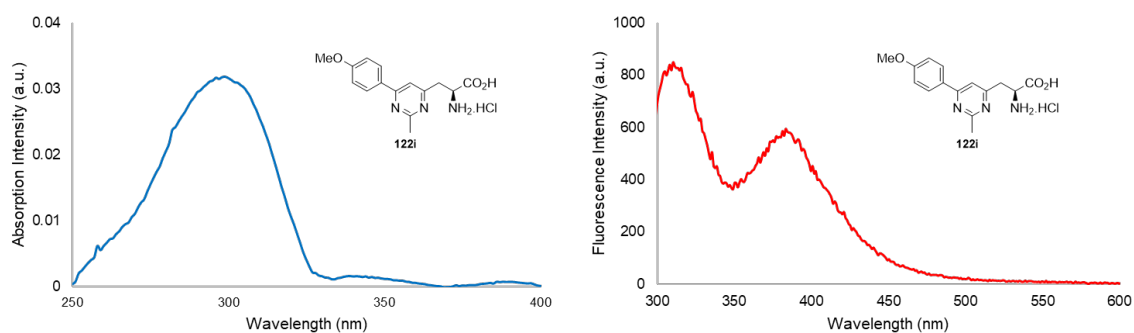


Figure 27: Absorption and emission spectra of **122i** recorded at 5 μM in methanol.

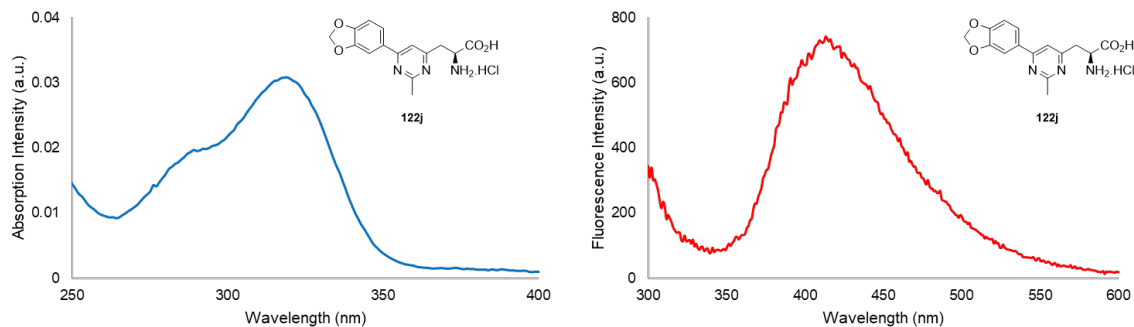


Figure 28: Absorption and emission spectra of **122j** recorded at 5 μM in methanol.

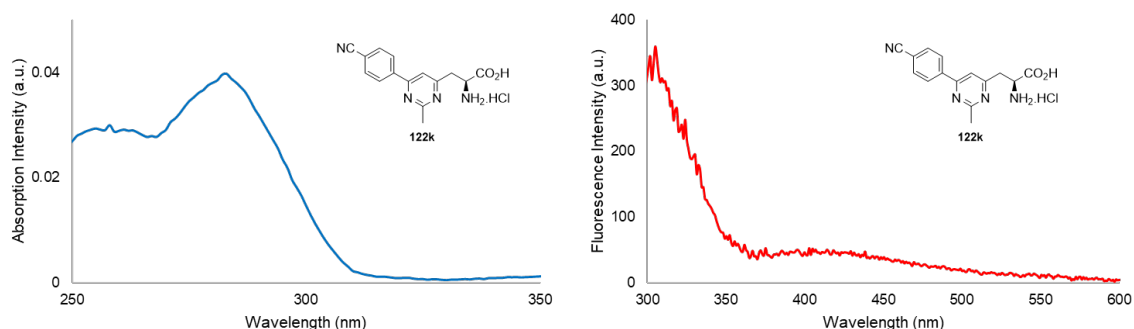
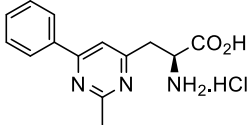
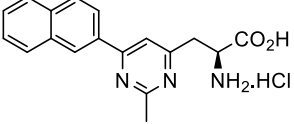
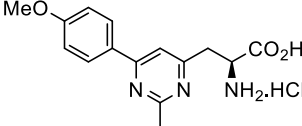
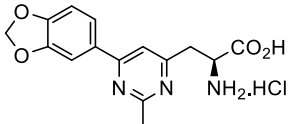
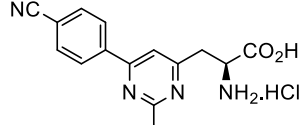


Figure 29: Absorption and emission spectra of **122k** recorded at 5 μM in methanol.

Overall, these amino acids exhibited emission bands from 306–485 nm, and all compounds (except for **122g**) displayed large Stoke Shifts (**Table 5**). Amino acids **122h** and **122j** displayed the most interesting properties. The naphthalene analogue **122h** exhibited the most red-shifted emission (485 nm), a Mega Stoke Shift of 180 nm and a good quantum yield of 11%. Similarly, the 3,4-benzodioxole analogue **122j** also displayed a good quantum yield (11%). The differences between amino acids **122g**–**122k** can be attributed to the different types of electronics associated with the side-chains. The highly conjugated and electron-rich side-chains with the π -deficient pyrimidine moiety display “push-pull” charge transfer character across the chromophore, while the electron-deficient 4-cyanophenyl analogue **122k** possessed weak fluorescence.

Table 5. Photophysical Data of Pyrimidine-Derived α -Amino Acids 122g–k.

	Absorption Maximum (nm)	Emission Maximum (nm)	Stokes Shift (nm)	Molar Extinction Coefficient (cm ⁻¹ M ⁻¹)	Quantum Yield (Φ_F)	Brightness (cm ⁻¹ M ⁻¹)
 122g	279	308	29	12,600	0.002	25
 122h	257, 305	390, 485	133, 180	12,800	0.11	1,408
 122i	259, 299	314, 385	55, 82	16,400	0.016	262
 122j	286, 319	309, 416	23, 94	10,100	0.11	1,111
 122k	258, 283	306, 418	48, 135	5,300	0.003	16

2.1.5.3 Fluorescent properties of the pyrimidine derived α -amino acids with no C2-substituent.

The photophysical properties of these analogues including Stokes shifts, quantum yields, molar attenuation, and brightness for each compound were investigated for each compound in methanol at a concentration of 5 μ M. Based on the results from the previous series, the phenyl analogue **122i** exhibited an absorption peak at 275 nm and an emission maximum at 387 nm (**Figure 30**). The highly conjugated **122m** exhibited a significant red-shift in absorption with a strong peak at 310 nm (**Figure 31**). Similarly, the electron-rich C4-substituted compound **122n** (**Figure 32**) also showed a good red-shift in absorption (306 nm) and a strong emission peak at 383 nm, while the other electron-rich analogue **122o** showed a more red-shifted

absorption (323 nm) and emission (430 nm) (**Figure 33**). In contrast, the amino acids bearing electron-withdrawing substituents **122p** displayed weak fluorescence and lowest brightness (**Figure 34**). It was confirmed that C2-unsubstituted pyrimidine analogues exhibited a trend of red-shifted spectra with large Stoke shifts and good quantum yields when compared to the previous analogues (**Table 6**).

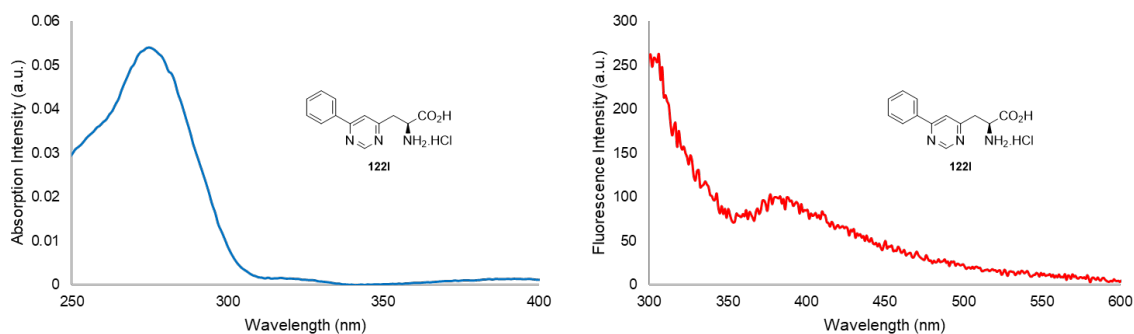


Figure 30: Absorption and emission spectra of **122i** recorded at 5 μM in methanol.

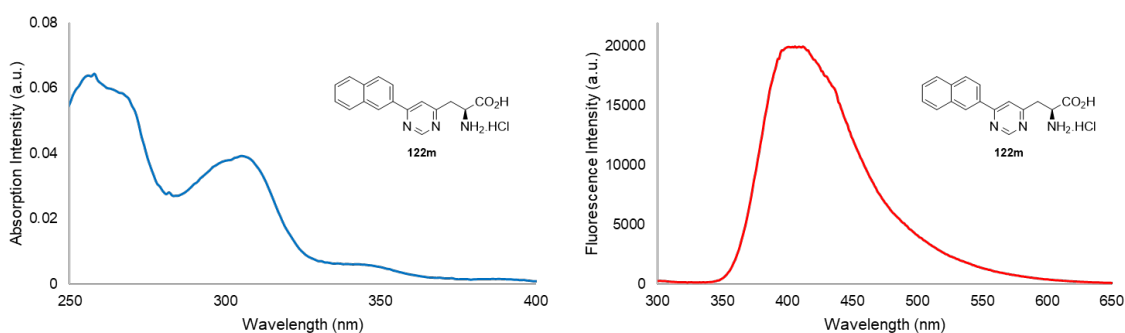


Figure 31: Absorption and emission spectra of **122m** recorded at 5 μM in methanol.

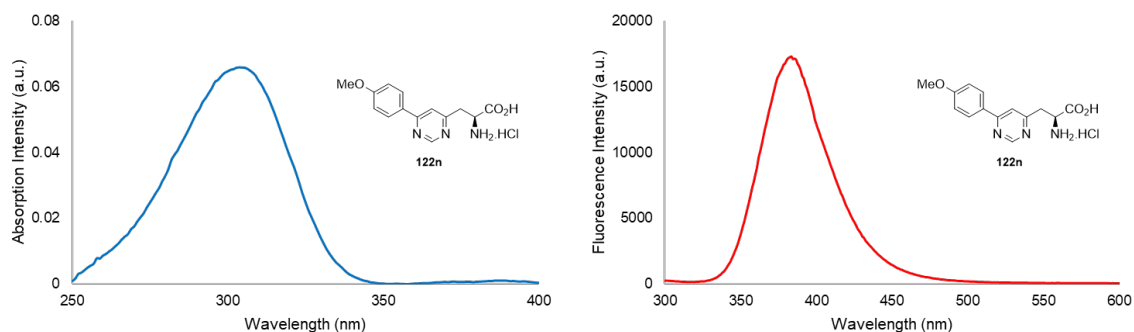


Figure 32: Absorption and emission spectra of **122n** recorded at 5 μM in methanol.

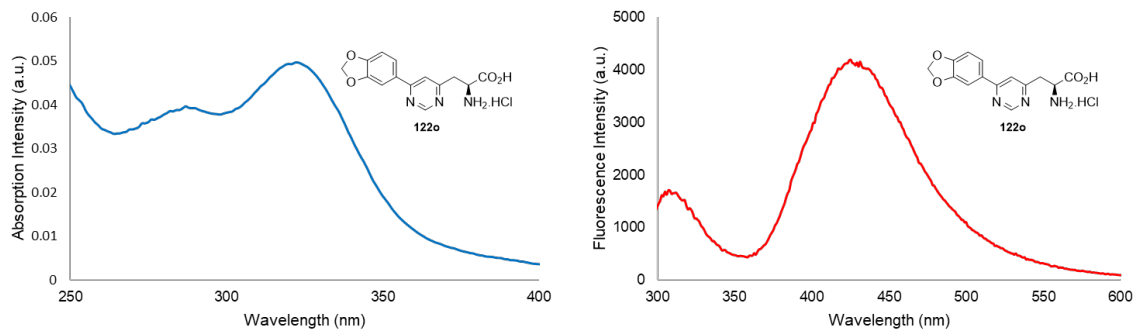


Figure 33: Absorption and emission spectra of **122o** recorded at 5 μM in methanol.

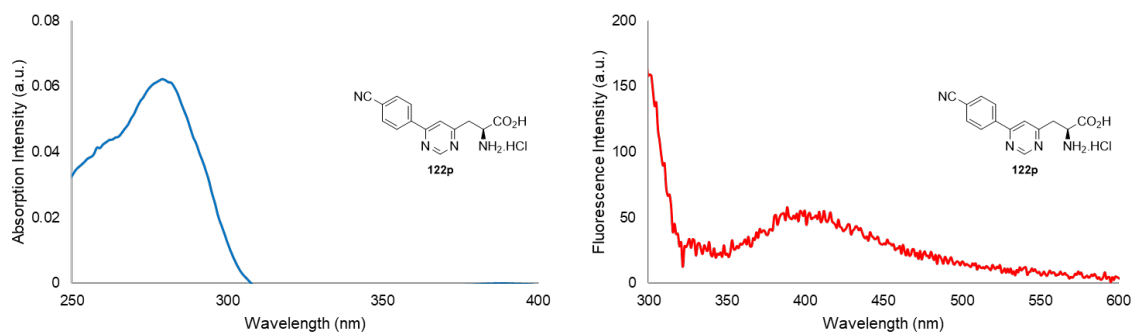
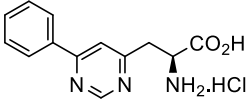
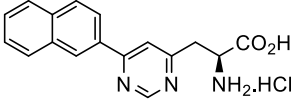
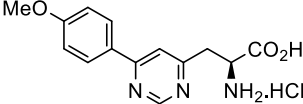
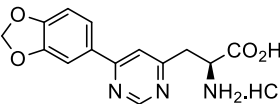
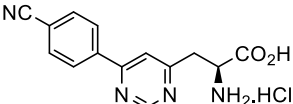


Figure 34: Absorption and emission spectra of **122p** recorded at 5 μM in methanol.

Table 6. Photophysical Data of Pyrimidine-Derived α -Amino Acids 122l–p.

	Absorption Maximum (nm)	Emission Maximum (nm)	Stokes Shift (nm)	Molar Extinction Coefficient ($\text{cm}^{-1} \text{M}^{-1}$)	Quantum Yield (Φ_F)	Brightness ($\text{cm}^{-1} \text{M}^{-1}$)
 122l	254, 275	387	48, 112	10,700	0.003	32
 122m	258, 310	314, 421	57, 111	10,400	0.30	3120
 122n	306	383	77	13,600	0.27	3,672
 122o	287, 323	309, 430	22, 107	7,900	0.20	1,580
 122p	279	415	136	12,800	0.0007	9

From the three series, it can be observed that substituents at C2 of the pyrimidine ring have an impact on the optical properties of these compounds. For example, the three amino acids with C4-naphthyl substituted pyrimidine rings show very different emission spectra (**Figure 35**). While the two compounds, **122b** and **122h** show emission maxima around 500 nm, the amino acid that lacks a C2-substituent **122m** has a hypsochromic shifted emission spectrum at 421 nm. It is proposed that this difference is due to the C2-substituent, which causes twisting of the chromophore and TICT emission for compounds **122b** and **122h**. For **122m**, this amino acid can adopt a more planar conformation resulting in locally excited emission at shorter wavelength.

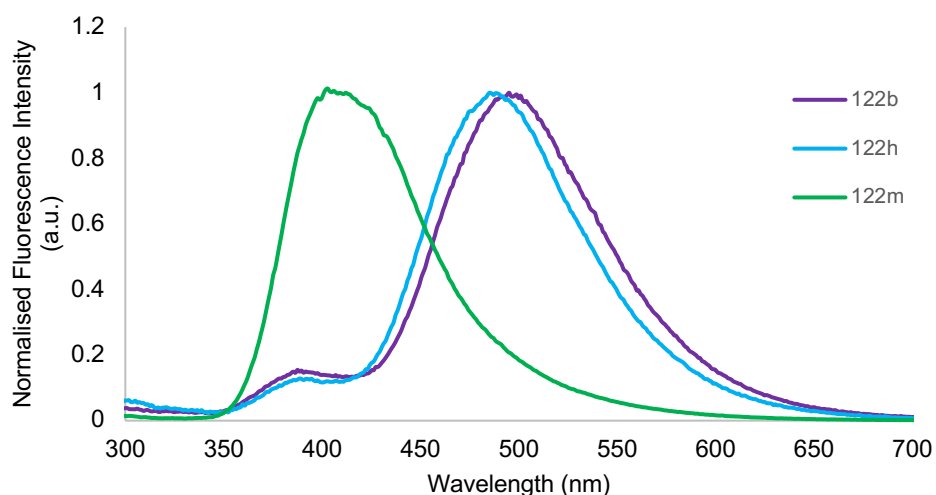


Figure 35: Emission spectra of **122b**, **122h** and **122m** recorded at 5 μM in methanol.

In the *p*-methoxyphenyl series, the C2-phenyl analogue **122c** displayed a brightness value of $90 \text{ cm}^{-1} \text{ M}^{-1}$. However, this brightness improved to $262 \text{ cm}^{-1} \text{ M}^{-1}$ for **122i** and $3,672 \text{ cm}^{-1} \text{ M}^{-1}$ for **122n**. For compounds **122i** and **122n**, the C2-substituent causes twisting between the two aryl rings, resulting in weak fluorescent emission (**Figure 36**). In comparison, C2-unsubstituted analogue **122n** can adopt a planar conformation across the chromophore in the excited state, resulting in strong emission via intramolecular charge transfer.

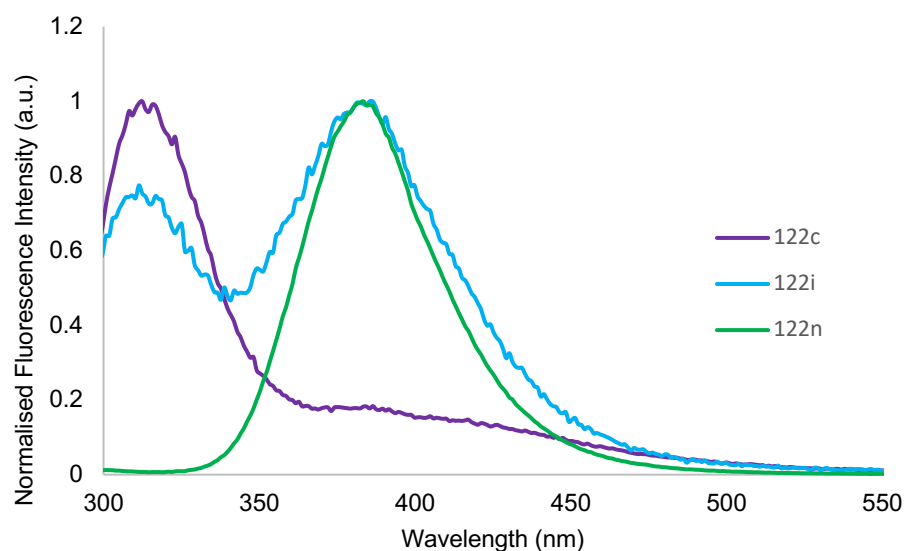


Figure 36: Emission spectra of **122c**, **122i** and **122n** recorded at 5 μM in methanol.

For the 3,4-benzodioxole series of compounds **122d**, **122j** and **122o**, while the emission maxima were similar (405–430 nm), only C2-phenyl substituted analogue **122d** showed weak fluorescence (**Figure 37**). In comparison, both **122j** and **122o** displayed significantly stronger fluorescence with quantum yields of 0.11 and 0.20, respectively. For this series, while the C2-phenyl analogue **122d** is significantly twisted resulting in poor conjugation and weak fluorescence, both **122j** and **122o** seem to be able to adopt relatively planar conformations resulting in effective charge transfer and strong fluorescence.

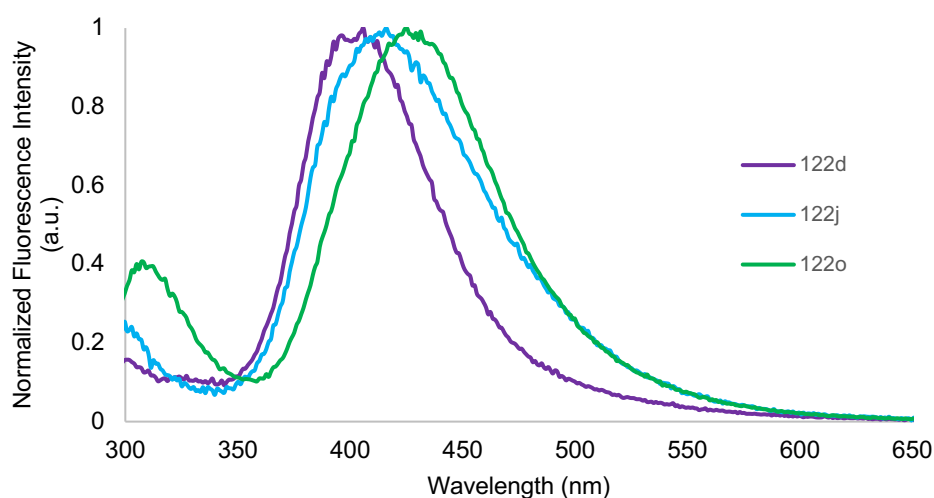


Figure 37: Emission spectra of **122d**, **122j** and **122o** recorded at 5 μM in methanol.

2.1.6 Further Analysis of Lead Analogue **122n**

Based on the findings of this study, the methoxy analogue **122n** was identified as the lead compound for further investigation of its environmental sensitivities, including solvatochromic properties and pH effects. The conjugation between the donor substituent and the acceptor pyrimidine core of compound **122n** suggested the potential for emission at longer wavelengths in more polar solvents. Therefore, it was expected that compound **122n** would display solvatochromism, with changes of emission in different solvents.

The solvatochromic properties of compound **122n** were investigated by measuring its absorption and emission spectra in various solvents. The results revealed that the absorption bands of **122n** underwent minimal changes in different solvents, showing that in the ground state, the absorbance of **122n** is not dependent on polarity (**Figure 38**).

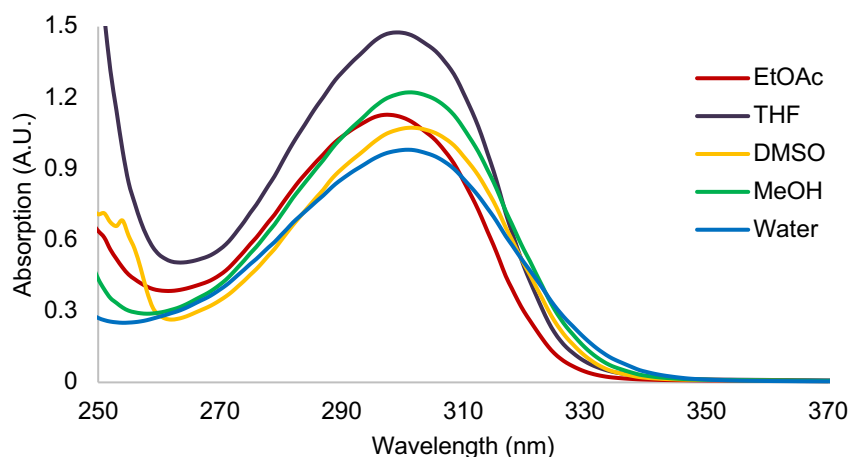


Figure 38: Absorption spectra of **122n** in various solvents. All spectra were recorded using a concentration of 5 μM .

In comparison, the emission spectra were found to be strongly solvent dependent (**Figure 39**). It was noted that the emission maxima of **122n** exhibited a significant red shift as the solvent polarity increased. For instance, in ethyl acetate, an emission maximum of 352 nm was observed, while in water, the emission maximum was observed at 384 nm. This result showed that **122n** is sensitive to the polarity of its surrounding environment. Consequently, the solvatochromic nature of amino acid **122n** makes it a valuable tool for investigating biomolecular microenvironment.

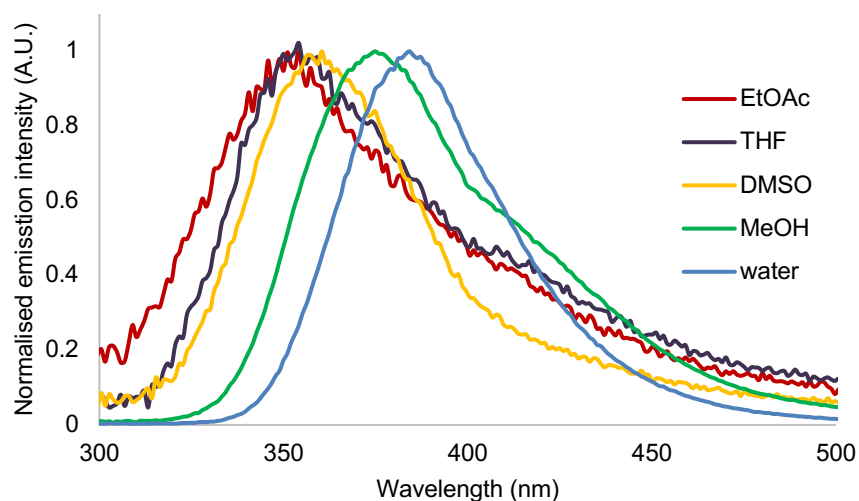


Figure 39. Emission spectra of **122n** in various solvents. All spectra were recorded using a concentration of 5 μM .

The observed solvatochromism of amino acid **122n** can be attributed to the greater dipole stabilisation provided by more polar solvents. The shift in wavelength observed for this compound suggests the presence of a strong dipole across the chromophore. The solvatochromism of **122n** was further supported by a Lippert-Mataga graph,^{87,122,123} which is a plot of Stokes shift versus solvent orientation polarisability (**Figure 40**). A straight line for a Lippert-Mataga graph confirms that the difference in emission wavelength in different solvents is due to solvatochromism. A straight-line plot was observed for amino acid **122n**, thus confirming the solvatochromic nature of this compound.

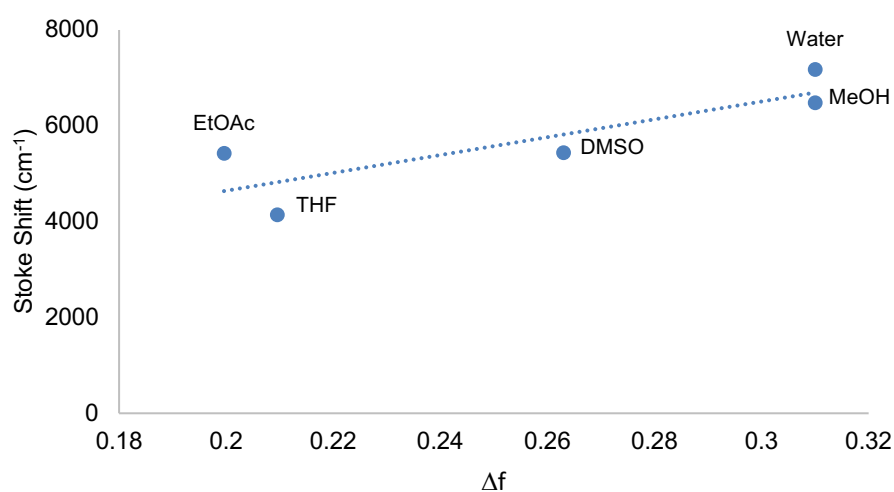


Figure 40: Lippert-Mataga graph for amino acid **122n**.

Having observed the interesting solvatochromism of amino acid **122n**, the effect of pH on its photophysical behaviour was next investigated. The pH-dependent investigation of compound **122n** revealed interesting changes in its photophysical properties. By subjecting compound **122n** to pH conditions from 7 to 1, stronger absorption and the formation of a weak second band at higher wavelength (~360 nm) was observed under increasing acidic conditions (**Figure 41**).

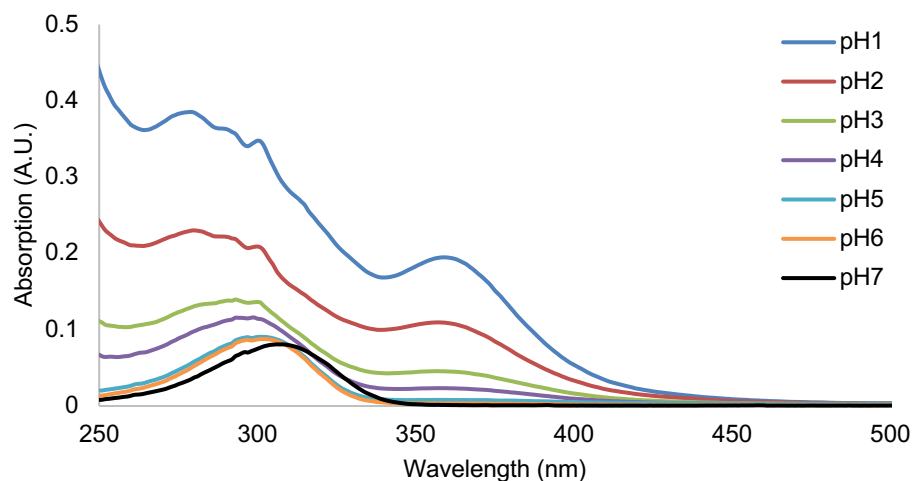


Figure 41: Absorption spectra of **122n** at various pH in methanol. All spectra were recorded using a concentration of 5 μM .

Similarly, the emission spectra of amino acid **122n** at various pH (1 to 7) showed no significant change in wavelength (**Figure 42**). However, changing from neutral pH to more acidic conditions resulted in quenching of fluorescence. Such protonation-induced effects of pyrimidines typically result in either hypsochromic¹²⁴ or bathochromic shifts of the emission band¹²⁵⁻¹²⁷ due to a change in conformation. For amino acid **122n**, protonation and possible twisting of the biaryl motif results in “turning off” of the fluorescence. This suggests that amino acid **122n** may have potential as a pH sensor in biological systems.

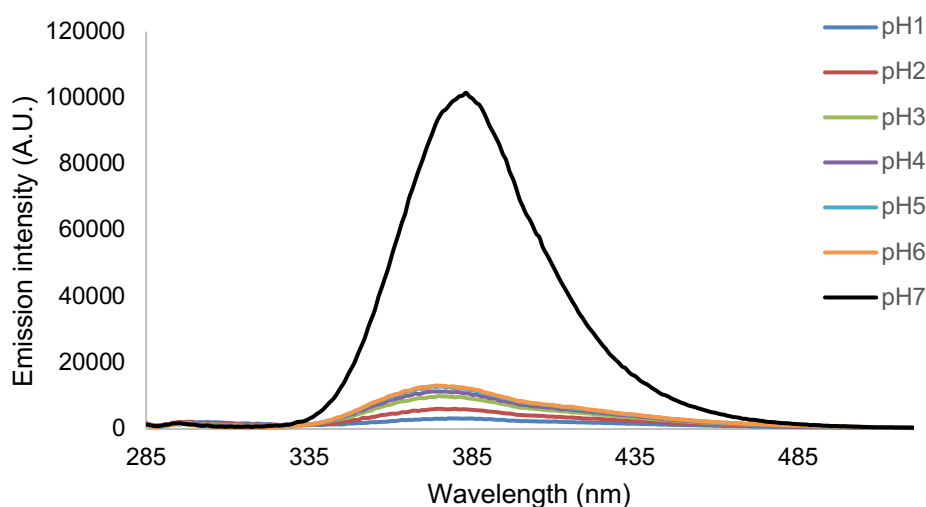


Figure 42: Emission spectra of **122n** at various pH in methanol. All spectra were recorded using a concentration of 5 μM .

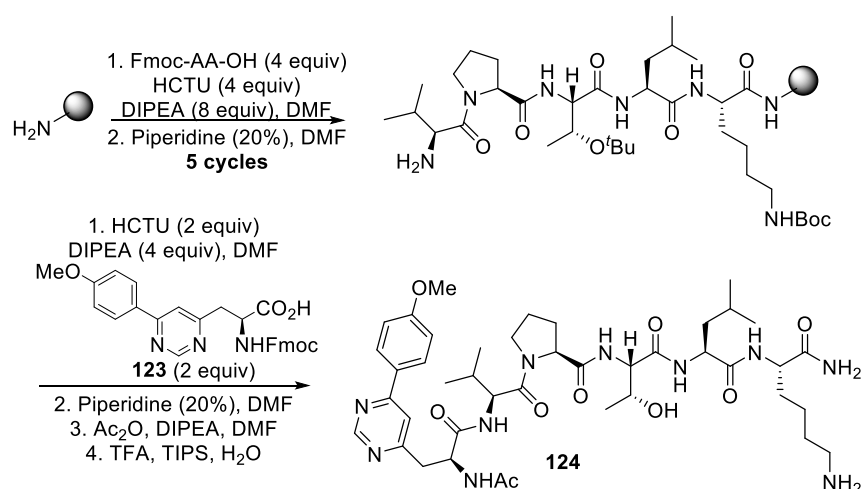
2.1.7 Conclusions

To conclude, a novel class of fluorescent pyrimidine-derived α -amino acids has been synthesised. The synthesis involved the conversion of an aspartic acid analogue to a Weinreb amide intermediate which was subsequently reacted with alkynyl lithium salts, which allowed the synthesis of ynone compounds. A ytterbium-catalysed heterocyclisation reaction with amidines was then developed for preparation of the pyrimidine ring system. By varying the alkyne side-chain, various analogues were prepared. Despite facing challenges with the yield of the last series, it was proposed that improving the yield of heterocyclisation reaction could be achieved by increasing the ytterbium catalyst to 20 mol%. This resulted in yield enhancement (45-64%). These compounds were easily deprotected, under mild conditions, in one step under acidic conditions to yield the parent amino acids. The study revealed that the combination of the electron-rich substituents (such as 4-methoxyphenyl and 3,4-benzodioxole) or the highly conjugated substituents (2-naphthyl) along with the π -deficient pyrimidine motif led to the formation of strong charge-transfer based fluorophores with large Stokes shifts, high overall brightness, and good quantum yields. The environment sensitive nature was demonstrated through solvatochromic studies, revealing distinct emission wavelengths in various solvents based on the polarity. Moreover, the behaviour of these compounds under varying pH condition was explored. A change from neutral to more acidic pH resulted in quenching of fluorescence, suggesting the potential of amino acid **122n** as a pH sensor in biological systems. The observed behaviour suggests that protonation and potential twisting of the biaryl motif leading to the “turning off” of the fluorescence.

2.1.8 Future Work

As the series of pyrimidine-derived amino acids have demonstrated interesting photophysical properties, such as red-shifted absorption and emission wavelength (compared to proteinogenic and previous pyridine-derived amino acids), large Stokes shifts and good quantum yields, these will be considered for biological applications. Future work will focus on expanding the structural diversity of these pyrimidine-derived amino acids by exploring different C2- and C4-substitutions. In particular, C2-unsubstituted pyrimidines with alkyne spaces between the aryl systems may lead to optimised properties. In the event that no further improvements are found, then lead compound **122n**, which has displayed remarkable fluorescent properties will be chosen for further investigation as a biological imaging agent. The next step could involve incorporation into a peptide sequence, aiming to assess the

suitability of the pyrimidine amino acids for solid-phase peptide synthesis (SPPS). An approach could involve the synthesis of a straightforward pentapeptide Val-Pro-Thr-Leu-Lys based on the Bax-binding domain of Ku70, which is known for its low cytotoxicity and efficient cell penetrating properties.¹²⁸ The preparation of this peptide would involve standard SPPS techniques, followed by incorporation of the Fmoc-protected pyrimidine amino acid, to produce a hexapeptide (**Scheme 31**).¹¹³ Following the synthesis of hexapeptide **124**, the fluorescent properties would be examined to understand any alteration in response to peptide incorporation. If the photophysical properties are retained, the peptide could be used for biological applications, such as cell imaging.



Scheme 31: Proposed synthesis of hexapeptide **124**.

2.2 Synthesis of Novel Fluorescent Biaryl α -amino acids

2.2.1 Introduction

As discussed in previous chapters, continuous efforts have been made to design unnatural amino acids which are highly fluorescent. Generally, fluorescent compounds often have conjugated aromatic ring structures that contain multiple π -bonds, which contribute to their fluorescence.¹²⁹⁻¹³¹ By modifying the substituent groups on the aromatic rings, the optical characteristics of these interconnected moieties can be enhanced. For example, extended p-conjugation of the tyrosine¹³⁰ and phenylalanine¹³² side-chains results in improved optical properties compared to the natural amino acid analogue (**Figure 43**).

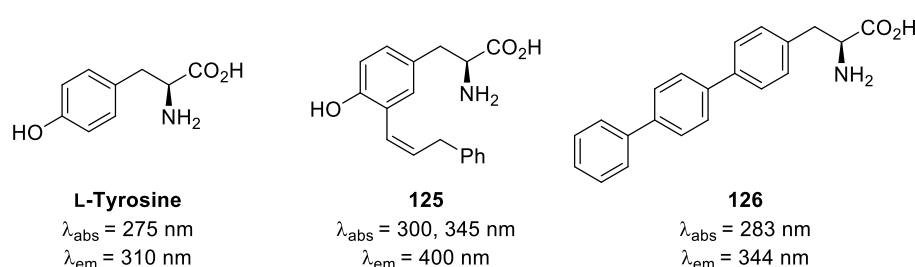
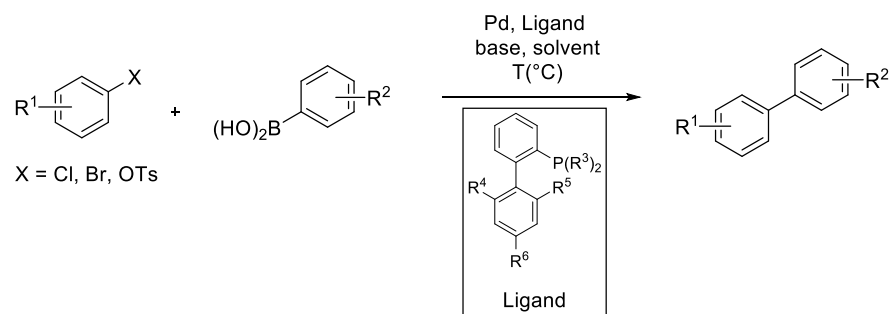


Figure 43: Fluorescent amino acids derived from tyrosine/phenylalanine with extended π -conjugation.

The main objective of this project was to develop new methodology that would allow fast access, in relatively few steps to biaryl α -amino acids. There are several established methods for constructing substituted biphenyl scaffolds; the most effective and widely used approach is the Suzuki–Miyaura cross-coupling reaction.^{133,134} Suzuki coupling is performed between aryl halide (R–X) as an electrophile and organoborane (R–B) as a nucleophile with a metal catalyst, suitable base, aqueous and organic solvent, and temperature (usually 60–100 °C). This method allows for the formation of carbon-carbon bonds between two sp^2 carbon atoms. Previous reports have detailed an effective approach for the synthesis of biphenyl derivatives by a simple aryl–aryl coupling procedure (**Scheme 32**).¹³⁵ Along with the widespread availability and stability of commercial boronic acids, these can be used with aryl (pseudo)halides for the palladium-catalysed Suzuki–Miyaura cross-coupling reaction,¹³⁶ resulting in the formation of the desired biaryl derivatives.¹³⁷



Scheme 32: Palladium-catalysed Suzuki-Miyaura cross-coupling reaction.

Among aryl (pseudo)halides, aryl iodides possess the highest reactivity, followed by aryl triflates, aryl bromides, and aryl chlorides (**Figure 44**). Despite their potential, some aryl triflates are sensitive to strong bases and are thermally labile, requiring the development of mild reaction conditions for coupling arylboronic acids with triflates.

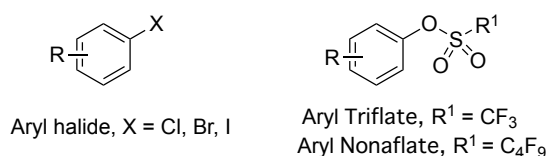
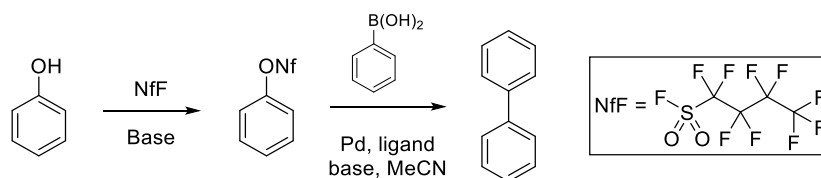


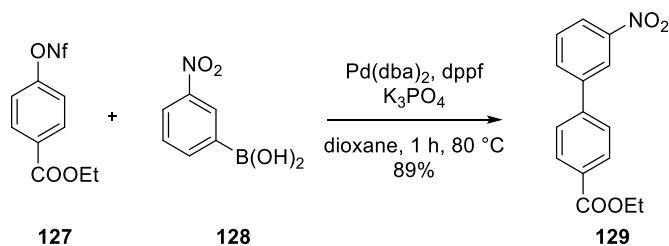
Figure 44: Cross coupling reagent; aryl halide, aryl triflate and aryl nonaflate

Due to the moderate reactivity of aryl triflates, their high cost, and undesired hydrolysis to the corresponding phenol as a side reaction, aryl fluoroalkanesulfonates such as nonaflates have been proposed as an alternative. Nonaflates can be more readily synthesised from cost-effective nonaflate fluoride. Additionally, nonaflates are more stable to hydrolysis compared to triflates. The advantage of using nonafluoro-1-butanefluoride (NfF), is due to its ease of handling compared to triflate reagents and its excellent leaving group properties, making it a useful strategy for palladium-catalysed coupling reactions (**Scheme 33**).¹³⁹



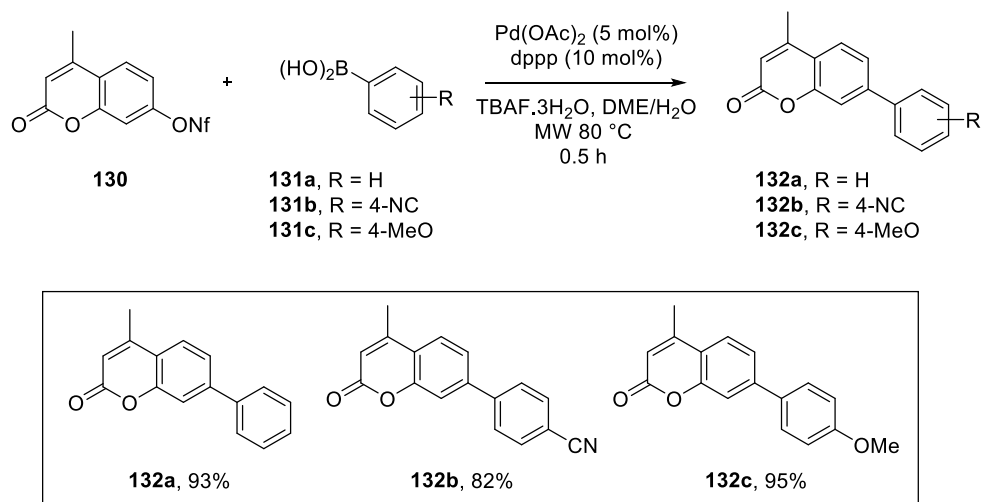
Scheme 33: The cross-coupling reactions of phenols using nonafluorobutanesulfonyl fluoride (NfF).

One example of this was shown by Rottlander and Knochel.¹⁴⁰ Aryl nonaflates were prepared and used for the selective formation of cross-coupling products. The palladium-catalysed cross-coupling reaction of the aryl nonaflate **127** with boronic acid **128** in the presence of K_3PO_4 as base gave expected biaryl product **129** in 89% yield (**Scheme 34**).



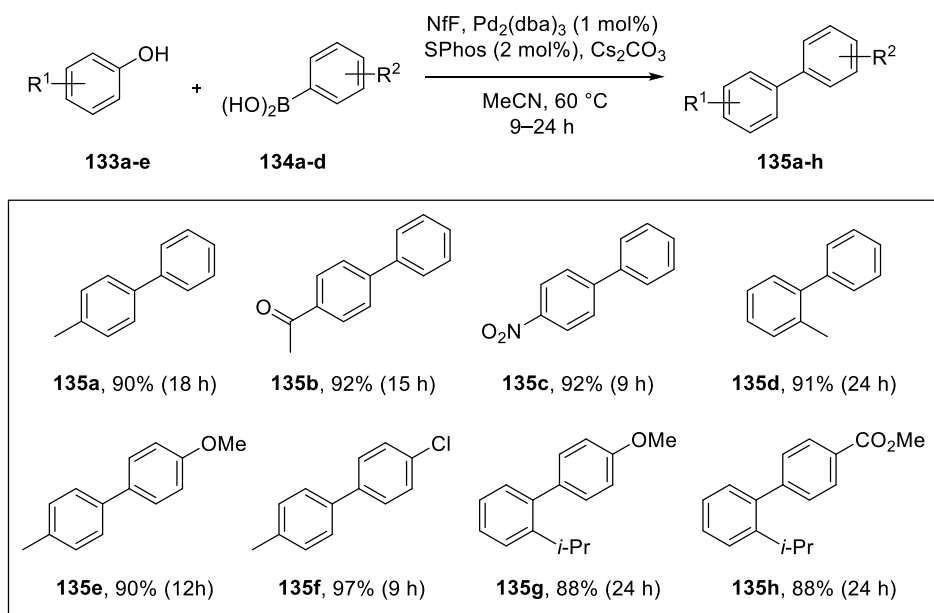
Scheme 34: Palladium-catalysed couplings of aryl compound with aryl nonaflate.

A further example of the use of aryl nonaflates during Suzuki–Miyaura cross-coupling reactions was reported by Kumar and coworkers,¹⁴¹ who demonstrated efficient reactions with $\text{Pd}(\text{OAc})_2$ and bidentate phosphine (dppp) as the catalyst system (**Scheme 35**). The cross-coupling of 4-methyl-7-nonafluorobutylsulfonyloxy coumarins **130** with aryl boronic acid **131a-c** utilised $\text{TBAF} \cdot 3\text{H}_2\text{O}$ as base under microwave irradiation conditions, resulting in the desired biaryl products **132a-c** with excellent yields.



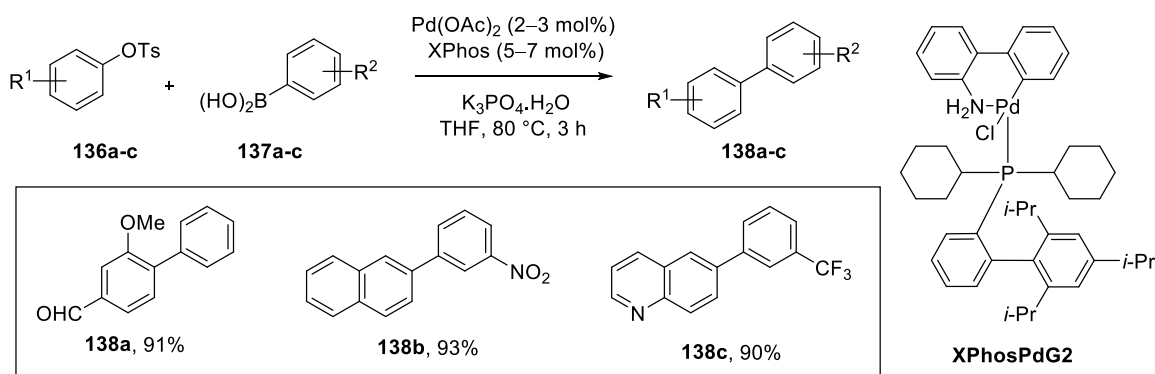
Scheme 35: Pd-catalysed Suzuki–Miyaura cross-coupling of aryl nonaflates.¹⁴¹

In 2012, Akai and coworkers¹³⁹ introduced an efficient one-pot cross-coupling reaction method of phenols and boronic acids, via a nonaflate, without the need for isolating the intermediate. A range of substituted phenols **133a–h** was subjected to the direct Suzuki–Miyaura coupling with arylboronic acids using Pd₂(dba)₃ and SPhos as ligand. The reactions were conducted under basic conditions with caesium carbonate, leading to the formation of the desired biphenyl products in excellent yields (**Scheme 36**).



Scheme 36: Formation of biphenyls via one-pot nonaflate Suzuki–Miyaura cross-coupling reaction.¹³⁹

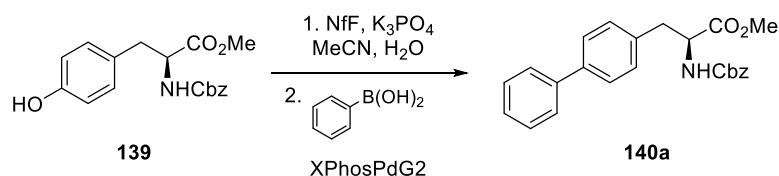
Also notable and of importance to this project, Buchwald and co-workers¹⁴² demonstrated the use of XPhosPdG2 as an effective catalyst for the coupling of sulfonates (in this case tosylates) with aryl boronic acids, for the efficient synthesis of a wide range of biaryl compounds (**Scheme 37**). This approach demonstrated the use of a catalyst system based on Pd(OAc)₂ and XPhos (which later become known as XPhosPdG2) in the presence of potassium phosphate. The reactions were complete in 3 h at 80 °C, resulting in 90–93% isolated yield.



Scheme 37: XPhosPdG2 catalysed Suzuki-Miyaura coupling of aryl tosylates.

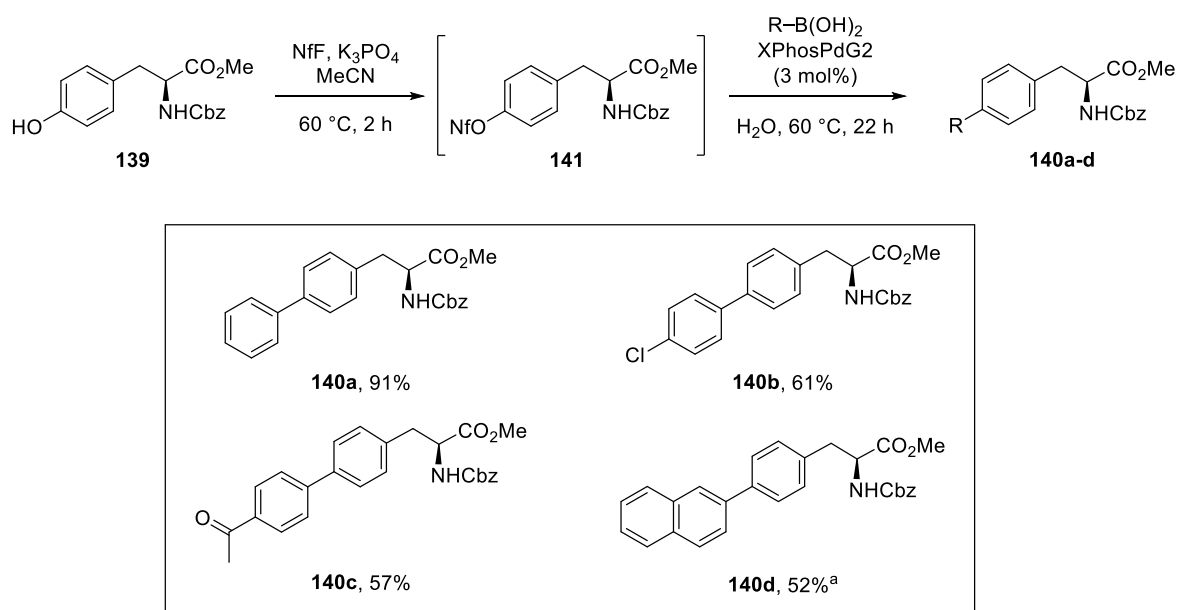
2.2.2 Project Aims

Previous work by Hecht and co-workers reported the synthesis and development of the poly-aromatic amino acid, 4-biphenyl-L-phenylalanine, as an effective fluorophore for application in chemical biology imaging applications.^{132,143} Based on this example, it was proposed that other polyaromatic amino acids and in particular, biphenyl analogues of L-phenylalanine, could act as effective fluorescent imaging probes. Furthermore, using the one-pot method of Akai,¹³⁹ it was proposed that access to biphenyl analogues of L-phenylalanine could be achieved in a single step from protected tyrosine derivatives (**Scheme 38**). It was also believed that Buchwald's second-generation XPhosPdG2 could be an effective catalyst for this transformation.



Scheme 38: Proposed one-pot nonaflate Suzuki-Miyaura cross-coupling reaction of tyrosine derivative **140a**.

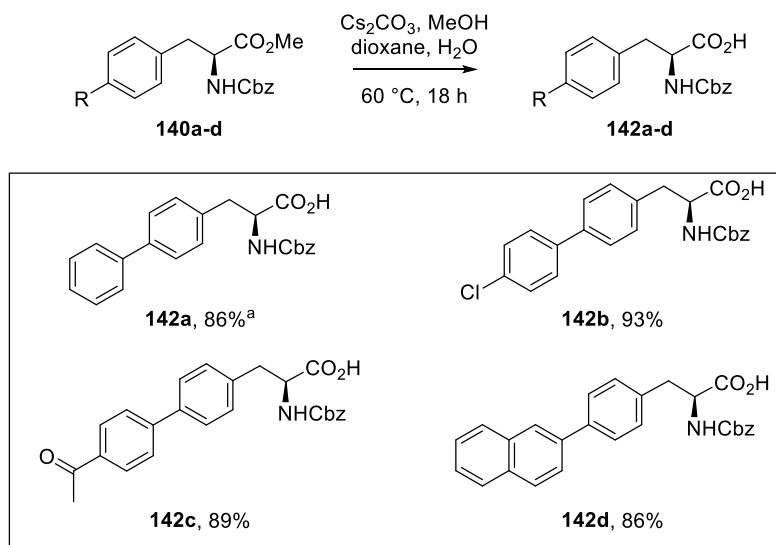
Initial studies were conducted by another PhD student from the Sutherland group, Rochelle McGrory, who showed that XPhosPdG2 was an effective catalyst for the cross-coupling step.¹⁴⁴ The other main difference to the Akai procedure,¹³⁹ was that water was required to solubilise the base, potassium phosphate. Using this one-pot method, the synthesis of biaryl amino acids was conducted from *N*-Cbz-L-tyrosine methyl ester **139** using various aryl boronic acids (**Scheme 39**). Using a reaction temperature of 60 °C, four different analogues were prepared in moderate to excellent yields.



Scheme 39: Substrate scope of one-pot synthesis of biaryl amino acids. ^aReaction carried out at 80 °C.

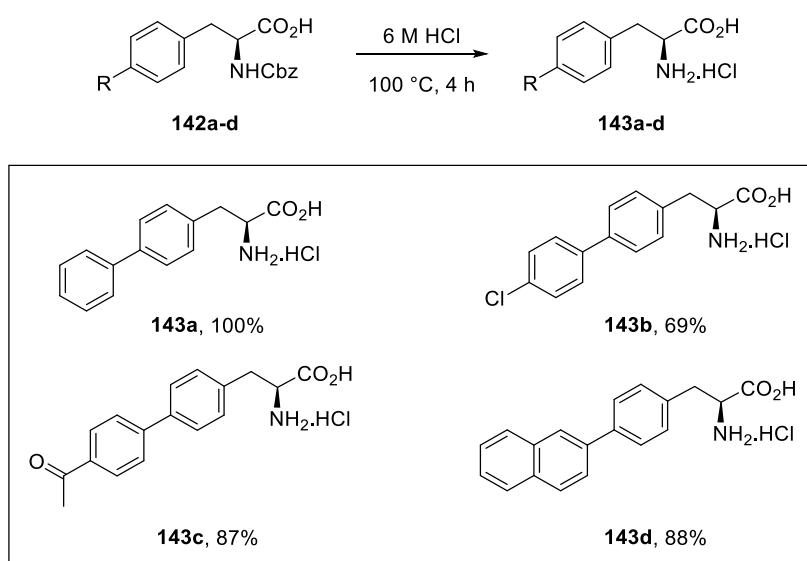
Having synthesised a small library of phenylalanine analogues, these were then subjected to a two-step strategy to access the parent amino acids for analysis of the photophysical properties. The first stage of this was methyl ester hydrolysis, which

was conducted using caesium carbonate as the base (**Scheme 40**). This gave the desired carboxylic acids **142a-d** in high yields.



Scheme 40: Methyl ester hydrolysis of biphenyl α -amino acids. ^aReaction carried out at room temperature.

The final deprotection step involved removal of the Cbz-group. Based on previous work in the group, this was done under acidic conditions, using 6 M hydrochloric acid (**Scheme 41**). For each amino acid analogue this was successful, resulting in the efficient synthesis of the four parent amino acids.



Scheme 41: Removal of the Cbz-protecting group under acidic conditions.

2.2.3 Fluorescent Properties of Biphenyl Amino Acids

The absorption and emission spectra of novel biphenyl amino acids **143a**–**143d** were recorded at 5 μM in methanol (**Figures 45–48**). In the case of **143a**, the amino acid with a biphenyl side-chain, the main absorption band was found at 254 nm with an emission band at 314 nm (**Figure 45**). The properties displayed by 4''-chlorophenyl analogue **143b** was an absorption band at 261 nm, with an emission maximum at 330 nm (**Figure 46**). The 4''-acetyl analogue **143c** displayed an absorption maximum at 289 nm and very weak fluorescence, with an emission maximum at 323 nm (**Figure 47**). The highly conjugated naphthyl analogue exhibited the most interesting properties (**Figure 48**). Amino acid **143d** displayed an absorption band above 289 nm and showed the strongest, most red-shifted fluorescence with an emission band at 356 nm.

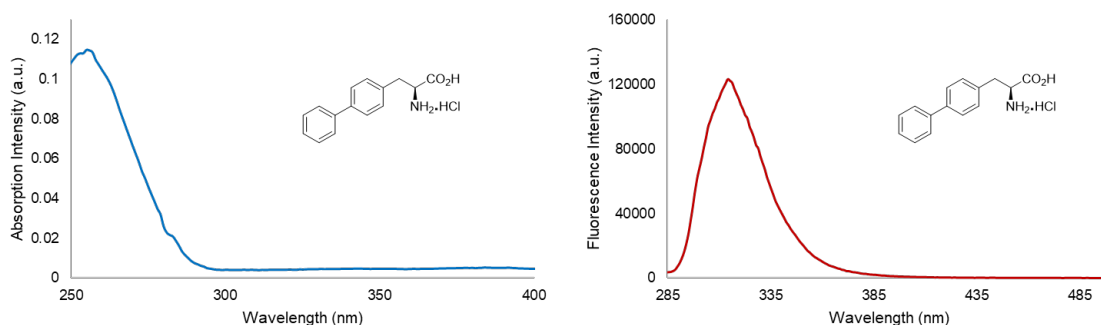


Figure 45: Absorption and emission spectra of **143a** (5 μM in MeOH, excitation at 275 nm).

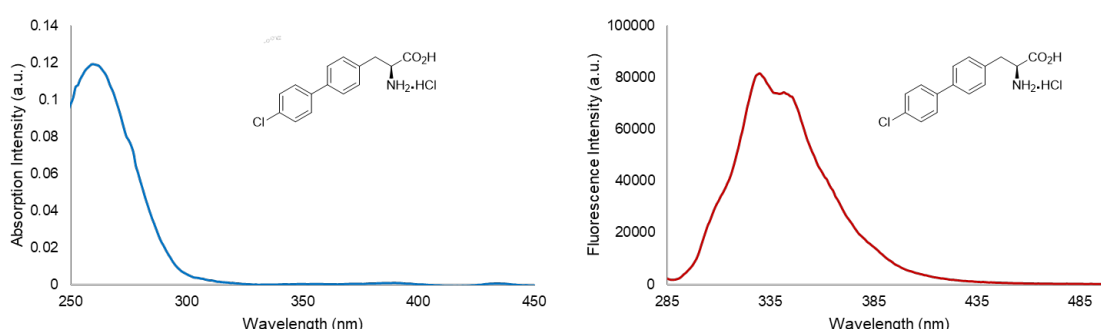


Figure 46: Absorption and emission spectra of **143b** (5 μM in MeOH, excitation at 275 nm).

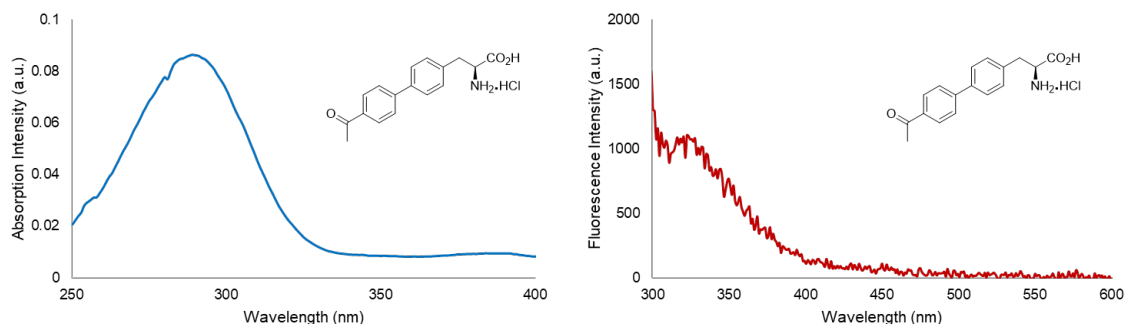


Figure 47: Absorption and emission spectra of **143c** (5 μM in MeOH, excitation at 275 nm).

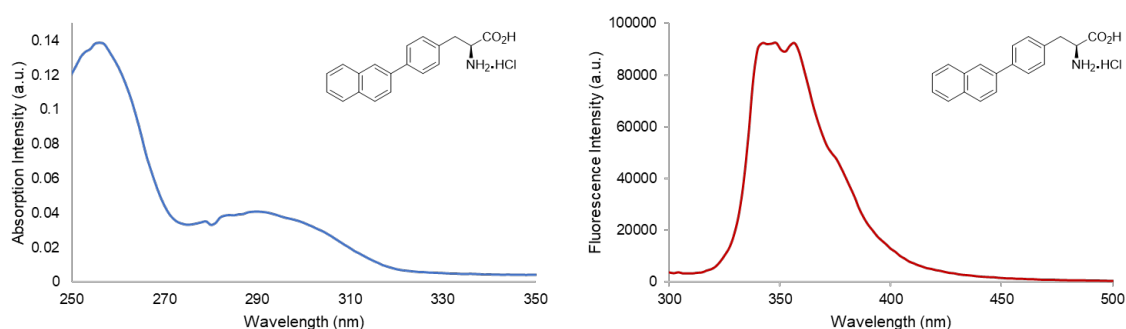
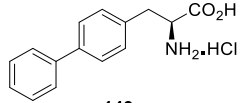
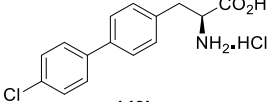
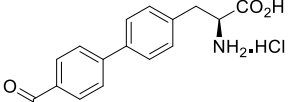
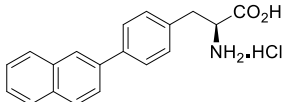


Figure 48: Absorption and emission spectra of **143d** (5 μM in MeOH, excitation at 275 nm).

As well as the absorption and emission spectra, other fluorescent data for biphenyl-derived amino acids **143a**, **143b**, **143c** and **143d** were measured (**Table 7**). Amino acids **143a**, **143b**, **143c** and **143d** exhibited excellent molar attenuation coefficients ($19700\text{--}32100\text{ cm}^{-1}\text{ M}^{-1}$) and large Stokes shifts (60–100 nm). In accordance with its weak fluorescence, 4'-acetylphenyl analogue **143c** showed a low quantum yield. However, the other three analogues all show significantly higher quantum yields than phenylalanine (0.024). For example, phenyl analogue **143a** possessed a quantum yield of 0.12, while naphthyl analogue **143d** was found to have the highest quantum yield of 0.18, resulting in an overall brightness of $5560\text{ cm}^{-1}\text{ M}^{-1}$.

Table 7: Photoluminescence properties of biphenyl α -amino acids.

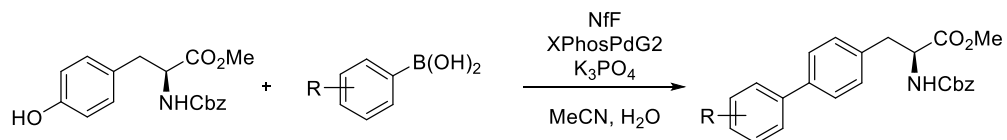
Compound	λ_{abs} (nm)	λ_{em} (nm)	Stokes Shift (nm)	Molar Attenuation Coefficient ($\text{cm}^{-1} \text{M}^{-1}$)	Quantum Yield (Φ_{F})	Brightness ($\text{cm}^{-1} \text{M}^{-1}$)
 143a	254	314	60	24200	0.12	2930
 143b	261	330	69	32100	0.08	2570
 143c	289	323	34	19700	0.002	390
 143d	256 289	356	87 100	30900	0.18	5560

2.2.4 Conclusions

In conclusion, novel biphenyl amino acids have been prepared using a one-pot, two-step transformation involving formation of a nonaflate intermediate, followed by a XPhosPdG2-catalysed Suzuki-Miyaura cross-coupling reaction. Following the preparation of four different analogues, these were deprotected over two steps, under standard conditions, allowing the rapid, three-step synthesis of biphenyl amino acids from commercially *N*-Cbz-L-tyrosine methyl ester. Full analysis of the photophysical properties of these biphenyl amino acids showed that these possessed interesting properties. In particular, the naphthyl analogue was found to have a quantum yield of 0.18 and showed the most red-shifted and brightest fluorescence. This initial work has shown that these polyaromatic amino acids have potential as fluorophores and deserve further examination.

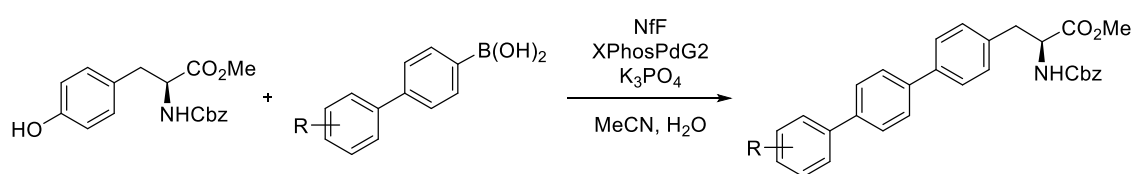
2.2.5 Future Work

To further explore the potential applications of these novel biphenyl amino acids, it would be necessary to expand the scope of the synthesis to encompass a broader series of analogues (**Scheme 42**). By introducing different substituents on the biphenyl framework, a more diverse library of compounds can be generated. This approach would enable the full evaluation of this class of amino acids and their fluorescent properties.



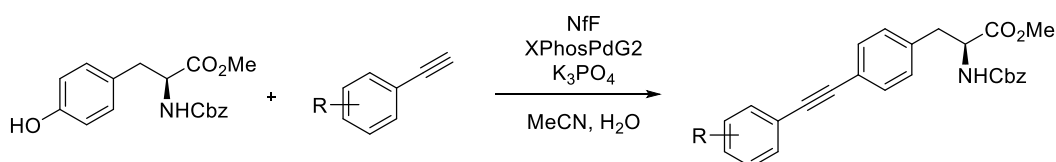
Scheme 42: Proposed synthesis of biphenyl α -amino acids.

As terphenyl α -amino acids are reported as having improved quantum yields and exhibit red-shifted absorption and emission in comparison to their corresponding biphenyl analogues, these could also be investigated.^{132,14} These compounds could be prepared in a similar manner as the corresponding biphenyl compounds using biphenyl boronic acids (**Scheme 43**).



Scheme 43: Proposed synthesis of terphenyl α -amino acids.

As biphenyl amino acids have shown interesting properties, one approach to improving their fluorescence is to modify the side-chain to include further conjugation. For example, stretched chromophores, incorporating alkyne units may lead to improved photophysical properties.¹¹⁵ These novel amino acids could be prepared by modification of the one-pot nonaflate synthesis and Suzuki-Miyaura reaction to include instead, a Sonogashira cross-coupling reaction (**Scheme 44**). Through optimisation, the range of suitable alkynes can be explored to generate a library of alkynyl amino acids with extended conjugation systems. The photophysical properties of the synthesised alkynyl amino acids would then be measured.



Scheme 44: Proposed synthesis of alkynyl α -amino acids.

2.3 New Applications of Enone Derived α -Amino Acids: The Stereoselective Synthesis of Diaminopimelic Acids.

2.3.1 Introduction

2,6-Diaminopimelic acid (DAP) and its analogues are of significant interest due to their intriguing biochemistry and potential as antimicrobial agents.^{120,145,146} In biological systems, *meso*-diaminopimelic acid (*meso*-DAP) **144** and L,L-diaminopimelic acid (L,L-DAP) **145** (Figure 49) play important roles as precursors in the biosynthesis of L-lysine in both bacteria and higher plants. Moreover, *meso*-DAP is the key cross-linking amino acid of peptidoglycan found in the cell walls of many pathogenic bacteria.^{147,148}

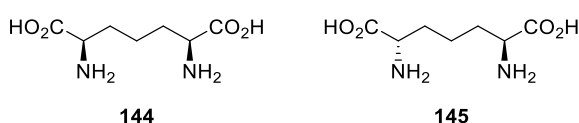


Figure 49: Chemical structures of *meso*-DAP **144** and L,L-DAP **145**.

Peptidoglycan is composed of cross-linked chains of peptidoglycan monomers, *N*-acetylglucosamine and *N*-acetylmuramic acid (NAG-NAM-pentapeptide). In gram-negative bacteria, *meso*-DAP is utilised as the cross-linking amino acid to connect the peptide chains of the peptidoglycan monomers. In gram-positive bacteria, L-lysine, the biosynthetic product of *meso*-DAP **144**, plays a similar role in forming the cross-links between the peptide chains (Figure 50).^{149,150}

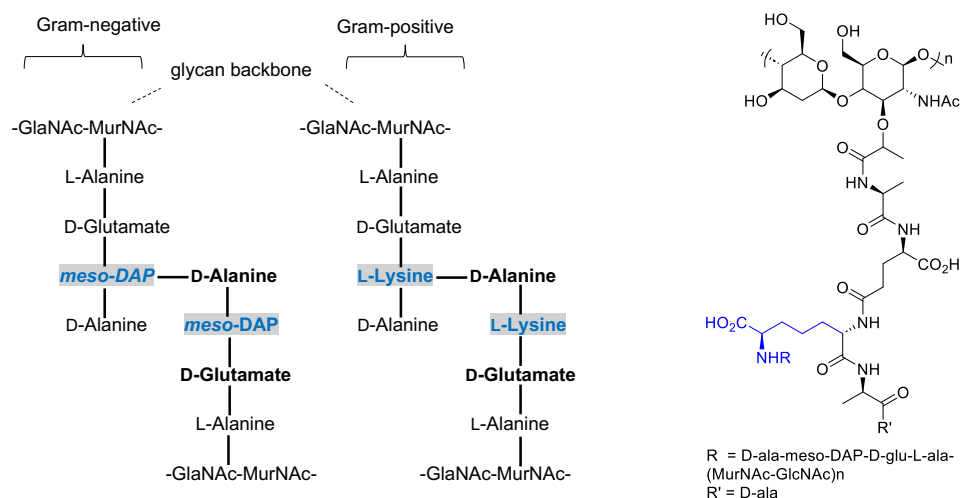


Figure 50: Peptidoglycan of a bacterial cell wall.

The biosynthesis of the key crosslinking amino acids in peptidoglycan can be divided into three main pathways,^{151,152} which share the first few steps from aspartate to tetrahydrodipicolinate. Pathway 1, the succinylase pathway uses succinylated intermediates and is the most widely distributed in bacteria (**Figure 51**). Pathway 2 involves the one-step reaction of L-tetrahydrodipicolinate to *meso*-DAP using DAP-dehydrogenase. Pathway 3 is the acetylase pathway and proceeds using an ammonium-incorporating dehydrogenase. Each variant of the DAP pathway relies on specific cofactors to carry out the enzymatic reactions. Analogues of diaminopimelic acid (DAP) have attracted significant interest as potential inhibitors of enzymes involved in the DAP pathway. By targeting these enzymes with specific inhibitors, it is possible to disrupt the DAP pathway leading to the inhibition of bacterial growth and viability.¹⁵³⁻¹⁵⁵

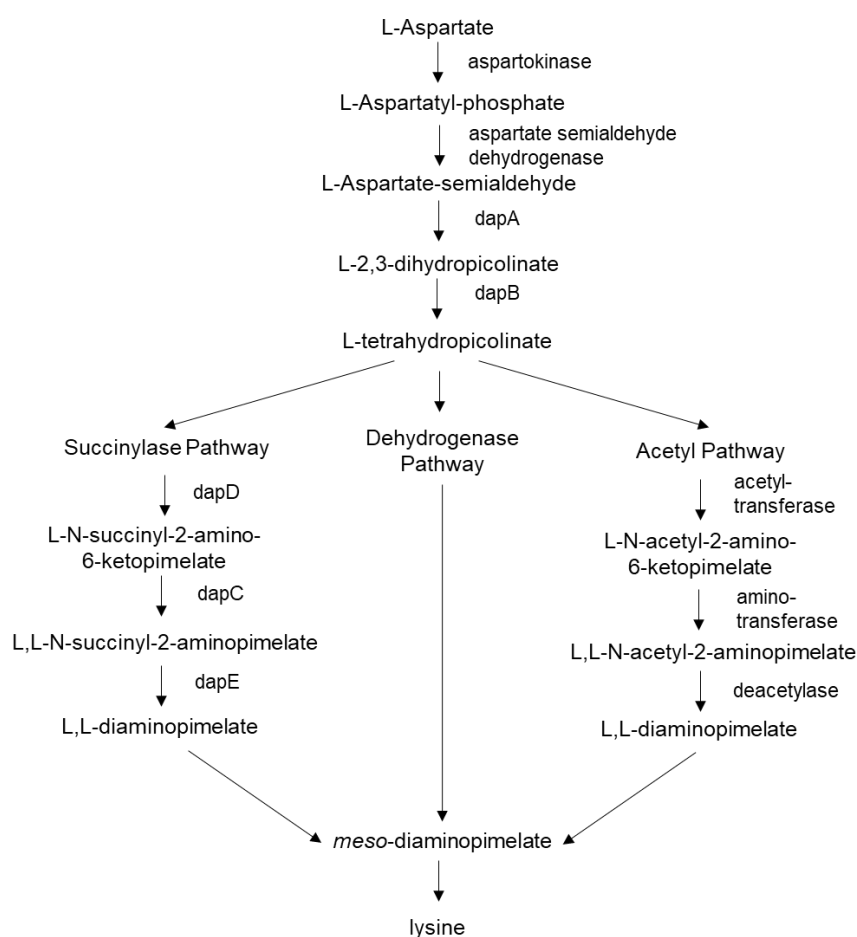


Figure 51: Bacterial biosynthesis of *meso*-DAP and Lysine.

The inhibition of cell wall biosynthesis has long been recognised as an effective approach to target bacterial infections.^{156, 157} Antibiotics such as β -lactams^{18, 158} and

glycopeptides (e.g. vancomycin)¹⁵⁹ have been shown to inhibit key steps in peptidoglycan synthesis, leading to antibacterial activity. However, the emergence of bacterial resistance to these antibiotics has necessitated the exploration of alternative approaches.

2.3.2 Antibiotic properties of DAP pathway inhibitors

Structural analogues of diaminopimelic acid (DAP) have been extensively studied as potential inhibitors of enzymes in the DAP pathway, in an effort to develop new antibiotics.^{120, 160, 161} In particular, the development of small molecules that mimic *meso*-DAP and inhibit cell wall biosynthesis holds promise as a broad-spectrum antibiotic against both gram-positive and gram-negative bacteria.¹⁶²⁻¹⁶⁴ Among them, compounds **146** and **147** have shown inhibition of *meso*-DAP dehydrogenase¹²⁰ (**Figure 52**), a critical enzyme involved in the biosynthesis of diaminopimelic acid/lysine. Additionally, compounds **148** and **149** have demonstrated significant antibacterial activity as inhibitors of L,L-DAP epimerase.¹⁶⁵ Notably, compounds **150** and **151** have emerged as particularly promising inhibitors, exhibiting a preliminary 75% inhibition for antibacterial growth.¹⁶⁵ These findings highlight the potential of DAP analogues as antimicrobial agents and advancements in the exploration and development of novel antibiotics targeting the DAP pathway.

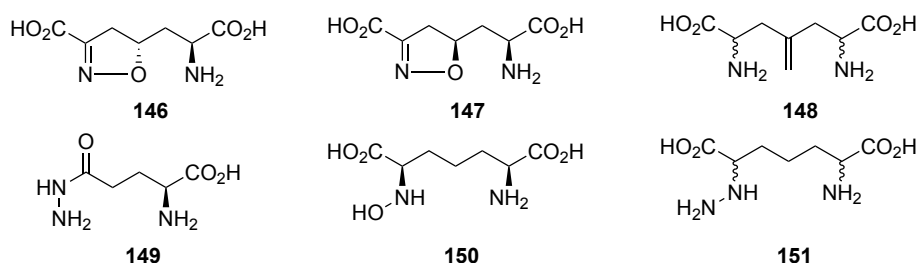


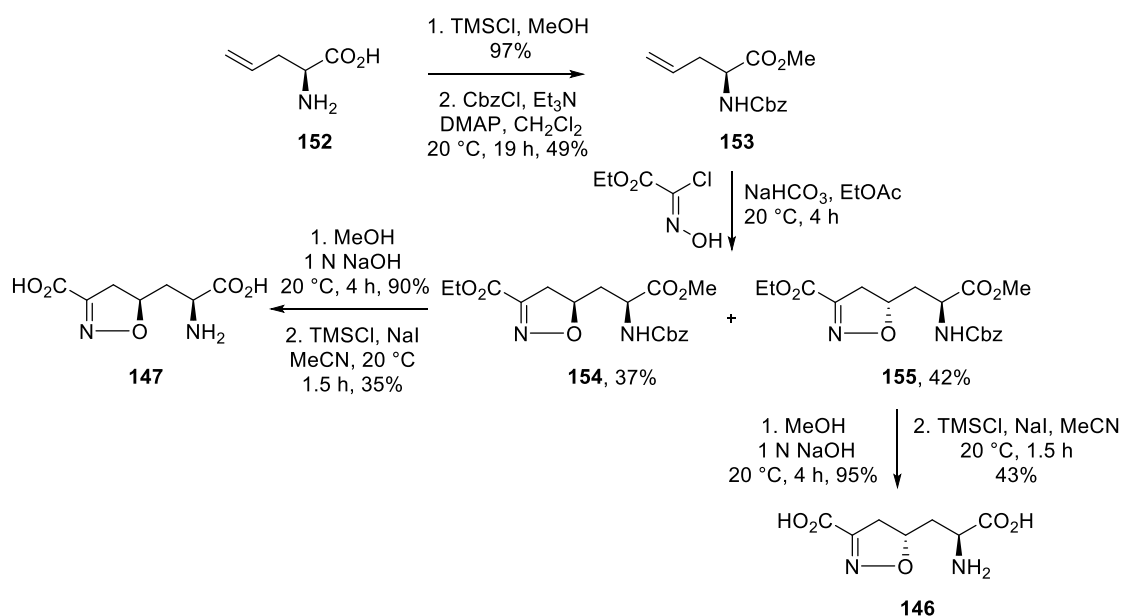
Figure 52: Analogues of DAP have potent biological activity.

2.3.2.1 Synthesis of diaminopimelic analogues

The development of inhibitors targeting the DAP pathway requires the stereoselective synthesis of DAP analogues and derivatives to establish the requisite stereogenic centres in these syntheses. Three general strategies have been employed; the use of chiral auxiliaries,^{163,166,167} the coupling of two fragments derived from the chiral pool,¹⁶⁸⁻¹⁷⁰ or the asymmetric reduction of an intermediate with one stereogenic centre already established.¹⁷¹⁻¹⁷⁴

2.3.2.2 Synthesis of protected DAP analogues

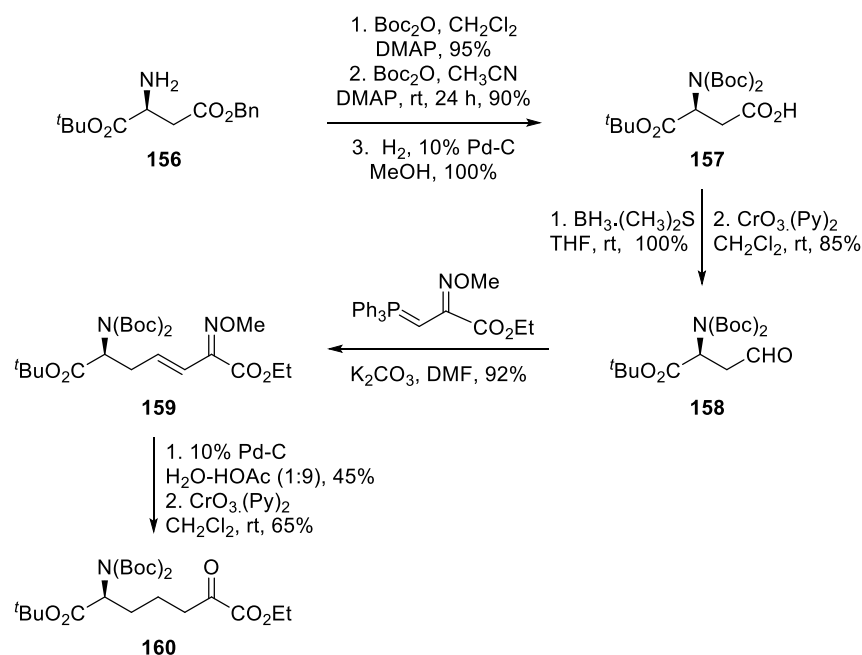
An early set of analogues of DAP, were isoxazoline derivatives **146** and **147**, reported by Zhang and co-workers.¹⁷⁵ The key step involved the 1,3-dipolar cycloaddition of protected allylglycine derivative **153** with a nitrile imine, derived from an oxime chloride under basic conditions, which gave a diastereomeric mixture of isoxazolines (**Scheme 45**). Separated diastereomer **154** was hydrolysed to afford the diacid in quantitative yield. Removal of the Cbz-protecting group using TMSCl and NaI gave *meso*-DAP analogue **147** (35% yield). Similarly, hydrolysis and deprotection of compound **155** gave compound **146** in 43% yield. The isoxazoline ring of compounds **146** and **147** was designed to mimic the imine intermediate of the *meso*-DAP dehydrogenase mechanism, thus allowing these compounds to act as active site inhibitors.¹⁷⁶ This enhanced understanding of the inhibitory mechanisms of DAP analogues towards *meso*-DAP dehydrogenase offered valuable insight for the future development of potent inhibitors targeting this enzyme.



Scheme 45: Synthetic route to isoxazoline analogues of *meso*-DAP.

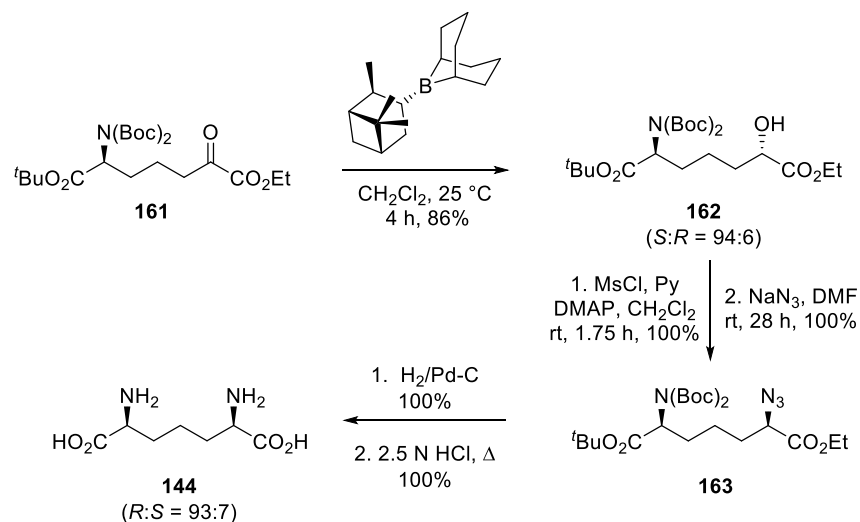
Several strategies have been developed for the synthesis of *meso*-DAP and protected analogues for peptide synthesis. Roberts and Chan described a new asymmetric synthesis of *meso*-DAP using a chiral pool approach (**Schemes 46 and 47**).¹⁷⁷ Protected aspartic acid analogue **156**, was converted to aldehyde **158** using a standard series of protecting groups and a reduction and oxidation sequence. Aldehyde **158** was then chain-extended via a Wittig reaction using a stabilised

phosphorane, bearing an oxime moiety. Hydrogenation of the resulting olefinic oxime under acidic conditions and oxidation of **159** gave α -keto ester **160** in 65% yield.



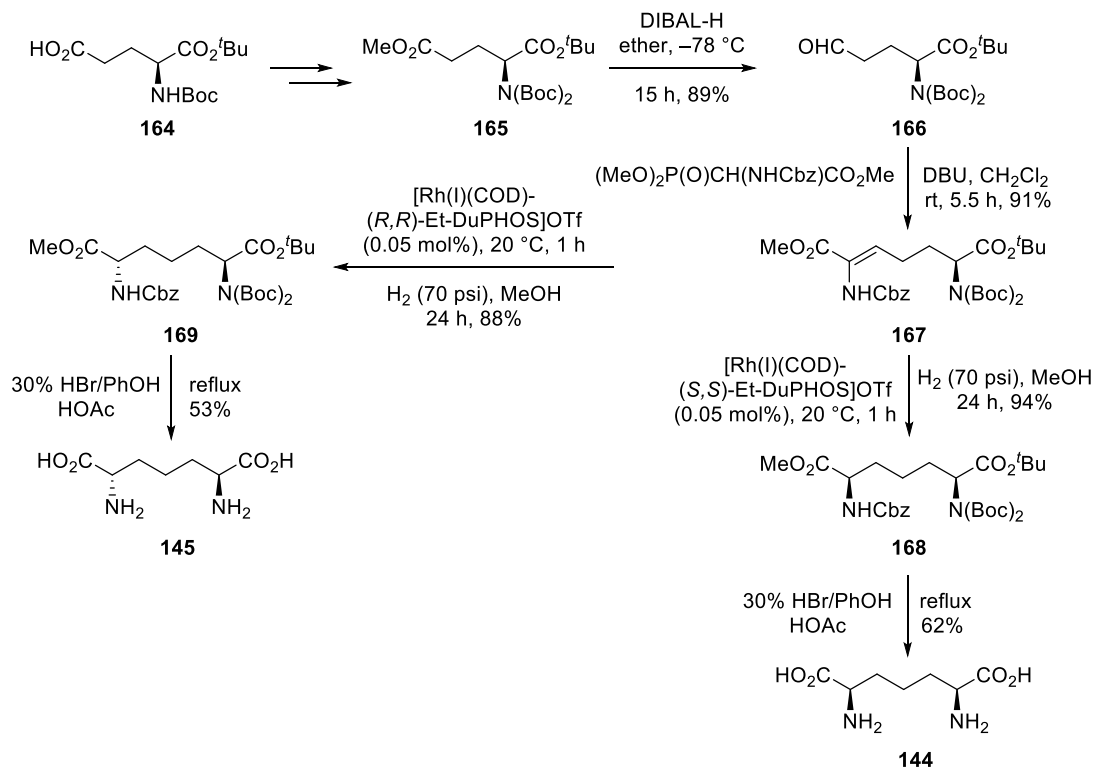
Scheme 46: Synthesis of α -keto ester **160** using a chiral pool approach.

The resulting α -keto ester **161** was subjected to an asymmetric reduction using (*R*)-alpine borane (**Scheme 47**). Activation of the secondary alcohol of **162** as a mesylate and displacement with sodium azide, gave azide **163** in quantitative yield over the two steps. Reduction of the azide and removal of the protecting groups under acidic conditions allowed completion of the synthetic route and access to *meso*-DAP **144**.



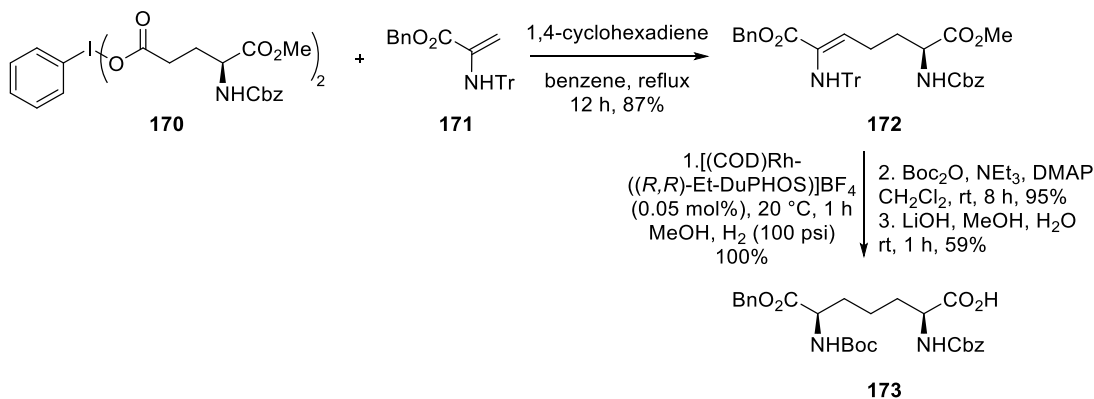
Scheme 47: Asymmetric reduction, introduction of nitrogen functionality and deprotection to *meso*-DAP **144**.

Hruby and co-workers have also reported a method for the synthesis of *meso*-DAP **144** and L,L-DAP **145** through asymmetric hydrogenation using Burk's catalyst as the key step (**Scheme 48**).¹⁷⁴ The rhodium-catalysed asymmetric hydrogenation of dehydroamino acid produced DAP compounds with orthogonal protecting groups in high ee (>95%). The synthesis started from commercially available Boc-protected glutamic acid *tert*-butyl ester **164** as the starting material. Methyl ester reduction of compound **165** using diisobutylaluminum hydride (DIBAL-H) at $-78\text{ }^\circ\text{C}$, resulted in the formation of aldehyde **166** in excellent yield (89%). Subsequently, aldehyde **166** underwent Horner-Wadsworth-Emmons (HWE) olefination with a phosphonate ester and DBU, leading to the synthesis of dehydroamino acid **167** (*Z/E* >95:5). Asymmetric hydrogenation of **167** using rhodium(I) catalysts with different chiral ligands gave **168** and **169** in 94% and 88% yields, respectively. Importantly, compounds **168** and **169** represent orthogonally protected versions of *meso*- and L,L-DAP that could be used for selective peptide synthesis. Removal of the protecting groups under reflux with 30% HBr in acetic acid and phenol gave *meso*- and L,L-DAP **144** and **145** in 62 and 53% yields, respectively.



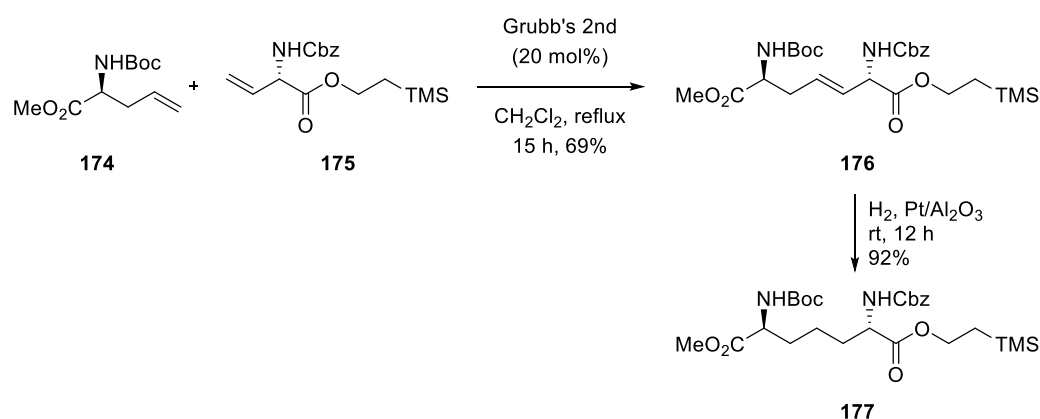
Scheme 48: Stereoselective synthesis of *meso*-DAP **144** and L,L-DAP **145**.

Vederas and co-workers developed a synthesis of protected *meso*-DAP analogues via the conjugate addition reaction of a protected amino acid radical derived from diacyloxyiodobenzenes **170** with dehydroamino acid **171**. This synthetic approach allowed for the preparation of selectively protected DAP derivatives (**Scheme 49**). The unsaturated adduct **172** was subjected to stereoselective hydrogenation resulting in the formation of the orthogonally protected *meso*-DAP derivative **173** in good overall yield.¹⁶⁹



Scheme 49: Synthesis of a protected *meso*-DAP derivative.

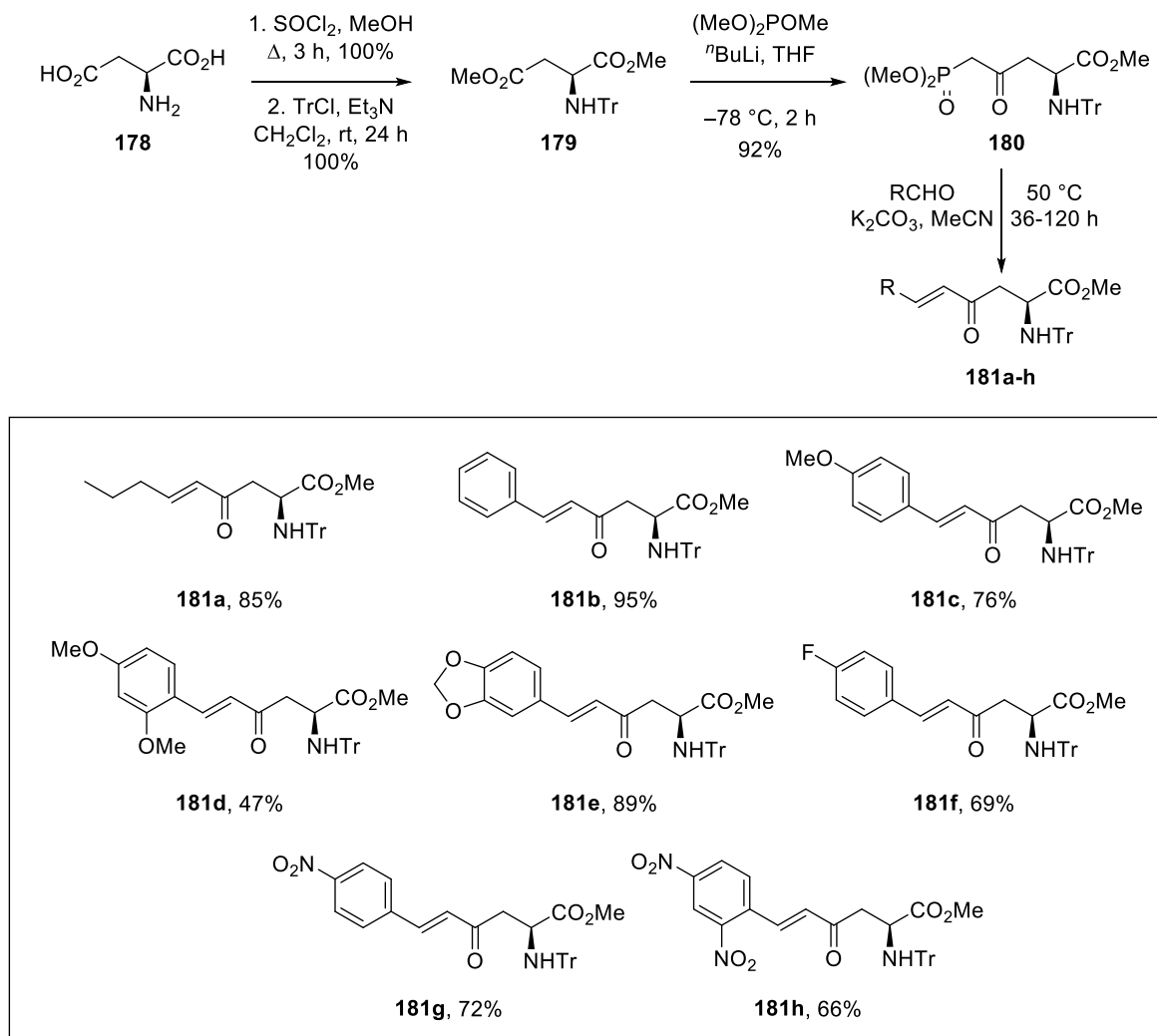
A modified strategy that uses a selective cross-metathesis reaction have been reported by Blicher and co-workers (**Scheme 50**).¹⁷⁶ In this case, reaction between (*S*)-allylglycine derivative **174** and (*S*)-vinylglycine derivative **175** in the presence of Grubbs 2nd generation catalyst provided the cross-metathesis adduct **176** in 69% yield. Hydrogenation of the metathesis product with Pt/Al₂O₃ furnished L,L-DAP derivative **177** in 92%.



Scheme 50: Cross metathesis protocol for the synthesis of a L,L-DAP analogue.

2.3.3 Previous Work in the Sutherland Group.

Previous work in the Sutherland group has investigated a simple and efficient regioselective method for the preparation of enone-derived amino acids.^{112,113,178,179} It should be noted that these compounds are prepared from simple starting materials and readily accessible aldehydes via a Horner-Wadsworth-Emmons (HWE) reaction with a phosphonate-derived amino acid.^{113,178} For example, L-aspartic acid derivative **178** was converted to phosphonate ester derivative **180**, using a regioselective reaction of the β -methyl ester with the anion of dimethyl methyl phosphonate (**Scheme 51**). Subsequent HWE reaction under mild basic conditions, with a range of aldehydes successfully synthesised enone-derived α -amino acids.¹¹³



Scheme 51: Synthetic approach to a diverse library of α -amino acids enones.

More recently, the Sutherland group has investigated the use of these enones for a one-pot condensation/aza-Michael process to produce heteroaromatic fluorescent amino acids as new biological probes (**Figure 53**).¹⁷⁹

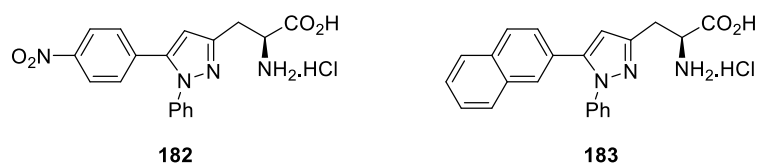
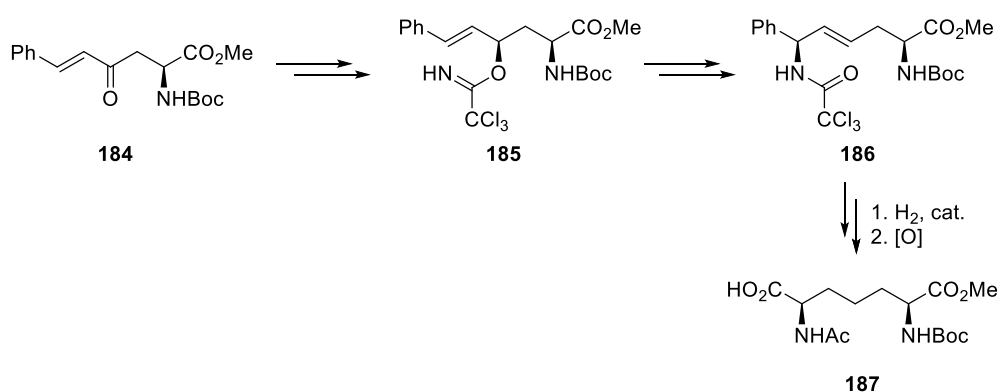


Figure 53: Fluorescent pyrazole-derived α -amino acids.

2.3.4 Project Aims

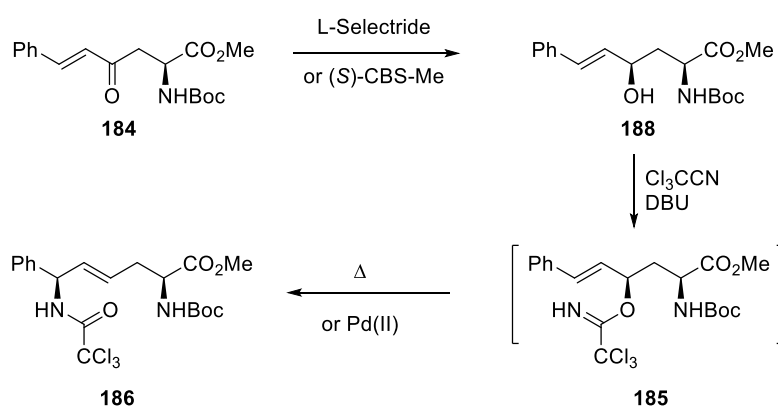
The aim of this project is the utilisation of enone-derived α -amino acids as key intermediates for a novel stereoselective synthesis of *meso*-DAP **144** and L,L-DAP **145** (**Scheme 52**). The approach would involve subjecting the enone-derived amino acids to a stereoselective reduction, resulting in the formation of an allylic alcohol. Subsequently, an allylic trichloroacetimidate would be formed, followed by an Overman rearrangement, which would allow the formation of the C-N bond with retention of stereochemistry. Hydrogenation of the alkene and oxidation of the phenyl ring would generate the core structure of a protected *meso*-DAP derivative. By switching the stereoselective outcome of the ketone reduction, a protected L,L-DAP derivative would also be accessible by this approach.



Scheme 52: Proposed synthetic pathway to protected *meso*-DAP **187**.

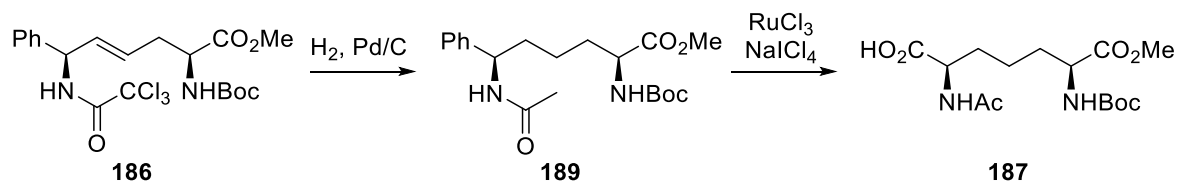
A key step of the proposed synthetic route involves the stereoselective reduction of the ketone moiety of the enone-derived α -amino acid. One approach is to use the chirality already present in the compound to induce a diastereoselective reduction. There are several studies in the literature which have investigated the reduction of 4-keto-2-amino acids with L-selectride and showed good selectivity for the *syn*-product.¹⁸⁰⁻¹⁸² In this project, the use of L-selectride for chemoselective reduction of the enone amino acid would be initially tested. Specific conditions would be developed to promote the formation of the *syn*-product while preventing 1,4-reduction or lactonisation of the resulting alcohol with the ester, as observed under some conditions. Other standard reducing agents would also be investigated as part of this study to develop an understanding of the limits of this reduction. Should this approach not allow a highly selective reduction, then the use of a chiral reducing agent would be investigated (**Scheme 53**). Previous work in the group has shown

that CBS-reagents work well with enones,¹⁸³ and in the case of this current substrate, the use of (*S*)-CBS-Me would represent an example of a matched pairing between chiral substrate and chiral reagent. This should result in a highly diastereoselective reduction. Following the successful reduction of the ketone, the allylic alcohol would then be converted to the allylic trichloroacetimidate under standard conditions and subjected to an Overman rearrangement under thermal conditions.¹⁸⁴⁻¹⁸⁶ As is commonly observed with this type of [3,3]-sigmatropic rearrangement, the stereochemistry of the allylic alcohol will be conserved during the transformation. As well as a thermal Overman rearrangement, a palladium(II)-catalysed process would also be studied to determine its efficiency.



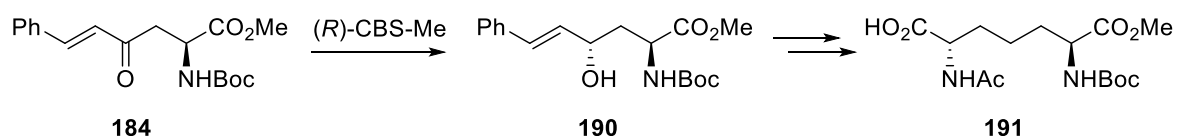
Scheme 53: The key steps for the synthesis of the *meso*-DAP core.

The final stage of the total synthesis of *meso*-DAP requires the oxidation of the phenyl ring to a carboxylic acid (**Scheme 54**). Before this reaction, the alkene will be hydrogenated. Under these conditions (H_2 , Pd/C), the C–Cl bonds of the trichloroacetamide will likely be cleaved, generating the acetyl group.¹⁸³ This would result in the two amino groups orthogonally protected. Phenyl ring oxidation will be done using ruthenium chloride in the presence of sodium periodate, as originally reported by Sharpless and coworkers.¹⁸⁷



Scheme 54: The final stage of the total synthesis of *meso*-DAP.

Once an approach has been optimised for the preparation of a *meso*-DAP analogue, then a similar route will be utilised for the preparation of L,L-DAP (**Scheme 55**). In this case, an asymmetric reduction of an enone will be performed using (*R*)-CBS-Me.¹⁸³ While this will be an example of a mismatched pairing between a chiral substrate and chiral reagent, it should still be selective enough to give the desired diastereoisomer as the major product. Then, using the optimised route, the Overman rearrangement, hydrogenation and oxidation steps will provide L,L-DAP analogue **191**.



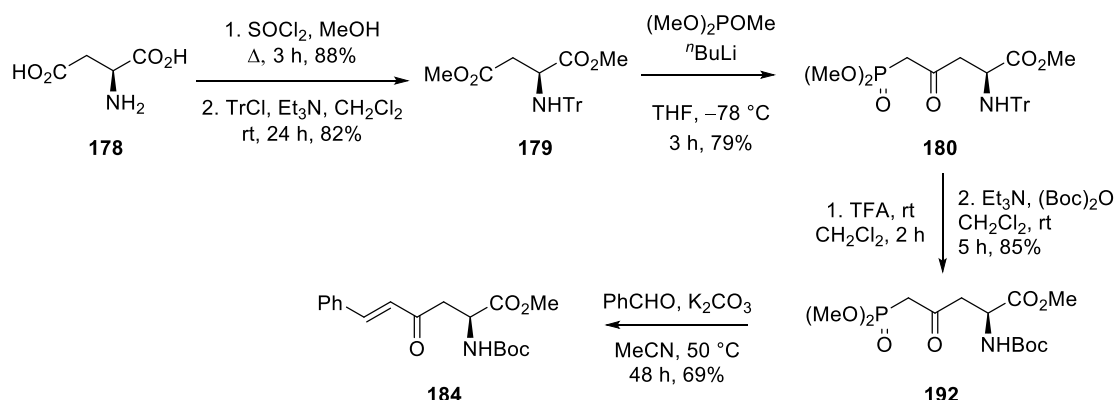
Scheme 55: Preparation of the L,L-DAP series.

2.3.5 Synthesis of Diaminopimelic acid

2.3.5.1 Synthesis of enone-derived α -amino acid **184**

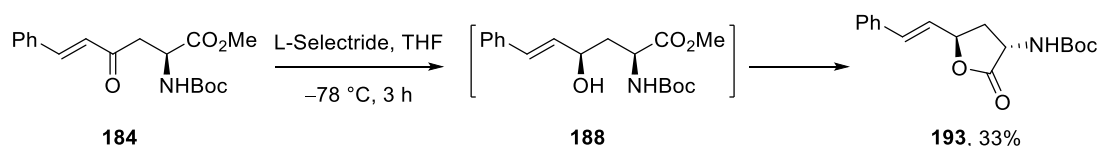
Initially, L-aspartic acid **178** was converted to the corresponding dimethyl ester using methanol and thionyl chloride (**Scheme 56**). The amino group was then protected using trityl chloride and triethylamine. This gave fully protected aspartate **179** in high yield over the two steps.¹⁷⁸ Regioselective reaction of the β -dimethyl ester of aspartate **179** with the anion of dimethyl methylphosphonate, formed by deprotonation with *n*-butyl lithium, gave β -ketophosphonate ester **180** in 79% yield.¹¹³ Trifluoroacetic acid (TFA) was used to remove the trityl group. Reprotection of the amine with di-*tert*-butyl dicarbonate allowed incorporation of the smaller protecting group. Previous work had shown that the presence of the very bulky *N*-trityl protecting group hindered most reactions of the enone moiety.^{37,39} The Boc-protected phosphonate ester **192** was then reacted with benzaldehyde via the HWE

reaction using potassium carbonate as a base and under standard conditions.¹¹³ This gave *E*-enone **184** with high stereoselectivity in 69% yield.



Scheme 56: Optimised synthetic route to enone **184**.

Initial studies of the stereoselective reduction of enone **184** with L-selectride were investigated.¹⁸² This reaction did allow reduction to the *syn*-product, however, on isolation, only lactone **193** was recovered in 33% yield (7:1 ratio with the minor *anti*-lactone) (**Scheme 57**). The expectation was that the reaction could potentially display diastereoselectivity, favouring attack from the less hindered back face. This would lead to the formation of the new *R*-stereocenter **193**. The key challenge observed was the occurrence of lactonisation, that had also been reported by Jackson.¹⁸⁸ Previous research within the group had similarly shown analogous outcomes when employing L-selectride with the methyl ester analogue. This result indicated the necessity for a more bulky ester group in order to prevent lactonisation.



Scheme 57: Lactonisation of desired *syn*-hydroxy amino ester.

Christina Bell, a final year MSci student in the group, originally investigated the reduction of enone **184** using L-selectride and confirmed the stereochemical outcome via Nuclear Overhauser Effect³⁸ spectroscopy of the major lactone **193** and the minor lactone **194** (**Figure 54**). When irradiating the hydrogen atom located at C2 of the major lactone, a strong coupling (1.3%) was observed with a hydrogen

atom at C3, specifically the one at 2.46 ppm. Subsequently, upon irradiation of the C4 hydrogen atom, it exhibited a strong correlation (0.7%) with the other C3 hydrogen atom, consistent with expectations, and demonstrated an even more pronounced 1.1% correlation with the NH hydrogen. Importantly, no correlation was noted between the hydrogens on C2 and C4, providing conclusive evidence for the identity of this molecule as originating from the *syn*-hydroxy amino ester. Conversely, when applying the same irradiation to the minor lactone, a substantial correlation of 0.8% was observed between the C2 and C4 hydrogen atoms. Furthermore, they both exhibited strong coupling (1.0%) to the hydrogen at 2.97 ppm at C3.

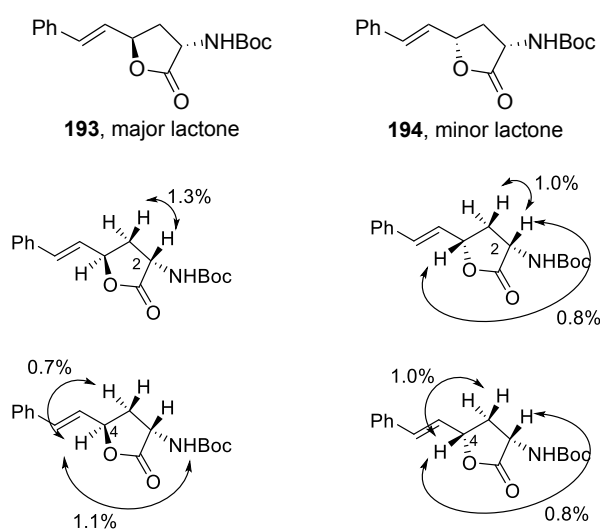
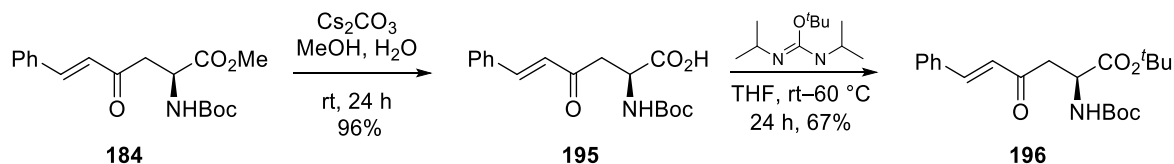


Figure 54: Results of NOE spectroscopy of the major and minor lactones.

2.3.5.2 Synthesis of *t*-butyl ester analogue **186**

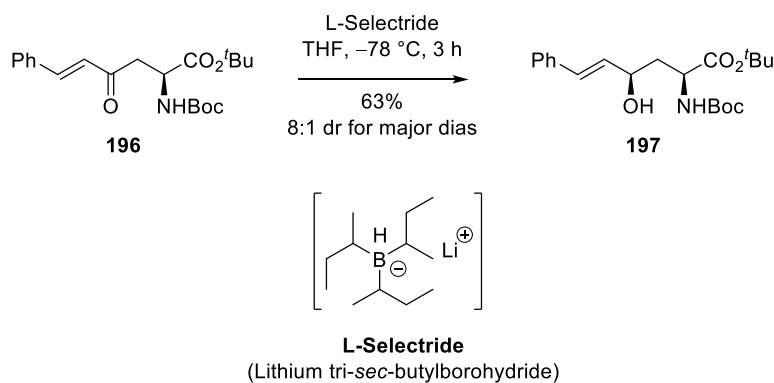
To overcome the previous issues of lactonisation with methyl ester analogue **184**, it was proposed to change the ester moiety to a *t*-butyl group (**Scheme 58**). It was proposed that this would prevent lactonisation, following L-selectride reduction. To access a *t*-butyl ester analogue quickly, methyl ester derivative **184** was hydrolysed using cesium carbonate. Under mild conditions, this gave the corresponding carboxylic acid **195** in 96% yield. The *t*-butyl ester was then formed using commercially available *O*-*tert*-butyl-*N,N*-diisopropylisourea. Using a previously reported method, this gave the desired *t*-butyl ester analogue of the enone-derived α -amino acid, compound **196** in 67% yield.¹⁸⁹



Scheme 58: Synthesis of *t*-butyl ester analogue **196**.

2.3.5.3 Stereoselective reduction of enone-derived α -amino acid **196**

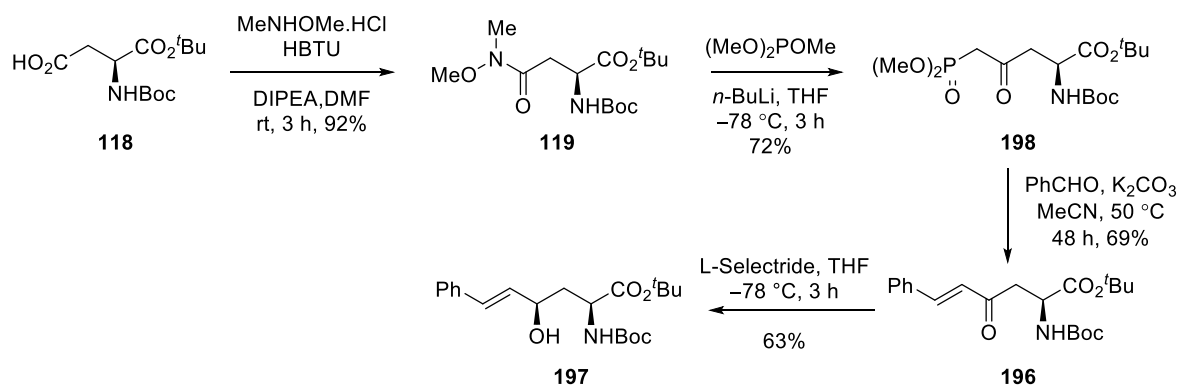
The next stage of the project investigated the stereoselective ketone reduction of *t*-butyl ester analogue **196** using L-selectride (**Scheme 59**).¹⁸² Reaction of the bulky L-selectride with **196** resulted in chemoselective reduction of the ketone from an open, non-chelated transition state and gave the *syn*-diastereomer as the major product with a diastereomeric ratio of 8:1. After separation of the diastereomers, the major product was isolated in 63% yield. It is proposed that the L-selectride reacts from the least hindered face of the enone, opposite to the *N*-Boc amino group. Having shown that *t*-butyl ester analogue could undergo reduction without lactonisation, it was decided that a more optimal route should be developed to access compound **197**. The current route required nine steps from L-aspartic acid, with six of these involving protection or deprotection reactions.



Scheme 59: Stereoselective reduction of enone **196**.

2.3.6 New approach for the efficient synthesis of enone-derived α -amino acid **196**.

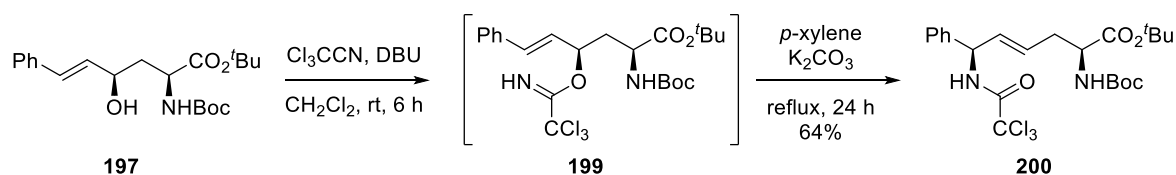
As described in Chapter 2, Weinreb amide **119** was prepared in one step from commercially available *N*-Boc-L-aspartic acid *t*-butyl ester **118**. This was used to prepared ynones by nucleophilic attack of the Weinreb amide with the lithium salt of alkynes. As this was highly efficient, it was proposed that a more efficient synthesis of enone **196** could be achieved by reaction of the same Weinreb amide with the lithium anion of dimethyl methylphosphonate (**Scheme 60**). As described before, *N*-Boc-L-aspartic acid *t*-butyl ester **118** was converted to Weinreb amide intermediate **119** by reaction of dimethyl hydroxylamine, in the presence of HBTU and DIPEA.¹¹⁶ This gave Weinreb amide **119** in 92% yield. Regioselective reaction of Weinreb amide **119** with dimethyl methylphosphonate anion led to the formation of β -ketophosphonate ester **198** in a 72% yield.¹¹³ Subsequently, employing standard conditions, the Horner-Wadsworth-Emmons reaction of Boc-protected phosphonate ester **198** with benzaldehyde, in the presence of potassium carbonate, gave *E*-alkene **196** as the sole product in 69% yield.¹¹³ Finally, as described above, L-selectride reduction of enone **196** gave allylic alcohol **197** in 63% yield.¹⁸² Overall, this new approach allowed the synthesis of allylic alcohol **197** in four steps versus nine steps for the previous route.



Scheme 60: A more efficient approach for the synthesis of allylic alcohol **197**.

2.3.6.1 Installation of the second amino group using an Overman rearrangement.

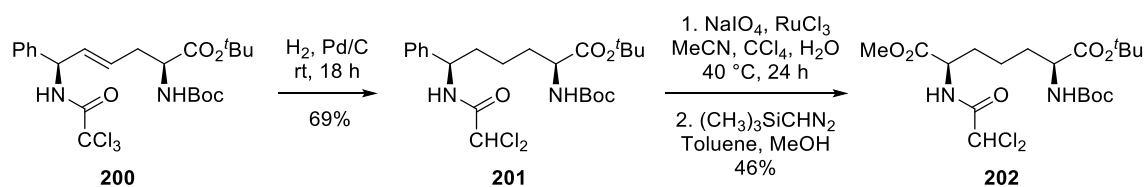
Following the successful development of a stereoselective reduction, the next stage involved the incorporation of the second amino group using an Overman rearrangement.⁴⁵ Allylic alcohol **197** was transformed into allylic amine **200** by an Overman rearrangement.⁴⁵ Allylic alcohol **197** was transformed into allylic amine **200** by an Overman rearrangement in two-steps (**Scheme 61**).¹⁸³ Initially, allylic trichloroacetimidate **199** was formed by reaction of **197** with trichloroacetonitrile and DBU. Thermal rearrangement of allylic trichloroacetimidate **199** gave allylic trichloroacetamide **200**, as a single diastereomer in 64% yield over the two steps. As thermal [3,3]-sigmatropic rearrangements are known to undergo concerted reactions, we propose that allylic trichloroacetamide is formed with retention of configuration as shown by the reacting conformer.



Scheme 61: Overman rearrangement of allylic alcohol **197**.

2.3.6.2 Completion of the synthetic route to a protected *meso*-DAP analogue.

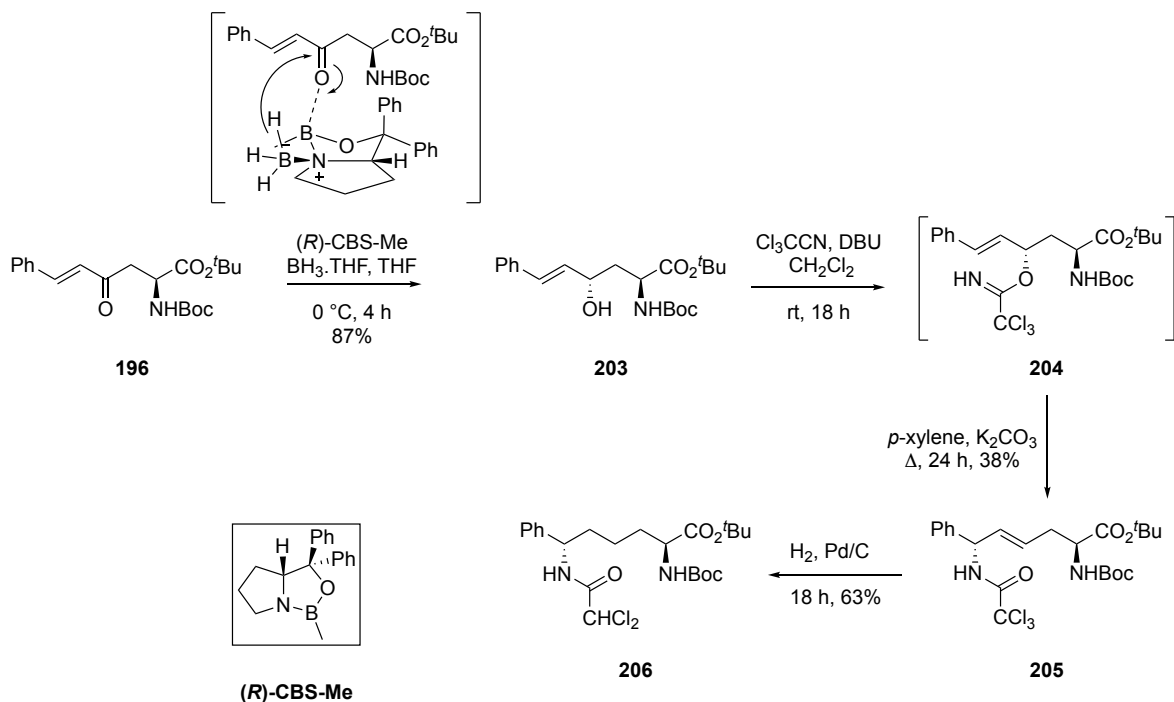
To complete the synthesis of a protected *meso*-DAP analogue required hydrogenation of the alkene, oxidation of the phenyl moiety and esterification of the resulting carboxylic acid (**Scheme 62**). Initially, allylic trichloroacetamide **200** was subjected to a hydrogenation reaction using atmospheric hydrogen and palladium on carbon, under standard conditions.¹⁸³ This resulted in hydrogenation of the alkene and partial reduction of the trichloroacetamide group. This gave compound **201** in 69% yield. Using the Sharpless protocol, the phenyl moiety of compound **201** was then oxidised using catalytic ruthenium(III) chloride (25 mol%) and sodium periodate.^{187,190} The reaction required a temperature of 40 °C and a reaction time of 24 h to reach full conversion. As the carboxylic acid was difficult to purify, it was proposed to isolate this as the corresponding methyl ester. Reaction with trimethylsilyldiazomethane gave the final product in 46% yield over the two steps.^{191,192} This completed the nine-step synthesis of a protected *meso*-DAP analogue using a stereoselective reduction and an Overman rearrangement as the key steps.



Scheme 62: The final stage of the synthesis of a protected *meso*-DAP analogue.

2.3.7 Synthesis of protected L,L-DAP 145

With the process for synthesis of *meso*-DAP in hand, we turned our attention to the diastereoselective synthesis of L,L-DAP **145** using a similar intermediate. This was prepared in a three-step approach from previously synthesised *E*-enone-derived amino acid **196** (**Scheme 63**). A study focused on the stereoselective reduction of the enone intermediate **196** using CBS oxazaborolidine.¹⁹³ This investigation aimed to explore the diastereoselective outcome for the synthesis of L,L-DAP. The results showed that under standard conditions,¹⁸³ reduction of **196** using (*R*)-CBS-Me in the presence of borane-THF gave (2*S*)-allylic alcohol **203** as the major product (9:1 dr) in excellent yield (87%). Subsequent Overman rearrangement of the resulting allylic alcohol provided access to trichloroacetamide **205**.¹⁸³ The synthesis of L,L-DAP was further progressed by hydrogenation of the alkene and trichloroacetamide group, ultimately yielding compound **206** in 63% yield. Due to time constraints, the last two steps of the synthesis of L,L-DAP is not yet complete. Future work is dedicated to exploring and optimising these last two steps in order to successfully complete the synthetic route for L,L-DAP.



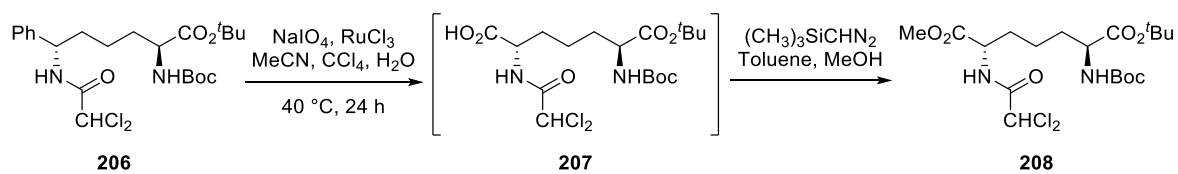
Scheme 63: The synthesis of a protected L,L-DAP.

2.3.8 Summary

A new synthesis of a protected *meso*-DAP analogue framework has been developed. Following the synthesis of an enone-derived amino acid, the key steps involved a stereoselective reduction of the enone using L-selectride, which gave a (2*R*)-allylic alcohol. Conversion to an allylic trichloroacetimidate and Overman rearrangement allowed the introduction of the second amino group. Finally, hydrogenation, oxidation and esterification completed a new nine-step approach for the synthesis of *meso*-DAP. Furthermore, this methodology was explored for the synthesis of L,L-DAP via an alternative stereoselective reduction of the enone intermediate. In this alternate approach, the use of the chiral reducing agent, (*R*)-CBS-Me in the presence of borane-THF led to the formation of (2*S*)-allylic alcohol as the major product. Use of the Overman rearrangement once again yield the corresponding allylic trichloroacetamide.

2.3.9 Future Work

To complete the synthesis of L,L-DAP analogue requires oxidation of the phenyl group and esterification of the resulting carboxylic acid (**Scheme 64**). Once this route is complete, a larger scale synthesis of either compound would provide material to investigate the synthesis of dipeptide analogues, through selective deprotection of one of the functional groups.



Scheme 64: The final stage of the synthesis of a protected L,L-DAP analogue.

3.0 Experimental

3.1 General Experimental

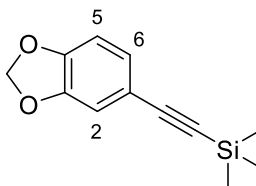
All reagents and starting materials were obtained from commercial sources and used as received. Dry solvents were purified using a PureSolv 500 MD solvent purification system. All reactions were performed under an atmosphere of argon unless otherwise mentioned. Brine refers to a saturated solution of sodium chloride. Flash column chromatography was carried out using Fisher matrix silica 60 (40 – 63 μM). Merck aluminium-backed plates pre-coated with silica gel 60 (UV₂₅₄) were used for thin-layer chromatography and visualised by staining with KMnO_4 , vanillin or ninhydrin. ^1H NMR and ^{13}C NMR spectra were recorded on a Bruker DPX 400 or 500 spectrometer with chemical shift values in ppm relative to tetramethylsilane ($\delta_{\text{H}} = 0.00$ ppm and $\delta_{\text{C}} = 0.00$ ppm), or solvent signals as the internal standard, for ^1H NMR spectra: CHCl_3 $\delta_{\text{H}} = 7.26$ ppm, DMSO, $\delta_{\text{H}} = 2.50$ ppm or CH_3OH , $\delta_{\text{H}} = 3.31$ ppm. For ^{13}C NMR spectra CDCl_3 $\delta_{\text{C}} = 77.2$ ppm DMSO- d_6 $\delta_{\text{C}} = 39.5$ ppm and $\text{CD}_3\text{OD}-d_4$ $\delta_{\text{C}} = 49.0$ ppm. Hydrogen and carbon assignments are based on two-dimensional COSY, HSQC, HMBC and DEPT experiments. Mass spectra were obtained using a JEOL JMS-700 spectrometer for EI and CI or Bruker Microtof-q or Agilent 6125B for ESI. Infrared spectra were obtained neat using a Shimadzu IR Prestige-21 spectrometer or Shimadzu 8400S spectrometer. Melting points were determined on a Reichert platform melting point apparatus or Stuart Scientific melting point apparatus. Optical rotations were determined as solutions irradiating with the sodium D line ($\lambda = 589$ nm) using an Autopol V polarimeter. $[\alpha]_{\text{D}}$ values are given in units $10^{-1} \text{ deg cm}^{-1} \text{ g}^{-1}$.

Absorption and emission data were recorded on one of two instruments:

1. UV-Vis spectra were recorded on a Pekin Elmer Lamda 25 instrument. Fluorescence spectra were recorded on a Shimadzu RF-5301PC spectrofluorometer. Emission data were measured using excitation and emission bandpass filters of 10 nm.
2. Both UV-Vis spectra and fluorescence spectra were recorded on a Horiba Duetta Fluorescence and Absorbance spectrometer. Absorbance spectra were recorded with an integration time of 0.05 s, and a band pass of 5 nm. Fluorescence spectra for pyrimidine derived amino acids were recorded with an excitation and emission band pass of 10 nm, an integration time of 0.1 or 2 s, and with detector accumulations set to 1. Respective standard samples were recorded with the same parameters.

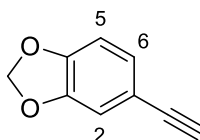
3.2 Aryl substituted pyrimidine derived α -amino acids experimental

1-(3',4'-Methylenedioxyphenyl)-2-trimethylsilylacetylene¹⁹⁴



To bis(triphenylphosphine)palladium(II) dichloride (0.102 g, 0.145 mmol) and copper iodide (0.0550 g, 0.29 mmol) in *N,N'*-dimethylformamide (0.6 mL) was added 4-bromo-1,2-(methylenedioxy)benzene (0.350 mL, 2.90 mmol) and triethylamine (17 mL). The solution was degassed and trimethylsilylacetylene (0.600 mL, 4.35 mmol) was added. The reaction mixture was stirred at 90 °C and after 6 h, further bis(triphenylphosphine)palladium(II) dichloride (0.102 g, 0.145 mmol) and copper iodide (0.0550 g, 0.290 mmol) were added. The reaction mixture was stirred at 90 °C for a further 18 h. Upon cooling, the reaction mixture was concentrated *in vacuo*. Purification by flash column chromatography eluting with 0–2% ethyl acetate in hexane gave 1-(3',4'-methylenedioxyphenyl)-2-trimethylsilylacetylene (0.569 g, 90%) as a yellow oil. Spectroscopic data were consistent with the literature.¹⁹⁴ δ_{H} (500 MHz, CDCl_3) 0.23 (9H, s, 3 \times CH_3), 5.96 (2H, s, OCH_2O), 6.73 (1H, d, J 8.0 Hz, 5'-H), 6.91 (1H, d, J 1.5 Hz, 2'-H), 7.00 (1H, dd, J 8.0, 1.5 Hz, 6'-H); δ_{C} (126 MHz, CDCl_3) 0.2 (3 \times CH_3), 92.4 (C), 101.4 (CH_2), 105.1 (C), 108.5 (CH), 112.0 (CH), 116.5 (C), 126.9 (CH), 147.4 (C), 148.2 (C); m/z (EI) 218 (M^+ , 80%), 203 (100).

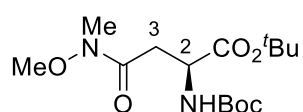
3,4-Methylenedioxyphenylethyne¹⁹⁵



To 1-(3',4'-methylenedioxyphenyl)-2-trimethylsilylacetylene (0.695 g, 3.18 mmol) in methanol (20 mL) was added potassium carbonate (1.30 g, 9.55 mmol). The reaction was stirred at room temperature for 1 h, and then concentrated *in vacuo*. The resulting residue was diluted with ethyl acetate (40 mL), washed with water (3 \times 30 mL) and brine (30 mL), dried (MgSO_4), filtered, and concentrated *in vacuo*.

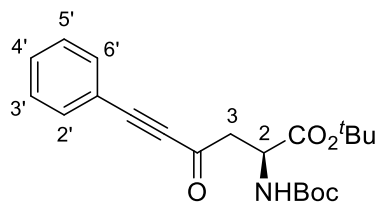
Purification by column chromatography eluting with 2% ethyl acetate in hexane gave 3,4-methylenedioxyphenylethyne as a yellow oil (0.320 g, 69%). Spectroscopic data were consistent with the literature.¹⁹⁵ δ_{H} (500 MHz, CDCl_3) 2.98 (1H, s, $\text{C}\equiv\text{CH}$), 5.97 (2H, s, OCH_2O), 6.75 (1H, d, J 8.0 Hz, 5-H), 6.93 (1H, d, J 1.5 Hz, 2-H), 7.02 (1H, dd, J 8.0, 1.5 Hz, 6-H); δ_{C} (126 MHz, CDCl_3) 75.6 (CH), 83.7 (C), 101.4 (CH_2), 108.4 (CH), 112.0 (CH), 115.3 (C), 126.9 (CH), 147.4 (C), 148.3 (C); m/z (EI) 146 (M^+ , 100%).

***tert*-Butyl (2*S*)-(tert-butoxycarbonylamino)-4-[methoxy(methyl)amino]-4-oxobutanoate (**119**)¹¹⁶**



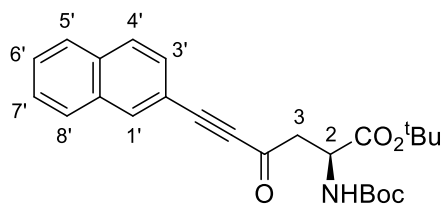
A mixture of 1-*tert*-butyl (2*S*)-(tert-butoxycarbonylamino)-4-butan-1,4-dioic acid (0.50 g, 1.76 mmol), *N,O*-dimethylhydroxyamine hydrochloride (0.24 g, 2.44 mmol), and *O*-(1*H*-benzotriazol-1-yl)-*N,N,N',N'*-tetramethyluronium tetrafluoroborate (0.73 g, 1.93 mmol) was stirred in *N,N*-dimethylformamide (3 mL) at 0 °C. Diisopropylethylamine (0.75 mL, 4.40 mmol) was then added dropwise. The mixture was stirred at room temperature for 3 h. An aqueous solution of 1 M sodium hydrogen sulfate (25 mL) was then added, and the mixture was extracted with ethyl acetate (3 × 20 mL). The combined organic layers were then washed with brine (3 × 20 mL), dried (MgSO_4), and concentrated under vacuum. Purification by flash column chromatography eluting with 20% ethyl acetate in dichloromethane gave *tert*-butyl (2*S*)-(tert-butoxycarbonylamino)-4-[methoxy(methyl)amino]-4-oxobutanoate **119** as a colourless oil (0.59 g, 92%). $[\alpha]_{\text{D}}^{20}$ -14.5 (c 0.6, MeOH) [lit.^{12b} $[\alpha]_{\text{D}}^{25}$ -12.3 (c 1.0, MeOH)]; δ_{H} (400 MHz, CDCl_3) 1.44 (9H, s, 3 × CH_3), 1.46 (9H, s, 3 × CH_3), 2.87 (1H, dd, J 16.8, 2.7 Hz, 3-*HH*), 3.14 (4H, m, 3-*HH* and NCH_3), 3.69 (3H, s, OCH_3), 4.43–4.47 (1H, m, 2-H), 5.67 (1H, d, J 8.3 Hz, NH); δ_{C} (101 MHz, CDCl_3) 27.9 (3 × CH_3), 28.3 (3 × CH_3), 32.0 (CH_3), 34.7 (CH_2), 50.4 (CH), 61.2 (CH_3), 79.4 (C), 81.7 (C), 155.7 (C), 170.5 (C), 171.8 (C); m/z (ESI) 355 (MNa^+ , 100%).

***tert*-Butyl (2*S*)-(tert-butoxycarbonylamino)-4-oxo-6-phenylhex-5-ynoate (120a)**



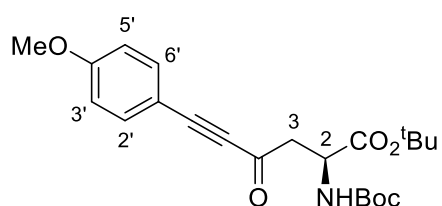
To a solution of phenylacetylene (0.20 mL, 1.9 mmol) in tetrahydrofuran (10 mL) at $-78\text{ }^{\circ}\text{C}$ was slowly added a solution of *n*-butyl lithium (2.5 M in hexane, 0.43 mL, 1.1 mmol). The mixture was stirred for 0.75 h and then added dropwise to a solution of *tert*-butyl (2*S*)-(tert-butoxycarbonylamino)-4-[methoxy(methyl)amino]-4-oxo butanoate **119** (0.12 g, 0.36 mmol) in tetrahydrofuran (25 mL) at $-78\text{ }^{\circ}\text{C}$. The reaction mixture was stirred at $-78\text{ }^{\circ}\text{C}$ for 1 h and then at $-20\text{ }^{\circ}\text{C}$ for 2 h. An aqueous 1 M solution of dipotassium hydrogen phosphate (10 mL) was added, and the mixture was extracted with diethyl ether (3 \times 30 mL). The combined organic layers were washed with brine (4 \times 30 mL) and dried (MgSO_4). After filtration, the solution was concentrated under vacuum. Purification by column chromatography eluting with 20% diethyl ether in petroleum gave *tert*-butyl (2*S*)-(tert-butoxycarbonylamino)-4-oxo-6-phenylhex-5-ynoate **120a** as a yellow oil (0.13 g, 89%). $[\alpha]_D^{20} -7.5$ (*c* 0.5, MeOH) [lit. ^{12b} $[\alpha]_D^{25} -3.8$ (*c* 1.0, MeOH)]; δ_{H} (400 MHz, CDCl_3) 1.45 (9H, s, 3 \times CH_3), 1.46 (9H, s, 3 \times CH_3), 3.18 (1H, dd, *J* 17.9, 4.6 Hz, 3-*HH*), 3.33 (1H, dd, *J* 17.9, 4.6 Hz, 3-*HH*), 4.49–4.53 (1H, m, 2-H), 5.42 (1H, d, *J* 8.1 Hz, NH), 7.36–7.42 (2H, m, 2 \times ArH), 7.43–7.50 (1H, m, ArH), 7.55–7.62 (2H, m, 2 \times ArH); δ_{C} (101 MHz, CDCl_3) 27.9 (3 \times CH_3), 28.3 (3 \times CH_3), 47.6 (CH_2), 50.2 (CH), 79.9 (C), 82.5 (C), 87.4 (C), 92.0 (C), 119.7 (C), 128.7 (2 \times CH), 131.0 (CH), 133.2 (2 \times CH), 155.5 (C), 169.9 (C), 184.7 (C); *m/z* (ESI) 396 (MNa^+ , 100%).

***tert*-Butyl (2*S*)-(tert-butoxycarbonylamino)-4-oxo-6-(2'-naphthyl)hex-5-ynoate (120b)**



The reaction was carried out according to the above procedure for the synthesis of *tert*-butyl (2*S*)-(tert-butoxycarbonylamino)-4-oxo-6-phenylhex-5-ynoate **120a** using 2-ethylnaphthalene (0.97 g, 6.4 mmol), *n*-butyl lithium (2.5 M in hexane, 1.5 mL, 3.8 mmol) and *tert*-butyl (2*S*)-(tert-butoxycarbonylamino)-4-[methoxy(methyl)amino]-4-oxobutanoate **119** (0.42 g, 1.3 mmol). Purification by flash column chromatography eluting with 20% diethyl ether in petroleum gave *tert*-butyl (2*S*)-(tert-butoxycarbonylamino)-4-oxo-6-(2'-naphthyl)hex-5-ynoate **120b** as a colourless oil (0.41 g, 77%). $\nu_{\max}/\text{cm}^{-1}$ (neat) 3342 (NH), 2977 (CH), 2197 (C \equiv C), 1708 (C=O), 1667 (C=O), 1496, 1366, 1215, 1080, 746; $[\alpha]_D^{24} +9.0$ (*c* 0.1, CHCl₃); δ_{H} (400 MHz, CDCl₃) 1.46 (9H, s, 3 × CH₃), 1.48 (9H, s, 3 × CH₃), 3.23 (1H, dd, *J* 17.9, 4.6 Hz, 3-*HH*), 3.37 (1H, dd, *J* 17.9, 4.6 Hz, 3-*HH*), 4.56 (1H, dt, *J* 8.6, 4.6 Hz, 2-*H*), 5.48 (1H, d, *J* 8.6 Hz, NH), 7.51–7.57 (3H, m, 5'-H, 6'-H and 7'-H), 7.80–7.85 (3H, m, 3'-H, 4'-H and 8'-H), 8.15 (1H, s, 1'-H); δ_{C} (101 MHz, CDCl₃) 27.9 (3 × CH₃), 28.4 (3 × CH₃), 47.6 (CH₂), 50.2 (CH), 79.9 (C), 82.5 (C), 87.7 (C), 92.6 (C), 116.8 (C), 127.1 (CH), 127.9 (CH), 128.2 (CH), 128.3 (CH), 128.4 (CH), 128.5 (CH), 132.6 (C), 134.0 (C), 134.6 (CH), 155.5 (C), 169.9 (C), 184.7 (C); *m/z* (ESI) 446.1948 (MNa⁺. C₂₅H₂₉NNaO₅ requires 446.1938).

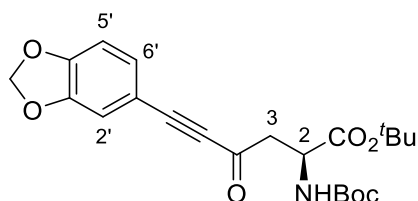
***tert*-Butyl (2*S*)-(tert-butoxycarbonylamino)-4-oxo-6-(4'-methoxyphenyl)hex-5-ynoate (120c)**



The reaction was carried out according to the above procedure for the synthesis of *tert*-butyl (2*S*)-(tert-butoxycarbonylamino)-4-oxo-6-(4'-methoxyphenyl)hex-5-

ynoate **120a** using 4-methoxyphenylacetylene (0.70 mL, 5.40 mmol), *n*-butyl lithium (2.5 M in hexane, 1.30 mL, 3.24 mmol) and *tert*-butyl (2*S*)-(tert-butoxy carbonylamino)-4-[methoxy(methyl)amino]-4-oxobutanoate **119** (0.35 g, 1.1 mmol). Purification by flash column chromatography eluting with 30% diethyl ether in petroleum gave *tert*-butyl (2*S*)-(tert-butoxycarbonylamino)-4-oxo-6-(4'-methoxyphenyl)hex-5-ynoate **120c** as a white solid (0.32 g, 74%). Mp 118–120 °C; $\nu_{\max}/\text{cm}^{-1}$ (neat) 3376 (NH), 2978 (CH), 2361, 2193 (C≡C), 1710 (C=O), 1665 (C=O), 1509, 1367, 1253, 1153, 1086, 739; $[\alpha]_D^{21} +16.4$ (c 0.1, CHCl₃); δ_{H} (400 MHz, CDCl₃) 1.44 (9H, s, 3 × CH₃), 1.46 (9H, s, 3 × CH₃), 3.16 (1H, dd, *J* 17.8, 4.5 Hz, 3-*HH*), 3.31 (1H, dd, *J* 17.8, 4.5 Hz, 3-*HH*), 3.85 (3H, s, OCH₃), 4.50 (1H, dt, *J* 8.5, 4.5 Hz, 2-H), 5.43 (1H, d, *J* 8.5 Hz, NH), 6.87–6.92 (2H, m, 3'-H and 5'-H), 7.51–7.57 (2H, m, 2'-H and 6'-H); δ_{C} (101 MHz, CDCl₃) 27.8 (3 × CH₃), 28.3 (3 × CH₃), 47.4 (CH₂), 50.2 (CH), 55.4 (CH₃), 79.8 (C), 82.4 (C), 87.5 (C), 93.3 (C), 111.4 (C), 114.4 (2 × CH), 135.3 (2 × CH), 155.5 (C), 161.9 (C), 169.9 (C), 184.6 (C); *m/z* (ESI) 426.1881 (MNa⁺. C₂₂H₂₉NNaO₆ requires 426.1887).

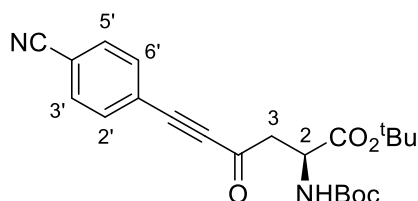
***tert*-Butyl (2*S*)-(tert-butoxycarbonylamino)-4-oxo-6-(3',4'-methylenedioxyphenyl)hex-5-ynoate (120d)**



The reaction was carried out according to the above procedure for the synthesis of *tert*-butyl (2*S*)-(tert-butoxycarbonylamino)-4-oxo-6-phenylhex-5-ynoate **120a** using 3,4-methylenedioxyphenylethyne (0.11 g, 0.77 mmol), *n*-butyl lithium (2.5 M in hexane, 0.18 mL, 0.46 mmol) and *tert*-butyl (2*S*)-(tert-butoxycarbonylamino)-4-[methoxy(methyl)amino]-4-oxobutanoate **119** (0.050 g, 0.15 mmol). Purification by flash column chromatography eluting with 20% diethyl ether in hexane gave *tert*-butyl (2*S*)-(tert-butoxycarbonylamino)-4-oxo-6-(3',4'-methylenedioxyphenyl)hex-5-ynoate **120d** as a yellow oil (0.042 g, 67%). $\nu_{\max}/\text{cm}^{-1}$ (neat) 3400 (NH), 2977 (CH), 2189 (C≡C), 1708 (C=O), 1667 (C=O), 1487, 1366, 1218, 1147, 1035, 845, 733; $[\alpha]_D^{25} +13.0$ (c 0.1, CHCl₃); δ_{H} (400 MHz, CDCl₃) 1.44 (9H, s, 3 × CH₃), 1.46 (9H, s, 3 × CH₃), 3.15 (1H, dd, *J* 17.8, 4.6 Hz, 3-*HH*), 3.30 (1H, dd, *J* 17.8, 4.6 Hz, 3-*HH*),

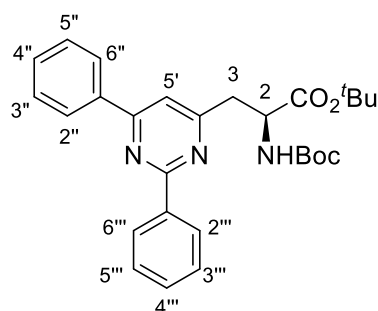
4.50 (1H, dt, J 8.4, 4.6 Hz, 2-H), 5.44 (1H, d, J 8.4 Hz, NH), 6.03 (2H, s, OCH₂O), 6.82 (1H, d, J 8.1 Hz, 5'-H), 7.01 (1H, d, J 1.5 Hz, 2'-H), 7.17 (1H, dd, J 8.1, 1.5 Hz, 6'-H); δ_c (101 MHz, CDCl₃) 27.8 (3 × CH₃), 28.3 (3 × CH₃), 47.4 (CH₂), 50.2 (CH), 79.9 (C), 82.5 (C), 86.8 (C), 92.9 (C), 101.9 (CH₂), 108.9 (CH), 112.6 (C), 112.7 (CH), 129.3 (CH), 147.8 (C), 150.4 (C), 155.5 (C), 170.0 (C), 184.6 (C); m/z (ESI) 440.1685 (MNa⁺. C₂₂H₂₇NNaO₇ requires 440.1680)

***tert*-Butyl (2*S*)-(tert-butoxycarbonylamino)-4-oxo-6-(4'-cyanophenyl)hex-5-ynoate (120e)**



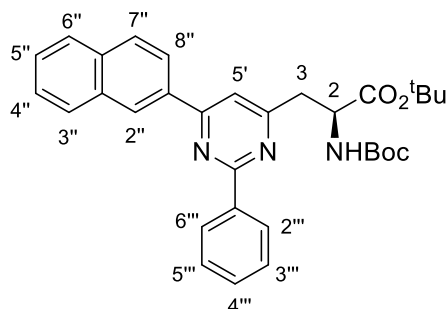
The reaction was carried out according to the above procedure for the synthesis of *tert*-butyl (2*S*)-(tert-butoxycarbonylamino)-4-oxo-6-phenylhex-5-ynoate **120a** using 4-cyanophenylacetylene (0.21 g, 1.7 mmol), *n*-butyl lithium (2.5 M in hexane, 0.40 mL, 1.0 mmol) and *tert*-butyl (2*S*)-(tert-butoxycarbonylamino)-4-[methoxy (methyl)amino]-4-oxobutanoate **119** (0.12 g, 0.33 mmol). Purification by flash column chromatography eluting with 30% diethyl ether in petroleum gave *tert*-butyl (2*S*)-(tert-butoxycarbonylamino)-4-oxo-6-(4'-cyano phenyl)hex-5-ynoate **120e** as a white solid (0.10 g, 61%). Mp 149–151 °C. ν_{\max} /cm⁻¹ (neat) 3391 (NH), 2978 (CH), 2366 (C≡C), 2207 (C≡N), 1710 (C=O), 1678 (C=O), 1500, 1367, 1252, 1150, 1086, 844, 736; $[\alpha]_D^{25}$ +9.2 (*c* 0.1, CHCl₃); δ_H (400 MHz, CDCl₃) 1.45 (9H, s, 3 × CH₃), 1.46 (9H, s, 3 × CH₃), 3.20 (1H, dd, J 17.8, 4.8 Hz, 3-*HH*), 3.31 (1H, dd, J 17.8, 4.8 Hz, 3-*HH*), 4.53 (1H, dt, J 8.2, 4.8 Hz, 2-H), 5.39 (1H, d, J 8.2 Hz, NH), 7.66–7.71 (4H, m, 2'-H, 3'-H, 5'-H and 6'-H); δ_c (101 MHz, CDCl₃) 27.9 (3 × CH₃), 28.3 (3 × CH₃), 47.6 (CH₂), 50.1 (CH), 80.0 (C), 82.8 (C), 88.4 (C), 89.6 (C), 114.3 (C), 117.8 (C), 124.5 (C), 132.3 (2 × CH), 133.4 (2 × CH), 155.4 (C), 169.6 (C), 184.1 (C); m/z (ESI) 421.1727 (MNa⁺. C₂₂H₂₆N₂NaO₅ requires 421.1734).

***tert*-Butyl (2*S*)-2-(*tert*-butoxycarbonylamino)-3-(2'-phenyl-4'-phenylpyrimidin-6'-yl)propanoate (121a)**



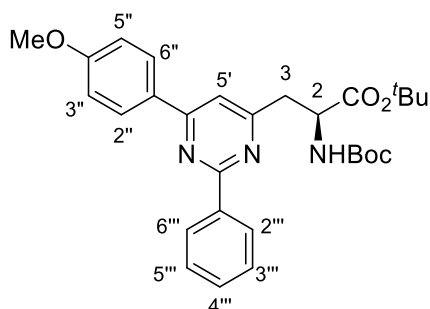
tert-Butyl (2*S*)-2-(*tert*-butoxycarbonylamino)-4-oxo-6-phenylhex-5-ynoate **120a** (0.046 g, 0.11 mmol) was dissolved in tetrahydrofuran (2 mL), followed by sequential addition of benzamidine hydrochloride (0.026 g, 0.17 mmol), potassium carbonate (0.018 g, 0.13 mmol) and ytterbium triflate (0.0070 g, 0.011 mmol). The mixture was heated to 50 °C for 48 h and then concentrated *in vacuo*. The residue was redissolved in dichloromethane (10 mL) and washed with a saturated solution of sodium hydrogen carbonate (5 mL) and then brine (5 mL). The organic layer was dried (MgSO₄) and concentrated *in vacuo*. Purification by flash column chromatography eluting with 30% ethyl acetate in petroleum ether gave *tert*-butyl (2*S*)-2-(*tert*-butoxycarbonylamino)-3-(2'-phenyl-4'-phenylpyrimidin-6'-yl)propanoate **121a** (0.039 g, 69%) as a yellow solid. Mp 95–100 °C; $\nu_{\max}/\text{cm}^{-1}$ (neat) 3429 (NH), 2977 (CH), 1706 (C=O), 1583 (C=C), 1501, 1364, 1250, 1149, 1031, 837, 729; $[\alpha]_D^{18} +26.0$ (c 0.1, CHCl₃); δ_{H} (400 MHz, CDCl₃) 1.34 (9H, s, 3 × CH₃), 1.44 (9H, s, 3 × CH₃), 3.36 (1H, dd, *J* 15.7, 5.1 Hz, 3-*HH*), 3.49 (1H, dd, *J* 15.7, 5.1 Hz, 3-*HH*), 4.73 (1H, dt, *J* 8.6, 5.1 Hz, 2-H), 5.94 (1H, d, *J* 8.6 Hz, NH), 7.47 (1H, s, 5'-H), 7.49–7.53 (6H, m, 6 × ArH), 8.19–8.23 (2H, m, 2 × ArH), 8.57–8.61 (2H, m, 2 × ArH); δ_{C} (101 MHz, CDCl₃) 28.0 (3 × CH₃), 28.4 (3 × CH₃), 39.3 (CH₂), 52.5 (CH), 79.7 (C), 81.9 (C), 114.2 (CH), 127.2 (2 × CH), 128.5 (2 × CH), 128.5 (2 × CH), 128.9 (2 × CH), 130.8 (CH), 130.9 (CH), 137.0 (C), 137.7 (C), 155.6 (C), 164.0 (C), 164.1 (C), 166.9 (C), 170.7 (C); *m/z* (ESI) 498.2355 (MNa⁺. C₂₈H₃₃N₃NaO₄ requires 498.2363).

***tert*-Butyl (2*S*)-2-(*tert*-butoxycarbonylamino)-3-[4'-(2''-naphthyl)-2'-phenylpyrimidin-6'-yl]propanoate (**121b**)**



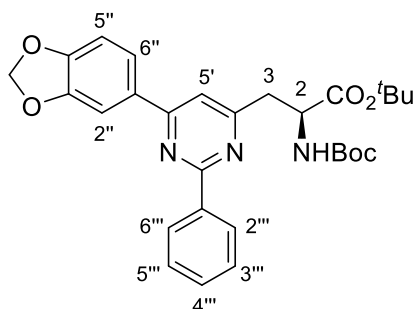
tert-Butyl (2*S*)-2-(*tert*-butoxycarbonylamino)-3-[4'-(2''-naphthyl)-2'-phenylpyrimidin-6'-yl]propanoate **121b** was synthesised as described for *tert*-butyl (2*S*)-2-(*tert*-butoxycarbonylamino)-3-(2'-phenyl-4'-phenylpyrimidin-6'-yl)propanoate **121a** using *tert*-butyl (2*S*)-(2-(*tert*-butoxycarbonylamino)-4-oxo-6-(2'-naphthyl)hex-5-ynoate **120b** (0.076 g, 0.18 mmol), benzamidine hydrochloride (0.042 g, 0.27 mmol), potassium carbonate (0.030 g, 0.22 mmol) and ytterbium triflate (0.010 g, 0.018 mmol). Purification by flash column chromatography eluting with 30% ethyl acetate in petroleum ether gave *tert*-butyl (2*S*)-2-(*tert*-butoxycarbonylamino)-3-[4'-(2''-naphthyl)-2'-phenylpyrimidin-6'-yl]propanoate **121b** (0.067 g, 71%) as a white solid. Mp 130–133 °C; $\nu_{\max}/\text{cm}^{-1}$ (neat) 3366 (NH), 2978 (CH), 1713 (C=O), 1571 (C=C), 1537, 1495, 1367, 1153, 1058, 760, 698; $[\alpha]_D^{24} +10.0$ (*c* 0.1, CHCl₃); δ_{H} (400 MHz, CDCl₃) 1.35 (9H, s, 3 × CH₃), 1.44 (9H, s, 3 × CH₃), 3.40 (1H, dd, *J* 15.7, 5.2 Hz, 3-*HH*), 3.53 (1H, dd, *J* 15.7, 5.2 Hz, 3-*HH*), 4.75 (1H, dt, *J* 8.6, 5.2 Hz, 2-H), 5.95 (1H, d, *J* 8.6 Hz, NH), 7.50–7.58 (5H, m, 5 × ArH), 7.63 (1H, s, 5'-H), 7.90–8.03 (3H, m, 3 × ArH), 8.33 (1H, dd, *J* 8.6, 1.7 Hz, 3''-H), 8.63–8.65 (2H, m, 2 × ArH), 8.72 (1H, br s, ArH); δ_{C} (101 MHz, CDCl₃) 28.0 (3 × CH₃), 28.4 (3 × CH₃), 39.4 (CH₂), 52.5 (CH), 79.7 (C), 82.0 (C), 114.4 (C), 116.8 (CH), 124.1 (CH), 126.6 (CH), 127.4 (CH), 127.5 (CH), 127.8 (2 × CH), 128.5 (2 × CH and C), 128.6 (2 × CH), 128.7 (CH), 129.0 (CH), 130.8 (C), 133.3 (C), 134.3 (C), 134.7 (C), 137.7 (C), 163.9 (C), 170.7 (C); *m/z* (ESI) 548.2520 (MNa⁺. C₃₂H₃₅N₃NaO₄ requires 548.2520).

***tert*-Butyl (2*S*)-2-(*tert*-butoxycarbonylamino)-3-[4'-(4''-methoxyphenyl)-2'-phenylpyrimidin-6'-yl]propanoate (**121c**)**



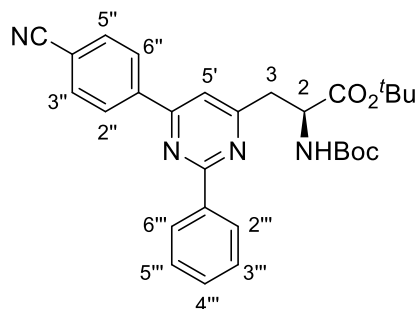
tert-Butyl (2*S*)-2-(*tert*-butoxycarbonylamino)-3-[4'-(4''-methoxyphenyl)-2'-phenylpyrimidin-6'-yl]propanoate **121c** was synthesised as described for *tert*-butyl (2*S*)-2-(*tert*-butoxycarbonylamino)-3-(2'-phenyl-4'-phenylpyrimidin-6'-yl)propanoate **121a** using *tert*-butyl (2*S*)-(tert-butoxycarbonylamino)-4-oxo-6-(4'-methoxyphenyl)hex-5-ynoate **120c** (0.44 g, 1.2 mmol), benzimidine hydrochloride (0.29 g, 1.8 mmol), potassium carbonate (0.20 g, 1.5 mmol) and ytterbium triflate (0.0070 g, 0.012 mmol). Purification by flash column chromatography eluting with 30% ethyl acetate in petroleum ether gave *tert*-butyl (2*S*)-2-(*tert*-butoxycarbonylamino)-3-[4'-(4''-methoxyphenyl)-2'-phenylpyrimidin-6'-yl]propanoate **121c** (0.31 g, 61%) as a white solid. Mp 205–210 °C; $\nu_{\text{max}}/\text{cm}^{-1}$ (neat) 3376 (NH), 2982 (CH), 1706 (C=O), 1573 (C=C), 1533, 1368, 1217, 1172, 763; $[\alpha]_{\text{D}}^{20} +24.5$ (*c* 0.1, CHCl₃); δ_{H} (400 MHz, CDCl₃) 1.34 (9H, s, 3 × CH₃), 1.44 (9H, s, 3 × CH₃), 3.33 (1H, dd, *J* 15.6, 4.5 Hz, 3-*HH*), 3.46 (1H, dd, *J* 15.6, 4.7 Hz, 3-*HH*), 3.89 (3H, s, OCH₃), 4.68–4.72 (1H, m, 2-H), 5.98 (1H, d, *J* 8.1 Hz, NH), 7.02–7.04 (2H, m, 3''-H and 5''-H), 7.40 (1H, s, 5'-H), 7.50–7.51 (3H, m, 3'''-H, 4'''-H and 5'''-H), 8.18–8.20 (2H, m, 2''-H and 6''-H), 8.57–8.59 (2H, m, 2'''-H and 6'''-H); δ_{C} (101 MHz, CDCl₃) 28.0 (3 × CH₃), 28.4 (3 × CH₃), 39.2 (CH₂), 52.5 (CH), 55.4 (OCH₃), 79.6 (C), 81.9 (C), 113.3 (CH), 114.3 (2 × CH), 128.4 (2 × CH), 128.5 (2 × CH), 128.8 (2 × CH), 129.4 (C), 130.6 (CH), 137.8 (C), 155.6 (C), 162.0 (C), 163.5 (C), 163.9 (C), 166.6 (C), 170.7 (C); *m/z* (ESI) 506.2647 (MH⁺. C₂₉H₃₆N₃O₅ requires 506.2649).

***tert*-Butyl (2*S*)-2-(*tert*-butoxycarbonylamino)-3-[4'-(3'',4''-methylenedioxyphenyl)-2'-phenylpyrimidin-6'-yl]propanoate (121d)**



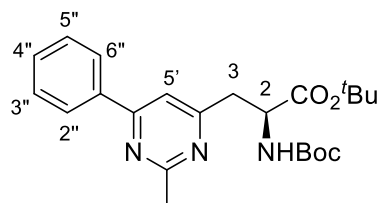
tert-Butyl (2*S*)-2-(*tert*-butoxycarbonylamino)-3-[4'-(3'',4''-methylenedioxyphenyl)-2'-phenylpyrimidin-6'-yl]propanoate **121d** was synthesised as described for *tert*-butyl (2*S*)-2-(*tert*-butoxycarbonylamino)-3-(2'-phenyl-4'-phenylpyrimidin-6'-yl)propanoate **121a** using *tert*-butyl (2*S*)-2-(*tert*-butoxycarbonylamino)-4-oxo-6-(3',4'-methylene dioxypheyl)hex-5-ynoate (0.093 g, 0.24 mmol), benzamidine hydrochloride (0.06 g, 0.36 mmol), potassium carbonate (0.040 g, 0.29 mmol) and ytterbium triflate (0.015 g, 0.024 mmol). Purification by flash column chromatography eluting with 30% ethyl acetate in petroleum ether gave *tert*-butyl (2*S*)-2-(*tert*-butoxycarbonylamino)-3-[4'-(3'',4''-methylenedioxyphenyl)-2'-phenyl pyrimidin-6'-yl]propanoate **121d** (0.083 g, 67%) as a colourless oil. $\nu_{\max}/\text{cm}^{-1}$ (neat) 3381 (NH), 2976 (CH), 1713 (C=O), 1573 (C=C), 1536, 1492, 1367, 1244, 1154, 1039, 772; $[\alpha]_D^{25} +18.0$ (*c* 0.1, CHCl₃); δ_{H} (400 MHz, CDCl₃) 1.34 (9H, s, 3 × CH₃), 1.44 (9H, s, 3 × CH₃), 3.33 (1H, dd, *J* 15.7, 5.0 Hz, 3-*HH*), 3.47 (1H, dd, *J* 15.7, 5.0 Hz, 3-*HH*), 4.71 (1H, dt, *J* 8.6, 5.0 Hz, 2-H), 5.95 (1H, d, *J* 8.6 Hz, NH), 6.07 (2H, s, OCH₂O), 6.94 (1H, d, *J* 8.2 Hz, 5''-H), 7.37 (1H, s, 5'-H), 7.49–7.54 (3H, m, 3''-H', 4'''-H and 5'''-H), 7.74 (1H, dd, *J* 8.2, 1.8 Hz, 6''-H), 7.77 (1H, d, *J* = 1.8 Hz, 2''-H), 8.54–8.59 (2H, m, 2'''-H and 6'''-H); δ_{C} (101 MHz, CDCl₃) 28.0 (3 × CH₃), 28.4 (3 × CH₃), 39.2 (CH₂), 52.4 (CH), 79.7 (C), 81.9 (C), 101.6 (CH₂), 107.4 (CH), 108.6 (CH), 113.5 (CH), 121.9 (CH), 128.5 (2 × CH), 128.5 (2 × CH), 130.7 (CH), 131.3 (C), 137.7 (C), 148.5 (C), 150.1 (C), 155.6 (C), 163.3 (C), 163.3 (C), 166.7 (C), 170.7 (C); *m/z* (ESI) 520.2445 (MH⁺. C₂₉H₃₄N₃O₆ requires 520.2442).

***tert*-Butyl (2*S*)-2-(*tert*-butoxycarbonylamino)-3-[4'--(4''-cyanophenyl)-2'-phenylpyrimidin-6'-yl]propanoate (121e)**



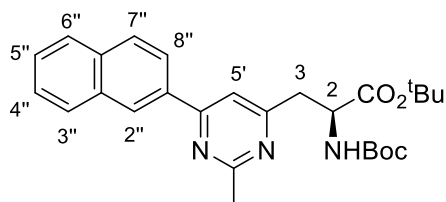
tert-Butyl (2*S*)-2-(*tert*-butoxycarbonylamino)-3-[4'--(4''-cyanophenyl)-2'-phenylpyrimidin-6'-yl]propanoate (**121e**) was synthesised as described for *tert*-butyl (2*S*)-2-(*tert*-butoxycarbonylamino)-3-(2'-phenyl-4'-phenylpyrimidin-6'-yl)propanoate **121a** using *tert*-butyl (2*S*)-(4-oxo-6-(4'-cyanophenyl)hex-5-ynoate **120e** (0.10 g, 0.25 mmol), benzamidine hydrochloride (0.059 g, 0.37 mmol), potassium carbonate (0.041 g, 0.30 mmol) and ytterbium triflate (0.015 g, 0.025 mmol). Purification by flash column chromatography eluting with 30% ethyl acetate in petroleum ether gave *tert*-butyl (2*S*)-2-(*tert*-butoxycarbonylamino)-3-[4'--(4''-cyanophenyl)-2'-phenylpyrimidin-6'-yl]propanoate **121e** (0.11 g, 89%) as a yellow oil. $\nu_{\max}/\text{cm}^{-1}$ (neat) 3425 (NH), 2978 (CH), 2229 (C \equiv N), 1705 (C=O), 1569 (C=C), 1533, 1367, 1150, 732, 695; $[\alpha]_D^{24} +30.2$ (c 0.1, CHCl₃); δ_{H} (400 MHz, CDCl₃) 1.36 (9H, s, 3 \times CH₃), 1.43 (9H, s, 3 \times CH₃), 3.41 (1H, dd, *J* 15.9, 5.2 Hz, 3-*HH*), 3.51 (1H, dd, *J* 15.9, 5.2 Hz, 3-*HH*), 4.74 (1H, dt, *J* 8.4, 5.2 Hz, 2-H), 5.80 (1H, d, *J* 8.4 Hz, NH), 7.51–7.55 (4H, m, 5'-H, 3''-H, 4''-H and 5''-H), 7.83 (2H, d, *J* 8.4 Hz, 2''-H and 6''-H), 8.32 (2H, d, *J* 8.4 Hz, 3''-H and 5''-H), 8.55–8.60 (2H, m, 2''-H and 6''-H); δ_{C} (101 MHz, CDCl₃) 28.0 (3 \times CH₃), 28.3 (3 \times CH₃), 39.5 (CH₂), 52.3 (CH), 79.9 (C), 82.1 (C), 114.3 (C), 114.6 (CH), 118.5 (C), 127.8 (2 \times CH), 128.6 (2 \times CH), 128.6 (2 \times CH), 131.1 (CH), 132.7 (2 \times CH), 137.2 (C), 141.2 (C), 155.5 (C), 161.9 (C), 164.4 (C), 167.8 (C), 170.6 (C); *m/z* (ESI) 523.2316 (MNa⁺. C₂₉H₃₂N₄NaO₄ requires 523.2316).

***tert*-Butyl (2*S*)-2-(*tert*-butoxycarbonylamino)-[3-(2'-methyl-4'-phenylpyrimidin-6'-yl)propanoate) (121g)**



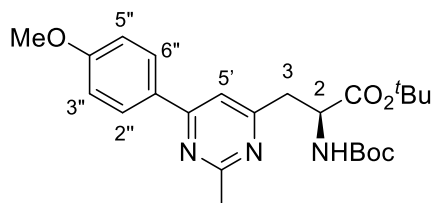
tert-Butyl (2*S*)-(*tert*-butoxycarbonylamino)-4-oxo-6-phenylhex-5-ynoate **120a** (0.34 g, 0.91 mmol) was dissolved in tetrahydrofuran (30 mL), followed by sequential addition of acetamidine hydrochloride (0.13 g, 1.4 mmol), potassium carbonate (0.30 g, 2.2 mmol) and ytterbium triflate (0.056 g, 0.091 mmol). The mixture was heated to 50 °C for 48 h and was concentrated *in vacuo*. The residue was redissolved in dichloromethane (30 mL), washed with a saturated solution of sodium hydrogen carbonate (20 mL), brine (20 mL), dried (MgSO₄) and concentrated *in vacuo*. Purification by flash column chromatography eluting with 30% ethyl acetate in petroleum ether gave *tert*-butyl (2*S*)-2-(*tert*-butoxycarbonylamino)-[3-(2'-methyl-4'-phenylpyrimidin-6'-yl)propanoate) **121g** (0.27 g, 71%) as a white solid. Mp 98–103 °C; $\nu_{\max}/\text{cm}^{-1}$ (neat) 3665 (NH), 2979 (CH), 1705 (C=O), 1580 (C=C), 1541, 1366, 1149, 1055, 752, 693; $[\alpha]_D^{25}$ +16.4 (*c* 0.1, CHCl₃); δ_{H} (400 MHz, CDCl₃) 1.40 (9H, s, 3 × CH₃), 1.42 (9H, s, 3 × CH₃), 2.76 (3H, s, 2'-CH₃), 3.27 (1H, dd, *J* 15.1, 5.2 Hz, 3-*HH*), 3.33 (1H, dd, *J* 15.1, 5.7 Hz, 3-*HH*), 4.62–4.67 (1H, m, 2-H), 5.65 (1H, d, *J* 8.1 Hz, NH), 7.41 (1H, s, 5'-H), 7.47–7.51 (3H, m, 3''-H, 4''-H and 5''-H), 8.04–8.06 (2H, m, 2''-H and 6''-H); δ_{C} (101 MHz, CDCl₃) 26.0 (CH₃), 27.9 (3 × CH₃), 28.3 (3 × CH₃), 39.4 (CH₂), 52.8 (CH), 79.7 (C), 82.0 (C), 113.8 (CH), 127.2 (2 × CH), 128.9 (2 × CH), 130.8 (CH), 136.9 (C), 155.4 (C), 164.3 (C), 166.4 (C), 167.7 (C), 170.4 (C); *m/z* (ESI) 436.2208 (MNa⁺. C₂₃H₃₁N₃NaO₄ requires 436.2207).

***tert*-Butyl (2*S*)-2-(*tert*-butoxycarbonylamino)-3-[2'-methyl-4'-(2''-naphthyl)pyrimidin-6'-yl]propanoate (121h)**



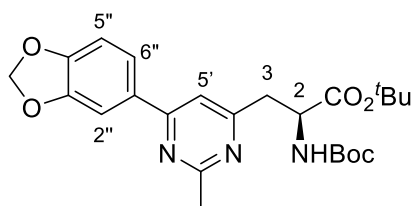
tert-Butyl (2*S*)-2-(*tert*-butoxycarbonylamino)-3-[2'-methyl-4'-(2''-naphthyl)pyrimidin-6'-yl]propanoate **121h** was synthesised as described for *tert*-butyl (2*S*)-2-(*tert*-butoxycarbonylamino)-3-(2'-methyl-4'-phenylpyrimidin-6'-yl)propanoate **121g** using *tert*-butyl (2*S*)-2-(*tert*-butoxycarbonylamino)-4-oxo-6-(2'-naphthyl)hex-5-ynoate **120b** (0.17 g, 0.39 mmol), acetamidine hydrochloride (0.092 g, 0.59 mmol), potassium carbonate (0.13 g, 0.94 mmol) and ytterbium triflate (0.024 g, 0.039 mmol). Purification by flash column chromatography eluting with 30% ethyl acetate in petroleum ether gave *tert*-butyl (2*S*)-2-(*tert*-butoxycarbonylamino)-3-[2'-methyl-4'-(2''-naphthyl)pyrimidin-6'-yl]propanoate **121h** (0.14 g, 76%) as a colourless oil. $\nu_{\max}/\text{cm}^{-1}$ (neat) 3361 (NH), 2980 (CH), 1716 (C=O), 1587 (C=C), 1541, 1364, 1254, 1160, 1024, 758; $[\alpha]_D^{20}$ +20.0 (*c* 0.1, CHCl₃); δ_{H} (400 MHz, CDCl₃) 1.42 (18H, br s, 6 × CH₃), 2.83 (3H, s, 2'-CH₃), 3.33–3.43 (2H, m, 3-H₂), 4.67–4.71 (1H, m, 2-H), 5.69 (1H, d, *J* 8.0 Hz, NH), 7.52–7.58 (2H, m, 2 × ArH), 7.62 (1H, s, 5'-H), 7.87–7.98 (3H, m, 3 × ArH), 8.16 (1H, d, *J* 8.5 Hz, 3''-H), 8.61 (1H, br s, 1''-H); δ_{C} (101 MHz, CDCl₃) 25.9 (CH₃), 27.9 (3 × CH₃), 28.3 (3 × CH₃), 39.3 (CH₂), 52.8 (CH), 79.8 (C), 82.1 (C), 114.0 (CH), 124.0 (CH), 126.6 (CH), 127.5 (C), 127.8 (2 × CH), 128.8 (CH), 129.1 (CH), 133.2 (CH), 134.0 (C), 134.6 (C), 155.5 (C), 164.3 (C), 166.2 (C), 167.5 (C), 170.4 (C); *m/z* (ESI) 464.2555 (MH⁺. C₂₇H₃₄N₃O₄ requires 464.244).

***tert*-Butyl (2*S*)-2-(*tert*-butoxycarbonylamino)-3-[4'-(4''-methoxyphenyl)-2'-methylpyrimidin-6'-yl]propanoate (121i)**



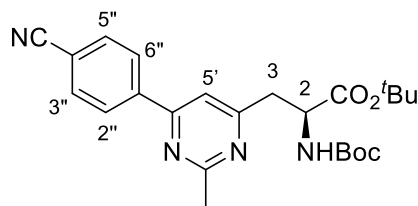
tert-Butyl (2*S*)-2-(*tert*-butoxycarbonylamino)-3-[4'-(4''-methoxyphenyl)-2'-methylpyrimidin-6'-yl]propanoate **121i** was synthesised as described for *tert*-butyl (2*S*)-2-(*tert*-butoxycarbonylamino)-[3-(2'-methyl-4'-phenylpyrimidin-6'-yl)]propanoate **121g** using *tert*-butyl (2*S*)-(4-oxo-6-(4'-methoxyphenyl)hex-5-ynoate) **120c** (0.093 g, 0.23 mmol), acetamidine hydrochloride (0.033 g, 0.34 mmol), potassium carbonate (0.076 g, 0.55 mmol) and ytterbium triflate (0.014 g, 0.023 mmol). Purification by flash column chromatography eluting with 30% ethyl acetate in petroleum ether gave *tert*-butyl (2*S*)-2-(*tert*-butoxycarbonylamino)-3-[4'-(4''-methoxyphenyl)-2'-methylpyrimidin-6'-yl]propanoate **121i** (0.065 g, 64%) as a white solid. Mp 110–114 °C; $\nu_{\text{max}}/\text{cm}^{-1}$ (neat) 3372 (NH), 2976 (CH), 1708 (C=O), 1584 (C=C), 1516, 1370, 1254, 1159, 840, 731; $[\alpha]_D^{19} +15.0$ (c 0.1, CHCl₃); δ_{H} (400 MHz, CDCl₃) 1.39 (9H, s, 3 × CH₃), 1.40 (9H, s, 3 × CH₃), 2.71 (3H, s, 2'-CH₃), 3.21 (1H, dd, *J* 15.0, 5.5 Hz, 3-HH), 3.29 (1H, dd, *J* 15.0, 5.5 Hz, 3-HH), 3.87 (3H, s, OCH₃), 4.62 (1H, dt, *J* 8.1, 5.5 Hz, 2-H), 5.65 (1H, d, *J* 8.1 Hz, NH), 6.97–7.01 (2H, m, 3''-H and 5''-H), 7.32 (1H, s, 5'-H), 8.03 (2H, d, *J* 8.8 Hz, 2''-H and 6''-H); δ_{C} (101 MHz, CDCl₃) 26.2 (CH₃), 27.9 (3 × CH₃), 28.3 (3 × CH₃), 39.5 (CH₂), 52.8 (CH), 55.4 (CH₃), 79.7 (C), 81.9 (C), 112.8 (CH), 114.3 (2 × CH), 128.7 (2 × CH), 129.4 (C), 155.4 (C), 161.9 (C), 163.6 (C), 166.1 (C), 167.7 (C), 170.5 (C); *m/z* (ESI) 444.2497 (MH⁺. C₂₄H₃₄N₃O₅ requires 444.2493).

***tert*-Butyl (2*S*)-2-(*tert*-butoxycarbonylamino)-3-[4'-(3'',4''-methylenedioxyphenyl)-2'-methylpyrimidin-6'-yl]propanoate (121j)**



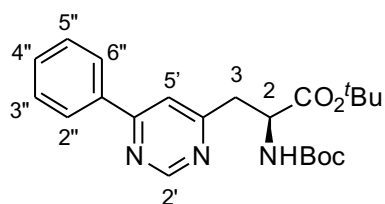
tert-Butyl (2*S*)-2-(*tert*-butoxycarbonylamino)-3-[4'-(3'',4''-methylenedioxyphenyl)-2'-methylpyrimidin-6'-yl]propanoate **121j** was synthesised as described for *tert*-butyl (2*S*)-2-(*tert*-butoxycarbonylamino)-3-(2'-methyl-4'-phenylpyrimidin-6'-yl)propanoate **121g** using *tert*-butyl (2*S*)-(*tert*-butoxycarbonylamino)-4-oxo-6-(3',4'-methylene dioxyphenyl)hex-5-ynoate **120d** (0.11 g, 0.25 mmol), acetamidine hydrochloride (0.035 g, 0.38 mmol), potassium carbonate (0.083 g, 0.60 mmol) and ytterbium triflate (0.015 g, 0.025 mmol). Purification by flash column chromatography eluting with 30% ethyl acetate in petroleum ether gave *tert*-butyl (2*S*)-2-(*tert*-butoxycarbonylamino)-3-[4'-(3'',4''-methylenedioxyphenyl)-2'-methylpyrimidin-6'-yl]propanoate **121j** (0.055 g, 50%) as a yellow oil. $\nu_{\max}/\text{cm}^{-1}$ (neat) 3384 (NH), 2979 (CH), 1708 (C=O), 1581 (C=C), 1495, 1362, 1241, 1130, 1035, 750; $[\alpha]_D^{25} +22.0$ (*c* 0.1, CHCl₃); δ_{H} (400 MHz, CDCl₃) 1.40 (9H, s, 3 × CH₃), 1.42 (9H, s, 3 × CH₃), 2.71 (3H, s, 2'-CH₃), 3.22 (1H, dd, *J* 15.0, 5.3 Hz, 3-*HH*), 3.29 (1H, dd, *J* 15.0, 5.9 Hz, 3-*HH*), 4.60–4.65 (1H, m, 2-H), 5.65 (1H, d, *J* 8.4 Hz, NH), 6.03 (2H, s, OCH₂O), 6.90 (1H, d, *J* 8.7 Hz, 5''-H), 7.29 (1H, s, 5'-H), 7.59–7.61 (2H, m, 2''-H and 6''-H); δ_{C} (101 MHz, CDCl₃) 26.1 (CH₃), 27.9 (3 × CH₃), 28.3 (3 × CH₃), 39.5 (CH₂), 52.7 (CH), 79.7 (C), 81.9 (C), 101.6 (CH₂), 107.4 (CH), 108.6 (CH), 113.0 (CH), 121.8 (CH), 131.3 (C), 148.5 (C), 150.0 (C), 155.5 (C), 163.4 (C), 166.3 (C), 167.7 (C), 170.5 (C); *m/z* (ESI) 458.2285 (MH⁺. C₂₄H₃₂N₃O₆ requires 458.2286).

***tert*-Butyl (2*S*)-2-(*tert*-butoxycarbonylamino)-3-[4'-(4''-cyanophenyl)-2'-methylpyrimidin-6'-yl]propanoate (**121k**)**



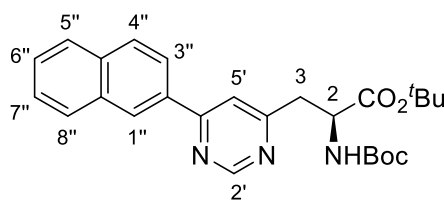
tert-Butyl (2*S*)-2-(*tert*-butoxycarbonylamino)-3-[4'-(4''-cyanophenyl)-2'-methylpyrimidin-6'-yl]propanoate **121k** was synthesised as described for *tert*-butyl (2*S*)-2-(*tert*-butoxycarbonylamino)-[3-(2'-methyl-4'-phenylpyrimidin-6'-yl)propanoate) **121g** using *tert*-butyl (2*S*)-(tert-butoxycarbonylamino)-4-oxo-6-(4'-cyanophenyl)hex-5-ynoate **120e** (0.084 g, 0.21 mmol), acetamidine hydrochloride (0.030 g, 0.32 mmol), potassium carbonate (0.070 g, 0.50 mmol) and ytterbium triflate (0.013 g, 0.021 mmol). Purification by flash column chromatography eluting with 30% ethyl acetate in petroleum ether gave *tert*-butyl (2*S*)-2-(*tert*-butoxycarbonylamino)-3-[4'-(4''-cyanophenyl)-2'-methylpyrimidin-6'-yl]propanoate **121k** (0.065 g, 65%) as a colourless oil. $\nu_{\max}/\text{cm}^{-1}$ (neat) 3393 (NH), 2885 (CH), 2237 (C≡N), 1744 (C=O), 1592 (C=C), 1501, 1450, 1247, 1033, 661; $[\alpha]_D^{24} +30.0$ (*c* 0.1, CHCl₃); δ_{H} (400 MHz, CDCl₃) 1.41 (18H, br s, 6 × CH₃), 2.76 (3H, s, 2'-CH₃), 3.26–3.37 (2H, m, 3-H₂), 4.62–4.67 (1H, m, 2-H), 5.54 (1H, d, *J* 8.1 Hz, NH), 7.44 (1H, s, 5'-H), 7.77–7.81 (2H, m, 2''-H and 6''-H), 8.18 (2H, d, *J* 8.0 Hz, 3''-H and 5''-H); δ_{C} (101 MHz, CDCl₃) 26.1 (CH₃), 27.9 (3 × CH₃), 28.3 (3 × CH₃), 39.7 (CH₂), 52.7 (CH), 79.8 (C), 82.2 (C), 114.1 (CH), 118.4 (C), 127.8 (2 × CH), 132.6 (2 × CH), 141.2 (C), 155.4 (C), 161.9 (C), 167.4 (C), 168.3 (C), 170.3 (2 × C); *m/z* (ESI) 439.2341 (MH⁺. C₂₄H₃₁N₄O₄ requires 439.2340).

***tert*-Butyl (2*S*)-2-(*tert*-butoxycarbonylamino)-3-(4'-phenylpyrimidin-6'-yl)propanoate (121I)**



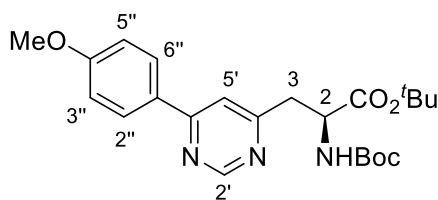
tert-Butyl (2*S*)-(*tert*-butoxycarbonylamino)-4-oxo-6-phenylhex-5-ynoate **120a** (0.083 g, 0.22 mmol) was dissolved in tetrahydrofuran (15 mL), followed by sequential addition of formamidine hydrochloride (0.18 g, 2.20 mmol), potassium carbonate (0.61 g, 4.40 mmol) and ytterbium triflate (0.027 g, 0.044 mmol). The mixture was heated to 50 °C for 48 h and was concentrated *in vacuo*. The residue was redissolved in dichloromethane (20 mL), washed with a saturated solution of sodium hydrogen carbonate (20 mL), brine (20 mL), dried (MgSO₄) and concentrated *in vacuo*. Purification by flash column chromatography eluting with 30% ethyl acetate in petroleum ether gave *tert*-butyl (2*S*)-2-(*tert*-butoxycarbonylamino)-3-(4'-phenylpyrimidin-6'-yl)propanoate (**121I**) (0.053 g, 64%) as a colourless oil. $\nu_{\text{max}}/\text{cm}^{-1}$ (neat) 3668 (NH), 2977 (CH), 1713 (C=O), 1587 (C=C), 1512, 1368, 1254, 1156, 1024, 840, 747; $[\alpha]_D^{19}$ +40.0 (c 0.1, CHCl₃); δ_{H} (400 MHz, CDCl₃) 1.39 (9H, s, 3 × CH₃), 1.42 (9H, s, 3 × CH₃), 3.29 (1H, dd, *J* 15.2, 5.0 Hz, 3-*HH*), 3.36 (1H, dd, *J* 15.2, 5.7 Hz, 3-*HH*), 4.64–4.69 (1H, m, 2-H), 5.69 (1H, d, *J* 8.5 Hz, NH), 7.49–7.53 (3H, m, 3''-H, 4''-H and 5''-H), 7.60 (1H, s, 5'-H), 8.05–8.09 (2H, m, 2''-H and 6''-H), 9.15 (1H, s, 2'-H); δ_{C} (101 MHz, CDCl₃) 27.9 (3 × CH₃), 28.3 (3 × CH₃), 39.7 (CH₂), 52.8 (CH), 79.8 (C), 82.2 (C), 116.8 (CH), 127.2 (2 × CH), 129.0 (2 × CH), 131.0 (CH), 136.6 (CH), 155.4 (C), 158.5 (C), 163.9 (C), 166.8 (C), 170.4 (C); *m/z* (ESI) 400.2229 (MH⁺. C₂₂H₃₀N₃O₄ requires 400.2231).

***tert*-Butyl (2*S*)-2-(*tert*-butoxycarbonylamino)-3-[4'-(2''-naphthyl)pyrimidin-6'-yl]propanoate (121m).**



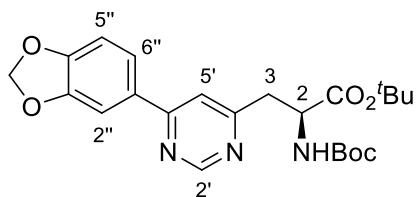
tert-Butyl (2*S*)-2-(*tert*-butoxycarbonylamino)-3-[4'-(2''-naphthyl)pyrimidin-6'-yl]propanoate **121m** was synthesised as described for *tert*-butyl (2*S*)-2-(*tert*-butoxycarbonylamino)-3-(4'-phenylpyrimidin-6'-yl)propanoate **121i** using *tert*-butyl (2*S*)-(2-(*tert*-butoxycarbonylamino)-4-oxo-6-(2'-naphthyl)hex-5-ynoate **120b** (0.050 g, 0.12 mmol), formamidine hydrochloride (0.097 g, 1.20 mmol), potassium carbonate (0.33 g, 2.40 mmol) and ytterbium triflate (0.015 g, 0.024 mmol). Purification by flash column chromatography eluting with 30% ethyl acetate in petroleum ether gave *tert*-butyl (2*S*)-2-(*tert*-butoxycarbonylamino)-3-[4'-(2''-naphthyl)pyrimidin-6'-yl]propanoate **121m** (0.028 g, 52%) as a white solid. Mp 162–165 °C; $\nu_{\max}/\text{cm}^{-1}$ (neat) 3430 (NH), 2979 (CH), 1715 (C=O), 1613 (C=C), 1497, 1366, 1152, 752, 694; $[\alpha]_D^{19} +34.0$ (*c* 0.1, CHCl₃); δ_{H} (400 MHz, CDCl₃) 1.40 (3H, s, 3 × CH₃), 1.43 (3H, s, 3 × CH₃), 3.33 (1H, dd, *J* 15.1, 5.1 Hz, 3-*HH*), 3.40 (1H, dd, *J* 15.1, 5.9 Hz, 3-*HH*), 4.67–4.72 (1H, m, 2-H), 5.71 (1H, d, *J* 8.2 Hz, NH), 7.53–7.59 (2H, m, 6''-H and 7''-H), 7.75 (1H, s, 5'-H), 7.87–7.92 (1H, m, 5''-H), 7.95–7.99 (2H, m, 4''-H and 8''-H), 8.16 (1H, dd, *J* 8.6, 1.5 Hz, 3''-H), 8.62 (1H, br s, 1''-H), 9.20 (1H, s, 2'-H); δ_{C} (101 MHz, CDCl₃) 27.9 (3 × CH₃), 28.3 (3 × CH₃), 39.7 (CH₂), 52.8 (CH), 79.8 (C), 82.2 (C), 116.9 (CH), 123.8 (CH), 126.7 (CH), 127.5 (2 × CH), 128.8 (CH), 128.9 (CH), 129.1 (CH), 133.3 (CH), 133.8 (C), 134.7 (C), 155.5 (C), 158.6 (C), 163.8 (C), 166.9 (C), 170.5 (C); *m/z* (ESI) 448.2230 ([M-H]⁻. C₂₆H₃₀N₃O₄ requires 448.2242).

***tert*-Butyl (2*S*)-2-(*tert*-butoxycarbonylamino)-3-[4'-(4''-methoxyphenyl)pyrimidin-6'-yl]propanoate (121n)**



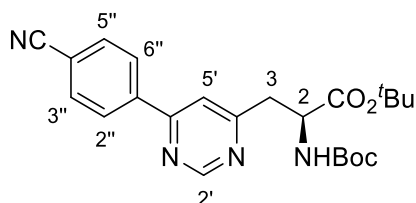
tert-Butyl (2*S*)-2-(*tert*-butoxycarbonylamino)-3-[4'-(4''-methoxyphenyl)pyrimidin-6'-yl]propanoate **121n** was synthesised as described for *tert*-butyl (2*S*)-2-(*tert*-butoxycarbonylamino)-3-(4'-phenylpyrimidin-6'-yl)propanoate **121i** using *tert*-butyl (2*S*)-(tert-butoxycarbonylamino)-4-oxo-6-(4'-methoxyphenyl)hex-5-ynoate **120c** (0.099 g, 0.25 mmol), formamidine hydrochloride (0.200 g, 2.50 mmol), potassium carbonate (0.69 g, 5.00 mmol) and ytterbium triflate (0.031 g, 0.050 mmol). Purification by flash column chromatography eluting with 30% ethyl acetate in petroleum ether gave *tert*-butyl (2*S*)-2-(*tert*-butoxycarbonylamino)-3-[4'-(4''-methoxyphenyl)pyrimidin-6'-yl]propanoate **121n** (0.054 g, 50%) as a colourless oil. $\nu_{\max}/\text{cm}^{-1}$ (neat) 3368 (NH), 2979 (CH), 1714 (C=O), 1592 (C=C), 1529, 1365, 1254, 1150, 1025; $[\alpha]_D^{18} +19.0$ (c 0.1, CHCl₃); δ_{H} (400 MHz, CDCl₃) 1.38 (9H, s, 3 × CH₃), 1.42 (9H, s, 3 × CH₃), 3.25 (1H, dd, *J* 15.1, 5.6 Hz, 3-*HH*), 3.33 (1H, dd, *J* 15.1, 5.6 Hz, 3-*HH*), 3.88 (3H, s, OCH₃), 4.65 (1H, dt, *J* 8.2, 5.6 Hz 2-H), 5.71 (1H, d, *J* 8.2 Hz, NH), 7.00–7.03 (2H, m, 3''-H and 5''-H), 7.53 (1H, s, 5'-H), 8.03–8.07 (2H, m, 2''-H and 6''-H), 9.08 (1H, s, 2'-H); δ_{C} (101 MHz, CDCl₃) 27.9 (3 × CH₃), 28.3 (3 × CH₃), 39.6 (CH₂), 52.8 (CH), 55.4 (CH₃), 79.8 (C), 82.1 (C), 114.4 (2 × CH), 115.8 (CH), 128.7 (2 × CH), 128.9 (CH), 155.5 (C), 158.4 (C), 162.1 (C), 163.4 (C), 166.4 (C), 170.5 (C); *m/z* (ESI) 430.2339 (MH⁺. C₂₃H₃₂N₃O₅ requires 430.2336).

***tert*-Butyl (2*S*)-2-(*tert*-butoxycarbonylamino)-3-[4'-(3'',4''-methylenedioxyphenyl)pyrimidin-6'-yl]propanoate (121o).**



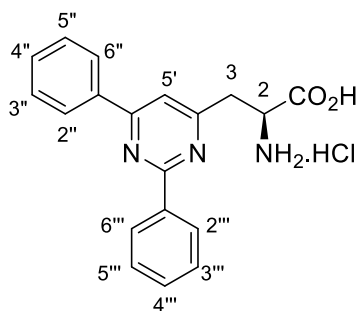
tert-Butyl(2*S*)-2-(*tert*-butoxycarbonylamino)-3-[4'-(3'',4''-methylenedioxyphenyl)pyrimidin-6'-yl]propanoate **121o** was synthesised as described for *tert*-butyl (2*S*)-2-(*tert*-butoxycarbonylamino)-3-(4'-phenylpyrimidin-6'-yl)propanoate **121i** using *tert*-butyl (2*S*)-(tert-butoxycarbonylamino)-4-oxo-6-(3',4'-methylenedioxyphenyl)hex-5-ynoate **120d** (0.17 g, 0.40 mmol), formamidinium hydrochloride (0.32 g, 4.0 mmol), potassium carbonate (1.1 g, 8.0 mmol) and ytterbium triflate (0.024 g, 0.040 mmol). Purification by flash column chromatography eluting with 30% ethyl acetate in petroleum ether gave *tert*-butyl (2*S*)-2-(*tert*-butoxycarbonylamino)-3-[4'-(3'',4''-methylenedioxyphenyl)pyrimidin-6'-yl]propanoate **121o** (0.079 g, 45%) as a yellow oil. $\nu_{\max}/\text{cm}^{-1}$ (neat) 3401 (NH), 2977 (CH), 2191, 1713 (C=O), 1533 (C=C), 1491, 1379, 1246, 1156, 1035, 844, 732; $[\alpha]_D^{22} +34.0$ (c 0.1, CHCl₃); δ_{H} (400 MHz, CDCl₃) 1.38 (9H, s, 3 × CH₃), 1.42 (9H, s, 3 × CH₃), 3.25 (1H, dd, *J* 15.1, 5.0 Hz, 3-*HH*), 3.33 (1H, dd, *J* 15.1, 5.6 Hz, 3-*HH*), 4.62–4.67 (1H, m, 2-H), 5.69 (1H, d, *J* 8.6 Hz, NH), 6.05 (2H, s, OCH₂O), 6.92 (2H, d, *J* 8.6 Hz, 5''-H), 7.49 (1H, s, 5'-H), 7.59–7.64 (2H, m, 2''-H and 6''-H), 9.08 (1H, s, 2'-H); δ_{C} (101 MHz, CDCl₃) 27.9 (3 × CH₃), 28.3 (3 × CH₃), 39.6 (CH₂), 52.8 (CH), 79.1 (C), 82.1 (C), 101.7 (CH₂), 107.3 (CH), 108.7 (CH), 116.0 (CH), 121.9 (CH), 127.3 (CH), 148.6 (C), 148.7 (C), 150.2 (C), 158.4 (C), 166.3 (C), 170.5 (C), 176.5 (C); *m/z* (ESI) 444.2138 (MH⁺. C₂₃H₃₀N₃O₆ requires 444.2129).

***tert*-Butyl (2*S*)-2-(*tert*-butoxycarbonylamino)-3-[4'-(4''-cyanophenyl)pyrimidin-6'-yl]propanoate (121p)**



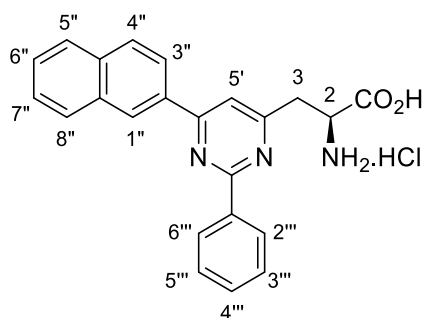
tert-Butyl (2*S*)-2-(*tert*-butoxycarbonylamino)-3-[4'-(4''-cyanophenyl)pyrimidin-6'-yl]propanoate **121p** was synthesised as described for *tert*-butyl (2*S*)-2-(*tert*-butoxycarbonylamino)-3-(4'-phenylpyrimidin-6'-yl)propanoate **121i** using *tert*-butyl (2*S*)-(*tert*-butoxycarbonylamino)-4-oxo-6-(4'-cyanophenyl)hex-5-ynoate **120e** (0.053 g, 0.13 mmol), formamidine hydrochloride (0.024 g, 1.30 mmol), potassium carbonate (0.036 g, 2.60 mmol) and ytterbium triflate (0.016 g, 0.026 mmol). Purification by flash column chromatography eluting with 30% ethyl acetate in petroleum ether gave *tert*-butyl (2*S*)-2-(*tert*-butoxycarbonylamino)-3-[4'-(4''-cyanophenyl)pyrimidin-6'-yl]propanoate (**121p**) (0.032 g, 60%) as a colourless oil. $\nu_{\max}/\text{cm}^{-1}$ (neat) 3436 (NH), 2979 (CH), 2230 (C \equiv N), 1710 (C=O), 1588 (C=C), 1499, 1367, 1253, 1153, 1024, 903, 725; $[\alpha]_D^{20}$ +20.0 (c 0.1, CHCl₃); δ_{H} (400 MHz, CDCl₃) 1.40 (9H, s, 3 \times CH₃), 1.41 (9H, s, 3 \times CH₃), 3.31–3.41 (2H, m, 3-H₂), 4.65–4.70 (1H, m, 2-H), 5.61 (1H, d, *J* 8.0 Hz, NH), 7.66 (1H, s, 5'-H), 7.79–7.82 (2H, m, 2''-H and 6''-H), 8.20 (2H, d, *J* 8.5 Hz, 3''-H and 5''-H), 9.20 (1H, s, 2'-H); δ_{C} (101 MHz, CDCl₃) 27.9 (3 \times CH₃), 28.3 (3 \times CH₃), 39.9 (CH₂), 52.7 (CH), 80.0 (C), 82.4 (C), 114.5 (CH), 117.2 (CH), 118.3 (C), 127.8 (2 \times CH), 132.8 (2 \times CH), 140.7 (C), 155.4 (C), 158.7 (C), 161.7 (C), 167.7 (C), 170.3 (C); *m/z* (ESI) 425.2183 (MH⁺. C₂₃H₂₉N₄O₄ requires 425.2183).

(2S)-2-Amino-3-(2'-phenyl-4'-phenylpyrimidin-6'-yl)propanoic acid hydrochloride (122a)



tert-Butyl (2S)-2-(*tert*-butoxycarbonylamino)-3-(2'-phenyl-4'-phenylpyrimidin-6'-yl)propanoate **121a** (0.11 g, 0.23 mmol) was dissolved in acetonitrile (1 mL). To the reaction mixture was added 1 M hydrochloric acid (10 mL) and the mixture was stirred at room temperature for 18 h. The reaction mixture was then concentrated *in vacuo*. This gave (2S)-2-amino-3-(2'-phenyl-4'-phenylpyrimidin-6'-yl)propanoic acid hydrochloride **122a** as a white solid (0.077 g, 95%). Mp 195–200 °C; $\nu_{\max}/\text{cm}^{-1}$ (neat) 3357 (NH/OH), 2932 (CH), 2158, 1717 (C=O), 1574 (C=C), 1537, 1377, 1029, 749, 688; $[\alpha]_D^{20} +19.8$ (c 0.1, MeOH); δ_{H} (400 MHz, CD₃OD) 3.62 (2H, d, *J* 5.4 Hz, 3-H₂), 4.65 (1H, t, *J* 5.4 Hz, 2-H), 7.47–7.60 (6H, m, 3''-H, 4''-H, 5''-H, 3'''-H, 4'''-H and 5'''-H), 7.84 (1H, s, 5'-H), 8.28–8.34 (2H, m, 2''-H and 6''-H), 8.53–8.60 (2H, m, 2'''-H and 6'''-H); δ_{C} (101 MHz, CD₃OD) 35.8 (CH₂), 50.7 (CH), 114.1 (CH), 127.0 (2 × CH), 128.2 (4 × CH), 128.7 (2 × CH), 130.7 (CH), 131.0 (CH), 136.5 (C), 137.4 (C), 164.2 (C), 164.6 (C), 164.9 (C), 169.9 (C); *m/z* (ESI) 342.1212 (MNa⁺. C₁₉H₁₇N₃NaO₂ requires 342.1213).

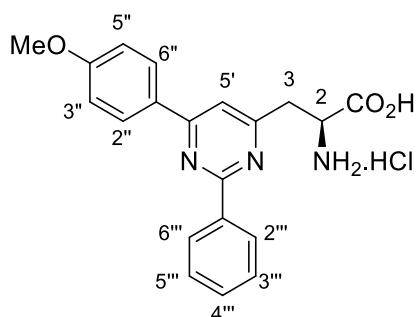
(2S)-2-Amino-3-[4'-(2''-naphthyl)-2'-phenylpyrimidin-6'-yl]propanoic acid hydrochloride (122b)



(2S)-2-Amino-3-[4'-(2''-naphthyl)-2'-phenylpyrimidin-6'-yl]propanoic acid hydrochloride **122b** was prepared as described for (2S)-2-amino-3-(2'-phenyl-4'-phenylpyrimidin-6'-yl)propanoic acid hydrochloride **122a** using *tert*-butyl (2S)-2-

(*tert*-butoxycarbonylamino)-3-[4'-(2''-naphthyl)-2'-phenylpyrimidin-6'-yl]propanoate **121b** (0.11 g, 0.23 mmol), acetonitrile (1 mL) and 1 M hydrochloric acid (10 mL). The reaction mixture was stirred at room temperature for 18 h and then concentrated *in vacuo*. This gave (2*S*)-2-amino-3-[4'-(2''-naphthyl)-2'-phenylpyrimidin-6'-yl]propanoic acid hydrochloride **122b** as a colourless oil (0.077 g, 95%). $\nu_{\max}/\text{cm}^{-1}$ (neat) 3305 (NH/OH), 2826 (CH), 1746 (C=O), 1571 (C=C), 1537, 1377, 1082, 760, 697; $[\alpha]_D^{24} +19.1$ (*c* 0.1, MeOH); δ_{H} (400 MHz, CD₃OD) 3.70 (2H, d, *J* 5.4 Hz, 3-H₂), 4.70 (1H, t, *J* 5.4 Hz, 2-H), 7.54–7.61 (5H, m, 5 × ArH), 7.93–7.96 (1H, m, ArH), 8.02–8.08 (3H, m, 3 × ArH), 8.40 (1H, dd, *J* 8.0, 3.6 Hz, ArH), 8.58–8.63 (2H, m, 2 × ArH), 8.85 (1H, br s, ArH); δ_{C} (101 MHz, CD₃OD) 35.8 (CH₂), 50.7 (CH), 114.5 (CH), 123.7 (CH), 126.5 (CH), 127.4 (CH), 127.5 (CH), 127.6 (CH), 128.3 (2 × CH), 128.3 (2 × CH), 128.4 (CH), 128.8 (CH), 130.9 (CH), 133.3 (C), 133.6 (C), 135.0 (C), 137.1 (C), 164.0 (C), 164.7 (C), 164.8 (C), 169.9 (C); *m/z* (ESI) 370.1558 (MH⁺. C₂₃H₂₀N₃O₂ requires 370.1550).

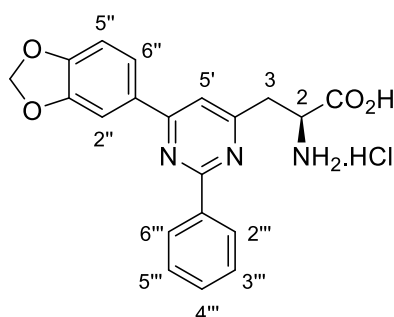
(2*S*)-2-Amino-3-[4'-(4''-methoxyphenyl)-2'-phenylpyrimidin-6'-yl]propanoic acid hydrochloride (122c)



(2*S*)-2-Amino-3-[4'-(4''-methoxyphenyl)-2'-phenylpyrimidin-6'-yl]propanoic acid hydrochloride **122c** was prepared as described for (2*S*)-2-amino-3-(2'-phenyl-4'-phenylpyrimidin-6'-yl)propanoic acid hydrochloride **122a** using *tert*-butyl (2*S*)-2-(*tert*-butoxycarbonylamino)-3-[4'-(4''-methoxyphenyl)-2'-phenylpyrimidin-6'-yl]propanoate **121c** (0.1240 g, 0.28 mmol), acetonitrile (1 mL) and 1 M hydrochloric acid (10 mL). The reaction mixture was stirred at room temperature for 18 h and then concentrated *in vacuo*. This gave (2*S*)-2-amino-3-[4'-(4''-methoxyphenyl)-2'-phenylpyrimidin-6'-yl]propanoic acid hydrochloride **122c** as a white solid (0.0764 g, 95%). Mp 175–180 °C; $\nu_{\max}/\text{cm}^{-1}$ (neat) 3354 (NH/OH), 2835 (CH), 1745 (C=O),

1588 (C=C), 1631, 1563, 1428, 1254, 1176, 1081, 840, 758; $[\alpha]_D^{18} +22.4$ (c 0.1, MeOH); δ_H (400 MHz, CD₃OD) 3.70 (2H, d, *J* 5.6 Hz, 3-H₂), 3.91 (3H, s, OCH₃), 4.71 (1H, t, *J* 5.6 Hz, 2-H), 7.13 (2H, d, *J* 8.6 Hz, 3''-H and 5''-H), 7.55–7.62 (3H, m, 3'''-H, 4'''-H and 5'''-H), 7.97 (1H, s, 5'-H), 8.34 (2H, d, *J* 8.6 Hz, 2''-H and 6''-H), 8.50–8.53 (2H, m, 2'''-H and 6'''-H); δ_C (101 MHz, CD₃OD) 35.1 (CH₂), 50.8 (CH), 54.9 (CH₃), 114.3 (CH), 114.4 (2 × CH), 127.1 (C), 128.6 (4 × CH), 129.9 (2 × CH), 131.9 (CH), 134.6 (C), 162.1 (C), 163.4 (C), 163.7 (C), 165.4 (C), 169.4 (C); *m/z* (ESI) 350.1500 (MH⁺. C₂₀H₂₀N₃O₃ requires 350.1499).

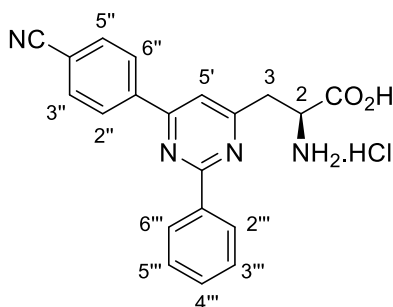
(2S)-2-Amino-3-[4'-(3'',4''-methylenedioxyphenyl)-2'-phenylpyrimidin-6'-yl]propanoic acid hydrochloride (122d)



(2S)-2-Amino-3-[4'-(3'',4''-methylenedioxyphenyl)-2'-phenylpyrimidin-6'-yl]propanoic acid hydrochloride **122d** was prepared as described for (2S)-2-amino-3-(2'-phenyl-4'-phenylpyrimidin-6'-yl)propanoic acid hydrochloride **122a** using *tert*-butyl (2S)-2-(*tert*-butoxy carbonylamino)-3-[4'-(3'',4''-methylenedioxyphenyl)-2'-phenylpyrimidin-6'-yl]propanoate **121d** (0.086 g, 0.23 mmol), acetonitrile (1 mL) and 1 M hydrochloric acid (10 mL). The reaction mixture was stirred at room temperature for 18 h and then concentrated *in vacuo*. This gave (2S)-2-amino-3-[4'-(3'',4''-methylenedioxyphenyl)-2'-phenylpyrimidin-6'-yl]propanoic acid hydrochloride **122d** as a yellow oil (0.079 g, 95%). $\nu_{\max}/\text{cm}^{-1}$ (neat) 3428 (NH/OH), 2977 (CH), 1706 (C=O), 1587 (C=C), 1491, 1362, 1153, 912, 729; $[\alpha]_D^{22} +32.0$ (c 0.1, MeOH); δ_H (400 MHz, CD₃OD) 3.65 (2H, d, *J* 4.3 Hz, 3-H₂), 4.67 (1H, t, *J* 4.3 Hz, 2-H), 6.07 (2H, s, OCH₂O), 6.99 (1H, d, *J* 7.9 Hz, 5''-H), 7.51–7.55 (3H, m, 3'''-H, 4'''-H and 5'''-H), 7.83 (1H, s, 5'-H), 7.85 (1H, br s, 2''-H), 7.91 (1H, d, *J* 7.9 Hz, 6''-H), 8.49–8.51 (2H, m, 2'''-H and 6'''-H); δ_C (101 MHz, CD₃OD) 35.5 (CH₂), 50.8 (CH), 102.0 (CH₂), 107.0 (CH), 108.3 (CH), 113.9 (CH), 122.7 (CH), 128.3 (2 × CH), 128.4 (2 × CH),

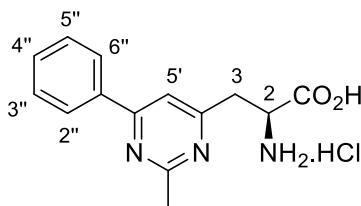
130.0 (C), 131.1 (CH), 136.3 (C), 148.7 (C), 151.0 (C), 163.3 (C), 164.1 (C), 164.5 (C), 169.7 (C); m/z (ESI) 364.1120 (MH^+ . $C_{20}H_{18}N_3O_4$ requires 364.2121).

(2S)-2-Amino-3-[4'-(4''-cyanophenyl)-2'-phenylpyrimidin-6'-yl]propanoic acid hydrochloride (122e)



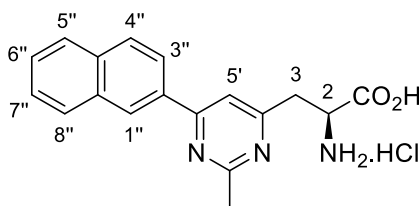
(2S)-2-Amino-3-[4'-(4''-cyanophenyl)-2'-phenylpyrimidin-6'-yl]propanoic acid hydrochloride **122e** was prepared as described for (2S)-2-amino-3-(2'-phenyl-4'-phenylpyrimidin-6'-yl)propanoic acid hydrochloride **122a** using *tert*-butyl (2S)-2-(*tert*-butoxycarbonylamino)-3-[4'-(4''-cyanophenyl)-2'-phenylpyrimidin-6'-yl]propanoate **121e** (0.088 g, 0.18 mmol), acetonitrile (1 mL) and 1 M hydrochloric acid (10 mL). The reaction mixture was stirred at room temperature for 18 h and then concentrated *in vacuo*. This gave (2S)-2-amino-3-[4'-(4''-cyanophenyl)-2'-phenylpyrimidin-6'-yl]propanoic acid hydrochloride **122e** as a yellow oil (0.057 g, 92%). ν_{max}/cm^{-1} (neat) 3354 (NH/OH), 2936 (CH), 1712 (C=O), 1646 (C=C), 1588, 1516, 1366, 1251, 1173, 770; $[\alpha]_D^{22} +15.0$ (c 0.1, MeOH); δ_H (400 MHz, CD_3OD) 3.69 (2H, d, J 4.6 Hz, 3-H₂), 4.69 (1H, t, J 4.6 Hz, 2-H), 7.50–7.55 (3H, m, 3'''-H, 4'''-H and 5'''-H), 7.92 (2H, d, J 7.9 Hz, 2''-H and 6''-H), 7.96 (1H, s, 5'-H), 8.49 (2H, d, J 7.9 Hz, 3''-H and 5''-H), 8.54–8.58 (2H, m, 2'''-H and 6'''-H); δ_C (101 MHz, CD_3OD) 36.0 (CH₂), 50.6 (CH), 114.2 (CH), 115.0 (C), 117.9 (C), 127.9 (2 × CH), 128.2 (2 × CH), 128.3 (2 × CH), 131.0 (CH), 132.6 (2 × CH), 137.0 (C), 140.8 (C), 162.6 (C), 164.4 (C), 165.7 (C), 169.8 (C); m/z (ESI) 345.1349 (MH^+ . $C_{20}H_{17}N_4O_2$ requires 345.1346).

(2S)-2-Amino-3-(2'-methyl-4'-phenylpyrimidin-6'-yl)propanoic acid hydrochloride (122g)



(2S)-2-Amino-3-(2'-methyl-4'-phenylpyrimidin-6'-yl)propanoic acid hydrochloride **122g** was prepared as described for (2S)-2-amino-3-(2'-phenyl-4'-phenylpyrimidin-6'-yl)propanoic acid hydrochloride **122a** using *tert*-butyl (2S)-2-(*tert*-butoxycarbonylamino)-3-(2'-methyl-4'-phenylpyrimidin-6'-yl)propanoate **121g** (0.22 g, 0.53 mmol), acetonitrile (1 mL) and 1 M hydrochloric acid (15 mL). The mixture was stirred at room temperature for 18 h and then concentrated *in vacuo*. This gave (2S)-2-amino-3-(2'-methyl-4'-phenylpyrimidin-6'-yl)propanoic acid hydrochloride **122g** as a white solid (0.13 g, 95%). Mp 145–149 °C; $\nu_{\max}/\text{cm}^{-1}$ (neat) 3371 (NH/OH), 2918 (CH), 1745 (C=O), 1612 (C=C), 1593, 1505, 1440, 1368, 1223, 1055, 752, 695; $[\alpha]_D^{24} +17.6$ (*c* 0.1, MeOH); δ_{H} (400 MHz, CD₃OD) 2.98 (3H, s, 2'-CH₃), 3.72 (1H, dd, *J* 16.4, 7.1 Hz, 3-HH), 3.80 (1H, dd, *J* 16.4, 6.1 Hz, 3-HH), 4.75–4.81 (1H, m, 2-H), 7.62–7.75 (3H, m, 3''-H, 4''-H and 5''-H), 8.22–8.26 (2H, m, 2''-H and 6''-H), 8.36 (1H, s, 5'-H); δ_{C} (101 MHz, CD₃OD) 22.0 (CH₃), 35.4 (CH₂), 50.6 (CH), 116.6 (CH), 128.5 (2 × CH), 129.3 (2 × CH), 132.4 (C), 133.2 (CH), 164.6 (C), 164.6 (C), 166.7 (C), 168.9 (C); *m/z* (ESI) 258.1238 (MH⁺). C₁₄H₁₆N₃O₂ requires 258.1237).

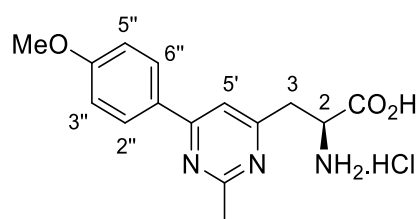
(2S)-2-Amino-3-[2'-methyl-4'-(2''-naphthyl)pyrimidin-6'-yl]propanoic acid hydrochloride (122h)



(2S)-2-Amino-3-[2'-methyl-4'-(2''-naphthyl)pyrimidin-6'-yl]propanoic acid hydrochloride **122h** was prepared as described for (2S)-2-amino-3-(2'-phenyl-4'-

phenylpyrimidin-6'-yl)propanoic acid hydrochloride **122a** using *tert*-butyl (2*S*)-2-(*tert*-butoxycarbonylamino)-3-[2'-methyl-4'-(2''-naphthyl)pyrimidin-6'-yl]propanoate **121h** (0.0650 g, 0.14 mmol), acetonitrile (1 mL) and 1 M hydrochloric acid (10 mL). The mixture was stirred at room temperature for 18 h and then concentrated *in vacuo*. This gave (2*S*)-2-amino-3-[2'-methyl-4'-(2''-naphthyl)pyrimidin-6'-yl]propanoic acid hydrochloride **122h** as a colourless oil (0.040 g, 93%). $\nu_{\max}/\text{cm}^{-1}$ (neat) 3354 (NH/OH), 2952 (CH), 1724 (C=O), 1512 (C=C), 1347, 1214, 1056, 812, 743; $[\alpha]_D^{22} +18.0$ (c 0.1, MeOH); δ_{H} (400 MHz, CD₃OD) 2.90 (3H, s, 2'-CH₃), 3.60 (1H, dd, *J* 16.5, 6.9 Hz, 3-*HH*), 3.69 (1H, dd, *J* 16.5, 4.9 Hz, 3-*HH*), 4.66–4.72 (1H, m, 2-H), 7.59–7.67 (2H, m, 6''-H and 7''-H), 7.97 (1H, d, *J* 8.9 Hz, 4''-H), 8.07 (2 H, d, *J* 8.4 Hz, 5''-H and 8''-H), 8.19 (1H, br s, 1'-H), 8.23 (1H, dd, *J* 8.9, 1.6 Hz, 3''-H), 8.78 (1H, s, 5'-H); δ_{C} (101 MHz, CD₃OD) 21.5 (CH₃), 35.0 (CH₂), 50.7 (CH), 117.2 (CH), 123.8 (CH), 127.3 (CH), 127.6 (CH), 128.9 (C), 129.2 (CH), 129.3 (CH), 129.4 (C), 130.9 (CH), 132.9 (CH), 135.8 (C), 163.7 (C), 165.4 (C), 168.0 (C), 168.7 (C); *m/z* (ESI) 308.1399 (MH⁺. C₁₈H₁₈N₃O₂ requires 308.1394).

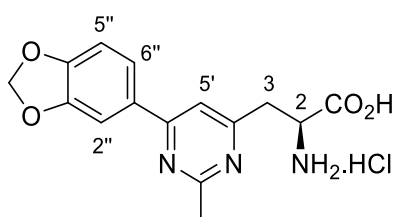
(2*S*)-2-Amino-3-[4'-(4''-methoxyphenyl)-2'-methylpyrimidin-6'-yl]propanoic acid hydrochloride (122i)



(2*S*)-2-Amino-3-[4'-(4''-methoxyphenyl)-2'-methylpyrimidin-6'-yl]propanoic acid hydrochloride **122i** was prepared as described for (2*S*)-2-amino-3-(2'-phenyl-4'-phenylpyrimidin-6'-yl)propanoic acid hydrochloride **122a** using *tert*-butyl (2*S*)-2-(*tert*-butoxycarbonylamino)-3-[4'-(4''-methoxyphenyl)-2'-methylpyrimidin-6'-yl]propanoate **121i** (0.12 g, 0.28 mmol), acetonitrile (1 mL) and 1 M hydrochloric acid (10 mL). The mixture was stirred at room temperature for 18 h and then concentrated *in vacuo*. This gave (2*S*)-2-amino-3-[4'-(4''-methoxyphenyl)-2'-methylpyrimidin-6'-yl]propanoic acid hydrochloride **122i** as a white solid (0.077 g, 95%). Mp 174–180 °C; $\nu_{\max}/\text{cm}^{-1}$ (neat) 3262 (NH/OH), 2830 (CH), 1742 (C=O), 1584 (C=C), 1251, 1180, 1031, 894, 621; $[\alpha]_D^{18} +13.0$ (c 0.1, MeOH); δ_{H} (400 MHz, CD₃OD) 2.90 (3H, s, 2'-CH₃), 3.60 (1H, dd, *J* 16.2, 7.1 Hz, 3-*HH*), 3.68 (1H, dd, *J* =

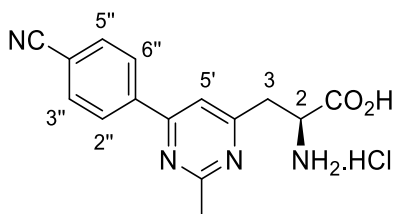
16.2, 6.1 Hz, 3-*HH*), 3.93 (3H, s, OCH₃), 4.70 (1H, t, *J* 6.6 Hz, 2-H), 7.17 (1H, dd, *J* 7.9, 2.1 Hz, 3''-H and 5''-H), 8.16 (1H, s, 5'-H), 8.23 (1H, dd, *J* 7.9, 2.1 Hz, 2''-H and 6''-H); δ_c (101 MHz, CD₃OD) 21.7 (CH₃), 35.1 (CH₂), 50.7 (CH), 55.0 (CH₃), 114.9 (C and 2 × CH), 115.4 (CH), 124.0 (C), 130.8 (2 × CH), 163.82 (C), 163.83 (C), 164.9 (C), 168.8 (C); *m/z* (ESI) 288.1349 (MH⁺. C₁₅H₁₈N₃O₃ requires 288.1343).

(2*S*)-2-Amino-3-[4'-(3'',4''-methylenedioxyphenyl)-2'-methylpyrimidin-6'-yl]propanoic acid hydrochloride (122j)



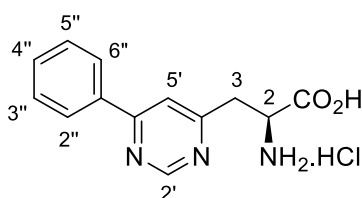
(2*S*)-2-Amino-3-[4'-(3'',4''-methylenedioxyphenyl)-2'-methylpyrimidin-6'-yl]propanoic acid hydrochloride **122j** was prepared as described for (2*S*)-2-amino-3-(2'-phenyl-4'-phenylpyrimidin-6'-yl)propanoic acid hydrochloride **122a** using *tert*-butyl (2*S*)-2-(*tert*-butoxycarbonylamino)-3-[4'-(3'',4''-methylenedioxyphenyl)-2'-methylpyrimidin-6'-yl]propanoate **121j** (0.050 g, 0.11 mmol), acetonitrile (1 mL) and 1 M hydrochloric acid (10 mL). The mixture was stirred at room temperature for 18 h and then concentrated *in vacuo*. This gave (2*S*)-2-amino-3-[4'-(3'',4''-methylenedioxyphenyl)-2'-methylpyrimidin-6'-yl]propanoic acid hydrochloride **122j** as a yellow oil (0.032 g, 95%). $\nu_{\max}/\text{cm}^{-1}$ (neat) 3317 (NH/OH), 2947 (CH), 1707 (C=O), 1450, 1407, 1114, 1018, 790; $[\alpha]_D^{23}$ +13.0 (c 0.1, MeOH); δ_H (400 MHz, CD₃OD) 2.84 (3H, s, 2'-CH₃), 3.53 (1H, dd, *J* 16.2, 7.1 Hz, 3-*HH*), 3.64 (1H, dd, *J* 16.2, 5.4 Hz, 3-*HH*), 4.63–4.67 (1H, m, 2-H), 6.12 (2H, s, OCH₂O), 7.05 (1H, d, *J* 8.2 Hz, 5''-H), 7.72 (1H, d, *J* 1.5 Hz, 2''-H) 7.83 (1H, dd, *J* 8.2, 1.5 Hz, 6''-H), 7.99 (1H, s, 5'-H); *m/z* (ESI) 302.1137 (MH⁺. C₁₅H₁₆N₃O₄ requires 302.1135).

(2S)-2-Amino-3-[4'-(4''-cyanophenyl)-2'-methylpyrimidin-6'-yl]propanoic acid hydrochloride (122k)



(2S)-2-Amino-3-[4'-(4''-cyanophenyl)-2'-methylpyrimidin-6'-yl]propanoic acid hydrochloride **122k** was prepared as described for (2S)-2-amino-3-(2'-phenyl-4'-phenylpyrimidin-6'-yl)propanoic acid hydrochloride **122a** using *tert*-butyl (2S)-2-(*tert*-butoxycarbonylamino)-3-[4'-(4''-cyanophenyl)-2'-methylpyrimidin-6'-yl]propanoate **121k** (0.065 g, 0.15 mmol), acetonitrile (1 mL) and 1 M hydrochloric acid (10 mL). The mixture was stirred at room temperature for 18 h and then concentrated *in vacuo*. This gave (2S)-2-amino-3-[4'-(4''-cyanophenyl)-2'-methylpyrimidin-6'-yl]propanoic acid **122k** as a yellow oil (0.040 g, 94%). $\nu_{\max}/\text{cm}^{-1}$ (neat) 3325 (NH/OH), 2922 (CH), 1641 (C=O), 1592 (C=C), 1526, 1490, 1362, 1011; $[\alpha]_D^{25} +14.0$ (c 0.1, MeOH); δ_{H} (400 MHz, CD₃OD) 2.79 (3H, s, 2'-CH₃), 3.51 (1H, dd, *J* 16.7, 7.4 Hz, 3-HH), 3.60 (1H, dd, *J* 16.7, 4.7 Hz, 3-HH), 4.61 (1H, dd, *J* 7.4, 4.7 Hz, 2-H), 7.89–7.94 (3H, m, 5'-H, 2''-H and 6''-H), 8.32–8.36 (2H, m, 3''-H and 5''-H); δ_{C} (101 MHz, CD₃OD) 24.1 (CH₃), 35.5 (CH₂), 50.8 (CH), 114.5 (CH), 114.6 (C), 117.8 (C), 128.0 (2 × CH), 132.6 (2 × CH), 140.2 (C), 162.9 (C), 165.8 (C), 167.8 (C), 169.4 (C); *m/z* (ESI) 283.1189 (MH⁺). C₁₅H₁₅N₄O₂ requires 283.1190).

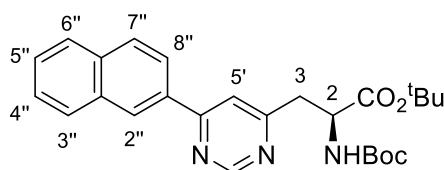
(2S)-2-Amino-3-(4'-phenylpyrimidin-6'-yl)propanoic acid hydrochloride (122l)



(2S)-2-Amino-3-(4'-phenylpyrimidin-6'-yl)propanoic acid hydrochloride **122l** was prepared as described for (2S)-2-amino-3-(2'-phenyl-4'-phenylpyrimidin-6'-yl)propanoic acid **122a** using *tert*-butyl (2S)-2-(*tert*-butoxycarbonylamino)-3-(4'-

phenylpyrimidin-6'-yl)propanoate **121l** (0.12 g, 0.31 mmol), acetonitrile (1 mL) and 1 M hydrochloric acid (10 mL). The mixture was stirred at room temperature for 18 h and then concentrated *in vacuo*. This gave (2S)-2-amino-3-(4'-phenylpyrimidin-6'-yl)propanoic acid hydrochloride **122i** as a white solid (0.073 g, 95%). Mp 68–70 °C; $\nu_{\max}/\text{cm}^{-1}$ (neat) 3440 (NH/OH), 2891 (CH), 1741 (C=O), 1631 (C=C), 1587, 1466, 1325, 1228, 1160, 970, 693; $[\alpha]_D^{18} +21.0$ (c 0.1, MeOH); δ_{H} (400 MHz, CD₃OD) 3.66 (1H, dd, *J* 16.5, 6.9 Hz, 3-HH), 3.74 (1H, dd, *J* 16.5, 5.3 Hz, 3-HH), 4.68–4.73 (1H, m, 2-H), 7.57–7.71 (3H, m, 3''-H, 4''-H and 5''-H), 8.22 (2H, d, *J* 8.0 Hz, 2''-H and 6''-H), 8.34 (1H, s, 5'-H), 9.33 (1H, s, 2'-H); δ_{C} (101 MHz, CD₃OD) 35.7 (CH₂), 50.7 (CH), 118.5 (CH), 127.9 (2 × CH), 129.2 (2 × CH), 132.7 (CH), 133.4 (CH), 155.1 (C), 163.9 (C), 166.8 (C), 169.1 (C); *m/z* (ESI) 244.1085 (MH⁺. C₁₃H₁₄N₃O₂ requires 244.1081).

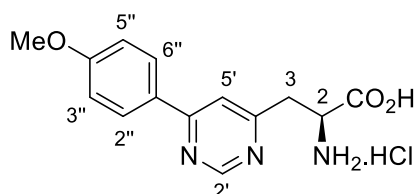
(2S)-2-Amino-3-[4'-(2''-naphthyl)pyrimidin-6'-yl]propanoic acid Hydrochloride (122m)



(2S)-2-Amino-3-[4'-(2''-naphthyl)pyrimidin-6'-yl]propanoic acid hydrochloride **122m** was prepared as described for (2S)-2-amino-3-(2'-phenyl-4'-phenylpyrimidin-6'-yl)propanoic acid hydrochloride **122a** using *tert*-butyl (2S)-2-(*tert*-butoxycarbonylamino)-3-[4'-(2''-naphthyl)pyrimidin-6'-yl]propanoate **121m** (0.029 g, 0.070 mmol), acetonitrile (0.5 mL) and 1 M hydrochloric acid (10 mL). The mixture was stirred at room temperature for 18 h and then concentrated *in vacuo*. This gave (2S)-2-amino-3-[4'-(2''-naphthyl)pyrimidin-6'-yl]propanoic acid hydrochloride **122m** as a white solid (0.019 g, 95%). Mp >155 °C (decomposition); $\nu_{\max}/\text{cm}^{-1}$ (neat) 3429 (NH/OH), 2977 (CH), 1706 (C=O), 1583 (C=C), 1364, 1250, 1149, 729; $[\alpha]_D^{19} +18.2$ (c 0.1, MeOH); δ_{H} (400 MHz, CD₃OD) 3.61 (1H, dd, *J* 16.8, 7.2 Hz, 3-HH), 3.70 (1H, dd, *J* 16.8, 4.7 Hz, 3-HH), 4.65–4.72 (1H, m, 2-H), 7.57–7.64 (2H, m, 6''-H and 7''-H), 7.94–7.96 (1H, m, 3''-H), 8.04–8.07 (2H, m, 5''-H and 8''-H), 8.25 (1H, d, *J* 8.4 Hz, 4''-H), 8.30 (1H, s, 5'-H), 8.78 (1H, br s, 1''-H), 9.27 (1H, s, 2'-H); δ_{C} (101 MHz, CD₃OD) 35.6 (CH₂), 50.8 (CH), 118.4 (CH), 123.5 (CH), 126.9 (CH), 127.5 (CH), 128.4 (CH), 129.0 (CH), 129.1 (CH), 129.2 (CH), 130.8 (C), 133.1 (CH), 135.4 (C),

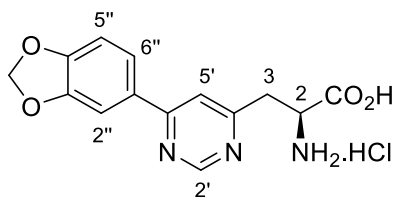
155.3 (C), 164.1 (C), 166.2 (C), 169.2 (C); m/z (ESI) 292.1093 ($[M-H]^-$. $C_{17}H_{14}N_3O_2$ requires 292.1092).

(2S)-2-Amino-3-[4'-(4''-methoxyphenyl)pyrimidin-6'-yl]propanoic acid hydrochloride (122n)



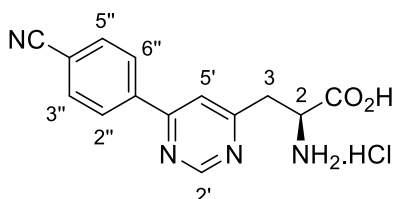
(2S)-2-Amino-3-[4'-(4''-methoxyphenyl)pyrimidin-6'-yl]propanoic acid hydrochloride **122n** was prepared as described for (2S)-2-amino-3-(2'-phenyl-4'-phenylpyrimidin-6'-yl)propanoic acid hydrochloride **122i** using *tert*-butyl (2S)-2-(*tert*-butoxycarbonylamino)-3-[4'-(4''-methoxyphenyl)pyrimidin-6'-yl]propanoate **121n** (0.73 g, 1.7 mmol), acetonitrile (1 mL) and 1 M hydrochloric acid (15 mL). The mixture was stirred at room temperature for 18 h and then concentrated *in vacuo*. This gave (2S)-2-amino-3-[4'-(4''-methoxyphenyl)pyrimidin-6'-yl]propanoic acid hydrochloride **122n** as a yellow oil (0.44 g, 95%); $\nu_{\max}/\text{cm}^{-1}$ (neat) 3401 (NH/OH), 2844 (CH), 1749 (C=O), 1591 (C=C), 1462, 1260, 1181, 1020, 841; $[\alpha]_D^{23} +15.0$ (c 0.1, MeOH); δ_H (400 MHz, CD_3OD) 3.55–3.74 (2H, m, 3-H₂), 3.91 (3H, s, OCH₃), 4.63–4.72 (1H, m, 2-H), 7.15 (2H, d, J 8.6 Hz, 3''-H and 5''-H), 8.21 (1H, s, 5'-H), 8.24 (2H, d, J 8.6 Hz, 2''-H and 6''-H), 9.23 (1H, s, 2'-H); δ_C (101 MHz, CD_3OD) 35.2 (CH₂), 50.7 (CH), 54.9 (CH₃), 114.7 (2 × CH), 117.2 (CH), 125.1 (CH), 130.0 (2 × CH), 154.4 (C), 163.4 (C), 164.3 (C), 165.9 (C), 169.1 (C); m/z (ESI) 274.1192 (MH⁺. $C_{14}H_{16}N_3O_3$ requires 274.1186).

(2S)-2-Amino-3-[4'-(3'',4''-methylenedioxyphenyl)pyrimidin-6'-yl]propanoic acid hydrochloride (122o)



(2S)-2-Amino-3-[4'-(3'',4''-methylenedioxyphenyl)pyrimidin-6'-yl]propanoic acid hydrochloride **122o** was prepared as described for (2S)-2-amino-3-(2'-phenyl-4'-phenylpyrimidin-6'-yl)propanoic acid hydrochloride **122a** using *tert*-butyl (2S)-2-(*tert*-butoxycarbonylamino)-3-[4'-(3'',4''-methylenedioxyphenyl)pyrimidin-6'-yl]propanoate **121o** (0.090 g, 0.20 mmol), acetonitrile (1 mL) and 1 M hydrochloric acid (10 mL). The mixture was stirred at room temperature for 18 h and then concentrated *in vacuo*. This gave (2S)-2-amino-3-[4'-(3'',4''-methylenedioxyphenyl)pyrimidin-6'-yl]propanoic acid hydrochloride **122o** as a colourless oil (0.055 g, 95%). $\nu_{\max}/\text{cm}^{-1}$ (neat) 3385 (NH/OH), 2913 (CH), 1742 (C=O), 1590 (C=C), 1457, 1252, 1035, 917; $[\alpha]_D^{25} +15.4$ (c 0.1, MeOH); δ_{H} (400 MHz, CD₃OD) 3.59–3.72 (2H, m, 3-H₂), 4.69 (1H, t, *J* 6.3 Hz, 2-H), 6.12 (2H, s, OCH₂O), 7.05 (1H, d, *J* 8.3 Hz, 5''-H), 7.74 (1H, d, *J* 1.6 Hz, 2''-H), 7.88 (1H, dd, *J* 8.3, 1.6 Hz, 6''-H), 8.26 (1H, s, 5'-H), 9.24 (1H, s, 2'-H); δ_{C} (101 MHz, CD₃OD) 35.4 (CH₂), 50.8 (CH), 102.2 (CH₂), 107.0 (CH), 108.5 (CH), 116.8 (CH), 123.2 (CH), 128.5 (CH), 149.0 (C), 151.7 (C), 156.0 (C), 163.8 (C), 165.2 (C), 169.3 (C); *m/z* (ESI) 288.0980 (MH⁺. C₁₄H₁₄N₃O₄ requires 288.0979).

(2S)-2-Amino-3-[4'-(4''-cyanophenyl)pyrimidin-6'-yl]propanoic acid hydrochloride (122p)



(2S)-2-Amino-3-[4'-(4''-cyanophenyl)pyrimidin-6'-yl]propanoic acid hydrochloride **122p** was prepared as described for (2S)-2-amino-3-(2'-phenyl-4'-phenylpyrimidin-

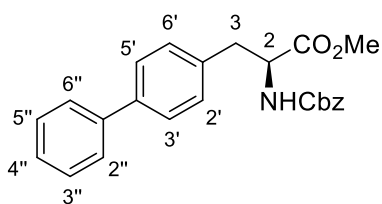
6'-yl)propanoic acid hydrochloride **122a** using *tert*-butyl (2*S*)-2-(*tert*-butoxycarbonylamino)-3-[4'-(4''-cyanophenyl)pyrimidin-6'-yl]propanoate **121p** (0.068 g, 0.16 mmol), acetonitrile (1 mL) and 1 M hydrochloric acid (10 mL). The mixture was stirred at room temperature for 18 h and then concentrated *in vacuo*. This gave (2*S*)-2-amino-3-[4'-(4''-cyanophenyl)pyrimidin-6'-yl]propanoic acid hydrochloride **122p** as a colourless oil (0.041 g, 95%); $\nu_{\max}/\text{cm}^{-1}$ (neat) 3372 (NH/OH), 2977 (CH), 1739 (C=O), 1595 (C=C), 1505, 1185, 1139, 837; $[\alpha]_D^{22} +12.0$ (c 0.1, MeOH); δ_{H} (400 MHz, CD₃OD) 3.55 (1H, dd, *J* 16.6, 7.2 Hz, 3-*HH*), 3.65 (1H, dd, *J* 16.6, 4.0 Hz, 3-*HH*), 4.60–4.65 (1H, m, 2-H), 7.91 (2H, d, *J* 8.1 Hz, 2''-H and 6''-H), 8.12 (1H, s, 5'-H), 8.37 (2H, d, *J* 8.1 Hz, 3''-H and 5''-H), 9.22 (1H, s, 2'-H); δ_{C} (101 MHz, CD₃OD) 35.5 (CH₂), 50.8 (CH), 114.7 (CH), 117.8 (C), 118.2 (CH), 128.2 (2 × CH), 132.7 (2 × CH), 139.5 (C), 157.1 (C), 162.8 (C), 165.9 (C), 169.3 (C); *m/z* (ESI) 269.1037 (MH⁺. C₁₄H₁₃N₄O₂ requires 269.1033).

3.3 Biaryl α -amino acid experimental

General Procedure for the Synthesis of Biphenyl Amino Acids

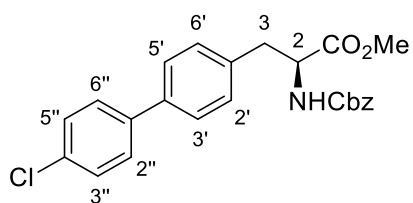
A solution of methyl (2*S*)-2-(benzyloxycarbonylamino)-3-(4-hydroxyphenyl)propanoate (1 equiv.) and potassium phosphate (3 equiv.) in acetonitrile (3 mL per mmol) was degassed under argon for 0.2 h. To this was added perfluoro-1-butanesulfonyl fluoride (1.5 equiv.). The reaction mixture was heated to 60 °C or 80 °C and stirred for 2 h. To this was added boronic acid (1.5 equiv.), XPhos Pd G2 (1 mol%) and water (2 mL per mmol). The reaction mixture was stirred at 60 °C or 80 °C for 2 h. Additional XPhos Pd G2 (1 mol%) was added and the reaction mixture was stirred at 60 °C or 80 °C for 2 h. A final portion of XPhos Pd G2 (1 mol%) was added and the reaction mixture was stirred at 60 °C or 80 °C for 18 h. After cooling to room temperature, the reaction mixture was diluted in ethyl acetate (30 mL) and washed with water (3 × 30 mL). The organic layer was dried (MgSO₄), filtered and concentrated *in vacuo*. Purification by flash column chromatography gave the biphenyl amino acids.

Methyl (2S)-2-(benzyloxycarbonylamino)-3-(biphen-4'-yl)propanoate (140a)¹⁹⁶



Methyl (2S)-2-(benzyloxycarbonylamino)-3-(biphen-4'-yl)propanoate was synthesised as described in general procedure using methyl (2S)-2-(benzyloxycarbonylamino)-3-(4-hydroxyphenyl)propanoate (0.150 g, 0.46 mmol), perfluoro-1-butanesulfonyl fluoride (0.12 mL, 0.68 mmol), phenylboronic acid (0.083 g, 0.68 mmol), XPhos Pd G2 (0.012 g, 0.015 mmol, 3 mol%) and potassium phosphate (0.290 g, 1.40 mmol) in acetonitrile (1.5 mL) and water (1 mL) at 60 °C. Purification by flash column chromatography, eluting with 30% ethyl acetate in hexane gave methyl (2S)-2-(benzyloxycarbonylamino)-3-(biphen-4'-yl)propanoate **140a** (0.16 g, 91%) as a white solid. Mp 85–90 °C (lit.¹⁹⁶ 83–85 °C); $[\alpha]_D^{22} +35.3$ (*c* 0.1, CHCl₃); δ_H (400 MHz, CDCl₃) 3.14 (1H, dd, *J* 13.9, 5.9 Hz, 3-HH), 3.21 (1H, dd, *J* 13.9, 5.9 Hz 3-HH), 3.75 (3H, s, OCH₃), 4.67–4.77 (1H, m, 2-H), 5.06–5.18 (2H, m, CH₂Ph), 5.29 (1H, d, *J* 8.3 Hz, 2-NH), 7.14–7.22 (2H, m, 2'-H and 6'-H), 7.28–7.62 (12H, m, Ph, 3'-H, 5'-H, 2''-H, 3''-H, 4''-H, 5''-H and 6''-H); δ_C (101 MHz, CDCl₃) 38.0 (CH₂), 52.5 (CH₃), 54.9 (CH), 67.1 (CH₂), 127.1 (2 × CH), 127.4 (CH), 127.4 (2 × CH), 128.2 (2 × CH), 128.3 (CH), 128.6 (2 × CH), 128.9 (2 × CH), 129.8 (2 × CH), 134.9 (C), 136.4 (C), 140.1 (C), 140.8 (C), 155.8 (C), 172.1 (C); *m/z* (ESI) 412 (MNa⁺. 100%).

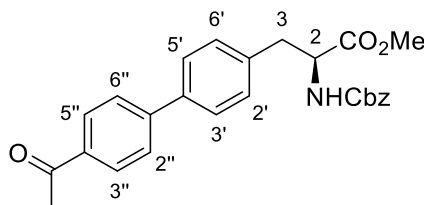
Methyl (2S)-2-(benzyloxycarbonylamino)-3-[4''-(chlorobiphen-4'-yl)]propanoate (140b)



Methyl (2S)-2-(benzyloxycarbonylamino)-3-[4''-(chlorobiphen-4'-yl)]propanoate was synthesised as described in general procedure using methyl (2S)-2-

(benzyloxycarbonylamino)-3-(4-hydroxyphenyl)propanoate (0.15 g, 0.46 mmol), perfluoro-1-butanesulfonyl fluoride (0.12 mL, 0.68 mmol), 4-chlorophenylboronic acid (0.13 g, 0.68 mmol), XPhos Pd G2 (0.012 g, 0.015 mmol, 3 mol%) and potassium phosphate (0.29 g, 1.40 mmol) in acetonitrile (1.5 mL) and water (1 mL) at 80 °C. Purification by flash column chromatography, eluting with 30% ethyl acetate in gave methyl (2*S*)-2-(benzyloxycarbonylamino)-3-[4''-(chlorobiphen-4'-yl)]propanoate **140b** (0.12 g, 61%) as a white solid. Mp 90–92 °C; $\nu_{\max}/\text{cm}^{-1}$ (neat) 3341 (NH), 3031, 2955 (CH), 1717 (C=O), 1515, 1487, 1347, 1258, 1212; $[\alpha]_{\text{D}}^{21} +53$ (c 0.1, CHCl₃); δ_{H} (400 MHz, CDCl₃) 3.11 (1H, dd, *J* 13.9, 5.7 Hz, 3-*HH*), 3.19 (1H, dd, *J* 13.9, 6.1 Hz 3-*HH*), 3.74 (3H, s, OCH₃), 4.67–4.72 (1H, m, 2-H), 5.07–5.14 (2H, m, CH₂Ph), 5.25 (1H, d, *J* 8.3 Hz, 2-NH), 7.15–7.20 (2H, m, 2'-H and 6'-H), 7.31–7.64 (11H, m, Ph, 3'-H, 5'-H, 2''-H, 3''-H, 5''-H and 6''-H); δ_{C} (101 MHz, CDCl₃) 37.8 (CH₂), 52.4 (CH₃), 54.7 (CH), 67.0 (CH₂), 127.1 (2 × CH), 127.5 (CH), 128.1 (2 × CH), 128.2 (2 × CH), 128.5 (2 × CH), 128.9 (2 × CH), 129.8 (2 × CH), 133.4 (C), 135.1 (C), 136.2 (C), 139.1 (C), 141.0 (C), 155.6 (C), 171.9 (C); *m/z* (ESI) 446.1131 (MNa⁺. C₂₄H₂₂³⁵ClINaO₄ requires 446.1130).

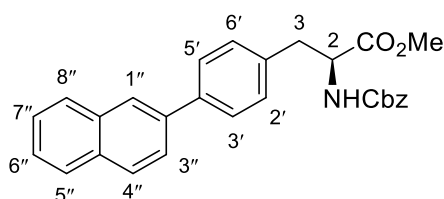
Methyl (2*S*)-2-(benzyloxycarbonylamino)-3-(4''acetylbiphen-4'-yl)propanoate (140c)



Methyl (2*S*)-2-(benzyloxycarbonylamino)-3-(4''-acetylbiphen-4'-yl)propanoate was synthesised as described in general procedure using methyl (2*S*)-2-(benzyloxycarbonylamino)-3-(4-hydroxyphenyl)propanoate (0.15 g, 0.46 mmol), perfluoro-1-butanesulfonyl fluoride (0.12 mL, 0.68 mmol), 4-acetylphenylboronic acid (0.10 g, 0.68 mmol), XPhos Pd G2 (0.012 g, 0.015 mmol, 3 mol%) and potassium phosphate (0.29 g, 1.4 mmol) in acetonitrile (1.5 mL) and water (1 mL) at 60 °C. Purification by flash column chromatography, eluting with 20% ethyl acetate in hexane gave methyl (2*S*)-2-(benzyloxycarbonylamino)-3-(4''-acetylbiphen-4'-yl)propanoate **140c** (0.11 g, 57%) as a white solid. Mp 125–128 °C; $\nu_{\max}/\text{cm}^{-1}$ (neat) 3336 (NH), 2955 (CH), 2890, 2251, 1713 (C=O), 1676, 1515, 1353,

1260, 1210; $[\alpha]_{\text{D}}^{25} +55.5$ (*c* 0.1, CHCl_3); δ_{H} (400 MHz, CDCl_3) 2.61 (3H, s, 4''-COCH₃), 3.12 (1H, dd, *J* 13.9, 6.2 Hz, 3-HH), 3.21 (1H, dd, *J* 13.9, 5.7 Hz, 3-HH), 3.74 (3H, s, OCH₃), 4.68–4.73 (1H, m, 2-H), 5.06–5.13 (2H, m, CH₂Ph), 5.37 (1H, d, *J* 8.2 Hz, 2-NH), 7.19–7.21 (2H, m, 2'-H and 6'-H), 7.29–7.35 (5H, m, Ph), 7.51–7.53 (2H, m, 3'-H and 5'-H), 7.63–7.65 (2H, m, 2''-H and 6''-H), 8.00–8.02 (2H, m, 3''-H and 5''-H); δ_{C} (101 MHz, CDCl_3) 26.7 (CH₃), 37.9 (CH₂), 52.4 (CH₃), 54.8 (CH), 67.0 (CH₂), 127.0 (2 × CH), 127.4 (2 × CH), 128.1 (2 × CH), 128.2 (2CH), 128.5 (2 × CH), 128.9 (2 × CH), 129.9 (2 × CH), 135.8 (C), 136.0 (C), 136.2 (C), 138.6 (C), 145.2 (C), 155.6 (C), 171.9 (C), 197.7 (C); *m/z* (ESI) 454.1631 (MNa⁺. C₂₆H₂₅NNaO₅ requires 454.1625).

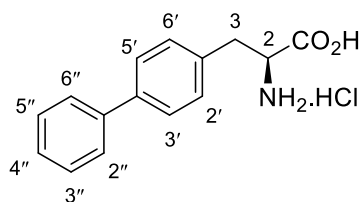
Methyl (2S)-2-(benzyloxycarbonylamino)-3-[(2''-naphthyl)phen-4'-yl]propanoate (140d)



Methyl (2S)-2-(benzyloxycarbonylamino)-3-[(2''-naphthyl)phen-4'-yl]propanoate was synthesised as described in general procedure using methyl (2S)-2-(benzyloxycarbonylamino)-3-(4-hydroxyphenyl)propanoate (0.15 g, 0.46 mmol), perfluoro-1-butanefluoride (0.12 mL, 0.68 mmol), 2-naphthaleneboronic acid (0.12 g, 0.68 mmol), XPhos Pd G2 (0.012 g, 0.015 mmol, 3 mol%) and potassium phosphate (0.29 g, 1.4 mmol) in acetonitrile (1.5 mL) and water (1 mL) at 80 °C. Purification by flash column chromatography, eluting with 30% ethyl acetate in hexane gave methyl (2S)-2-(benzyloxycarbonylamino)-3-[(2''-naphthyl)phen-4'-yl]propanoate **140d** (0.11 g, 52%) as a colourless oil. $\nu_{\text{max}}/\text{cm}^{-1}$ (neat) 3346 (NH), 3320, 3059, 2978 (CH), 1776 (C=O), 1651, 1538, 1318, 1249, 1050, 1022; $[\alpha]_{\text{D}}^{25} +62.8$ (*c* 0.1, CHCl_3); δ_{H} (400 MHz, CDCl_3) 3.14 (1H, dd, *J* 13.9, 6.1 Hz, 3-HH), 3.21 (1H, dd, *J* 13.9, 5.7 Hz 3-HH), 3.75 (3H, s, OCH₃), 4.69–4.74 (1H, m, 2-H), 5.07–5.15 (2H, m, CH₂Ph), 5.30 (1H, d, *J* 8.3 Hz, 2-NH), 7.18–7.22 (2H, m, 2'-H and 6'-H), 7.27–7.36 (5H, m, Ph), 7.45–7.52 (2H, m, 3'-H and 5'-H), 7.61–7.64 (2H, m, 6''-H and 7''-H), 7.70 (1H, dd, *J* 8.5, 1.8 Hz, 3''-H), 7.84–7.91 (3H, m, 4''-H, 5''-H and 8'-H), 8.00 (1H, d, *J* 1.8 Hz, 1''-H); δ_{C} (101 MHz, CDCl_3)

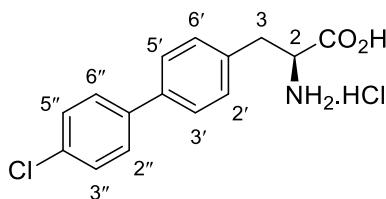
37.9 (CH₂), 52.4 (CH₃), 54.8 (CH), 67.0 (CH₂), 125.4 (CH), 125.7 (CH), 125.9 (CH), 126.3 (CH), 127.6 (2 × CH), 127.7 (CH), 128.1 (2 × CH), 128.2 (CH), 128.2 (CH), 128.4 (CH), 128.5 (2 × CH), 129.8 (2 × CH), 132.6 (CH), 133.7 (C), 134.9 (C), 136.3 (C), 138.0 (C), 139.9 (C), 155.7 (C), 172.0 (C); *m/z* (ESI) 462.1688 (MNa⁺. C₂₈H₂₅NNaO₄ requires 462.1676).

(2S)-2-Amino-3-(biphen-4'-yl)propanoic acid hydrochloride (143a)¹⁹⁷



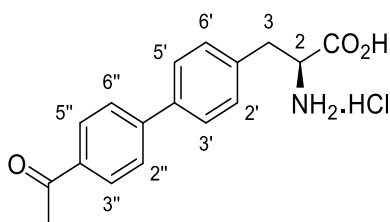
To a stirred solution of methyl (2S)-2-(benzyloxycarbonylamino)-3-(biphen-4'-yl)propanoate (0.031 g, 0.08 mmol) **140a** in methanol (2 mL), dioxane (1.75 mL) and water (1.75 mL) was added caesium carbonate (0.033 g, 0.10 mmol). The reaction mixture was stirred at room temperature for 18 h. The reaction mixture was concentrated *in vacuo*, diluted in water (5 mL), acidified to pH 1 using 1 M aqueous hydrochloric acid and then extracted with ethyl acetate (3 × 20 mL). The organic layers were combined, dried (MgSO₄), filtered and concentrated *in vacuo* to give (2S)-2-(benzyloxycarbonylamino)-3-(biphen-4'-yl)propanoic acid (0.028 g, 94%) **142a** as a yellow solid. (2S)-2-(Benzyloxycarbonylamino)-3-(biphen-4'-yl)propanoic acid (0.024 g, 0.06 mmol) was dissolved in 6 M hydrochloric acid (2 mL) and heated under reflux for 4 h. The reaction mixture was cooled to room temperature and concentrated *in vacuo* to give (2S)-2-amino-3-(biphen-4'-yl)propanoic acid **143a** (0.012 g, 84%) as a white solid. Mp 256–258 °C (lit.¹⁹⁷ 256–258 °C); [α]_D¹⁸ –80.7 (c 0.1, MeOH); δ_H (400 MHz, CD₃OD) 3.20 (1H, dd, *J* 14.5, 7.9 Hz, 3-*HH*), 3.38 (1H, dd, *J* 14.5, 5.4 Hz 3-*HH*), 4.29 (1H, dd, *J* 7.9, 5.4 Hz, 2-H), 7.38–7.49 (5H, m, 2'-H, 6'-H, 3''-H, 4''-H and 5''-H), 7.59–7.68 (4H, m, 3'-H, 5'-H, 2''-H and 6''-H); δ_C (101 MHz, CD₃OD) 36.9 (CH₂), 55.1 (CH), 127.9 (2 × CH), 128.5 (CH), 128.7 (2 × CH), 129.9 (2 × CH), 131.0 (2 × CH), 134.6 (C), 141.8 (C), 142.0 (C), 171.1 (C); *m/z* (ESI) 242 (MH⁺. 100%).

(2S)-2-Amino-3-(4''-chlorobiphen-4'-yl)propanoic acid hydrochloride (143b)



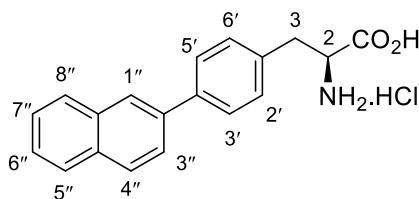
(2S)-2-Amino-3-(4''-chlorobiphen-4'-yl)propanoic acid hydrochloride **143b** was synthesised as described for (2S)-2-amino-3-(biphen-4'-yl)propanoic acid hydrochloride **143a** using methyl (2S)-2-(benzyloxycarbonylamino)-3-(4''-chlorobiphen-4'-yl)propanoate **140b** (0.091 g, 0.27 mmol), methanol (3 mL), dioxane (1.75 mL), water (1.75 mL) and caesium carbonate (0.089 g, 0.27 mmol). This gave (2S)-2-(benzyloxycarbonylamino)-3-(4''-chlorobiphen-4'-yl)propanoic acid **142b** (0.080 g, 93%) as a white solid which was used for the next reaction. (2S)-2-(Benzyloxycarbonylamino)-3-(4''-chlorobiphen-4'-yl)propanoic acid (0.051 g, 0.12 mmol) was dissolved in 6 M hydrochloric acid (2 mL) and heated under reflux for 4 h. The reaction mixture was cooled to room temperature and concentrated *in vacuo*. Purification by recrystallisation from a mixture of methanol and diethyl ether to give (2S)-2-amino-3-(4''-methoxybiphen-4'-yl)propanoic acid **143b** (0.033 g, 69%) as a white solid. Mp 235–237 °C; $\nu_{\max}/\text{cm}^{-1}$ (neat) 3457 (NH), 2883 (CH), 2176, 1730 (C=O), 1497, 1213; $[\alpha]_{\text{D}}^{23} -12.0$ (c 0.1, MeOH); δ_{H} (400 MHz, CD₃OD) 3.20 (1H, dd, *J* 14.5, 7.5 Hz, 3-*HH*), 3.36 (1H, dd, *J* 14.5, 7.6 Hz, 3-*HH*), 4.27–4.30 (1H, m, 2-H), 7.38–7.51 (4H, m, 2'-H, 3'-H, 5' H and 6'-H), 7.56–7.72 (4H, m, 2''-H, 3''-H, 5'' and 6''-H); δ_{C} (101 MHz, CD₃OD) 35.5 (CH₂), 56.1 (CH), 127.1 (2 × CH), 128.0 (2 × CH), 128.6 (2 × CH), 129.7 (2 × CH), 133.2 (C), 133.7 (C), 139.0 (C), 139.2 (C), 170.0 (C); *m/z* (ESI) 276.0794 (MH⁺. C₁₅H₁₅³⁵ClNO₂ requires 276.0786).

(2S)-2-Amino-3-(4''-acetylbiphen-4'-yl)propanoic acid hydrochloride (143c)



(2S)-2-Amino-3-(4''-acetylbiphen-4'-yl)propanoic acid hydrochloride **143c** was synthesised as described for (2S)-2-amino-3-(biphen-4'-yl)propanoic acid hydrochloride **143a** using methyl (2S)-2-(benzyloxycarbonylamino)-3-(biphen-4'-yl)propanoate **140c** (0.052 g, 0.12 mmol) in methanol (3 mL), dioxane (1.75 mL), water (1.75 mL) and caesium carbonate (0.051 g, 0.16 mmol). This gave (2S)-2-(benzyloxycarbonylamino)-3-(4''-acetylbiphen-4'-yl)propanoic acid **142c** (0.045 g, 89%) as a yellow solid which was used for the next reaction. (2S)-2-(Benzyloxycarbonylamino)-3-(4''-acetylbiphen-4'-yl)propanoic acid (0.040 g, 0.09 mmol) was dissolved in 6 M hydrochloric acid (2 mL) and heated under reflux for 4 h. The reaction mixture was cooled to room temperature and concentrated *in vacuo* to give (2S)-2-amino-3-(4''-acetylbiphen-4'-yl)propanoic acid **143c** (0.022 g, 87%) as a white solid. Mp 230–234 °C; $\nu_{\max}/\text{cm}^{-1}$ (neat) 3480 (NH), 2888 (CH), 1762 (C=O), 1645, 1551, 1479, 1294, $[\alpha]_{\text{D}}^{23}$ –8.0 (*c* 0.1, MeOH); δ_{H} (400 MHz, CD₃OD) 3.21 (1H, dd, *J* 14.5, 7.6 Hz, 3-HH), 3.38 (1H, dd, *J* 14.5, 7.1 Hz 3-HH), 4.28 (1H, dd, *J* 7.1, 5.6 Hz 2-H), 7.38–7.44 (2H, m, 2'-H and 6'-H), 7.59–7.68 (4H, m, 3'-H, 5'-H, 2''-H and 6''-H), 8.07–8.09 (2H, m, 3''-H and 5''-H); δ_{C} (101 MHz, CD₃OD) 25.3 (CH₃), 35.7 (CH₂), 58.7 (CH), 126.7 (2 × CH), 127.5 (2 × CH), 128.7 (2 × CH), 129.8 (2 × CH), 133.9 (C), 135.8 (C), 136.9 (C), 140.5 (C), 170.0 (C), 198.6 (C); *m/z* (ESI) 284.1287 (MH⁺. C₁₇H₁₈NO₃ requires 284.1281).

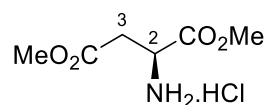
(2S)-2-Amino-3-[(2''-naphthyl)phen-4'-yl]propanoic acid hydrochloride (143d)



(2S)-2-Amino-3-(4''-naphthylbiphen-4'-yl)propanoic acid hydrochloride **143d** was synthesised as described for (2S)-2-amino-3-(biphen-4'-yl)propanoic acid hydrochloride **143a** using methyl (2S)-2-(benzyloxycarbonylamino)-3-[(2''-naphthyl)phen-4'-yl]propanoate **140d** (0.072 g, 0.16 mmol), methanol (3 mL), dioxane (1.75 mL), water (1.75 mL) and caesium carbonate (0.068 g, 0.21 mmol). This gave (2S)-2-(benzyloxycarbonylamino)-3-[(2''-naphthyl)phen-4'-yl]propanoic acid **142d** (0.059 g, 86%) as a white solid which was used for the next reaction. (2S)-2-(Benzyloxycarbonylamino)-3-[(2''-naphthyl)phen-4'-yl]propanoic acid (0.050 g, 0.12 mmol) was dissolved in 6 M hydrochloric acid (2 mL) and heated under reflux for 4 h. The reaction mixture was cooled to room temperature and concentrated *in vacuo*. Purification by recrystallisation from methanol and diethyl ether gave (2S)-2-amino-3-[(2''-naphthyl)phen-4'-yl]propanoic acid hydrochloride **143d** (0.030 g, 88%) as a white solid. Mp 236–240 °C; $\nu_{\max}/\text{cm}^{-1}$ (neat) 3331 (NH), 2856 (CH), 1768 (C=O), 1692, 1598, 1491, 1392, 1324, 1183, 1119; $[\alpha]_{\text{D}}^{23}$ -11.0 (*c* 0.1, MeOH); δ_{H} (400 MHz, CD₃OD) 3.00 (1H, dd, *J* 14.1, 9.4 Hz, 3-*HH*), 3.26 (1H, dd, *J* 14.1, 8.9 Hz, 3-*HH*), 4.49 (1H, dd, *J* 8.9, 4.6 Hz, 2-H), 7.23–7.51 (8H, m, 2'-H, 3'-H, 5'-H, 6'-H, 1''-H, 3''-H, 6''-H and 7''-H), 7.65–7.76 (3H, m, 4''-H, 5''-H and 8''-H); δ_{C} (101 MHz, CD₃OD) 36.9 (CH₂), 55.3 (CH), 125.5 (CH), 125.9 (CH), 126.8 (CH), 127.2 (CH), 127.5 (CH), 128.8 (CH), 128.0 (2 × CH), 129.5 (2 × CH), 132.7 (CH), 133.8 (C), 136.5 (C), 136.8 (C), 138.0 (C), 139.3 (C), 173.7 (C); *m/z* (ESI) 292.1335 (MH⁺. C₁₉H₁₈NO₂ requires 292.1332).

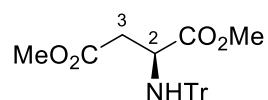
3.4 Enone Derived α -amino acids experimental

Dimethyl (2S)-2-aminobutandioate hydrochloride¹⁹⁸



To a suspension of L-aspartic acid **178** (5.00 g, 37.6 mmol) in methanol (30 mL) at 0 °C under argon was added dropwise thionyl chloride (4.00 mL, 52.6 mmol). The reaction mixture was warmed to room temperature and then heated under reflux for 3 h. The solution was concentrated *in vacuo* to give a colourless oil. This was triturated with diethyl ether which gave dimethyl (2S)-2-aminobutandioate hydrochloride as a colourless solid (7.55 g, 100%). Mp 115–116 °C (lit.¹⁹⁸ 114–115 °C); $[\alpha]_D^{24}$ +22.0 (c 1.0, MeOH); δ_H (400 MHz, DMSO- d_6) 2.99 (1H, dd, J 18.0, 5.5 Hz, 3-*HH*), 3.05 (1H, dd, J 18.0, 5.5 Hz, 3-*HH*), 3.66 (3H, s, OMe), 3.74 (3H, s, OMe), 4.35 (1H, t, J 5.5 Hz, 2-H), 8.72 (3H, s, CHNH_3^+); δ_C (101 MHz, DMSO- d_6) 34.0 (CH_2), 48.4 (CH), 52.2 (CH_3), 53.0 (CH_3), 168.7 (C), 169.6 (C); m/z (CI) 162 (MH^+ , 100%), 148¹⁹⁹, 102 (20).

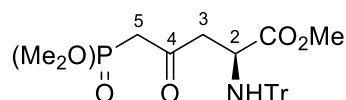
Dimethyl (2S)-2-(tritylamino)butandioate (**179**)²⁰⁰



To a solution of dimethyl (2S)-2-aminobutandioate hydrochloride (7.46 g, 37.7 mmol) in dichloromethane (150 mL) at 0 °C was added dropwise triethylamine (11.0 mL, 75.4 mmol) and triphenylmethylchloride (10.5 g, 37.7 mmol). The reaction mixture was allowed to warm to room temperature and stirred for 24 h. The reaction mixture was washed with 2 M citric acid (100 mL), water (100 mL), brine (100 mL), then dried (MgSO_4) and concentrated *in vacuo* to give a colourless oil. Purification by column chromatography eluting with 50% diethyl ether in petroleum ether gave dimethyl (2S)-2-(tritylamino)butandioate **179** as a colourless solid (15.2 g, 100%). Mp 71–72 °C (lit.²⁰⁰ 70–71 °C); $[\alpha]_D^{24}$ +36.6 (c 1.0, CHCl_3); δ_H (400 MHz, CDCl_3) 2.51 (1H, dd, J 14.7, 7.0 Hz, 3-*HH*), 2.66 (1H, dd, J 14.7, 5.4 Hz, 3-*HH*), 2.93 (1H, d, J 10.1 Hz, NH), 3.25 (3H, s, OMe), 3.67 (3H, s, OMe), 3.68–3.73 (1H, m, 2-H), 7.15–

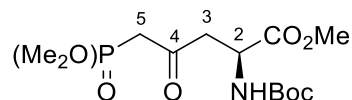
7.20 (3H, m, 3 × ArH), 7.23–7.28 (6H, m, 6 × ArH), 7.46–7.51 (6H, m, 6 × ArH); δ_{C} (101 MHz, CDCl_3) 39.0 (CH_2), 50.5 (CH), 50.7 (CH_3), 52.4 (CH_3), 69.9 (C), 125.2 (3 × CH), 126.6 (6 × CH), 127.5 (6 × CH), 144.4 (3 × C), 169.7 (C), 172.6 (C); m/z (EI) 403 (M^+ , 1%), 326 (35), 243 (100), 165 (30), 83 (70).

Methyl (2S)-5-(dimethoxyphosphoryl)-4-oxo-2-(tritylamino)pentanoate (180)²⁰¹



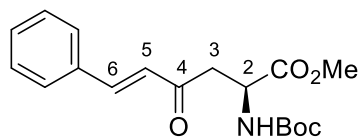
A solution of dimethyl methylphosphonate (3.00 mL, 27.3 mmol) in THF (50 mL) was cooled to $-78\text{ }^\circ\text{C}$ under an argon atmosphere. *n*-Butyl lithium (2.5 M in hexane, 11.0 mL, 28.6 mmol) was added dropwise and the reaction mixture stirred for 1 h. In a separate reaction vessel, a solution of dimethyl (2S)-2-(tritylamino)butandioate **179** (5.00 g, 12.4 mmol) in THF (100 mL) was cooled to $-78\text{ }^\circ\text{C}$ and then the dimethyl methylphosphonate/*n*-butyl lithium solution was cannulated into the flask and the reaction mixture stirred at $-78\text{ }^\circ\text{C}$ for 2 h to give a yellow solution. The reaction was quenched with a saturated solution of ammonium chloride (3 mL) and allowed to warm to room temperature. The mixture was concentrated *in vacuo*. The resulting residue was diluted with ethyl acetate (100 mL), washed with water (2 × 100 mL), brine (100 mL) then dried (MgSO_4) and concentrated *in vacuo*. Purification by column chromatography eluting with 40% ethyl acetate in dichloromethane gave methyl (2S)-5-(dimethoxyphosphoryl)-4-oxo-2-(tritylamino)pentanoate **180** as a white solid (5.71 g, 93%). Mp $117\text{--}118\text{ }^\circ\text{C}$ (lit.²⁰¹ $117\text{--}118.5\text{ }^\circ\text{C}$); $[\alpha]_{\text{D}}^{24} +31.1$ (c 1.0, CHCl_3); δ_{H} (400 MHz, CDCl_3) 2.78 (1H, dd, J 16.7, 6.9 Hz, 3-*HH*), 2.85–2.95 (2H, m, 3-*HH* and NH), 3.06 (2H, d, $J_{\text{H-C-P}}$ 22.7 Hz, 5- H_2), 3.29 (3H, s, OCH_3), 3.65–3.73 (1H, m, 2-H), 3.76 (3H, s, OCH_3), 3.79 (3H, s, OCH_3), 7.15–7.21 (3H, m, 3 × ArH), 7.26 (6H, t, J 7.7 Hz, 6 × ArH), 7.47 (6H, d, J 7.7 Hz, 6 × ArH); δ_{C} (101 MHz, CDCl_3) 41.8 (d, $J_{\text{C-P}}$ 128 Hz, CH_2), 48.8 (CH_2), 52.0 (CH_3), 52.9 (CH_3), 53.0 (CH_3), 53.1 (CH), 71.3 (C), 126.6 (3 × CH), 127.9 (6 × CH), 128.8 (6 × CH), 145.7 (3 × C), 174.0 (C), 199.3 (C); m/z (CI) 496 (MH^+ , 1%), 301¹⁹⁹, 254 (90), 243 (100), 237 (55), 167 (45).

Methyl (2S)-2-(tert-butoxycarbonylamino)-5-(dimethoxyphosphoryl)-4-oxopentanoate (192)



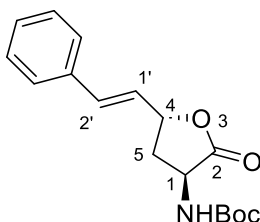
To a solution of methyl (2S)-5-(dimethoxyphosphoryl)-4-oxo-2-(tritylamino) pentanoate **180** (6.23 g, 12.6 mmol) in dichloromethane (100 mL) was added trifluoroacetic acid (9.62 mL, 126 mmol). The reaction mixture was stirred at room temperature for 2 h and then concentrated *in vacuo*. The resulting residue was dissolved in water (100 mL) and washed with diethyl ether (2 × 80 mL). The aqueous layer was concentrated *in vacuo* to give the TFA salt. This was dissolved in dichloromethane (40 mL), cooled to 0 °C and di-*tert*-butyl dicarbonate (5.50 g, 25.1 mmol) and triethylamine (3.60 mL, 25.1 mmol) were added. The reaction mixture was warmed to room temperature and stirred for 16 h. The reaction mixture was diluted with dichloromethane (50 mL), washed with 1 M aqueous hydrochloric acid (50 mL) and brine (50 mL). The organic layer was dried (MgSO₄) and concentrated *in vacuo*. Purification by flash chromatography using silica gel eluting with 2% methanol in dichloromethane gave methyl (2S)-2-(tert-butoxycarbonylamino)-5-(dimethoxyphosphoryl)-4-oxopentanoate **192** as a clear oil (4.12 g, 93%). $\nu_{\max}/\text{cm}^{-1}$ (neat) 3291 (NH), 2957 (CH), 1713 (C=O), 1506, 1368, 1252, 1165, 1026; $[\alpha]_{\text{D}}^{22} +25.2$ (*c* 1.0, CHCl₃); δ_{H} (400 MHz, CDCl₃) 1.42 (9H, s, 3 × CH₃), 3.09 (2H, d, *J* 22.7 Hz, 5-H₂), 3.13 (1H, dd, *J* 18.4, 4.3 Hz, 3-HH), 3.29 (1H, dd, *J* 18.4, 4.7 Hz, 3-HH), 3.71 (3H, s, OCH₃), 3.75 (3H, s, OCH₃), 3.78 (3H, s, OCH₃), 4.50 (1H, ddd, *J* 8.4, 4.7, 4.3 Hz, 2-H), 5.45 (1H, d, *J* 8.4 Hz, NH); δ_{C} (101 MHz, CDCl₃) 28.4 (3 × CH₃), 41.6 (d, *J*_{C-P} 128 Hz, CH₂) 45.9 (CH₂), 49.5 (CH), 52.7 (CH₃), 53.2 (d, *J*_{C-O-P} 5.4 Hz, CH₃), 53.3 (d, *J*_{C-O-P} 5.1 Hz, CH₃), 80.2 (C), 155.5 (C), 171.7 (C), 199.9 (C); *m/z* (ESI) 376.1121 (MNa⁺. C₁₃H₂₄NNaO₈P requires 376.1132).

Methyl (2S,5E)-4-oxo-6-phenyl-2-(tert-butoxycarbonylamino)hex-5-enoate (184)²⁰²



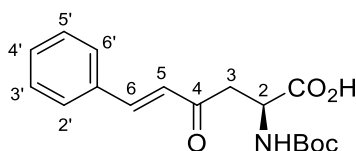
Methyl (2S)-2-(tert-butoxycarbonylamino)-5-(dimethoxyphosphoryl)-4-oxo pentanoate **183** (1.51 g, 4.27 mmol) was dissolved in acetonitrile (30 mL) at room temperature under argon. Anhydrous potassium carbonate (1.24 g, 8.97 mmol) was added to the solution and stirred for 0.5 h. Benzaldehyde (0.87 mL, 8.54 mmol) was added to the suspension and heated at 50 °C for 48 h. The reaction mixture was allowed to cool to room temperature and then concentrated *in vacuo*. The resultant residue was dissolved in ethyl acetate (50 mL) and washed with water (30 mL), brine (30 mL), then dried (MgSO₄) and concentrated *in vacuo*. Purification by column chromatography eluting with 20–40% diethyl ether in petroleum ether gave methyl (2S,5E)-4-oxo-6-phenyl-2-(tert-butoxycarbonylamino)hex-5-enoate **184** as a colourless oil (**175**) (0.980 g, 69%). $\nu_{\max}/\text{cm}^{-1}$ (NaCl) 3368 (NH), 2979 (CH), 1747 (C=O), 1713 (C=O), 1663 (C=C), 1496, 1367, 1168; $[\alpha]_{\text{D}}^{17} +56.9$ (*c* 1.0, CHCl₃); δ_{H} (400 MHz, CDCl₃) 1.44 (9H, s, O^tBu), 3.33 (1H, dd, *J* 17.8, 4.3 Hz, 3-HH), 3.44 (1H, dd, *J* 17.8, 4.1 Hz, 3-HH), 3.75 (3H, s, OMe), 4.62 (1H, ddd, *J* 8.5, 4.3, 4.1 Hz, 2-H), 5.60 (1H, d, *J* 8.5 Hz, NH), 6.71 (1H, d, *J* 16.1 Hz, 5-H), 7.38–7.42 (3H, m, 3 × ArH), 7.52–7.55 (2H, m, 2 × ArH), 7.57 (1H, d, *J* 16.1 Hz, 6-H); δ_{C} (101 MHz, CDCl₃) 28.3 (3 × CH₃), 42.4 (CH₂), 49.6 (CH), 52.6 (CH₃), 79.9 (C), 125.6 (CH), 128.4 (2 × CH), 129.2 (2 × CH), 130.9 (CH), 134.1 (C), 143.9 (CH), 155.6 (C), 172.0 (C), 197.6 (C); *m/z* (CI) 334.1653 (MH⁺. C₁₈H₂₄NO₅ requires 334.1654), 320 (4%), 278 (100), 234 (13).

tert-Butyl N-[(1S,4S)-2-oxo-4-[(E)-2-phenylethenyl]cyclopentyl]carbamate (193).



To a solution of the Boc-protected amino acid **175** (0.090 g, 0.27 mmol) in dry THF (3.0 mL) was added sodium borohydride (0.016 g, 0.43 mmol) at room temperature and under argon. The reaction mixture was reflux for 3 h before being quenched with an aqueous solution of ammonium chloride (5 mL). The reaction mixture was extracted with ethyl acetate (3 × 20 mL). The combined organic layers were washed with water (20 mL), brine (20 mL), dried (MgSO₄), filtered and concentrated *in vacuo*. The crude products were separated by column chromatography on silica, eluting with 30% ethyl acetate in petroleum ether to give **193** as colourless oil (0.020 g, 25%). $\nu_{\max}/\text{cm}^{-1}$ (NaCl) 3356 (NH), 2981 (CH), 1772 (C=O), 1684 (C=O), 1526, 1365, 1162; $[\alpha]_{\text{D}}^{24}$ -59.3 (c 1.0, CHCl₃); δ_{H} (400 MHz, CDCl₃) 1.47 (9H, s, O^tBu), 1.99–2.09 (1H, m, 5-HH), 2.95–2.98 (1H, m, 5-HH), 4.47–4.52 (1H, m, 4-H), 5.11 (1H, s, NH), 4.98–5.04 (1H, m, 1-H), 6.19 (1H, dd, *J* 15.9, 7.2 Hz, 1'-H), 6.73 (1H, d, *J* 15.9 Hz, 2'-H), 7.27–7.41 (5H, m, ArH); δ_{C} (101 MHz, CDCl₃) 28.3 (3 × CH₃), 37.6 (CH₂), 51.5 (CH), 78.3 (CH), 80.6 (C), 125.2 (CH), 126.8 (2 × CH), 128.6 (CH), 128.7 (2 × CH), 134.5 (CH), 135.4 (C), 155.4 (C), 175.0 (C); *m/z* (ESI) 326.1350 (MNa⁺. C₁₇H₂₁NNaO₄ requires 326.1363).

(2S,5E)-4-Oxo-6-phenyl-2-(tert-butoxycarbonylamino)hex-5-enoic acid (195)

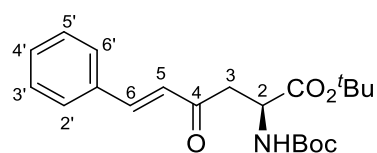


To a solution of methyl (2S,5E)-4-oxo-6-phenyl-2-(tert-butoxycarbonylamino)hex-5-enoate **184** (1.00 g, 3.00 mmol) in methanol/water (1:1, 12 mL) was added cesium carbonate (1.27 g, 3.90 mmol). The resultant suspension was stirred at room temperature for 24 h. The reaction mixture was concentrated *in vacuo* and the

residue was dissolved in water (15 mL) and acidified to pH 1 with 1 M hydrochloric acid. The aqueous layer was washed with dichloromethane (3 × 30 mL) and the combined organic layers were dried (MgSO₄), filtered and concentrated *in vacuo* to give (2*S*,5*E*)-4-oxo-6-phenyl-2-(*tert*-butoxycarbonylamino)hex-5-enoic acid **195** as a white solid (0.920 g, 96%). Mp 58–60 °C; $\nu_{\max}/\text{cm}^{-1}$ (neat) 3433 (NH), 2981 (CH), 1693 (C=O), 1660 (C=O), 1609 (C=C), 1495, 1367, 1159, 908, 728; $[\alpha]_{\text{D}}^{22} +15.7$ (c 0.1, CHCl₃); δ_{H} (400 MHz, CDCl₃) 1.44 (9H, s, 3 × CH₃), 3.26 (1H, dd, *J* 18.0, 4.4 Hz, 3-*HH*), 3.48 (1H, dd, *J* 18.0, 4.4 Hz, 3-*HH*), 4.65 (1H, dt, *J* 8.5, 4.4 Hz, 2-H), 5.64 (1H, d, *J* 8.5 Hz, NH), 6.74 (1H, d, *J* 16.2 Hz, 5-H), 7.35–7.43 (3H, m, 6-H and 2 × ArH), 7.54–7.63 (3H, m, 3 × ArH); δ_{C} (101 MHz, CDCl₃) 28.3 (3 × CH₃), 42.3 (CH₂), 49.5 (CH), 80.3 (C), 125.4 (CH), 128.5 (2 × CH), 129.0 (2 × CH), 130.9 (CH), 134.1 (CH), 144.4 (C), 155.8 (C), 175.8 (C), 198.0 (C); *m/z* (ESI) 342.1301 (MNa⁺. C₁₇H₂₁NNaO₅ requires 342.1312).

***tert*-Butyl (2*S*,5*E*)-4-oxo-6-phenyl-2-(*tert*-butoxycarbonylamino)hex-5-enoate**

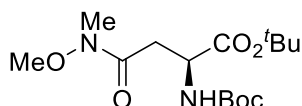
199



A solution of (2*S*,5*E*)-4-oxo-6-phenyl-2-(*tert*-butoxycarbonylamino)hex-5-enoic acid (**195**) (3.96 g, 17.1 mmol) in tetrahydrofuran (60 mL) was treated with *O*-*tert*-butyl *N,N*-diisopropylisourea (5.14 g, 25.7 mmol) at room temperature and then stirred for 2.5 h at 60 °C. Additional *O*-*tert*-butyl *N,N*-diisopropylisourea (3.43 g, 17.1 mmol) was added to the mixture and then stirring was continued overnight. The reaction mixture was filtered through celite, which was washed with diethyl ether (2 × 50 mL). The filtrate was then evaporated *in vacuo* and the crude product was purified by flash chromatography eluting with 30–50% ethyl acetate in hexane to give *tert*-butyl (2*S*,5*E*)-4-oxo-6-phenyl-2-(*tert*-butoxycarbonylamino)hex-5-enoate ¹⁹⁹ as a colourless oil (3.93 g, 80%). $\nu_{\max}/\text{cm}^{-1}$ (neat) 3337 (NH), 2978 (CH), 1711 (C=O), 1665 (C=O), 1610 (C=C), 1392, 1153, 758; $[\alpha]_{\text{D}}^{22} +19.0$ (c 0.1, CHCl₃); δ_{H} (400 MHz, CDCl₃) 1.44 (9H, s, 3 × CH₃), 1.45 (9H, s, 3 × CH₃), 3.17 (1H, dd, *J* 17.6, 4.3 Hz, 3-*HH*), 3.37 (1H, dd, *J* 17.6, 4.3 Hz, 3-*HH*), 4.48 (1H, dt, *J* 8.6, 4.3 Hz, 2-H), 5.54 (1H, d, *J* 8.6 Hz, NH), 6.72 (1H, d, *J* 16.3 Hz, 5-H), 7.40–7.42 (3H, m, 6-H and 2 × ArH),

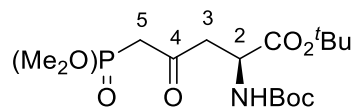
7.54–7.59 (3H, m, 3 × ArH); δ_{C} (101 MHz, CDCl_3) 27.9 (3 × CH_3), 28.3 (3 × CH_3), 42.5 (CH_2), 50.3 (CH), 79.7 (C), 82.0 (C), 125.8 (CH), 128.4 (2 × CH), 129.0 (2 × CH), 130.7 (CH), 134.2 (CH), 143.6 (C), 155.6 (C), 170.4 (C), 197.0 (C); m/z (ESI) 398.1938 (MNa^+ . $\text{C}_{21}\text{H}_{29}\text{NNaO}_5$ requires 398.1935).

***tert*-Butyl (2*S*)-(*tert*-butoxycarbonylamino)-4-[methoxy(methyl)amino]-4-oxobutanoate (**119**)¹¹⁶**



A mixture of 1-*tert*-butyl (2*S*)-(*tert*-butoxycarbonylamino)-4-butan-1,4-dioic acid **118** (0.500 g, 1.76 mmol), *N,O*-dimethylhydroxyamine hydrochloride (0.240 g, 2.44 mmol), and *O*-(benzotriazol-1-yl)-*N,N,N',N'*-tetramethyluronium hexafluorophosphate (HBTU), (0.730 g, 1.93 mmol) were stirred in *N,N'*-dimethylformamide (3 mL) at 0 °C. Diisopropylethylamine (0.75 mL, 4.40 mmol) was then added dropwise. The mixture was stirred at room temperature for 3 h. An aqueous solution of 1 M sodium hydrogen sulfate (25 mL) was then added, and the mixture was extracted with ethyl acetate (3 × 20 mL). The combined organic layers were then washed with brine (3 × 20 mL), dried (MgSO_4), and concentrated under vacuum. Purification by flash column chromatography eluting with 20% ethyl acetate in dichloromethane gave *tert*-butyl (2*S*)-(*tert*-butoxycarbonylamino)-4-[methoxy(methyl)amino]-4-oxobutanoate **119** as a colourless oil (0.590 g, 92%). $[\alpha]_{\text{D}}^{20}$ -14.5 (c 0.6, MeOH) (lit.¹¹⁶ $[\alpha]_{\text{D}}^{25}$ -12.3 (c 1.0, MeOH)); δ_{H} (400 MHz, CDCl_3) 1.44 (9H, s, 3 × CH_3), 1.46 (9H, s, 3 × CH_3), 2.88 (1H, dd, J 17.0, 3.6 Hz, 3-*HH*), 3.11–3.18 (4H, m, 3-*HH*, NCH_3), 3.69 (3H, s, OCH_3), 4.43–4.47 (1H, m 2-H), 5.67 (1H, d, J 8.7 Hz, NH); δ_{C} (101 MHz, CDCl_3) 27.9 (3 × CH_3), 28.3 (3 × CH_3), 32.0 (CH_3), 34.7 (CH_2), 50.4 (CH), 61.2 (CH_3), 79.5 (C), 81.7 (C), 155.8 (C), 170.6 (C), 171.8 (C); m/z (ESI) 355 (MNa^+ . 100%).

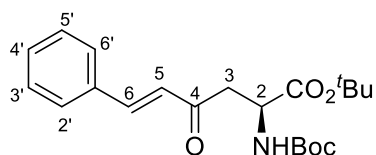
***tert*-Butyl (2*S*)-2-(*tert*-butoxycarbonylamino)-5-(dimethoxyphosphoryl)-4-oxopentanoate (**198**)**



A solution of dimethyl methylphosphonate (1.22 mL, 11.3 mmol) in tetrahydrofuran (20 mL) was cooled to $-78\text{ }^{\circ}\text{C}$ under an argon atmosphere. *n*-Butyl lithium (2.5 M in hexane, 4.50 mL, 11.3 mmol) was added dropwise and the reaction mixture stirred for 1 h. In a separate reaction vessel, a solution of dimethyl *tert*-butyl (2*S*)-(*tert*-butoxycarbonylamino)-4-[methoxy(methyl)amino]-4-oxobutanoate **119** (1.09 g, 3.23 mmol) in tetrahydrofuran (40 mL) was cooled to $-78\text{ }^{\circ}\text{C}$ and then the dimethyl methylphosphonate/*n*-butyl lithium solution was cannulated into the flask and the reaction mixture stirred at $-78\text{ }^{\circ}\text{C}$ for 2 h to give a yellow solution. The reaction was quenched with a saturated solution of ammonium chloride (2 mL) and allowed to warm to room temperature. The mixture was concentrated *in vacuo*. The resulting residue was diluted with ethyl acetate (50 mL), washed with water (2 \times 50 mL), brine (50 mL) then dried (MgSO_4) and concentrated *in vacuo*. Purification by flash column chromatography eluting with 75% ethyl acetate in dichloromethane gave *tert*-butyl (2*S*)-5-(dimethoxyphosphoryl)-4-oxo-2-(*tert*-butoxycarbonylamino)pentanoate **198** as a white solid (0.91 g, 70%). Mp $72\text{--}75\text{ }^{\circ}\text{C}$; $\nu_{\text{max}}/\text{cm}^{-1}$ (neat) 3290 (NH), 2976 (CH), 1713 (C=O), 1612, 1490, 1361, 1246, 1153, 851, 751; $[\alpha]_{\text{D}}^{22} +23.7$ (*c* 1.0, CHCl_3); δ_{H} (400 MHz, CDCl_3) 1.44 (9H, s, 3 \times CH_3), 1.45 (9H, s, 3 \times CH_3), 3.04–3.17 (3H, m, 3- H_2 and 5-*HH*), 3.27 (1H, dd, $J_{\text{H-C-P}}$ 18.3, 4.5 Hz, 5-*HH*), 3.78 (3H, s, OCH_3), 3.81 (3H, s, OCH_3), 4.37 (1H, dt, J 8.4, 4.5 Hz, 2-H), 5.45 (1H, d, J 8.4 Hz, NH); δ_{C} (101 MHz, CDCl_3) 27.8 (3 \times CH_3), 28.3 (3 \times CH_3), 41.4 (d, $^1J_{\text{C-P}}$ 128 Hz, CH_2), 46.1 (CH_2), 50.1 (CH), 53.1 (d, $J_{\text{C-O-P}}$ 3.3 Hz, CH_3), 53.1 (d, $J_{\text{C-O-P}}$ 3.5 Hz, CH_3), 79.8 (C), 82.3 (C), 155.5 (C), 170.0 (C), 199.7 (d, $^2J_{\text{C-P}}$ 6.2 Hz, C); m/z (ESI) 418.1603 (MNa^+ , $\text{C}_{16}\text{H}_{30}\text{NNaO}_8\text{P}$ requires 418.1601).

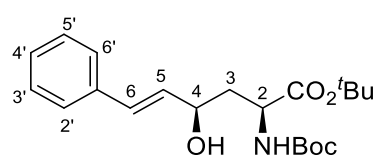
***tert*-Butyl (2*S*,5*E*)-4-oxo-6-phenyl-2-(*tert*-butoxycarbonylamino)hex-5-enoate**

199, 202



tert-Butyl (2*S*)-2-(*tert*-butoxycarbonylamino)-5-(dimethoxyphosphoryl)-4-oxo pentanoate **198** (2.81 g, 7.11 mmol) was dissolved in acetonitrile (80 mL) at room temperature under argon. Anhydrous potassium carbonate (1.08 g, 7.82 mmol) was added to the solution and stirred for 0.5 h. Benzaldehyde (1.45 mL, 14.22 mmol) was added to the suspension and heated at 50 °C for 48 h. The reaction mixture was allowed to cool to room temperature and then concentrated *in vacuo*. The resultant residue was dissolved in ethyl acetate (50 mL) and washed with water (30 mL), brine (30 mL), then dried (MgSO₄) and concentrated *in vacuo*. Purification by column chromatography eluting with 30% diethyl ether in petroleum ether gave methyl (2*S*,5*E*)-4-oxo-6-phenyl-2-(*tert*-butoxycarbonylamino)hex-5-enoate **196** as a colourless oil (2.10 g, 79%). Spectroscopic data as described above.

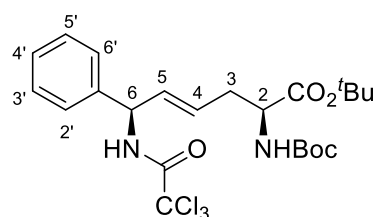
***tert*-Butyl (2*S*,4*R*,5*E*)-4-hydroxy-6-phenyl-2-(*tert*-butoxycarbonylamino)hex-5-enoate (**197**)**



To a solution of *tert*-butyl (2*S*,5*E*)-4-oxo-6-phenyl-2-(*tert*-butoxycarbonylamino)hex-5-enoate **196** (0.12 g, 0.31 mmol) in tetrahydrofuran (15 mL) was added *L*-selectride (0.11 mL, 0.49 mmol) dropwise at -78 °C and under argon. The mixture was allowed to stir for 3 h before being quenched with an aqueous solution of ammonium chloride (5 mL). The reaction mixture was extracted with ethyl acetate (3 × 20 mL). The combined organic layers were washed with water (20 mL), brine (20 mL), dried (MgSO₄), filtered and concentrated *in vacuo*. Purification by flash column chromatography on silica eluting with 50% diethyl ether in hexane gave *tert*-butyl (2*S*,4*R*,5*E*)-4-hydroxy-6-phenyl-2-(*tert*-butoxycarbonylamino)hex-5-enoate **197** as

a white solid (0.087 g, 75%). Mp 103–108 °C; $\nu_{\max}/\text{cm}^{-1}$ (neat) 3361 (NH), 2978 (CH), 1698 (C=O), 1495, 1366, 1250, 1152, 748; $[\alpha]_{\text{D}}^{19} +30.6$ (c 0.1, CHCl_3); δ_{H} (400 MHz, CDCl_3) 1.42 (9H, s, 3 × CH_3), 1.48 (9H, s, 3 × CH_3), 1.95 (1H, dt, J 12.0, 8.0 Hz, 3- HH), 2.11–2.18 (1H, m, 3- HH), 2.65 (1H, br s, OH), 4.31–4.33 (1H, m, 2-H), 4.49–4.52 (1H, m, 4-H), 5.35 (1H, d, J 6.8 Hz, NH), 6.23 (1H, dd, J 15.9, 6.0 Hz, 5-H), 6.61 (1H, d, J 15.9 Hz, 6-H), 7.21–7.39 (5H, m, 5 × ArH); δ_{C} (101 MHz, CDCl_3) 28.0 (3 × CH_3), 28.3 (3 × CH_3), 40.3 (CH_2), 51.9 (CH), 70.0 (CH), 80.1 (C), 82.2 (C), 126.5 (2 × CH), 127.7 (CH), 128.5 (2 × CH), 130.1 (CH), 131.7 (CH), 136.7 (C), 155.6 (C), 171.8 (C); m/z (ESI) 400.2085 (MNa^+). $\text{C}_{21}\text{H}_{31}\text{NNaO}_5$ requires 400.2094).

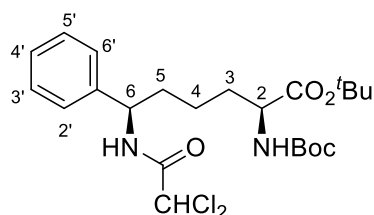
***tert*-Butyl (2*S*,4*E*,6*R*)-6-phenyl-2-(*tert*-butoxycarbonylamino)-6-(trichloromethyl carbonylamino)hex-4-ene (200)**



A stirred solution of (2*S*,4*R*,5*E*)-4-hydroxy-6-phenyl-2-(*tert*-butoxycarbonylamino)hex-5-enoate **197** (0.087 g, 0.23 mmol) in dichloromethane (5 mL) was cooled to 0 °C before 1,8-diazabicyclo[5.4.0]undec-7-ene (0.05 mL, 0.34 mmol) was added, followed by trichloroacetonitrile (0.012 mL, 0.11 mmol). The reaction mixture was stirred at 0 °C for 0.5 h and then at room temperature for 16 h. The mixture was then filtered through a plug of silica. This was washed with diethyl ether (30 mL) and the filtrate was concentrated *in vacuo* to give a yellow oil. The crude residue was then dissolved in *p*-xylene (10 mL) and potassium carbonate (0.030 g, 0.23 mmol) was added. The reaction mixture was then heated under reflux for 24 h before being concentrated *in vacuo*. Purification by flash column chromatography eluting with 20% ethyl acetate in petroleum ether gave *tert*-butyl (2*S*,4*E*,6*R*)-6-phenyl-2-(*tert*-butoxycarbonylamino)-6-(trichloromethylcarbonylamino)hex-4-ene **200** as a colourless oil (0.076 g, 64%). $\nu_{\max}/\text{cm}^{-1}$ (neat) 3427 (NH), 3323 (NH), 2978 (CH), 2926 (CH), 1698 (C=O), 1504, 1367, 1153, 759; $[\alpha]_{\text{D}}^{20} +17.2$ (c 0.5, CHCl_3); δ_{H} (400 MHz, CDCl_3) 1.43 (9H, s, 3 × CH_3), 1.44 (9H, s, 3 × CH_3), 2.46 (1H, dt, J 16.0, 8.0 Hz, 3- HH), 2.63 (1H, dt, J 16.0, 8.0 Hz, 3- HH), 4.24–4.29 (1H, m, 2-H), 5.10 (1H, d, J 7.7 Hz, NH), 5.52–5.55

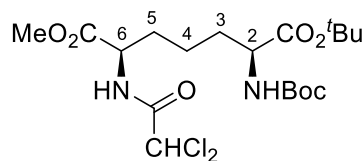
(1H, m, 6-H), 5.64 (1H, dt, J 15.4, 8.0 Hz, 4-H), 5.78 (1H, dd, J 15.4, 5.7 Hz, 5-H), 6.95 (1H, d, J 7.7 Hz, NH), 7.29–7.39 (5H, m, 5 × ArH); δ_{C} (101 MHz, CDCl₃) 28.0 (3 × CH₃), 28.4 (3 × CH₃), 35.7 (CH₂), 53.5 (CH), 56.4 (CH), 79.8 (C), 82.3 (C), 92.6 (C), 127.0 (2 × CH), 128.2 (CH), 128.2 (CH), 129.0 (2 × CH), 131.6 (CH), 139.1 (C), 155.2 (C), 160.9 (C), 170.9 (C); m/z (ESI) 543.1173 (MNa⁺. C₂₃H₃₁³⁵Cl₃N₂NaO₅ requires 543.1191).

***tert*-Butyl (2*S*,6*R*)-6-phenyl-2-(*tert*-butoxycarbonylamino)-6-(dichloromethyl carbonylamino)hexanoate (201)**



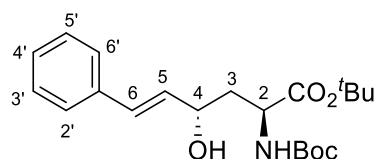
To a solution of *tert*-butyl (2*S*,4*E*,6*R*)-6-phenyl-2-(*tert*-butoxycarbonylamino)-6-(trichloromethylcarbonylamino)hex-4-ene **200** (0.050 g, 0.12 mmol) in methanol (4 mL) was added 10% palladium on carbon (0.0040 g). The reaction mixture was allowed to stir under an atmosphere of hydrogen at room temperature for 18 h. The reaction mixture was filtered through a short pad of celite, which was washed with methanol and concentrated *in vacuo*. Purification by flash column chromatography eluting with 50% diethyl ether in petroleum ether gave *tert*-butyl (2*S*,6*R*)-6-phenyl-2-(*tert*-butoxycarbonylamino)-6-(dichloromethylcarbonylamino)hexanoate **201** (0.020 g, 42% yield) as colourless oil. $\nu_{\text{max}}/\text{cm}^{-1}$ (neat) 3433 (NH), 2981 (CH), 2254, 1693 (C=O), 1609 (C=O), 1495, 1367, 1254, 1159, 908, 728; $[\alpha]_{\text{D}}^{20}$ -3.0 (c 0.1, CHCl₃); δ_{H} (400 MHz, CDCl₃) 1.31–1.38 (2H, m, 4-H₂), 1.42 (9H, s, 3 × CH₃), 1.43 (9H, s, 3 × CH₃), 1.59–1.66 (1H, m, 3-HH), 1.73–1.80 (1H, m, 3-HH), 1.88–1.94 (2H, m, 5-H₂), 4.14 (1H, q, J 7.8 Hz, 6-H), 4.90 (1H, q, J 7.4 Hz, 2-H), 5.03 (1H, d, J 7.8 Hz, NH), 5.93 (1H, s, CHCl₂), 6.86 (1H, d, J 7.4 Hz, NH), 7.26–7.43 (5H, m, 5 × ArH); δ_{C} (101 MHz, CDCl₃) 21.8 (CH₂), 28.0 (3 × CH₃), 28.4 (3 × CH₃), 32.8 (CH₂), 35.2 (CH₂), 53.5 (CH), 54.3 (CH), 66.5 (CH), 79.8 (C), 82.0 (C), 126.4 (2 × CH), 127.9 (CH), 128.9 (2 × CH), 140.5 (C), 155.5 (C), 163.4 (C), 171.8 (C); m/z (ESI) 511.1736 (MNa⁺. C₂₃H₃₄³⁵Cl₂N₂NaO₅ requires 511.1737).

1-*tert*-Butyl 7-methyl (2*S*,6*R*)-2-(*tert*-butoxycarbonylamino)-6-(dichloromethyl carbonylamino)hexan-1,7-dioate (202)



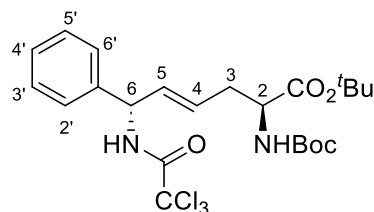
A suspension of *tert*-butyl (2*S*,6*R*)-6-phenyl-2-(*tert*-butoxycarbonylamino)-6-(dichloromethylcarbonylamino)hexanoate **201** (0.050 g, 0.12 mmol) and sodium periodate (0.32 g, 1.5 mmol) in acetonitrile (2.0 mL), carbon tetrachloride (2.0 mL) and water (3.0 mL) was treated with ruthenium(III) chloride hydrate (0.0046 g, 0.030 mmol). The reaction mixture was vigorously stirred at room temperature for 4 h. The mixture was diluted with ethyl acetate (5 mL), and the organic phase was washed with a 0.3 M aqueous solution of hydrochloric acid (5 mL) and brine (5 mL). The organic layer was dried (Na₂SO₄), filtered and concentrated *in vacuo*. The resulting residue was dissolved in toluene (5 mL) and methanol (5 mL), and (trimethylsilyl) diazomethane solution (2.0 M in diethyl ether, 2.2 mL, 4.4 mmol) was added dropwise. The reaction mixture was stirred at room temperature for 2 h and concentrated *in vacuo*. Purification by column chromatography eluting with 10% diethyl ether in petroleum ether gave 1-*tert*-butyl 7-methyl (2*S*,6*R*)-2-(*tert*-butoxycarbonylamino)-6-(dichloromethylcarbonylamino)hexan-1,7-dioate **202** as a colourless oil (0.02 g, 41%). $\nu_{\max}/\text{cm}^{-1}$ (neat) 2956 (CH), 1712 (C=O), 1510, 1367, 1254, 1165, 1050; $[\alpha]_{\text{D}}^{20} +32.0$ (c 0.1, CHCl₃); δ_{H} (400 MHz, CDCl₃) 1.28–1.66 (21H, m, 4-*HH*, 5-H₂ and 6 × CH₃), 1.75–1.83 (2H, m, 3-H₂), 1.92–2.01 (1H, m, 4-*HH*), 3.78 (3H, s, OCH₃), 4.12–4.17 (1H, m, 6-H), 4.54–4.61 (1H, m, 2-H), 5.06 (1H, d, *J* 7.5 Hz, NH), 5.95 (1H, s, CHCl₂), 7.11 (1H, d, *J* 7.8 Hz, NH); δ_{C} (101 MHz, CDCl₃) 20.9 (CH₂), 28.0 (3 × CH₃), 28.3 (3 × CH₃), 31.5 (CH₂), 32.6 (CH₂), 51.6 (CH), 52.7 (CH₃), 53.5 (CH), 66.1 (CH), 79.8 (C), 82.1 (C), 155.4 (C), 163.8 (C), 169.0 (C), 171.6 (C); *m/z* (ESI) 493.1478 (MNa⁺. C₁₉H₃₂³⁵Cl₂N₂NaO₇ requires 493.1479).

***tert*-Butyl (2*S*,4*S*,5*E*)-4-hydroxy-6-phenyl-2-(*tert*-butoxycarbonylamino)hex-5-enoate (**203**)**



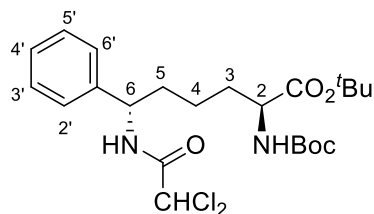
To a solution of *tert*-butyl (2*S*,5*E*)-4-oxo-6-phenyl-2-(*tert*-butoxycarbonylamino)hex-5-enoate **196** (0.10 g, 0.27 mmol) in tetrahydrofuran (10 mL) was added dropwise with stirring (*R*)-(+)-2-methyl-CBS-oxazaborolidine (0.30 mL, 0.30 mmol, 1 M solution in toluene) at 0 °C. The mixture was allowed to stir for 0.5 h at 0 °C. Borane (0.80 mL, 0.80 mmol, 1 M in tetrahydrofuran) was added dropwise and stirring was continued at 0 °C for 4 h. The mixture was quenched with methanol (5 mL), warmed to room temperature, and concentrated *in vacuo*. The reaction mixture was dissolved in diethyl ether (30 mL) and washed with 1 M citric acid (3 × 50 mL), water (50 mL), brine (50 mL) and dried (MgSO₄), filtered and concentrated *in vacuo*. Purification by flash column chromatography on silica eluting with ethyl acetate and petroleum ether (1:6) gave *tert*-butyl (2*S*,4*S*,5*E*)-4-hydroxy-6-phenyl-2-(*tert*-butoxycarbonylamino)hex-5-enoate **203** as a white solid (0.092 g, 87%). Mp 120–123 °C $\nu_{\max}/\text{cm}^{-1}$ (neat) 3457 (NH), 2981 (CH), 2365, 1723 (C=O), 1502, 1361, 1243, 1152, 909, 746; $[\alpha]_{\text{D}}^{25} +47.0$ (c 0.1, CHCl₃); δ_{H} (400 MHz, CDCl₃) 1.46 (18H, m, 6 × CH₃), 1.64–1.70 (1H, m, 3-*HH*), 2.03 (1H, ddd, *J* 13.9, 10.7, 4.0 Hz, 3-*HH*), 4.29–4.39 (2H, m, OH and 2-H), 4.44 (1H, ddd, *J* 10.7, 8.1, 4.0 Hz, 4-H), 5.49 (1H, d, *J* 7.8 Hz, NH), 6.23 (1H, dd, *J* 15.9, 8.1 Hz, 5-H), 6.66 (1H, d, *J* 15.9 Hz, 6-H), 7.19–7.24 (1H, m, ArH), 7.28–7.31 (2H, m, 2 × ArH), 7.36–7.39 (2H, m, 2 × ArH); δ_{C} (101 MHz, CDCl₃) 28.0 (3 × CH₃), 28.3 (3 × CH₃), 42.2 (CH₂), 51.2 (CH), 67.9 (CH), 80.6 (C), 82.5 (C), 126.4 (2 × CH), 127.5 (CH), 128.5 (2 × CH), 129.5 (CH), 131.0 (CH), 136.9 (C), 157.0 (C), 171.8 (C); *m/z* (ESI) 400.2114 (MNa⁺. C₂₁H₃₁NNaO₅ requires 400.2094).

***tert*-Butyl (2*S*,4*E*,6*S*)-6-phenyl-2-(*tert*-butoxycarbonylamino)-6-(trichloromethyl carbonylamino)hex-4-ene (205)**



A stirred solution of *tert*-butyl (2*S*,4*S*,5*E*)-4-hydroxy-6-phenyl-2-(*tert*-butoxy carbonylamino)hex-5-enoate **203** (0.31 g, 0.81 mmol) in dichloromethane (20 mL) was cooled to 0 °C before 1,8-diazabicyclo[5.4.0]undec-7-ene (0.18 mL, 1.2 mmol) was added followed by trichloroacetonitrile (0.41 mL, 0.50 mmol). The reaction mixture was stirred at 0 °C for 0.5 h and then at room temperature for 16 h. The mixture was then filtered through a plug of silica. This was washed with diethyl ether (50 mL) and the filtrate was concentrated *in vacuo* to give a yellow oil. The crude residue was then dissolved in *p*-xylene (20 mL) and potassium carbonate (0.11 g, 0.80 mmol) was added. The reaction mixture was then heated under reflux for 24 h before being concentrated *in vacuo*. Purification by flash column chromatography eluting with 20% ethyl acetate in petroleum ether gave *tert*-butyl (2*S*,4*E*,6*S*)-6-phenyl-2-(*tert*-butoxycarbonylamino)-6-(trichloromethylcarbonylamino)hex-4-ene **205** as a colourless oil (0.16 g, 38%). $\nu_{\max}/\text{cm}^{-1}$ (neat) 3327 (NH), 2905 (CH), 1700 (C=O), 1506 (C=O), 1362 (CO), 1217, 1152, 913, 768; $[\alpha]_{\text{D}}^{25}$ +31.0 (*c* 0.1, CHCl₃); δ_{H} (400 MHz, CDCl₃) 1.42 (18H, s, 6 × CH₃), 2.51 (1H, dt, *J* 13.8, 6.1 Hz, 3-*HH*), 2.63 (1H, dt, *J* 13.8, 6.9, Hz, 3-*HH*), 4.25–4.30 (1H, m, 2-H), 5.10 (1H, d, *J* 8.0 Hz, NH), 5.50–5.54 (1H, m, 6-H), 5.60–5.66 (1H, m, 4-H), 5.77 (1H, dd, *J* 15.4, 5.8 Hz, 5-H), 6.89 (1H, d, *J* 7.6 Hz, NH), 7.30–7.40 (5H, m, 5 × ArH); δ_{C} (101 MHz, CDCl₃) 28.0 (3 × CH₃), 28.4 (3 × CH₃), 35.4 (CH₂), 53.4 (CH), 56.6 (CH), 79.8 (C), 82.3 (C), 92.6 (C), 127.0 (2 × CH), 127.8 (CH), 128.3 (CH), 129.1 (2 × CH), 131.6 (CH), 139.0 (C), 154.8 (C), 160.8 (C), 170.8 (C); *m/z* (ESI) 543.1194 (MNa⁺. C₂₃H₃₁³⁵Cl₃N₂NaO₅ requires 543.1191).

***tert*-Butyl (2*S*,6*S*)-6-phenyl-2-(*tert*-butoxycarbonylamino)-6-(dichloromethyl carbonylamino)hexanoate (206)**



To a solution of *tert*-butyl (2*S*,4*E*,6*S*)-6-phenyl-2-(*tert*-butoxycarbonylamino)-6-(trichloromethylcarbonylamino)hex-4-ene **205** (0.16 g, 0.30 mmol) in methanol (15 mL) was added 10% palladium on carbon (0.012 g). The reaction mixture was allowed to stir under an atmosphere of hydrogen at room temperature for 18 h. The reaction mixture was filtered through a short pad of celite, which was washed with methanol and concentrated *in vacuo*. Purification by flash column chromatography eluting with 50% diethyl ether in petroleum ether gave *tert*-butyl (2*S*,6*S*)-6-phenyl-2-(*tert*-butoxycarbonylamino)-6-(dichloromethylcarbonylamino)hexanoate **206** (0.092 g, 63% yield) as colourless oil. $\nu_{\max}/\text{cm}^{-1}$ (neat) 3289 (NH), 2926 (CH), 1676 (C=O), 1540 (C=O), 1368, 1153, 847, 701; $[\alpha]_{\text{D}}^{25} -7.2$ (*c* 0.1, CHCl₃); δ_{H} (400 MHz, CDCl₃) 1.24–1.35 (2H, m, 4-H₂), 1.40 (9H, s, 3 × CH₃), 1.43 (9H, s, 3 × CH₃), 1.55–1.67 (1H, m, 3-HH), 1.75–2.00 (3H, m, 3-HH and 5-H₂), 4.08–4.17 (1H, m, 6-H), 4.89 (1H, q, *J* 7.8 Hz, 2-H), 5.06 (1H, d, *J* 7.8 Hz, NH), 5.92 (1H, s, CHCl₂), 6.83 (1H, d, *J* 5.7 Hz, NH), 7.27–7.37 (5H, m, 5 × ArH); δ_{C} (101 MHz, CDCl₃) 21.8 (CH₂), 28.0 (3 × CH₃), 28.4 (3 × CH₃), 32.7 (CH₂), 35.4 (CH₂), 53.5 (CH), 54.3 (CH), 66.5 (CH), 79.7 (C), 82.0 (C), 126.4 (2 × CH), 127.8 (CH), 128.9 (2 × CH), 140.8 (C), 155.5 (C), 163.5 (C), 171.7 (C); *m/z* (ESI) 511.1734 (MNa⁺. C₂₃H₃₄³⁵Cl₂N₂NaO₅ requires 511.1737).

4.0 References

1. R. J. Ouellette and J. D. Rawn, in *Organic Chemistry Study Guide*, eds. R. J. Ouellette and J. D. Rawn, Elsevier, Boston, 2015, DOI: <https://doi.org/10.1016/B978-0-12-801889-7.00027-3>.
2. V. K. Ahluwalia, L. S. Kumar and S. Kumar, in *Chemistry of Natural Products: Amino Acids, Peptides, Proteins and Enzymes*, eds. V. K. Ahluwalia, L. S. Kumar and S. Kumar, Springer International Publishing, Cham, 2022, DOI: 10.1007/978-3-030-86698-3_1.
3. S. Paudel, G. Wu and X. Wang, Springer International Publishing, 2021, DOI: 10.1007/978-3-030-74180-8_2.
4. P. Staszek, L. A. Weston, K. Ciacka, U. Krasuska and A. Gniazdowska, *Phytochem. Rev.*, 2017, **16**, 1269-1282.
5. M. Fichtner, K. Voigt and S. Schuster, *Biochim Biophys Acta Gen Subj*, 2017, **1861**, 3258-3269.
6. Y. Ding, J. P. Ting, J. Liu, S. Al-Azzam, P. Pandya and S. Afshar, *Amino acids*, 2020, **52**, 1207–1226.
7. E. W. Hancock Robert and S. Chapple Daniel, *Antimicrob. Agents Chemother.*, 1999, **43**, 1317-1323.
8. M. Agirre, A. Arrieta, I. Arrastia and F. P. Cossio, *Chem. Asian J.*, 2019, **14**, 44.
9. R. Iwata, S. Furumoto, C. Pascali, A. Bogni and K. Ishiwata, *J. Labelled Compd. Radiopharm.*, 2003, **46**, 555-566.
10. R. H. Newman, M. D. Fosbrink and J. Zhang, *Chem. Rev.*, 2011, **111**, 3614-3666.
11. W. Niu and J. Guo, *Mol. BioSyst.*, 2013, **9**, 2961.
12. J. W. Lichtman and J.-A. Conchello, *Nat. Methods*, 2005, **2**, 910-919.
13. J. R. Lakowicz, *Introduction to Fluorescence.*, Springer, Boston, MA., 2006.
14. G. O. F. Parikesit, in *Encyclopedia of Microfluidics and Nanofluidics*, ed. D. Li, Springer US, Boston, MA, 2013, DOI: 10.1007/978-3-642-27758-0_580-2, pp. 1-10.
15. E. Tully and R. O'Kennedy, *Fluorescent Labeling*, Springer, Boston, MA, 2008.
16. J. R. Lakowicz, Springer US, 2006.
17. K.-L. Wong, J.-C. G. Bünzli and P. A. Tanner, *J. Lumin.*, 2020, **224**, 117256.

18. M. M. Ochomogo and C. T. Lohans, *RSC med. chem*, 2021, **12**, 1623-1639.
19. AL. Botelho, Y. Shin, J. Liu and X. Lin, *PLOS ONE*, 2014, **9**, e86370.
20. Y. Ha and H.-K. Choi, *Chem. Biol. Interact.*, 2016, **248**, 36-51.
21. L. D. Lavis and R. T. Raines, *ACS Chem. Biol.*, 2008, **3**, 142-155.
22. J. M. Hicks, *Hum Pathol*, 1984, **15**, 112-116.
23. A. Loudet and K. Burgess, *Chem. Rev.*, 2007, **107**, 4891-4932.
24. T. Terai and T. Nagano, *Pflügers Arch - Eur. J. Physiol*, 2013, **465**, 347-359.
25. C. Wu, J. Wang, J. Shen, C. Bi and H. Zhou, *Sens. Actuators B Chem.*, 2017, **243**, 678-683.
26. G. T. Dempsey, M. Bates, W. E. Kowtoniuk, D. R. Liu, R. Y. Tsien and X. Zhuang, *J. Am. Chem. Soc.*, 2009, **131**, 18192-18193.
27. C. P. Toseland, *J. Chem. Biol.*, 2013, **6**, 85-95.
28. C. M. Jones, D. M. Robkis, R. J. Blizzard, M. Munari, Y. Venkatesh, T. S. Mihaila, A. J. Eddins, R. A. Mehl, W. N. Zagotta, S. E. Gordon and E. J. Petersson, *Chem. Sci.*, 2021, **12**, 11955-11964.
29. W. Zhang, Z. Ma, L. Du and M. Li, *The Analyst*, 2014, **139**, 2641-2649.
30. D. Altman, D. Goswami, T. Hasson, J. A. Spudich and S. Mayor, *PLOS Biol.*, 2007, **5**, e210.
31. T. Zhou and M. Szostak, *Catal. Sci. Technol.*, 2020, **10**, 5702-5739.
32. Z. Zhang, W. Xu, M. Kang, H. Wen, H. Guo, P. Zhang, L. Xi, K. Li, L. Wang, D. Wang and B. Z. Tang, *Adv. Mater.*, 2020, **32**, 2003210.
33. M. Hirshberg, K. Henrick, L. Lloyd Haire, N. Vasisht, M. Brune, J. E. T. Corrie and M. R. Webb, *Biochem.*, 1998, **37**, 10381-10385.
34. B. Hein, K. I. Willig, C. A. Wurm, V. Westphal, S. Jakobs and S. W. Hell, *Biophys. J.*, 2010, **98**, 158-163.
35. R. Sjöback, J. Nygren and M. Kubista, *Spectrochim. Acta A Mol. Biomol. Spectrosc.*, 1995, **51**, L7-L21.
36. W.-C. Sun, K. R. Gee, D. H. Klaubert and R. P. Haugland, *J. Org. Chem.*, 1997, **62**, 6469-6475.
37. J. L. Turnbull, B. R. Benlian, R. P. Golden and E. W. Miller, *J. Am. Chem. Soc.*, 2021, **143**, 6194-6201.
38. N. Boens, V. Leen and W. Dehaen, *Chem. Soc. Rev.*, 2012, **41**, 1130-1172.
39. P. Chinna Ayya Swamy, G. Sivaraman, R. N. Priyanka, S. O. Raja, K. Ponnuvel, J. Shanmugpriya and A. Gulyani, *Coord. Chem. Rev.*, 2020, **411**, 213233.

40. R. He, Y. Zhang, S. Madhu, Q. Gao, Q. Lian, S. S. Raghavan and J. Geng, *Chem. Commun.*, 2020, **56**, 14717-14720.
41. J. B. Grimm and L. D. Lavis, *Nat. Methods*, 2022, **19**, 149-158.
42. A. C. Benniston and G. Copley, *Phys. Chem. Chem. Phys.*, 2009, **11**, 4124.
43. I. Johnson, *Histochem. J.*, 1998, **30**, 123-140.
44. M. Farinone, J. Cybińska and M. Pawlicki, *Org. Chem. Front.*, 2020, **7**, 2391-2398.
45. P. Majumdar, X. Yuan, S. Li, B. Le Guennic, J. Ma, C. Zhang, D. Jacquemin and J. Zhao, *J. Mater. Chem. B*, 2014, **2**, 2838-2854.
46. X. Ji, N. Wang, J. Zhang, S. Xu, Y. Si and W. Zhao, *Dyes Pigm.*, 2021, **187**, 109089.
47. T. Rohand, E. Dolusic, T. H. Ngo, W. Maes and W. Dehaen, *Arkivoc*, 2007, **2007**, 307-324.
48. K. V. Ksenofontova, A. A. Ksenofontov, I. A. Khodov and E. V. Rumyantsev, *J. Mol. Liq.*, 2019, **283**, 695-703.
49. L. Mendive-Tapia, R. Subiros-Funosas, C. Zhao, F. Albericio, N. D. Read, R. Lavilla and M. Vendrell, *Nat. Protoc.*, 2017, **12**, 1588-1619.
50. M. Beija, C. A. M. Afonso and J. M. G. Martinho, *Chem. Soc. Rev.*, 2009, **38**, 2410-2433.
51. J. B. Grimm, L. M. Heckman and L. D. Lavis, *Prog Mol Biol Transl Sci*, 2013, **113**, 1-34.
52. S. J. Dwight and S. Levin, *Org. Lett.*, 2016, **18**, 5316-5319.
53. J. B. Grimm and L. D. Lavis, *Org. Lett.*, 2011, **13**, 6354-6357.
54. W. B. Swanson, M. Durdan, M. Eberle, S. Woodbury, A. Mauser, J. Gregory, B. Zhang, D. Niemann, J. Herremans, P. X. Ma, J. Lahann, M. Weivoda, Y. Mishina and C. F. Greineder, *RSC Chem. Biol.*, 2022, **3**, 748-764.
55. D. Cao, Z. Liu, P. Verwilst, S. Koo, P. Jangjili, J. S. Kim and W. Lin, *Chem. Rev.*, 2019, **119**, 10403-10519.
56. J. Gordo, J. Avó, A. J. Parola, J. C. Lima, A. Pereira and P. S. Branco, *Org. Lett.*, 2011, **13**, 5112-5115.
57. M. Levitus and S. Ranjit, *Q. Rev. Biophys.*, 2011, **44**, 123-151.
58. H. A. Shindy, *Dyes Pigm.*, 2017, **145**, 505-513.
59. A. Mishra, R. K. Behera, P. K. Behera, B. K. Mishra and G. B. Behera, *Chem. Rev.*, 2000, **100**, 1973-2012.
60. C. N. Njiojob, E. A. Owens, L. Narayana, H. Hyun, H. S. Choi and M. Henary, *J. Med. Chem.*, 2015, **58**, 2845-2854.

61. E. A. Owens, M. Henary, G. El Fakhri and H. S. Choi, *Acc. Chem. Res.*, 2016, **49**, 1731-1740.
62. Y. Cho, H. J. An, T. Kim, C. Lee and N. K. Lee, *J. Am. Chem. Soc.*, 2021, **143**, 14125-14135.
63. M. E. Cooper, S. Gregory, E. Adie and S. Kalinka, *J. Fluoresc.*, 2002, **12**, 425-429.
64. W. R. Lovett, A. Al Hamd, S. Casa and M. Henary, *Dyes Pigm.*, 2021, **190**, 109268.
65. X. Qian, Y. Xiao, Y. Xu, X. Guo, J. Qian and W. Zhu, *Chem. Commun.*, 2010, **46**, 6418.
66. Y. Xiao, F. Liu, X. Qian and J. Cui, *Chem. Commun.*, 2005, DOI: 10.1039/b413537g, 239.
67. F. Liu, Y. Xiao, X. Qian, Z. Zhang, J. Cui, D. Cui and R. Zhang, *Tetrahedron*, 2005, **61**, 11264-11269.
68. T. Gunnlaugsson, A. P. Davis and M. Glynn, *Chem. Commun.*, 2001, DOI: 10.1039/b107608f, 2556-2557.
69. T. Gunnlaugsson, A. P. Davis, G. M. Hussey, J. Tierney and M. Glynn, *Org. Biomol. Chem.*, 2004, **2**, 1856.
70. J. Han and K. Burgess, *Chem. Rev.*, 2010, **110**, 2709-2728.
71. R. Nandi and N. Amdursky, *Acc. Chem. Res.*, 2022, **55**, 2728-2739.
72. Y. Li, Q. Chen, X. Pan, W. Lu and J. Zhang, *Top. Curr. Chem.*, 2022, **380**, 22.
73. T. Terai and T. Nagano, *Curr. Opin. Chem. Biol.*, 2008, **12**, 515-521.
74. A. Ghisaidoobe and S. Chung, *Int. J. Mol. Sci.*, 2014, **15**, 22518-22538.
75. Y. Xiong, C. Shi, L. Li, Y. Tang, X. Zhang, S. Liao, B. Zhang, C. Sun and C. Ren, *New J. Chem.*, 2021, **45**, 15180-15194.
76. Z. Cheng, E. Kuru, A. Sachdeva and M. Vendrell, *Nat. Rev. Chem.*, 2020, **4**, 275-290.
77. G. W. Gokel, *Dean's Handbook of Organic Chemistry*, McGraw-Hill, 2004.
78. J. A. Ross and D. M. Jameson, *Photochem. Photobiol. Sci.*, 2008, **7**, 1301-1312.
79. Y. Xiong, C. Shi, L. Li, Y. Tang, X. Zhang, S. Liao, B. Zhang, C. Sun and C. Ren, *New J. Chem.*, 2021, **45**, 15180-15194.
80. J. M. Antosiewicz and D. Shugar, *Biophys. Rev.*, 2016, **8**, 151-161.
81. P. Horx and A. Geyer, *Chem. Sci.*, 2021, **12**, 11455-11463.

82. Y. S. Moroz, W. Binder, P. Nygren, G. A. Caputo and I. V. Korendovych, *Chem. Commun.*, 2013, **49**, 490-492.
83. A. V. Smirnov, D. S. English, R. L. Rich, J. Lane, L. Teyton, A. W. Schwabacher, S. Luo, R. W. Thornburg and J. W. Petrich, *J. Phys. Chem. B*, 1997, **101**, 2758-2769.
84. J. B. Alexander Ross, A. G. Szabo and C. W. V. Hogue, in *Methods in Enzymology*, Academic Press, 1997, vol. 278, pp. 151-190.
85. P. Cheruku, J.-H. Huang, H.-J. Yen, R. S. Iyer, K. D. Rector, J. S. Martinez and H.-L. Wang, *Chem. Sci.*, 2015, **6**, 1150-1158.
86. A. Gupta, B. P. Garreffi and M. Guo, *Chem. Commun.*, 2020, **56**, 12578-12581.
87. A. Filarowski, M. Kluba, K. Cieřlik-Boczula, A. Koll, A. Kochel, L. Pandey, W. M. De Borggraeve, M. Van Der Auweraer, J. Catalán and N. Boens, *Photochem. Photobiol. Sci.*, 2010, **9**, 996–1008.
88. R. J. Micikas, A. Acharyya, A. B. Smith and F. Gai, *Chem. Phys. Lett.*, 2022, **795**, 139553.
89. B. H. Jhun, K. Ohkubo, S. Fukuzumi and Y. You, *J. Mater. Chem. C*, 2016, **4**, 4556-4567.
90. M. P. Brun, L. Bischoff and C. Garbay, *Angew Chem Int Ed Engl*, 2004, **43**, 3432-3436.
91. F. Bureř, *RSC Adv.*, 2014, **4**, 58826-58851.
92. F. Würthner, F. Effenberger, R. Wortmann and P. Krämer, *Chem. Phys.*, 1993, **173**, 305-314.
93. C. Dehu, F. Meyers and J. L. Bredas, *J. Am. Chem. Soc.*, 1993, **115**, 6198-6206.
94. A. E. Stiegman, E. Graham, K. J. Perry, L. R. Khundkar, L. T. Cheng and J. W. Perry, *J. Am. Chem. Soc.*, 1991, **113**, 7658-7666.
95. S. R. Marder, L.-T. Cheng and B. G. Tiemann, *J. Chem. Soc.*, 1992, 672.
96. A. Adhikari, B. R. Bhattarai, A. Aryal, N. Thapa, P. Kc, A. Adhikari, S. Maharjan, P. B. Chanda, B. P. Regmi and N. Parajuli, *RSC Adv.*, 2021, **11**, 38126-38145.
97. A. H. Harkiss and A. Sutherland, *Org. Biomol. Chem.*, 2016, **14**, 8911-8921.
98. M. Eugenio Vázquez, D. M. Rothman and B. Imperiali, *Org. Biomol. Chem.*, 2004, **2**, 1965-1966.
99. G. Loving and B. Imperiali, *J. Am. Chem. Soc.*, 2008, **130**, 13630-13638.

100. E. Azuma, N. Nakamura, K. Kuramochi, T. Sasamori, N. Tokitoh, I. Sagami and K. Tsubaki, *J Org Chem*, 2012, **77**, 3492-3500.
101. S. Chen, N. E. Fahmi, C. Bhattacharya, L. Wang, Y. Jin, S. J. Benkovic and S. M. Hecht, *Biochem.*, 2013, **52**, 8580-8589.
102. D. A. Dougherty, *Chem. Biol.*, 2000, **4**, 645–652.
103. A. R. Katritzky and T. Narindoshvili, *Org. Biomol*, 2009, **7**, 627-634.
104. C. M. Haney, R. F. Wissner and E. J. Petersson, *Chem. Biol.*, 2015, **28**, 123-130.
105. I. Coin, *Synth.Biol.*, 2018, **46**, 156-163.
106. K. L. Kiick, E. Saxon, D. A. Tirrell and C. R. Bertozzi, *Proc. Natl Acad. Sci. USA*, 2002, **99**, 19–24.
107. M.-L. sao, F. Tian and P. G. Schultz, *Chembiochem*, 2005, **6**, 2147-2149.
108. G. V. M. Sharma, B. S. Babu, K. V. S. Ramakrishna, P. Nagendar, A. C. Kunwar, P. Schramm, C. B. and H. and J. Hofmann, *Chem.–Eur. J.*, 2009, **15**, 5552.
109. R. Huisgen, *Chem. Int. Ed.*, 1963, **2**, 566-598.
110. M. Meldal and C. W. Tornøe, *Chem. Rev.*, 2008, **108**, 2952-3018.
111. I. Avan, C. D. Hal and A. R. Katri, *Chem.Soc.Rev* 2014, **43**, 3575.
112. L. S. Fowler, D. Ellis and A. Sutherland, *Org. Biomol. Chem.*, 2009, **7**.
113. A. H. Harkiss, J. D. Bell, A. Knuhtsen, A. G. Jamieson and A. Sutherland, *J. Org. Chem.*, 2019, **84**, 2879–2890.
114. J. D. Bell, T. E. F. Morgan, N. Buijs, A. H., Harkiss, C. R. Wellaway and A. Sutherland, *J. Org. Chem* . 2019, **84**, 10436.
115. L. M. Riley, T. N. Mclay and A. Sutherland, *J. Org. Chem.*, 2023, **88**, 2453-2463.
116. H.-D. Vu, J. Renault, L. Toupet, P. Uriac and N. Gouault, *Eur. J. Org. Chem*, 2013, 6677.
117. A. S. Karpov and J. J. Muller, *Org. Lett* . 2003, **5**, 3451.
118. R. M. Adlington, J. E. Baldwin, D. Catterick and G. J. Pritchard, *Chem. Commun.*, 1997, 1757.
119. R. M. Adlington, J. E. Baldwin, D. Catterick and G. J. Pritchard, *J. Chem. Soc., Perkin Trans.* , 1999, **1**, 855-866.
120. H. Wang, G. E. Kellogg, P. Xu and Y. Zhang, *J. Mol. Graph. Model*, 2018, **83**, 100-111.
121. A. J. Wolf and D. M. Underhill, Peptidoglycan recognition by the innate immune system, *Nature Reviews Immunology*, 2018, **18**, 243-254.

122. E. Lippert, *Z. Naturforsch.*, 1995, **A 10**, 541-545.
123. L. Espinar-Barranco, M. Meazza, A. Linares-Perez, R. Rios, J. M. Paredes and L. Crovetto, *Sensors*, 2019, **19**, 4932.
124. S. Wörner, F. Röncke, A. S. Ulrich and H. A. Wagenknecht, 4-Aminophthalimide Amino Acids as Small and Environment-Sensitive Fluorescent Probes for Transmembrane Peptides, *Chembiochem*, 2020, **21**, 618-622.
125. C. Hadad, S. Achelle, J. C. García-Martinez and J. Rodríguez-López, *J. Org. Chem.*, 2011, **76**, 3837–3845.
126. S. Achelle, A. Barsella, C. Baudequin, B. Caro and F. R.-I. Guen, *J. Org. Chem.*, 2012, **77**, 4087–4096.
127. B. Aydiner and Z. Seferoglu, *Eur. J. Org. Chem.*, 2018, 5921–5934.
128. J. A. Gomez, V. Gama, T. Yoshida, W. Sun, P. Hayes, K. Leskov, D., Boothman and S. Matsuyama, *Biochem. Soc. Trans.*, 2007, **35**, 797–801.
129. G. Mata and N. W. Luedtke, *Organic Letters*, 2013, **15**, 2462-2465.
130. P. Cheruku, J.-H. Huang, H.-J. Yen, R. S. Iyer, K. D. Rector, J. S. Martinez and H.-L. Wang, *Chemical Science*, 2015, **6**, 1150-1158.
131. L. Gilfillan, R. Artschwager, A. H. Harkiss, R. M. J. Liskamp and A. Sutherland, *Organic & Biomolecular Chemistry*, 2015, **13**, 4514-4523.
132. S. Chen, N. E. Fahmi, C. Bhattacharya, L. Wang, Y. Jin, S. J. Benkovic and S. M. Hecht, *Biochemistry*, 2013, **52**, 8580-8589.
133. A. Suzuki, *Angew. Chem. Int. Ed.*, 2011, **50**, 6722-6737.
134. H. A. Ali, M. A. Ismail, A. E.-A. S. Fouda and E. A. Ghaith, *RSC Advances*, 2023, **13**, 18262-18305.
135. R. Martin and S. L. Buchwald, *Accounts of Chemical Research*, 2008, **41**, 1461-1473.
136. N. Miyaura and A. Suzuki, *Chemical Reviews*, 1995, **95**, 2457-2483.
137. K. Billingsley, T. Barder and S. Buchwald, *Angew Chem Int Ed Engl.*, 2007, **46**, 5359–5363
138. M. A. Blanchette, W. Choy, J. T. Davis, A. P. Essinfeld, S. Masamune, W. R. Roush and T. Sakai, *Tetrahedron Lett.*, 1984, **25**, 2183-2186.
139. S. Akai, T. Ikawa and K. Saito, *Synlett*, 2012, **23**, 2241-2246.
140. M. Rottlander and P. Knochel, *J. Org. Chem.*, 1998, **63**, 203.
141. M. N. Joy, D. Y. Bodke, K. K. AbdulKhader, A. M. Sajith, T. Venkatesh and A. K. A. Kumar, *J. Fluor. Chem.*, 2016, **182**, 109-120.

142. H. N. Nguyen, X. Huang and S. L. Buchwald, *Journal of the American Chemical Society*, 2003, **125**, 11818-11819.
143. S. Chen, N. E. Fahmi, L. Wang, C. Bhattacharya, S. J. Benkovic and S. M. Hecht, *Journal of the American Chemical Society*, 2013, **135**, 12924-12927.
144. R. McGrory, PhD Thesis, University of Glasgow, 2023.
145. L. K. Lam, L. D. Arnold, T. H. Kalantar, J. G. Kelland, P. M. Lane-Bell, M. M. Palcic, M. A. Pickard, J. C. and Vederas, *J. Biol. Chem.*, 1988, **263**, 11814.
146. H. Ma, V. N. Stone, H. Wang, G. E. Kellogg, P. Xu and Y. Zhang, *Bioorg. Med. Chem. Lett.*, 2017, **27**, 3840-3844.
147. K. H. Schleifer and O. Kandler, *Bacteriol. Rev.*, 1972, **36**, 407-477.
148. J. M. Ghuysen and B. Hackenbeck, *Bacterial Cell Wall.*, Hackenbeck, R., Ed. Elsevier, Amsterdam, 1994.
149. W. Vollmer, D. Blanot and M. A. d. Pedro, *FEMS Microbial. Rev.*, 2008, **32**, 149-167.
150. B. Chatterjee, D. Mondal and S. Bera, *Tetrahedron*, 2021, **100**, 132403.
151. Y. Liu, R. White and W. Whitman, *J. Bacteriol.*, 2010, **192**, 3304-3310.
152. D. M. Gillner, D. P. Becker and R. C. Holz, *J. Biol. Inorg. Chem.*, 2012, **18**, 155-163.
153. D. A. Berges, W. E. DeWolf Jr, G. L. Dunn, D. J. Newman, S. J. Schmidt, J. J. Taggart and C. Gilvarg, *J. Biol. Chem.*, 1986, 6160.
154. J. M. Girondeau, C. Agouridas, M. Masson, R. Pineau and F. LeGoffic, *J. Med. Chem.*, 1986, **29**, 1023.
155. R. J. Cox, J. A. Schouten, R. A. Stentiford and K. J. Wareing, *Bioorg. Med. Chem. Lett.*, 1998, **8**, 945.
156. R. Gupta, N. Gupta and S. Bindal, *Fundamentals of Bacterial Physiology and Metabolism*, Springer, Singapore, 2021.
157. P. Sarkar, V. Yarlagadda, C. Ghosh and J. Haldar, *MedChemComm*, 2017, **8**, 516-533.
158. K. Bush and P. A. Bradford, *Cold Spring Harb. Perspect. Med.*, 2016, **6**, a025247.
159. M. S. Butler, K. A. Hansford, M. A. T. Blaskovich, R. Halai and M. A. Cooper, *J. Antibiot*, 2014, **67**, 631-644.
160. J. G. Kelland, L. D. Arnold, M. M. Palcic, M. A. Pickard and J. C. Vederas, *J. Biol. Chem*, 1986, **261**, 13216-13223.
161. G. Auger, J. v Heijenoort, J. C. Vederas and D. Blanot, *FEBS Lett.*, 1996, **391**, 171-174.

162. S. D. Abbott, P. Lane-Bell, K. P. S. Sidhu and J. C. Vederas, *J. Am. Chem. Soc.*, 1994, **116**, 6513–6520.
163. C. M. Diaper, A. Sutherland, B. Pillai, M. N. G. James, P. Semchuk, J. S. Blanchard and J. C. Vederas, *Org. Biomol. Chem*, 2005, **3**, 4402.
164. B. A. Boughton, R. C. J. Dobson, J. A. Gerrard and C. A. Hutton, *Bioorganic Med. Chem. Lett.*, 2008, **18**, 460-463.
165. L.K. Lam, L. D. Arnold, T. H. Kalantar, J. G. Kelland, P. M. Lane-Bell, M. M. Palcic, M. A. Pickard and J. C. Vederas, *J. Biol. Chem.* , 1988, **263**, 11814.
166. Y. Gao, P. Lane-Bell and J. C. Vederas, *J. Org. Chem.*, 1998, **63**, 2133–2143.
167. J. L. Roberts and C. Chan, *Tetrahedron Lett.*, 2002, **43**, 7679-7682.
168. A. R. Jurgens, *Tetrahedron Lett.*, 1992, **33**, 4727.
169. A. Sutherland and J.C. Vederas, *ChemComm.*, 2002, 224-225.
170. Y. Saito, Y. Yoshimura, H. Wakamatsu and H. Takahata, *Molecules.*, 2013, **18**, 1162-1173.
171. R. M. Williams, M. -N. Im and J. Cao, *J. Am. Chem. Soc.*, 1991, **113**, 6976.
172. R. M. Williams and C. Yuan, *J. Org. Chem*, 1992, **57**, 6519–6527.
173. P. Collier, I. Patel and R. Taylor, *Tetrahedron Lett.*, 2001, **42**, 5953-5954.
174. W. Wang, C. Xiong, J. Yang and V. J. Hruby, *Synth.*, 2002, **1**, 94-98.
175. H. Ma, V.N. Stone, H. Wang, G.E. Kellogg, P. Xu and Y. Zhang, *Bioorg. Med. Chem. Lett.*, 2017, **27**, 3840-3844.
176. E. G. Nolen, C. J. Fedorka and B. Blicher, *Synth Commun*, 2006, **36**, 1707–1713.
177. J. L. Roberts and C. Chan, *Tetrahedron Lett.*, 2002, **43**, 7679-7682.
178. L. S. Fowler, L. Thomas, D. Ellis, A. and Sutherland, *ChemComm*, 2011, **47**, 6569.
179. J. D. Bell, A. H. Harkiss, D. Nobis, E. Malcolm, A., Knuhtsen, C. R. Wellaway, A. G. Jamieson, S. W. Magennis and A. Sutherland, *Chem. Commun* . 2020, **56**, 1887.
180. T. H. Keller and L. weike, *Tetrehedron Lett.*, 1990, **31**, 6307-6310.
181. S. K. Chung and D. H. Kang, *Tetrahedron*, 1997, **8**, 3027-3030.
182. J. Rudolph, F. Hannig, H. Theis and R. Wischnat, *Org. Lett*, 2001, **3**, 3153–3155.
183. E. D. D. Calder, A. M. Zaed and A. Sutherland, *J. Org. Chem.*, 2013, **78**, 7223–7233.

184. L. E. Overman and N. E. Carpenter, *In Organic Reactions*, L. E. Overman, Ed. , Wiley: Hoboken, NJ, 2005. Vol. 66, 1-107.
185. A. A. Tjeng, K. L. Handore and R. A. Batey, *Org. Lett.*, 2020, **22**, 3050–3055.
186. T. K. Hollis and L. E. J. Overman, *Organomet. Chem.* , 1999, **576**, 290-299.
187. P. H., A. Carlsen, T. Katsuki, V. S. Martin and K. B. Sharpless, *J. Org. Chem* . 1981, **46**, 3936.
188. R. F. W. Jackson, A. B. Rettie, A. Wood and M. J. Wythes, *J. Chem. Soc., Perkin Trans. 1*, 1994, 1719-1726.
189. A. M. P. Koskinen, J. Helaja, E. T. T. Kumpulainen, J. Koivisto, H. Mansikkamäki and K. Rissanen, *J. Org. Chem.*, 2005, **70**, 6447–6453.
190. M. T. Nuñez and V. S. Martín, *J. Org. Chem* . 1990, **55**, 1928.
191. N. Hashimoto, T. Aoyama and T. Shioiri, *Chem. Pharm. Bull.*, 1981, **29**, 1475–1478.
192. E. Kühnel, D. D. P. Laffan, G. C. Lloyd-Jones, T. Martínez Del Campo, I. R. Shepperson and J. L. Slaughter, *Angew. Chem. Int. Ed.*, 2007, **46**, 7075–7078.
193. E. J. Corey and C. J. Helal, *Angew. Chem. Int. Ed.*, 1998, 1986-2012
194. Y. Jeong, J. Lee and J. Ryu., *Bioorg. Med. Chem*, 2016, **24**.
195. W. H. Pearson and M. J. Postich, *J. Org. Chem.*, 1994, **59**, 5662-5671.
196. W. Wang, C. Xiong, J. Zhang and V. J. Hruby, *Tetrahedron*, 2002, **58**, 3101-3110.
197. A. Varnavas, L. Lassiani, V. Valenta, L. Mennuni, F. Makovec and D. Hadjipavlou-Litina, *Eur. J. Med. Chem.*, 2005, **40**, 563-581.
198. P. Gmeiner, P. L. Feldman, M. Y. Chu-Moyer and H. Rapoport, *J. Org. Chem.*, 1990, **55**, 3068–3074.
199. R. Huisgen, 3-Dipolar cycloadditions past and future. *Angew. Chem. Int. Ed.* 2, 566–598.
200. I. Abrunhosa-Thomas, A. Plas, A. Vogrig, N. Kandepedu, P. Chalard and Y. Troin, *J. Org. Chem.*, 2013, **78**, 2511-2526.
201. D. E. Rudisill and J. P. Whitten, *Synthesis*, 1994, **8**, 851-854.
202. Fowler. L. S., Ellis. D. and Sutherland. A, *Org. Biomol. Chem.*, 2009, **7**, 4309-4316.